SANDIA REPORT

SAND91—0244 • TTC—1058 • UC—722
Unlimited Release
Printed June 1991

Structural Testing of the Los Alamos National Laboratory Heat Source/Radioisotopic Thermoelectric Generator Shipping Container

D. R. Bronowski, M. M. Madsen

Prepared by
Sandia National Laboratories
Albuquerque, New Mexico 87185 and Livermore, California 94550
for the United States Department of Energy
under Contract DE-AC04-76DP00789

Issued by Sandia National Laboratories, operated for the United States Department of Energy by Sandia Corporation.

Available to DOE and DOE contractors from
Office of Scientific and Technical Information
PO Box 62
Oak Ridge, TN 37831

Prices available from (615) 576-8401, FTS 626-8401

Available to the public from
National Technical Information Service
US Department of Commerce
5285 Port Royal Rd
Springfield, VA 22161

NTIS price codes
Printed copy: A08
Microfiche copy: A01

SAND 91-0244
TTC-1058
Unlimited Distribution
Printed June 1991

Distribution
Category UC-722

STRUCTURAL TESTING OF THE LOS ALAMOS NATIONAL LABORATORY HEAT SOURCE/RADIOISOTOPIC THERMOELECTRIC GENERATOR SHIPPING CONTAINER*

D. R. Bronowski and M. M. Madsen
Transportation System Development Department
Sandia National Laboratories**
Albuquerque, NM 87185

ABSTRACT

The Heat Source/Radioisotopic Thermoelectric Generator shipping container is a Type B packaging design currently under development by Los Alamos National Laboratory. Type B packaging for transporting radioactive material is required to maintain containment and shielding after being exposed to the normal and hypothetical accident environments defined in Title 10 Code of Federal Regulations Part 71. A combination of testing and analysis is used to verify the adequacy of this package design. This report documents the test program portion of the design verification, using several prototype packages. Four types of testing were performed: 30-foot hypothetical accident condition drop tests in three orientations, 40-inch hypothetical accident condition puncture tests in five orientations, a 21 psi external overpressure test, and a normal conditions of transport test consisting of a water spray and a 4 foot drop test.

---

*This work was performed at Sandia National Laboratories, Albuquerque, New Mexico, supported by the U.S. Department of Energy under Contract DE-AC04-76DP00789.
**A United States Department of Energy Facility.

ACKNOWLEDGMENTS

The authors are indebted to a large group of individuals who have contributed to this test program. The cooperation and work of the following individuals are greatly appreciated: H. Kovaschetz and E. Barreras of Mechanical Measurements Division 7485-3, D. Cotter, K. Babb, and L. Abeyta of Dynamic Loads and Facilities Development Division 7531, T. Miller, Jr. of Track and Cables Division 7535, K. Sobilik, D. Schulze, and J. Bonner of Thermal Test and Analysis Division 7537, the staff of Photometrics and Optical Development Division 7556, C. Edwards and the staff of Welding and Plasma Spray Section 7473-4, and the staff of Secondary Standards Division 7414, especially W. Leisher and J. Lamarr. Special thanks are due to W. Uncapher and D. Stenberg of Transportation Systems Development Division 6323 for their technical expertise. The technical editing and typing of Creative Computer Services of Albuquerque, NM are gratefully acknowledged.

CONTENTS

CONTENTS (Continued)

CONTENTS (Continued)

LIST OF FIGURES

LIST OF FIGURES (Continued)

LIST OF FIGURES (Continued)

LIST OF TABLES

1.0 INTRODUCTION

This report describes testing performed on the heat source/radioisotopic thermoelectric generator (HS/RTG) shipping container. The container was designed and fabricated by Los Alamos National Laboratory (LANL) to transport HS or RTG components. Sandia National Laboratories, Albuquerque (SNL) was contracted to perform a series of tests on a structural test unit.

These tests will provide data to verify container design adequacy under normal conditions of transport or following a hypothetical accident, and secondarily, to provide structural response data that will verify analytical predictions. This data will support LANL's Safety Analysis Report for Packaging (SARP) for the container.

The test series consisted of an overpressure test, a water spray test, a 4-foot drop test, three 30-foot drop tests, and five 40-inch puncture tests. Extensive instrumentation was used to gather structural response data during the 30-foot drop tests. Tests on these units also evaluated the worst case orientation. This orientation was later used on a separate, certification test unit. All tests were conducted in accordance with Title 10 Code of Federal Regulations, Part 71 (10 CFR 71).[1]

Data obtained from the test series include leakage test results, acceleration and strain data, dimensional inspection data, and photometric/photographic documentation. No conclusions are presented here nor are test results interpreted.

2.0 PACKAGE DESCRIPTION

The HS/RTG package is a Type-B shipping container consisting of an inner and an outer container. The outer container is a 12-gallon military specification drum (MIL-D-6054) with a modified locking ring (Figure 2-1) 14.75 inches in diameter and 21 inches high. Average weight of the units tested was 71.25 pounds.

Acting as a thermal insulator and shock absorption material, layered Celotex® mineral board fills the area between the inner and outer containers. The Celotex layers are bonded into a body section and a lid section (Figure 2-1).

Inner container components are shown in Figure 2-2. The inner container body (Figure 2-3) is a flow-turned stainless steel payload container 12 inches long and 4 inches in diameter. A machined stainless steel lid incorporates a double O-ring seal, which provides the required level of leak containment and provides a test cavity for leak-testing. Closure of the inner container is made by a bolted V-clamp produced commercially by Aeroquip® Corporation. The RTG configuration payload (Figure 2-4) with two mock-up RTGs was used for all tests since it provided the highest weight content.

Specific component orientation was maintained at each assembly by aligning the most vulnerable area of each component with the actual location of impact. The welded drum seam, the bolt lug of the drum lid locking ring, and the bolt of the inner container V-clamp were oriented at the 180° side of the drum, the side nearest the impact in the corner and side drop tests. Orientation of the V-clamp dictated orientation of the body Celotex, aligning the area of minimum insulation with the 180° side.

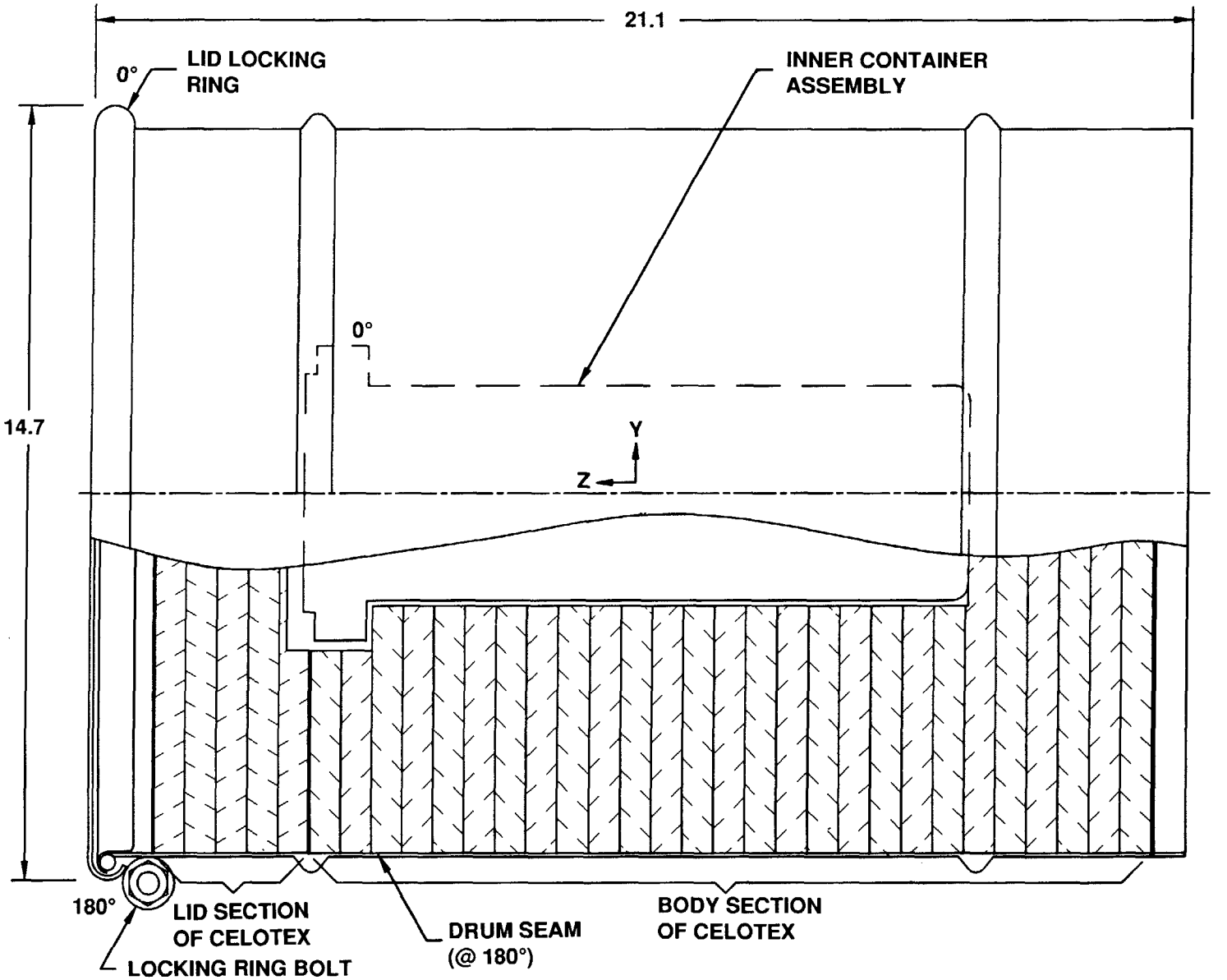

Figure 2-1. Outer Drum Components

Figure 2-2. Inner Container Components

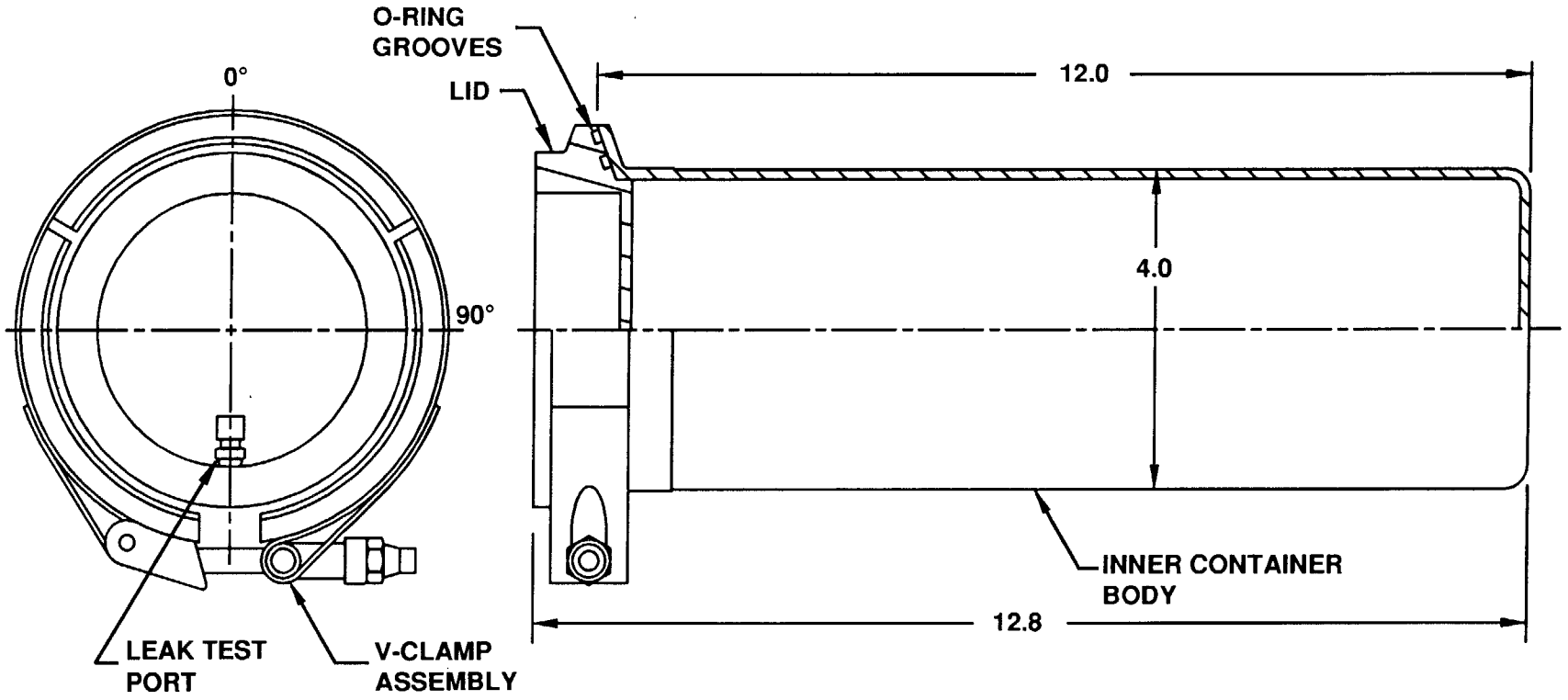

Figure 2-3. Inner Container Assembly

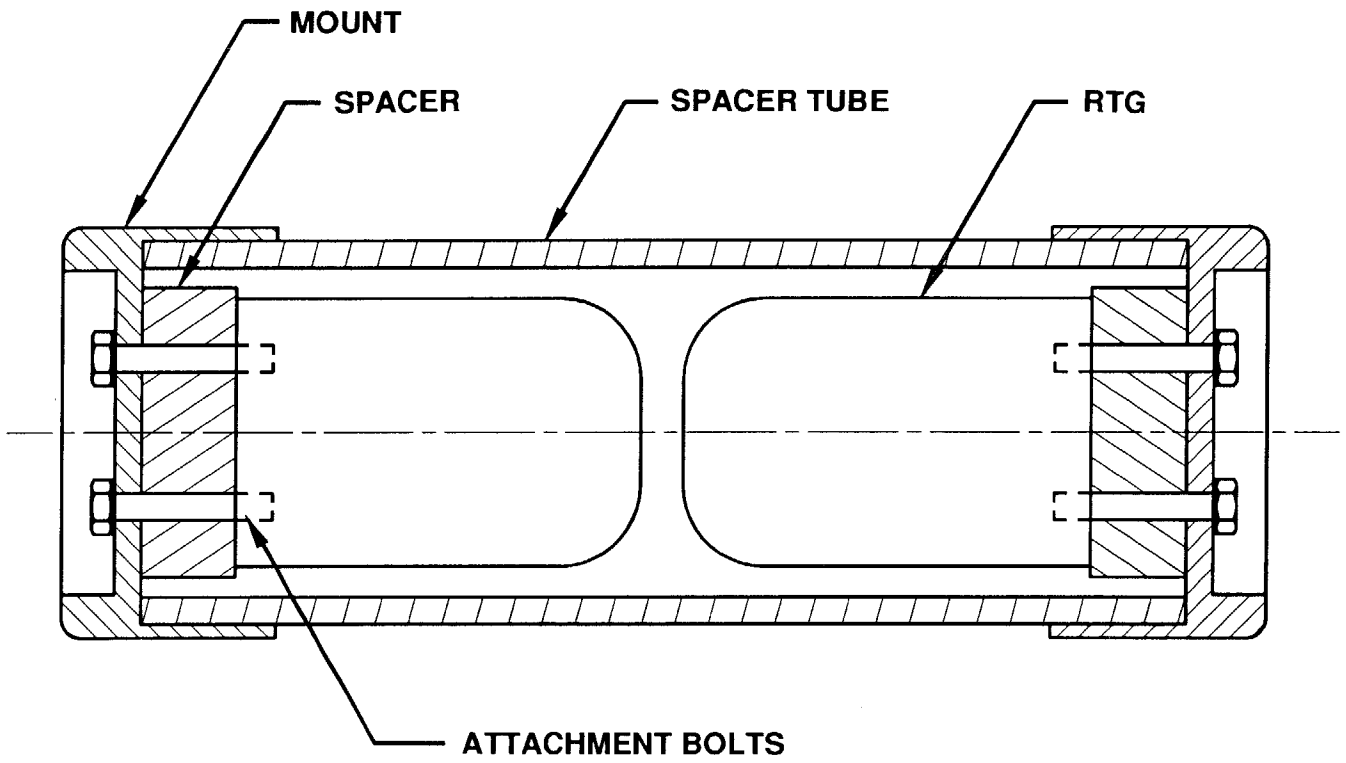

Figure 2-4. Payload Assembly

3.0 TEST PROGRAM DESCRIPTION

To verify the structural integrity of the HS/RTG shipping container design, the test series shown in Table 3-1 was performed. This series was defined by LANL in the HS/RTG Shipping Container Test Specification.[2] The series contains tests for both normal conditions of transport and hypothetical accidents, as defined in 10 CFR 71.[1] All tests were performed at ambient temperature.

Pretest measurements were made to establish baseline data for the inner container of the package through dimensional inspections and leakage rate measurements. These nondestructive evaluation (NDE) procedures were repeated periodically during the testing sequence. Table 3-2 illustrates the application of NDE, assembly, and disassembly procedures. Posttest results of NDE and disassembly tasks are presented in the sections related to each individual test.

3.1 Overpressure Test

This test simulated a 50-foot immersion test as specified by 10 CFR 71.[1] The package was placed in a hydrostatic test chamber for a period of 8 hours at a minimum pressure of 21 psig. Both pretest and posttest leakage rate measurements and mechanical inspections of the inner container body and lid were performed.

3.2 Normal Conditions of Transport Tests

Normal conditions of transport tests consist of a water spray test followed by a 4-foot free fall drop test. The water spray test simulated exposure to a rainfall of at least 2 inches per hour for a minimum period of 1 hour. The 4-foot drop test was conducted aligning the center of gravity over the lid locking ring bolt, an orientation for which maximum drum deformation was expected. Leakage rate was measured before the water spray test and again after the drop test. A mechanical inspection of the inner container body and lid was performed after the drop test.

3.3 30-Foot Drop Tests

Three drop tests were performed, one in each of the following orientations: center of gravity (CG) over corner, side, and end on. Each test was a guided free fall drop impacting an essentially unyielding target at 44 feet per second. An additional 2.3 feet was added to the standard 30-foot free fall drop height to compensate for friction in the guidance system. The test facility and guidance system are described in detail in Section 4.2.

TABLE 3-1

Test Sequence

Test No.	Test Description	Unit No.	Drop Height	Impact Angle
1	Overpressure	S-1	NA	NA
2	Water Spray	S-1	NA	NA
3	Normal Conditions Drop	S-1	4 ft	58°
4	Center of Gravity Over Corner Drop	S-2	32.3 ft	58°
5	Side Drop	S-3	32.3 ft	0°
6	End Drop	S-1	32.3 ft	90°
7	Locking Ring Punch	S-2	40 in.	54°
8	Center of Gravity Over Corner Punch	S-2	40 in.	54°
9	Side Punch	S-3	40 in.	0°
10	End Punch	S-1	40 in.	90°
11	Locking Ring Punch	S-1	40 in.	60°

For each of the tests, the inner container of the structural test unit was assembled in a new outer drum using new Celotex insulation. The inner container was leak-tested before and after each test. Inner container components were inspected after the third drop test.

The package was instrumented with accelerometers, strain gages, and instrumented bolts for each of these tests. Data was recorded during the drop events using a high-speed data acquisition system. Transducer information is described in detail in Section 5; data relating to each drop test is presented in following sections.

3.4 Puncture Tests

Five puncture tests were performed on the three drop tested units. Each test was a 40-inch free falls onto a

TABLE 3-2

HS/RTG Shipping Container Test Matrix

Test	Test Description	Inspect	Instrument	Leak Test	Assembly	Test Procedure	Dis-Assembly	Leak Test	Inspect
S-0	Overpressure	X		X	X	LANL-0 (Ref. 3)	X	X	X
S-1	Norm Cond			X	X	LANL-1 (Ref. 4)	X	X	X
S-2	CG Drop		X	X	X	LANL-S2 (Ref. 5)	X	X	
S-3	Side Drop		X	X	X	LANL-S3 (Ref. 6)	X	X	
S-4	End Drop		X	X	X	LANL-S4 (Ref. 7)	X	X	X
S-5a	Puncture			X	X	LANL-S5 (Ref. 8)			
S-5b	Puncture					LANL-S5 (Ref. 8)	a	X	
S-5c	Puncture				b	LANL-S5 (Ref. 8)	a	X	
S-5d	Puncture				b	LANL-S5 (Ref. 8)			
S-5e	Puncture					LANL-S5 (Ref. 8)	X	X	X

a. Test unit required only partial disassembly.
b. Test unit required only partial re-assembly.

6-inch-diameter puncture bar as defined in 10 CFR 71.[1]. One punch was performed on each of the three drop-tested units with the punch attacking the damaged area. Two additional tests directed the punch at the drum lid locking ring in an attempt to remove the ring.

Leak-testing was conducted on the inner container before and after each test (or pair of tests). Dimensions of the inner container body and lid were inspected after the final test.

3.5 Documentation/Quality Assurance

All testing and related activities were conducted under the SNL Transporatation System Development Department 6320 Quality Assurance Program Plan.[9] Project-specific program plans for testing[10] and quality assurance[11] were prepared. Detailed written test procedures with quality assurance (QA) hold points were assigned to control testing and recording of all data. Additional procedures directed assembly, instrumentation, leak-testing, inspection, and disassembly of the package and provided directions for recording related data. Before use, all procedures were approved by SNL and LANL project and QA personnel. Documentation included hardware identification, transducer calibrations or specification data, laboratory instrument identification and calibration, assembly and disassembly torque values and notes, deformation sketches with dimensions, NDE results and notes, and high-speed and still photographic records.

For each test, applicable test procedures and all related data were organized into test books maintained as permanent records in the SNL Department 6320 Quality Assurance Records Storage Facility.

Photometric documentation data consisted of 400 frame per second photos of all dynamic tests. An additional 2,000 frame per second camera recorded each 30-foot drop test. To aid in photometric analysis the test facility used grid boards and striped the test unit with contrasting colors.

A copy of the test books, photos, films, and data will be supplied to LANL test engineers. At the conclusion of the test program, all test hardware will be returned to LANL.

4.0 TEST FACILITY DESCRIPTION

4.1 Hydrostatic Test Chamber

SNL Experimental Mechanics Division 7542 supplied and operated the hydrostatic test chamber used for the over-pressure test. The 18 inch diameter by 36 inch deep chamber is rated for 125 psig air and 400 psig water. Compressed air regulated at the target pressure was used to pressurize the water-filled chamber. Chamber pressure was monitored with a calibrated pressure gauge and recorded continuously on a strip chart recording system.

4.2 185-Foot Drop Tower

All drop and puncture tests were conducted at the SNL 185-foot drop tower facility located in Area III. The target at this facility meets the International Atomic Energy Agency (IAEA) essentially unyielding criteria[12]. This target consists of a block of reinforced concrete covered with a steel plate 4 feet by 6 feet by 8 inches thick. Total target weight is more than 55,000 pounds.

The test facility is illustrated in Figure 4-1. For the 4-foot drop and 40-inch puncture tests, the test unit was attached to an adjustable cradle using wire rope. Release was made using an explosive cable cutter, allowing the test unit to free fall onto the target or puncture bar.

Because of the light weight of the test package and the large number of instrumentation cables, a guidance system was used for the 30-foot drop tests, enabling the impact angle of the package to be controlled accurately. Actual drop height for the guided tests was 32 feet, 4 inches. Additional height (above the regulatory 30-foot free fall test) was required to compensate for friction in the guidance system and resulted in the required 44 feet per second impact velocity.

For the 44 feet per second tests the package was attached to the adjustable cradle with wire rope. The cradle was attached to a sliding beam which guided the assembly through the first part of the fall. At approximately 8 feet above the target, the wire rope was cut using an explosive cable cutter or explosive bolts, allowing the package to free fall the remaining distance. The sliding beam and cradle assembly was stopped approximately 1 foot after package release using a water braking system.

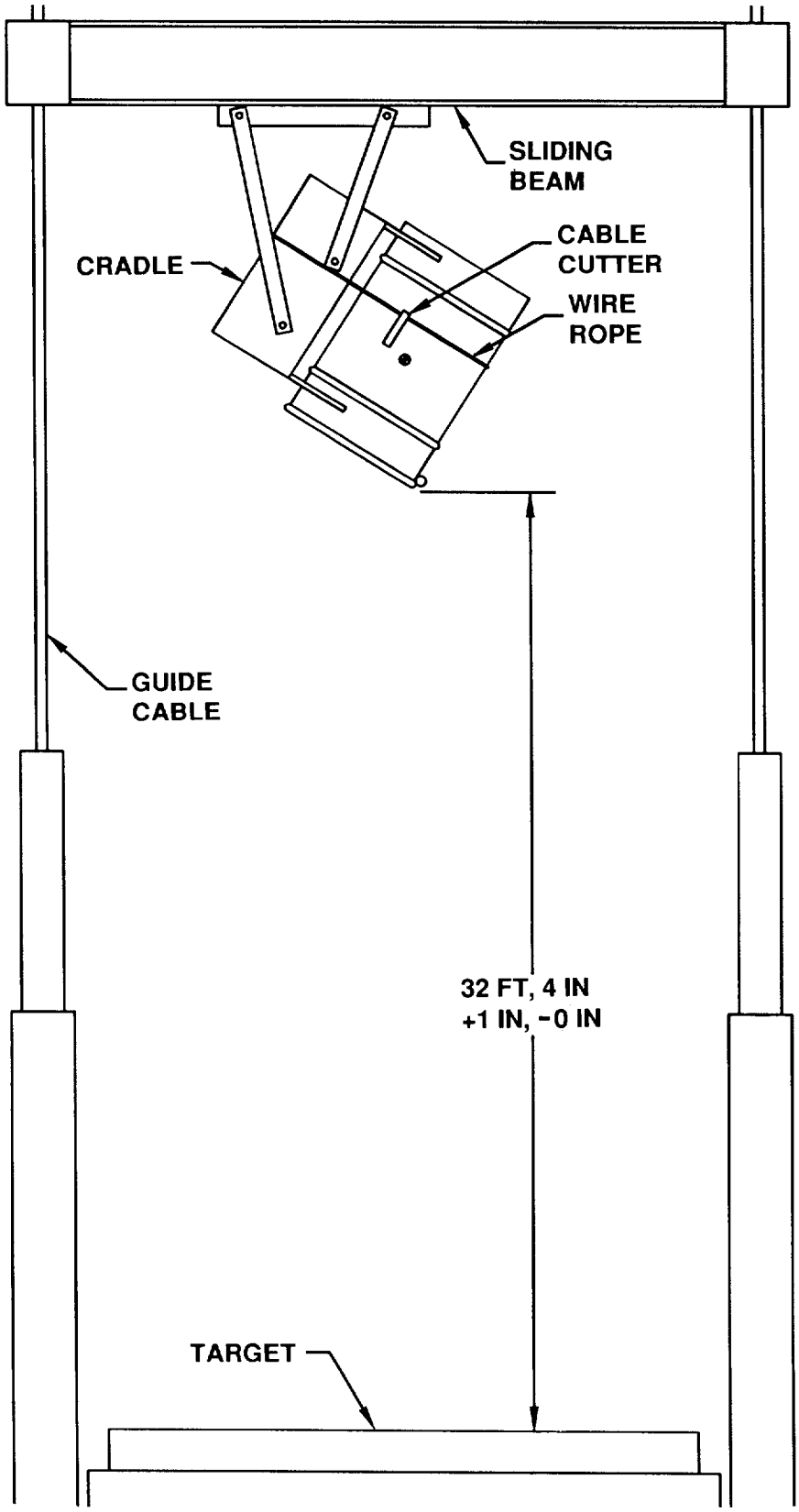

Figure 4-1. Drop Test Facility

5.0 STRUCTURAL RESPONSE INSTRUMENTATION

Extensive instrumentation measured structural responses of the package for the 30-foot drop tests. Instrumentation devices included accelerometers, strain gages, and strain-gaged bolts. Each type of instrumentation, collectively known as transducers, provided a different kind of experimental data. Accelerometers measured decelerations of various package components. Strain gages measured surface strains at various locations on the inner container components. Strain-gaged bolts in the drum lid locking ring and in one RTG measured tensile strains in these bolts.

Locations and general descriptions of transducers used in the drop tests are described in following sections. A description of the data acquisition system, discussions of signal filtering rates, and expected uncertainties for each instrumentation device are also included in this section.

Each instrumentation channel was assigned a unique designation to maintain identification throughout the test series. An "S" followed by a numeric character was used for strain gage channels. "A" followed by both a numeric character and an axis direction was used for accelerometer channels. "SB" followed by a numeric character was used for strain-gaged bolts.

5.1 Strain Gages

Strain gages were mounted on the exterior surfaces of the inner container body, lid, and V-clamp. Single and biaxial foil-type gages manufactured by Measurement Group®, Inc., were used. Gage patterns (illustrated in Figures 5-1, 5-2, and 5-3) were used for all three drop tests. Table 5-1 lists the gage type, location, and direction (axial, hoop, or radial). Figure 5-4 illustrates a typical gage installation.

5.2 Accelerometers

Accelerometers were mounted on the exterior of the outer drum, on the exterior of the inner container body and lid, and on the payload assembly. The accelerometers selected for the program were Endevco® Model 7270A $\pm$ 20,000 g piezoresistive transducers. Accelerometer mounting locations were unique for each drop test to align the measuring axis of the transducer with the test unit line of action (pairs of accelerometers mounted at right angles to each other were used for the corner drop test.) Accelerometer layouts for the three tests are shown in Figures 5-5, 5-6, and 5-7. Table 5-2 lists the locations of accelerometers. A typical installation is illustrated in Figure 5-8. Accelerometers were attached with screws to mounting blocks, which were attached to the test unit with quick-setting adhesive. Each accelerometer was

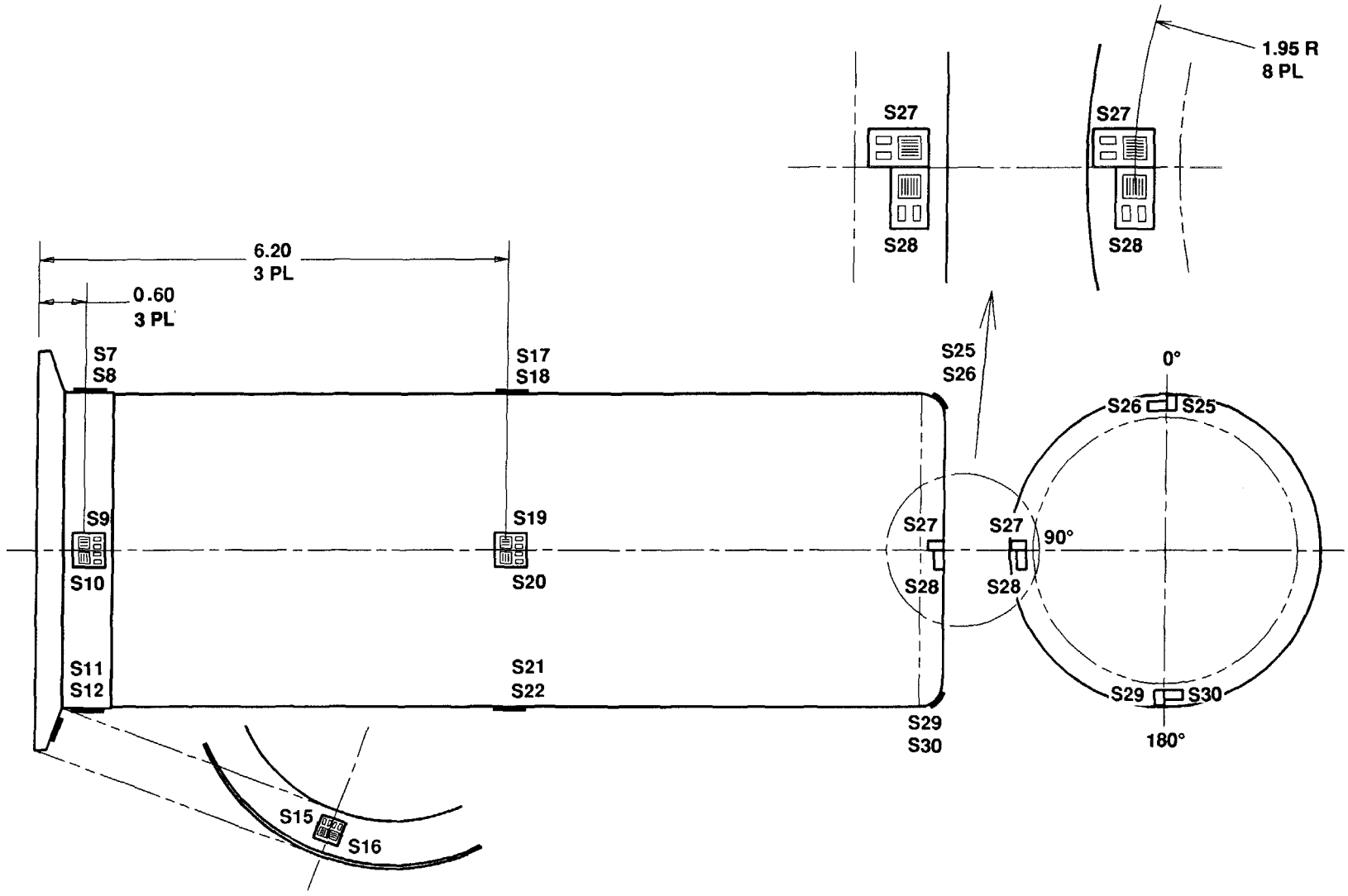

Figure 5-1. Strain Gage Locations--Inner Container Body

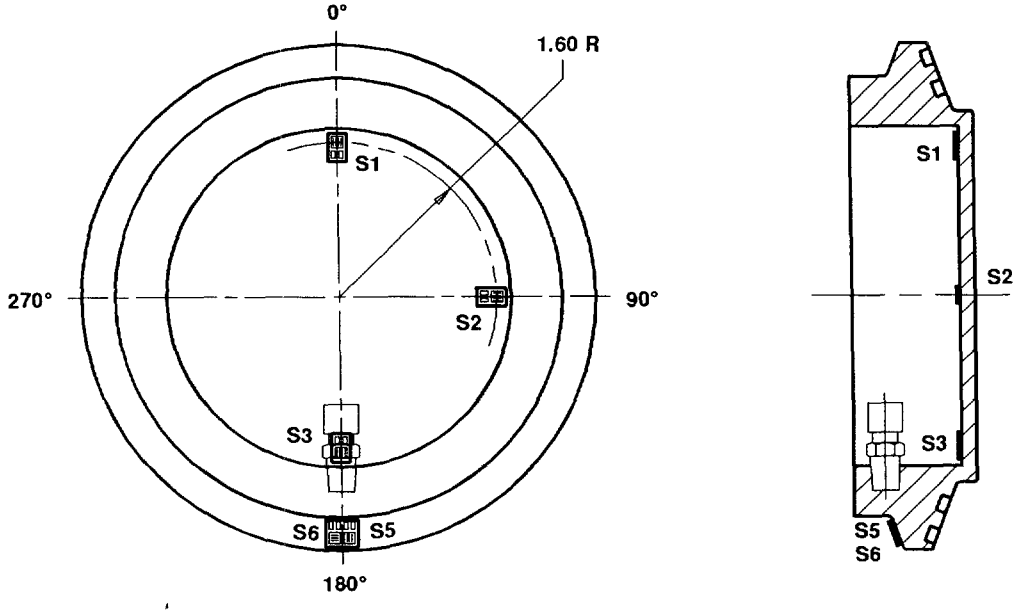

Figure 5-2. Strain Gage Locations--Inner Container Lid

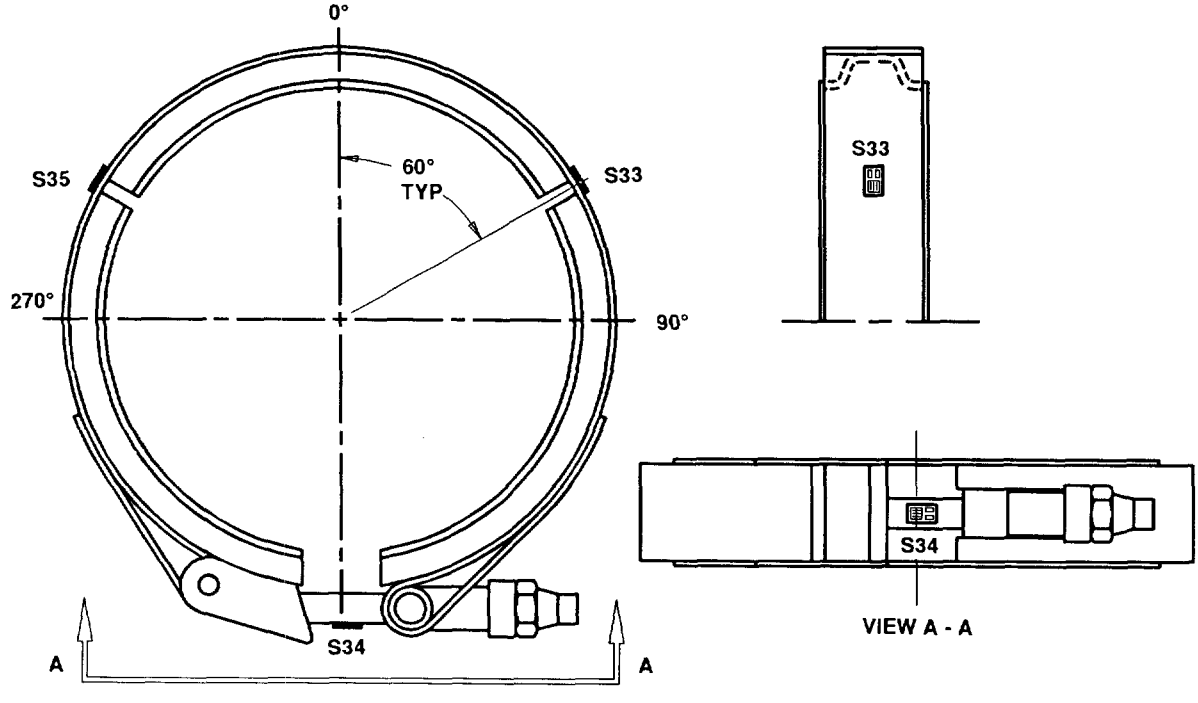

Figure 5-3. Strain Gage Locations--Inner Container V-Clamp

TABLE 5-1

Strain Gages--Inner Container Components

Strain Desig.	Type/Catalog Number	Component	Location	Direction
S1	CEA-09-062UW-350	Lid	0°/top	radial
S2	CEA-09-062UW-350	Lid	90°/top	radial
S3	CEA-09-062UW-350	Lid	180°/top	radial
S4	CEA-09-062UW-350	Lid	270°/top	radial
S5	CEA-09-062UT-350	Lid	180°/flange	radial
S6	CEA-09-062UT-350	Lid	180°/flange	hoop
S7	CEA-09-125UT-350	Body	0°/top	axial
S8	CEA-09-125UT-350	Body	0°/top	hoop
S9	CEA-09-125UT-350	Body	90°/top	axial
S10	CEA-09-125UT-350	Body	90°/top	hoop
S11	CEA-09-125UT-350	Body	180°/top	axial
S12	CEA-09-125UT-350	Body	180°/top	hoop
S13	CEA-09-125UT-350	Body	270°/top	axial
S14	CEA-09-125UT-350	Body	270°/top	hoop
S15	CEA-09-062UT-350	Body	180°/flange	radial
S16	CEA-09-062UT-350	Body	180°/flange	hoop
S17	CEA-09-125UT-350	Body	0°/center	axial
S18	CEA-09-125UT-350	Body	0°/center	hoop
S19	CEA-09-125UT-350	Body	90°/center	axial
S20	CEA-09-125UT-350	Body	90°/center	hoop
S21	CEA-09-125UT-350	Body	180°/center	axial
S22	CEA-09-125UT-350	Body	180°/center	hoop
S23	CEA-09-125UT-350	Body	270°/center	axial
S24	CEA-09-125UT-350	Body	270°/center	hoop
S25	CEA-09-062UW-350	Body	0°/bottom	axial
S26	CEA-09-062UW-350	Body	0°/bottom	hoop
S27	CEA-09-062UW-350	Body	90°/bottom	axial
S28	CEA-09-062UW-350	Body	90°/bottom	hoop
S29	CEA-09-062UW-350	Body	180°/bottom	axial
S30	CEA-09-062UW-350	Body	180°/bottom	hoop
S31	CEA-09-062UW-350	Body	270°/bottom	axial
S32	CEA-09-062UW-350	Body	270°/bottom	hoop
S33	CEA-09-062UW-350	V-clamp	60°/band	
S34	CEA-05-062UW-350	V-clamp	180°/bolt	
S35	CEA-09-062UW-350	V-clamp	300°/band	

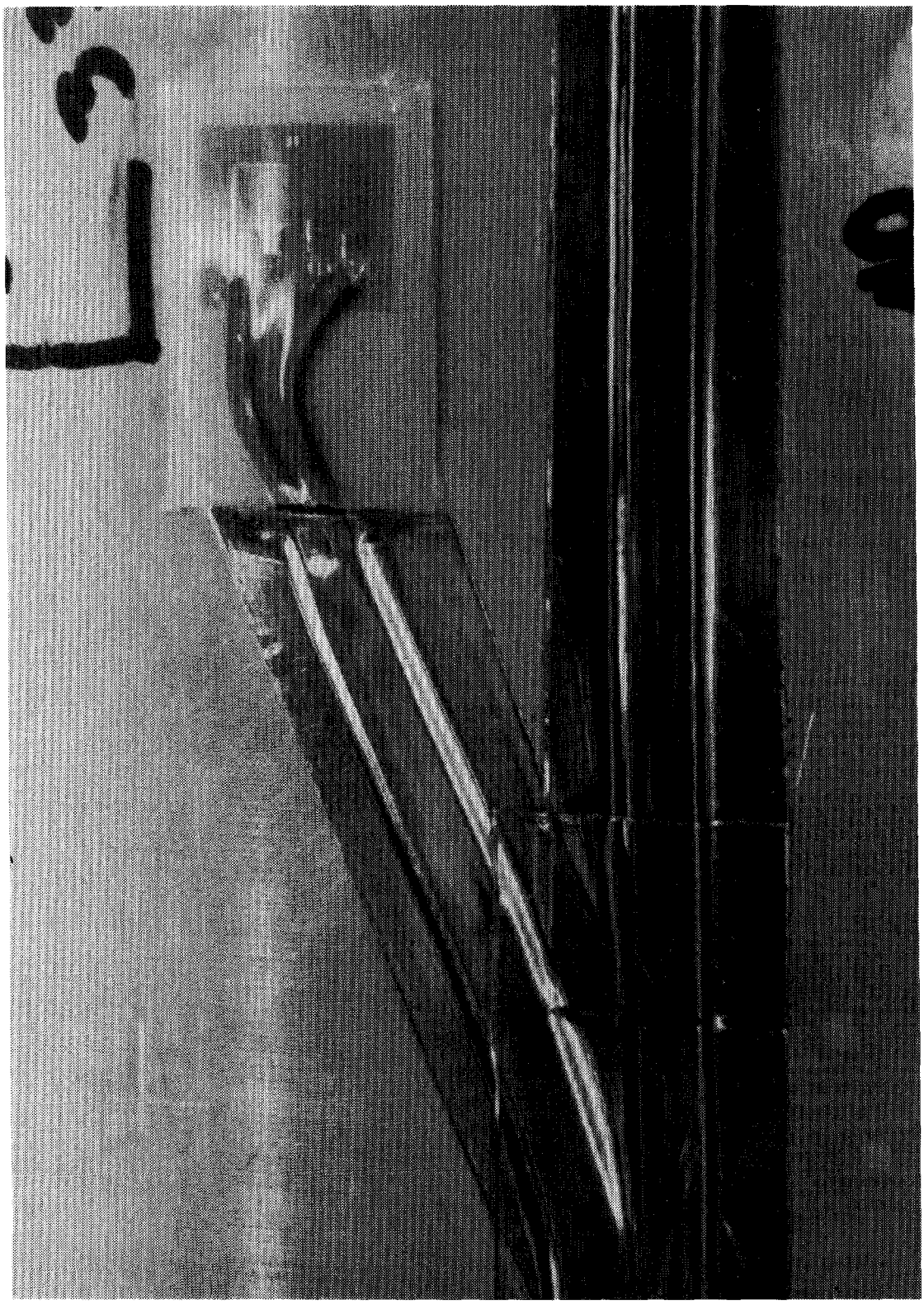

Figure 5-4. Typical Strain Gage Installation

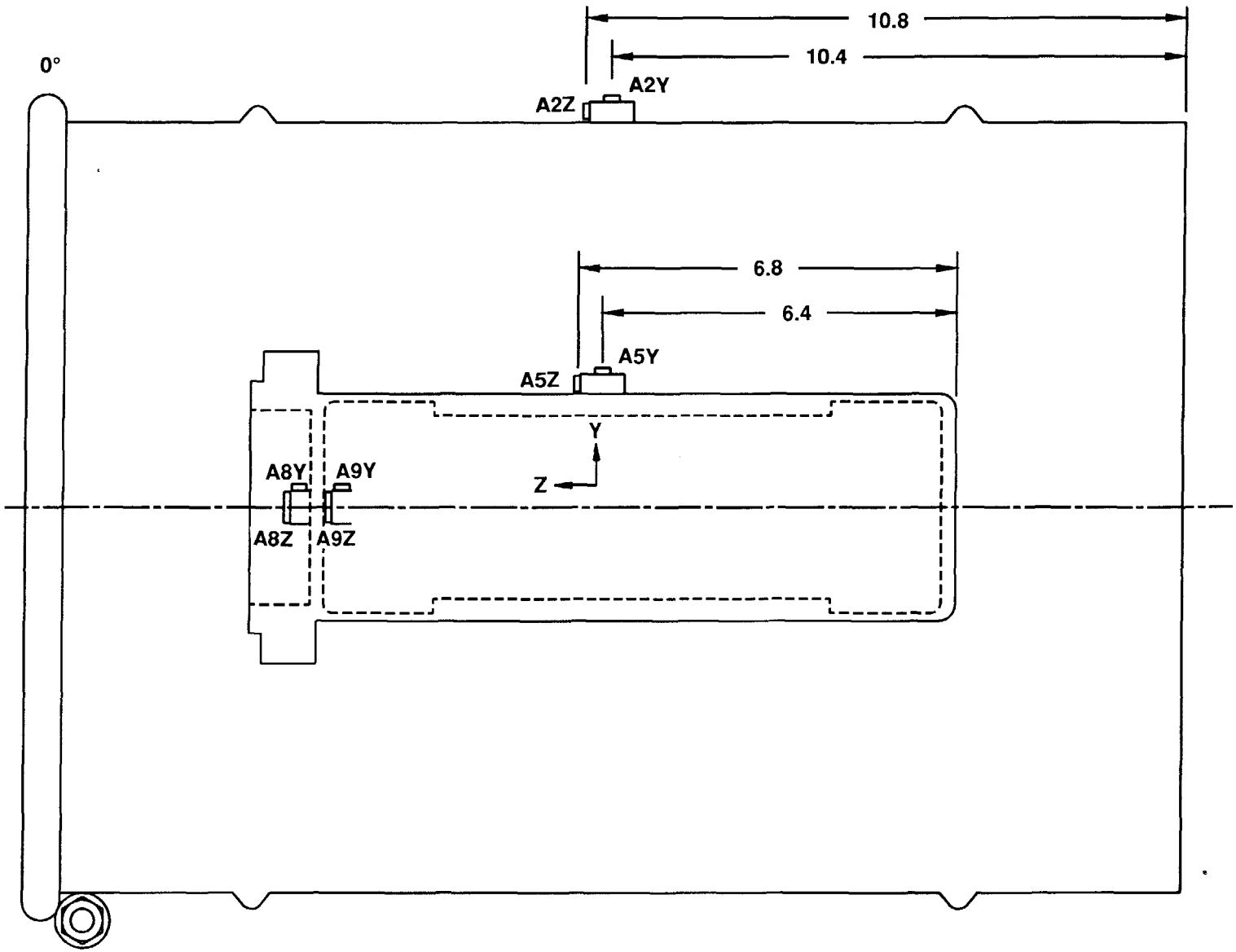

Figure 5-5. Accelerometer Locations--Center of Gravity Over Corner Drop Test

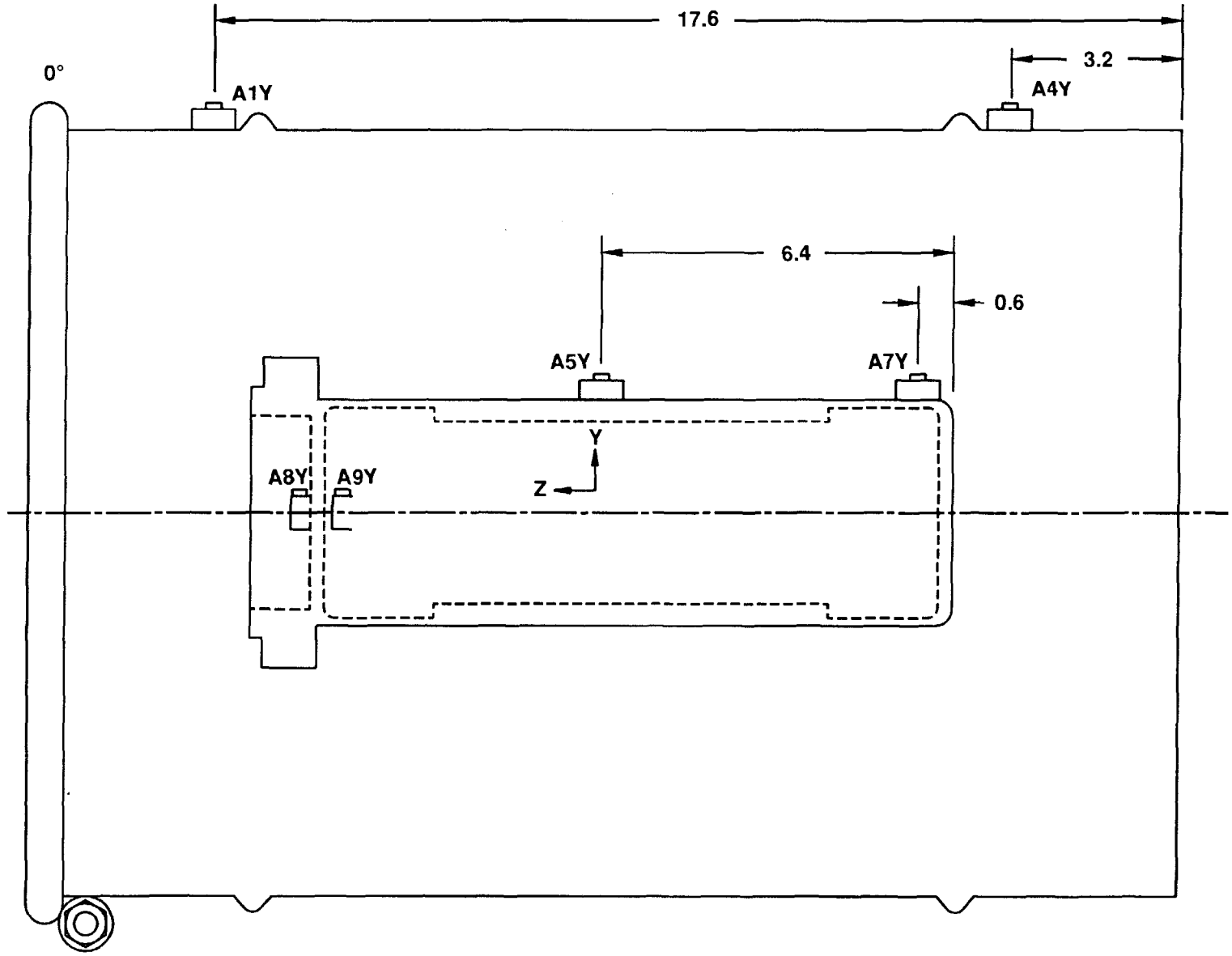

Figure 5-6. Accelerometer Locations--Side Drop Test

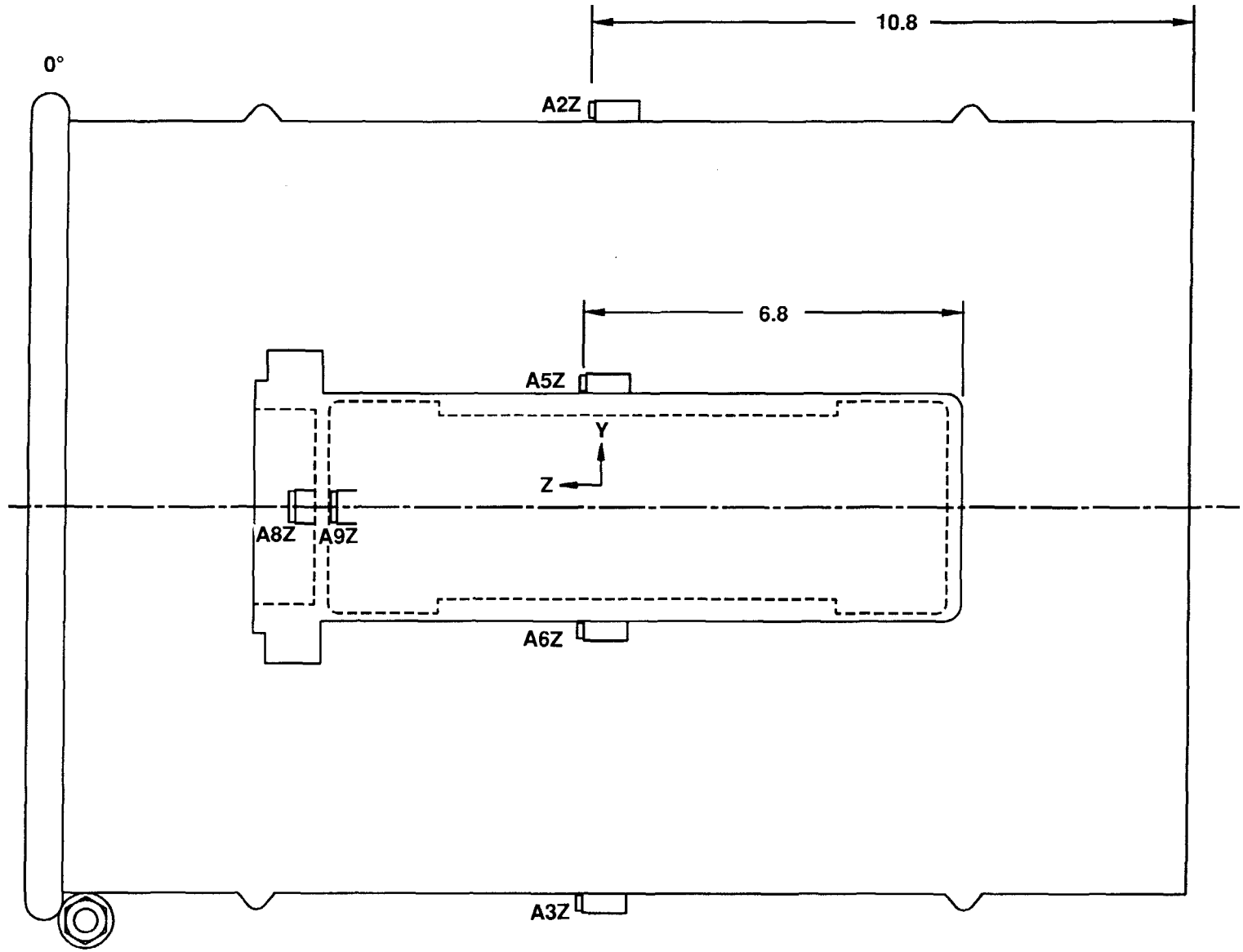

Figure 5-7. Accelerometer Locations--End Drop Test

TABLE 5-2

Accelerometer Locations

Accel. Desig.	Type/Catalog Number	Component	Location	Direction
		CG OVER CORNER DROP TEST		
A2Y	7270A-20K	Drum	0°/center	Y
A2Z	7270A-20K	Drum	0°/center	Z
A5Y	7270A-20K	Canister	0°/center	Y
A5Z	7270A-20K	Canister	0°/center	Z
A8Y	7270A-20K	Lid	Centerline	Y
A8Z	7270A-20K	Lid	Centerline	Z
A9Y	7270A-20K	Payload	Centerline	Y
A9Z	7270A-20K	Payload	Centerline	Z
		SIDE DROP TEST		
A1Y	7270A-20K	Drum	0°/top	Y
A4Y	7270A-20K	Drum	0°/bottom	Y
A5Y	7270A-20K	Canister	0°/center	Y
A7Y	7270A-20K	Canister	0°/bottom	Y
A8Y	7270A-20K	Lid	Centerline	Y
A9Y	7270A-20K	Payload	Centerline	Y
		END DROP TEST		
A2Z	7270A-20K	Drum	0°/center	Z
A3Z	7270A-20K	Drum	180°/top	Z
A5Z	7270A-20K	Canister	0°/center	Z
A6Z	7270A-20K	Canister	180°/center	Z
A8Z	7270A-20K	Lid	Centerline	Z
A9Z	7270A-20K	Payload	Centerline	Z

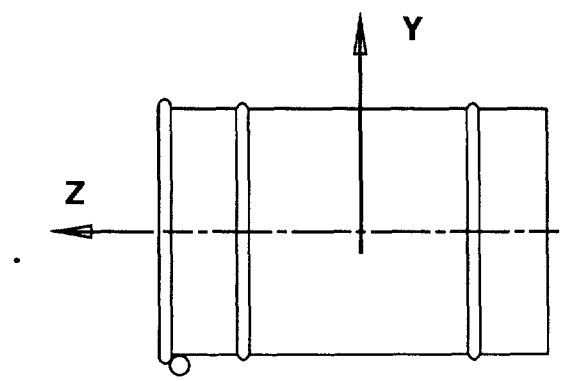

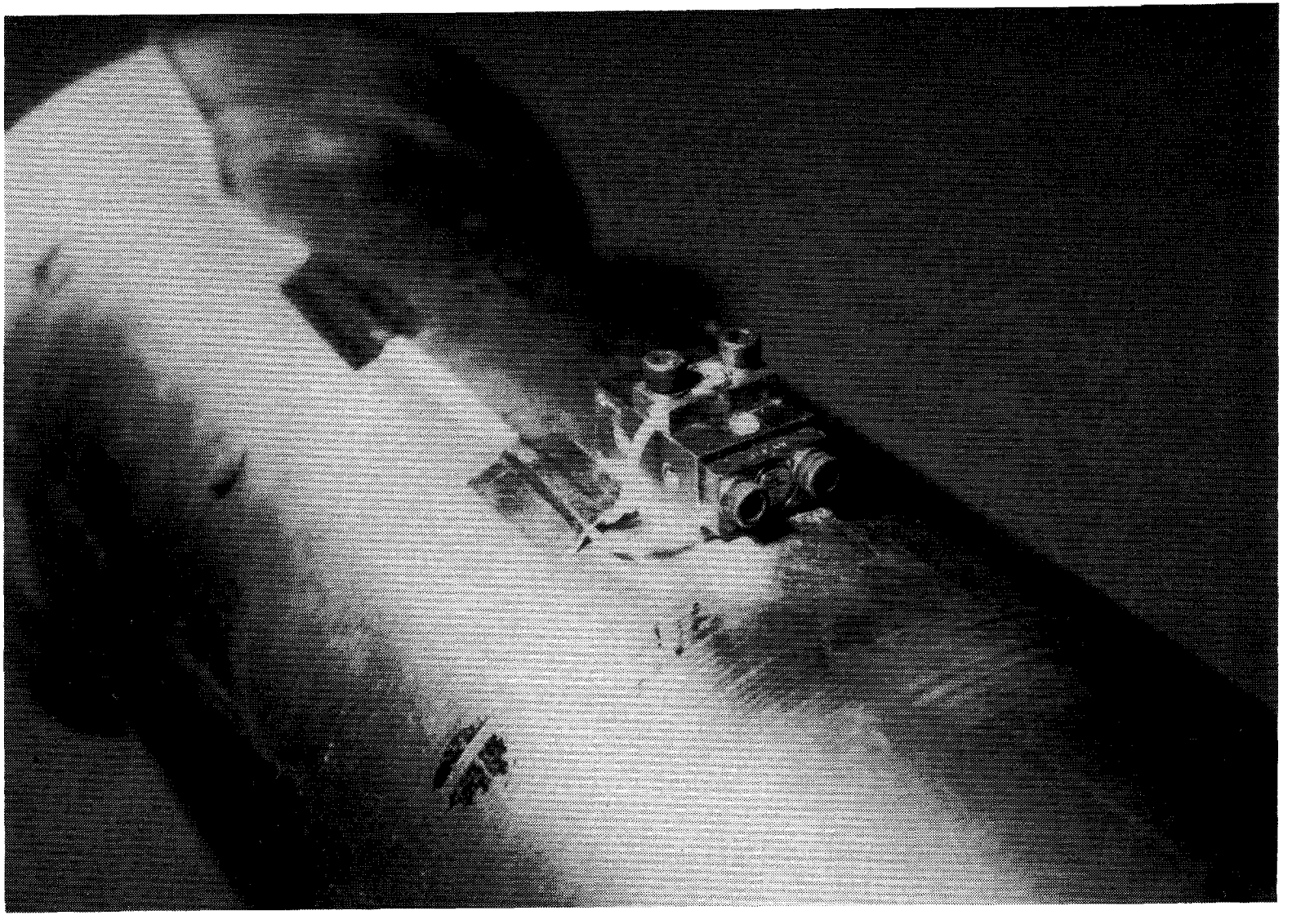

Figure 5-8. Typical Accelerometer Installation

assigned a designation consisting of a number and coordinate direction.

5.3 Instrumented Bolts

Instrumented (internally strain-gaged) bolts were used to measure loads on the outer drum locking ring bolt and the two mounting bolts in the lid end RTG (Figure 5-9). The bolts, 1/4-inch diameter for the RTG and 1/2-inch diameter for the locking ring (Figure 5-10), were procured from Strainsert® Company and were internally gaged with a quarter bridge strain gage. To measure preloads in the bolts, static strains were measured at installation and disassembly.

5.4 Transducer Interconnections

Transducer lead wires were routed to terminal strips on the 0° side of the outer drum (Figure 5-11). Wiring was routed so as to minimize the chance for damage during testing. Two bundles of field cable connected these terminal strips to the data acquisition system. To verify continuity, resistance measurements were made at various points along the assembly and test set-up sequence.

5.5 Data Acquisition and Reduction System

Output from the transducers was converted into electrical signals and recorded on the data acquisition system shown in Figure 5-12. This system includes signal conditioners, which supply input voltages, and bridge balance and calibration capabilities. The signals then passed through amplifiers and were recorded on high-speed digital recorders. Data were also simultaneously recorded on analog tape machines as a backup.

All transducer signals were recorded at 100,000 samples/second which produced a frequency response of ~10,000 Hz. All data were then filtered at 1,000 Hz using a digital Bessel filter. This filter rate reduces high frequency components and presents data representative of the structural response of the package.

Data from the tests were displayed in the form of plots (engineering units versus time). A systematic review of all data was performed, including a comparison of data from each transducer to data from other transducers on the test unit. Conclusions were drawn, and each data channel was assigned a confidence level. Possible uncertainty in collected data is estimated to be $\pm$15 percent.[13] All data plots (1,000 Hz and wide band-10,000 Hz) and evaluation information are presented on the microfiche attached to the back cover of this report. Representative plots, presented in the following sections, detail the results of each test.

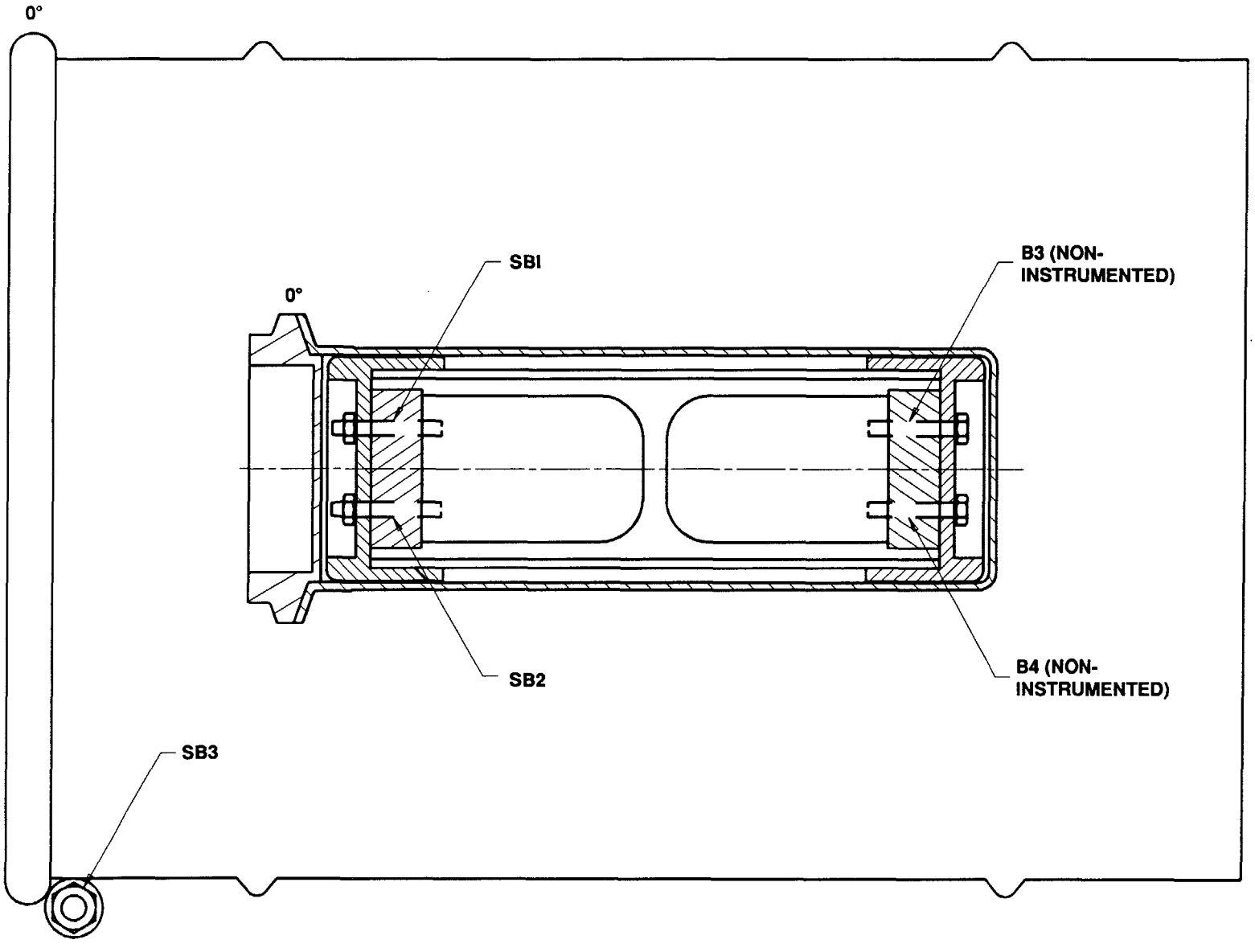

Figure 5-9. Instrumented Bolt Locations

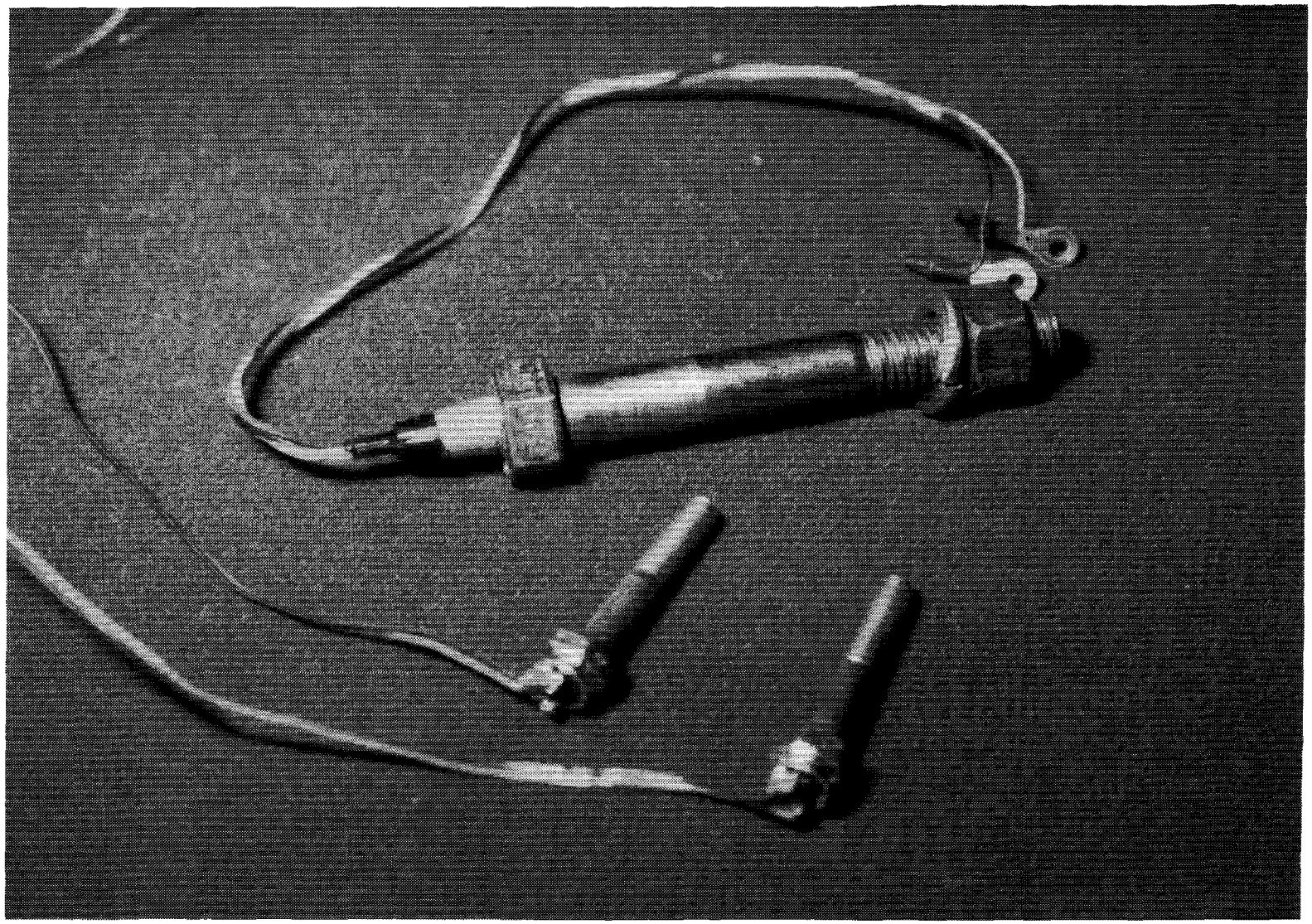

Figure 5-10. Instrumented Bolts

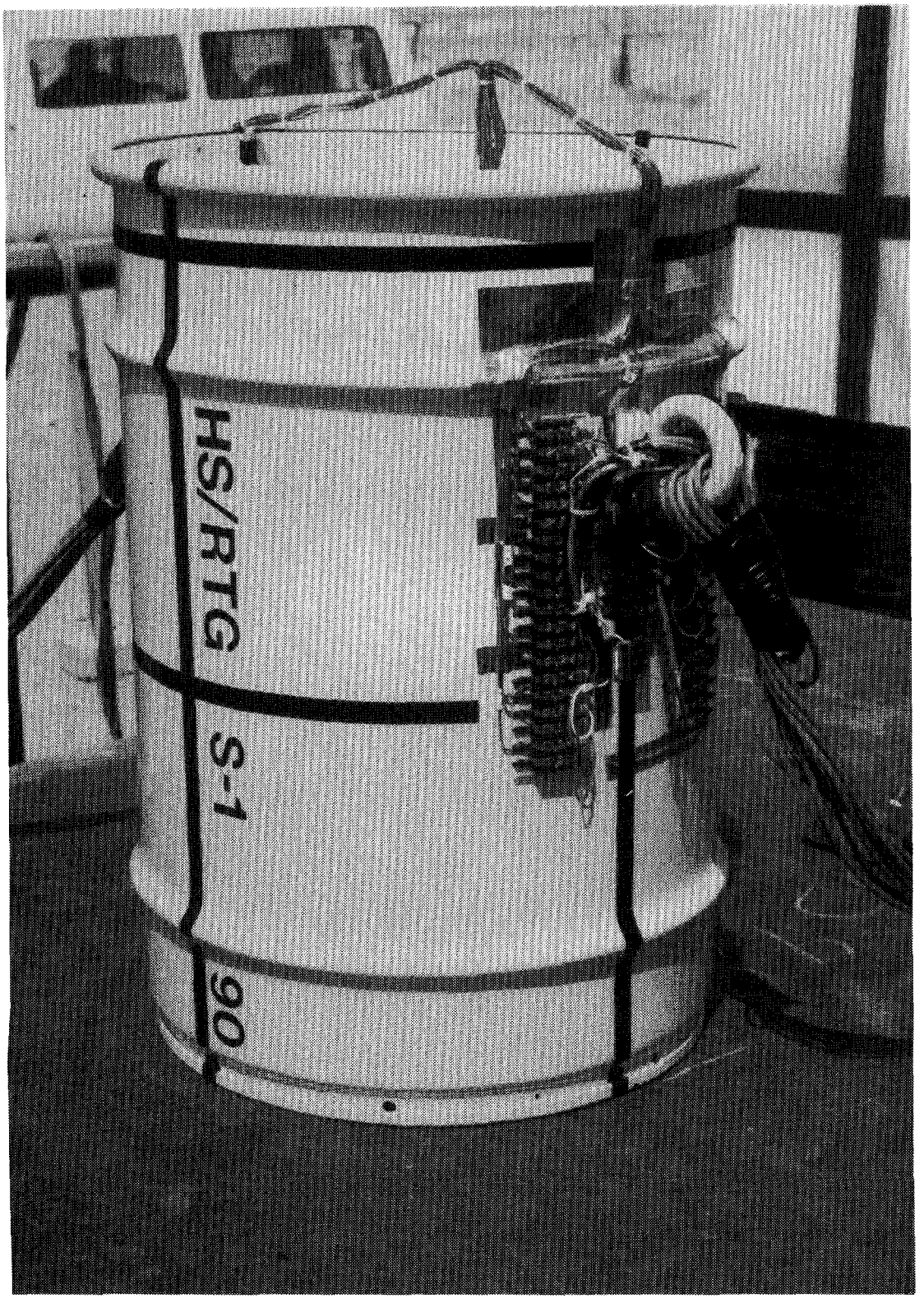

Figure 5-11. Transducer Wiring

Figure 5-12. Data Acquisition System

6.0 OVERPRESSURE TEST

An overpressure test was performed in accordance with the immersion test requirement of 10 CFR 71.73.[1] This test requires immersing the container in 50 feet (minimum) of water for at least 8 hours. Regulations allow a 21 psig hydrostatic test as an acceptable alternate test method. The pressurized chamber test was selected because of the small size of the package and the availability of an appropriate chamber. Testing was performed following the HS/RTG Overpressure Test Procedure.[3]

6.1 Test Unit Preparation

A previously untested inner container body and lid were inspected before the test for baseline data using a written inspection procedure.[14] The payload assembly and inner container were assembled following the Instrumentation and Assembly Procedure.[15] The V-clamp bolt was tightened to 100 inch-pounds.

Helium leak-testing was performed on the inner container seal in accordance with a project-specific leak test procedure[16] and ANSI N14.5.[17] The leakage rate measured 6.4×10^{-9} atm $cm^3/sec.$; this small rate was a result of cavity background (outgassing) and helium permeation. Appendix A presents a detailed description of the leak-testing and a discussion of permeation.

The inner container assembly was installed in a previously untested outer drum (identified as S-1A) with new Celotex (identified as S-1A). Then the drum lid and lid locking ring were installed. Each of the locking ring bolts was torqued to 30 inch-pounds. One-inch-diameter disks of vinyl-covered adhesive tape were placed over each of the four vent holes in the outer drum.

Test unit weight was measured at 83 pounds. Because the unit was buoyant, a weight was attached to the bottom of the package to keep it submerged in the chamber (Figure 6-1).

6.2 Test Set-Up

The hydrostatic test chamber is shown in Figure 6-2. Internal dimensions of the chamber are 18 inches in diameter by 36 inches deep. It is rated for 400 psi water, 125 psi air. The test unit was placed into the chamber and the chamber filled with water. After the chamber lid was installed, a calibrated pressure transducer was installed through the lid. Pressure to the chamber was provided by a continuous supply of pressurized air, regulated at the specified pressure. This system would maintain the required pressure if water leaked into the package. Pressure data were

Figure 6-1. Test Unit with Weight Attached

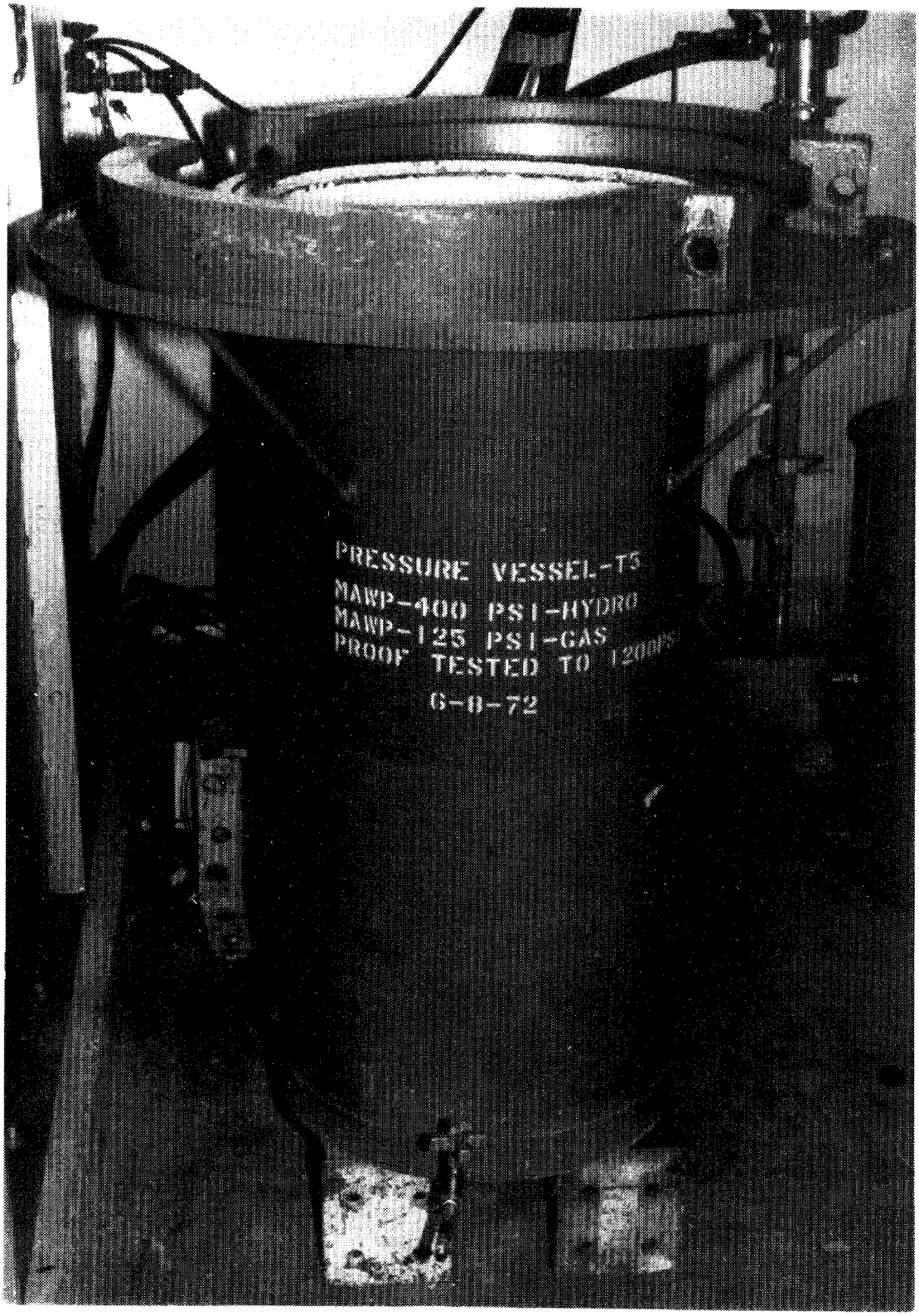

Figure 6-2. Hydrostatic Test Chamber

monitored using a calibrated strain indicator and recorded using a strip chart recording system.

6.3 Overpressure Test

Bubbles were observed streaming from the unit near the 0° side as the chamber was filled. (A vent hole was located at approximately 5°.) The chamber lid was installed and sealed.

The chamber was pressurized to 21.10 psig and held for a period of 8 hours and 5 minutes. Pressure varied between 21.05 and 21.20 psig during the test. At the conclusion of the test, pressure was released and the chamber opened.

6.4 Posttest Observations

An obvious drop in the water level was noted after the test. This change of approximately 5 inches represented an inleakage to the unit of 5.5 gallons. Bubbles were observed streaming from the unit's 0° side, and an intermittent flow of bubbles was noted near the 90° side. The unit was then removed from the chamber and positioned vertically on a table.

The vent hole near 0° was covered by the locking ring lug; tape over this vent may have been damaged during ring installation, causing the bubbles observed immediately after immersion. Tape over the vent near 90° was partially detached.

No deformations were visible on the exterior of the drum. An internal pressure was evident from a release of air and bubbles from the vent at 0°.

After the weight was removed from the drum bottom, the unit was weighed. A posttest weight of 137.5 pounds represented a net increase of 54.5 pounds.

6.5 Disassembly

Complete disassembly was performed after the overpressure test. Posttest torque on the locking ring bolts was measured at ~25 foot-pounds, a 5 foot-pound decrease from the assembly torque. The locking ring and lid were easily removed. The top surface of the Celotex was damp to the touch. The lid section of Celotex was slightly snug in the drum because of swelling but was removed intact.

Water (~1/8 inch) was observed in the depression of the inner container lid. The inner container assembly was removed easily. Approximately 1/4 inch of water was apparent in the cavity of the body section of Celotex, which was also swollen slightly but removable. All Celotex had a spongy feel and the layers of each section appeared to be held together by only the coating of paint on the exterior.

After visual inspection and leak-testing of the inner container, the inner container was disassembled. Posttest torque on the V-clamp bolt measured at 95 inch-pounds, a decrease of 5 inch-pounds from the torque applied at assembly.

6.6 Results--Nondestructive Examination

6.6.1 Leak Test

A posttest leak test of the inner container seal showed no detectable leak above the existing background of the leak-test cavity (1.0×10^{-9} atm cm^3/sec).

6.6.2 Inspection

A posttest dimensional inspection was performed on the inner container body and lid. No dimensional changes within the accuracy of the inspection process were detected for the inner container lid. The only apparent change to the inner container body was a slight change to the angular measurement of the flange. An increase of approximately 0.15° was noted near 180°. This change may have been caused by loads induced during assembly of the V-clamp, rather than by the test itself. The V-clamp was oriented to close at the 180° side. Complete inspection data and a discussion of accuracy are contained in Appendix B.

7.0 NORMAL CONDITIONS OF TRANSPORT TESTS

Two tests were performed on the structural test unit to evaluate the package under normal conditions of transport. These tests consisted of a water spray and a 4-foot free fall drop test, performed in series, as defined in 10 CFR 71.71[1]. Both tests were conducted following the HS/RTG Normal Conditions Test Procedure.[4]

The first test was a water spray test, subjecting the test unit to a simulated rainfall of a minimum of 2 inches of rain per hour for a period of at least 1 hour. The second test was a 4-foot free fall drop test of the unit onto a flat, essentially unyielding target. The drop test was required to be performed between 1.5 and 2.5 hours after the conclusion of the water spray test.

7.1 Test Unit Preparation

Posttest inspection from the overpressure test served as the pretest inspection for the normal conditions tests. The payload assembly and inner container were assembled and the V-clamp bolt tightened to 100 inch-pounds.

Helium leak-testing was conducted on the inner container seal. There was no detectable leak within the sensitivity of the leak detector, i.e., $<2 \times 10^{-10}$ atm cm^3/sec. Appendix A contains a detailed description of the leak-testing.

The inner container assembly was installed in the outer drum used for the overpressure test (S-1A), with new Celotex (S-1B). The drum lid and lid locking ring were then installed. Locking ring bolts were torqued to 120 inch-pounds each. One-inch-diameter disks of vinyl-covered adhesive tape were placed over each of the four vent holes in the outer drum.

The assembled test unit weighed 82 pounds.

7.2 Test Set-Up--Water Spray Test

Figure 7-1 illustrates the water spray test configuration. This configuration conformed to International Atomic Energy Agency (IAEA) advisory material for water delivery[12] and maximum wetting of the package. The test unit was suspended horizontally from a crane hook with a swivel feature that permitted rotation of the package. The spray nozzle was adjusted to deliver even coverage in a 30-inch-diameter pattern at a distance of 10.5 feet. This pattern was sufficient to envelop the entire test unit. Water consumption was measured at 3 gallons per minute. This consumption equated to

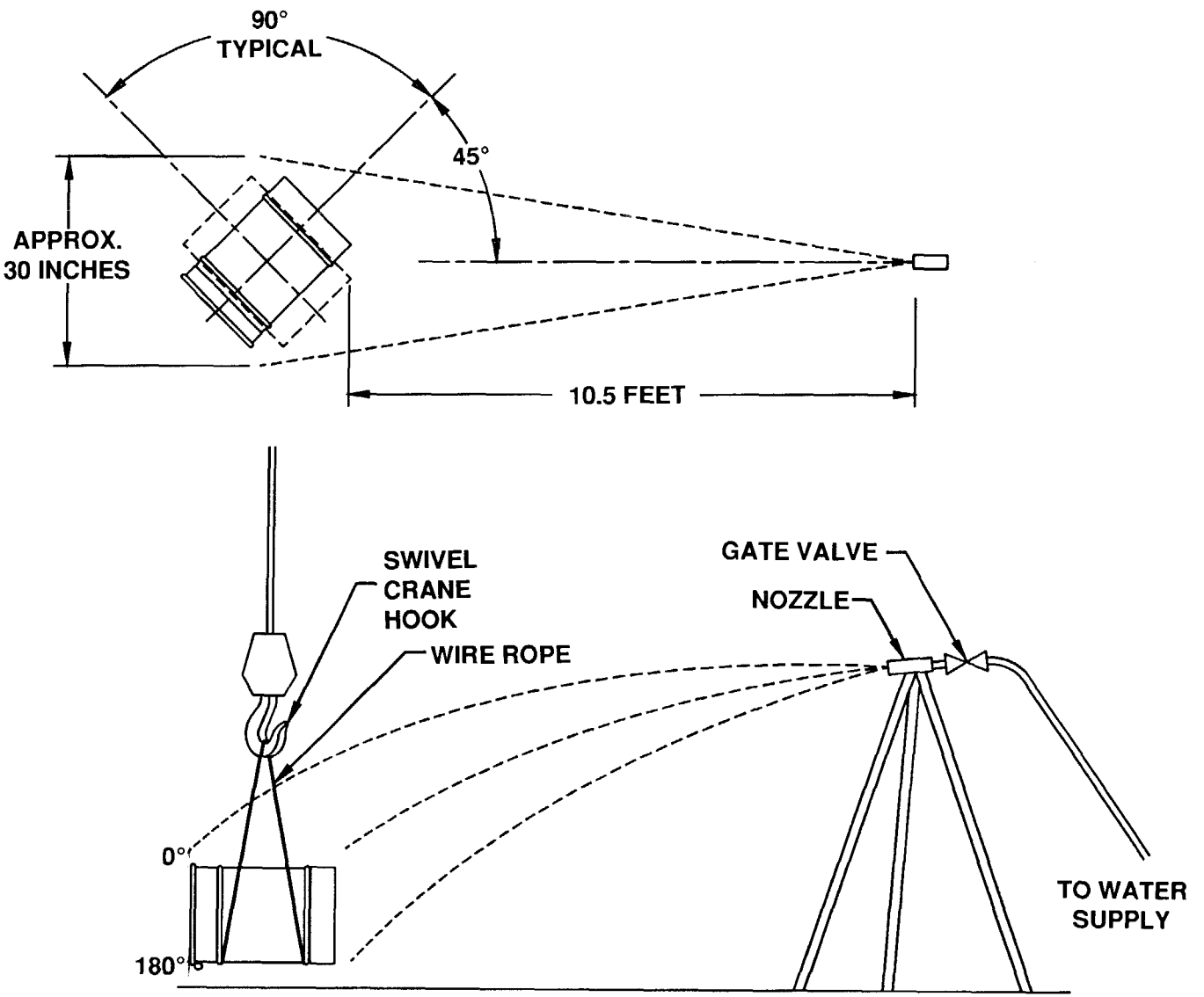

Figure 7-1. Water Spray Test Configuration

a delivery of 58 inches per hour in the area of the spray at the 10-foot distance. This was far in excess of the required 2 inches per hour, but necessary in order to meet the 10-foot distance recommendation.

7.3 Water Spray Test

A water spray nozzle was directed at the test unit with nozzle adjustments made during test set-up (Figure 7-2). The water was turned on, and start time recorded. During this test, ambient air temperature was 40°F with winds of 1 to 2 mph. After 15 minutes of spray, the test unit was rotated 90° clockwise, continuing the water spray. Two more 90°-clockwise rotations were made at 15- to 17-minute intervals. After spraying 15 minutes at the fourth position, the water was stopped. Total test time was 1 hour, 2 minutes, with each position being sprayed for a minimum of 15 minutes. The unit was then removed from the crane and immediately transported to the drop test facility.

7.4 Test Set-Up--4-Foot Drop Test

For this test, the unit was mounted in the cradle at an angle of 58° with respect to horizontal, with the 0° side facing down. This aligned the center of gravity of the unit over the lid locking ring and the bolt lug (Figure 7-3). The cradle and test unit were raised so that the lowest point of the unit, the edge of the bolt lug, was 48-1/16 inches above the target surface.

7.5 4-Foot Drop Test

The 4-foot drop test is shown in Figure 7-4. The test unit impacted at a velocity of 16.0 feet per second and an angle of 53°. Photographs A and B show the unit at decreasing heights above the target. Photograph D shows the unit just after impact. The unit rebounded and rotated toward the lid (Photographs E and F) but remained on the target, coming to rest on its lid. Environmental conditions at test time were 44°F with winds of approximately 3 mph.

7.6 Exterior Deformations

Damage to the outer drum is shown in Figures 7-5 and 7-6. The outer drum deformed in the area of impact, shortening the drum corner approximately 0.3 inch. All damage was limited to the side of the drum in the area of impact. Collapsing of the rolled ring resulted in the 0.25-inch height decrease. This area was also deformed by the bolt lug which rotated into the side of the drum during impact. Two small cuts were observed in the side of the drum under the inner corners of the bolt lug where deformation was sufficient to tear the sheet metal.

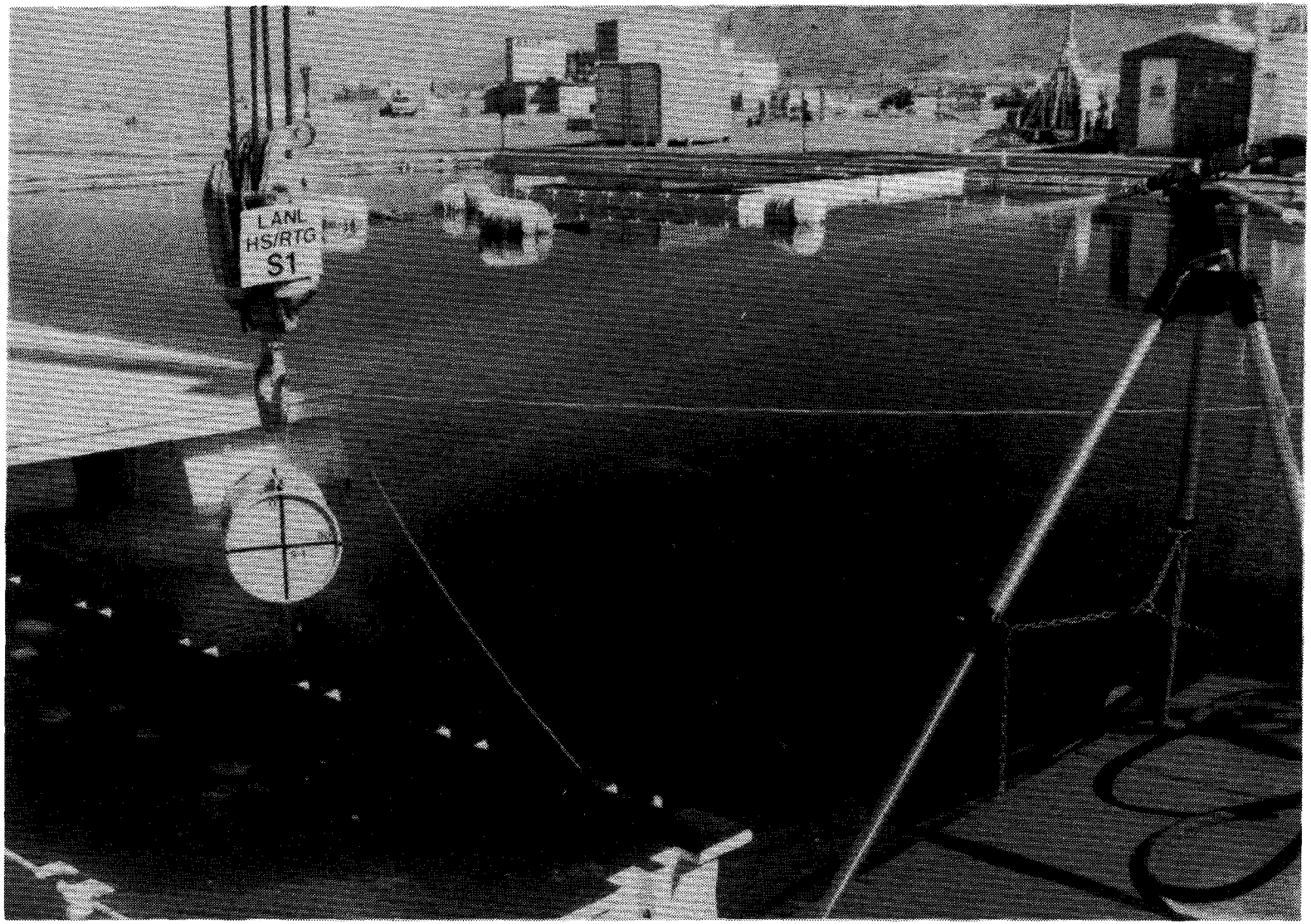

Figure 7-2. Water Spray Test

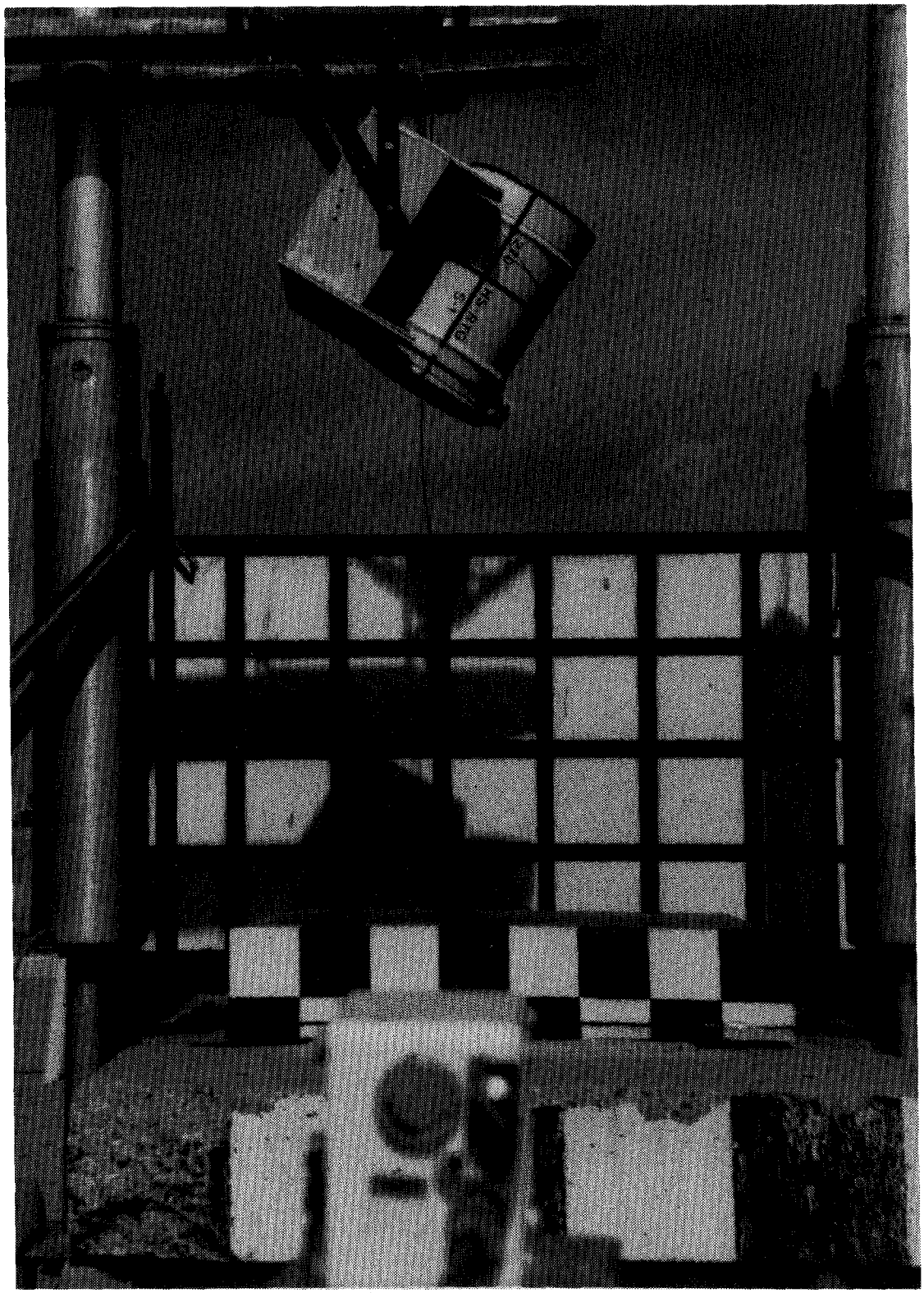

Figure 7-3. Test Unit in Cradle

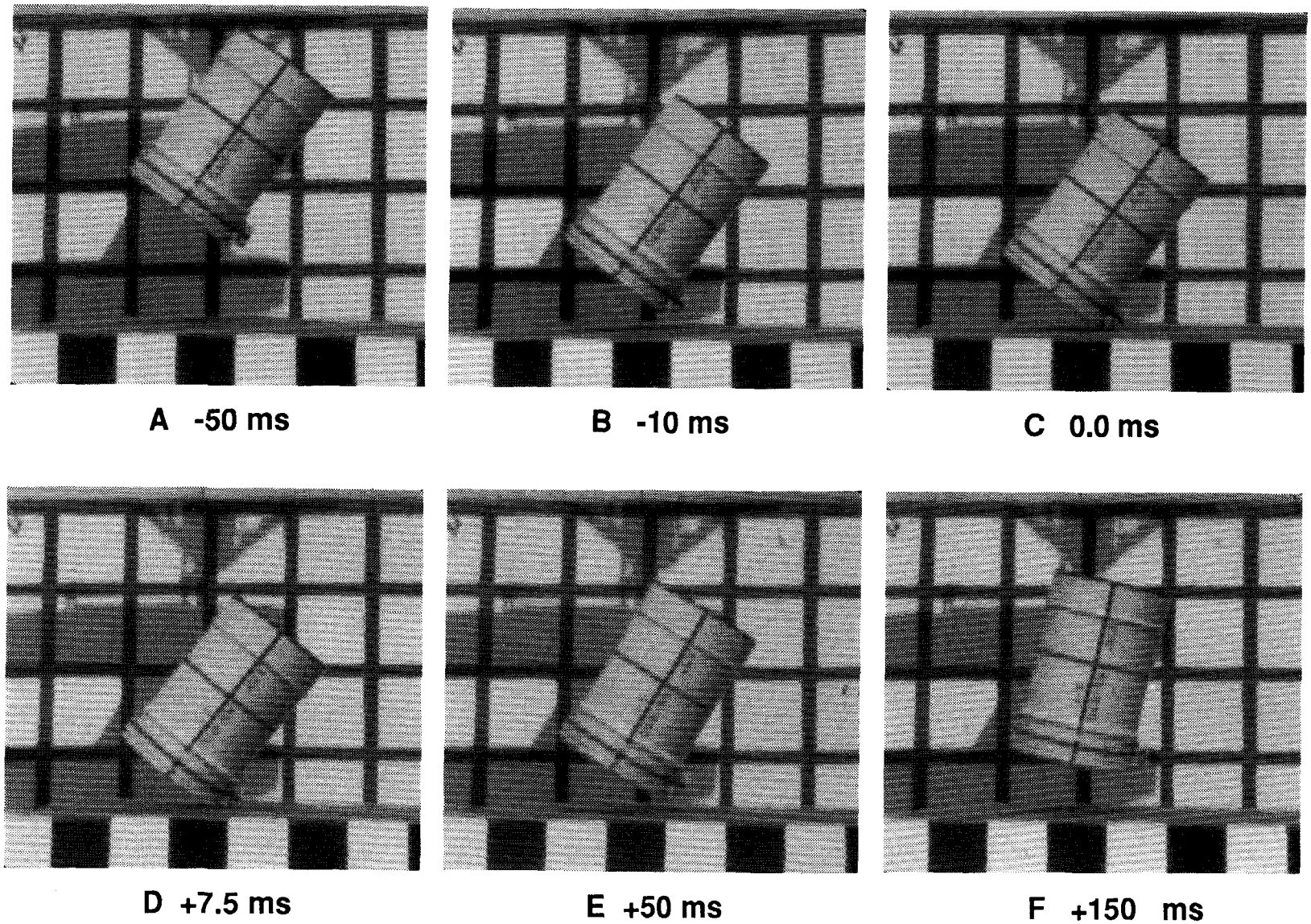

Figure 7-4. Test Sequence

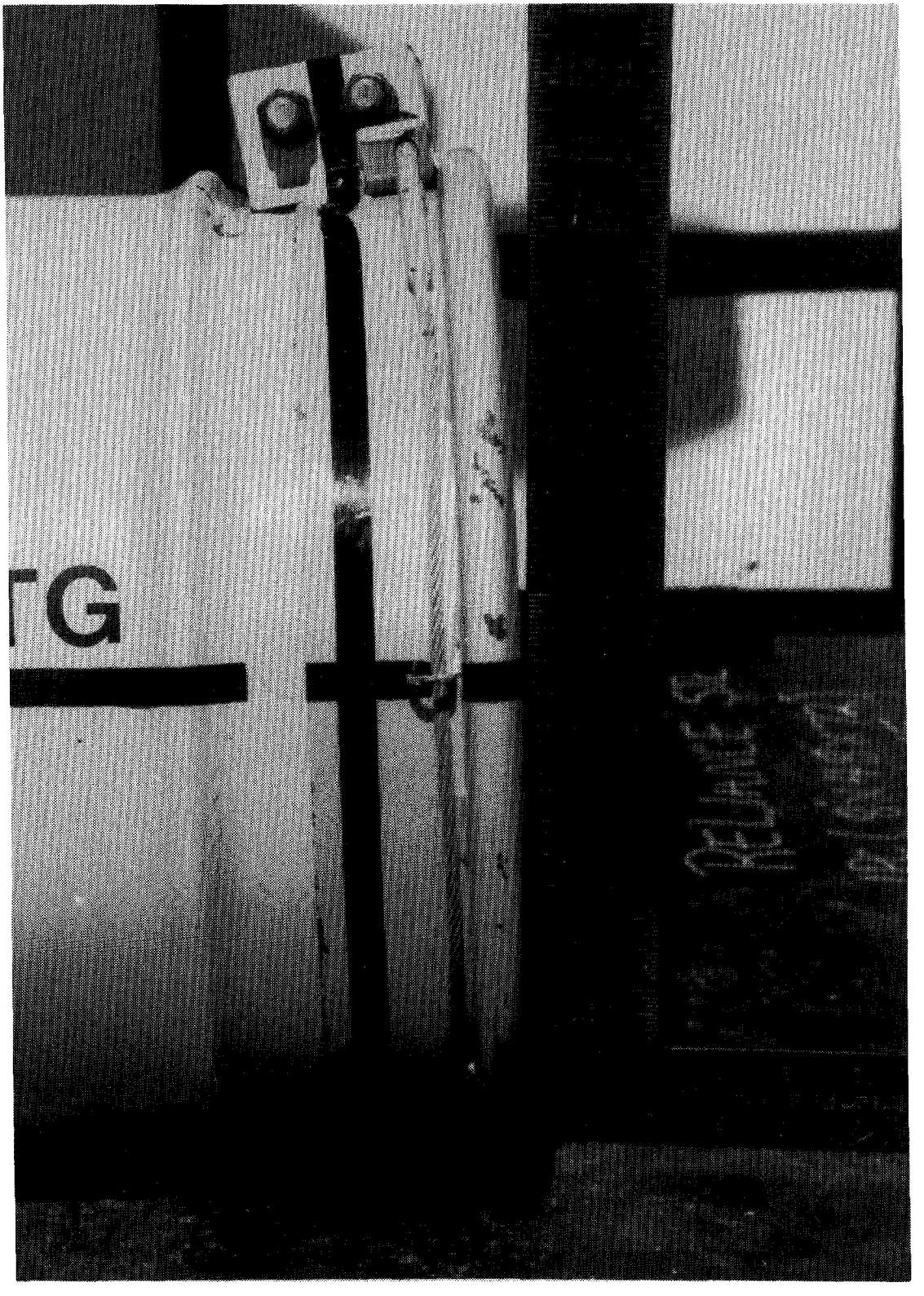

Figure 7-5. Drum and Locking Ring Deformations

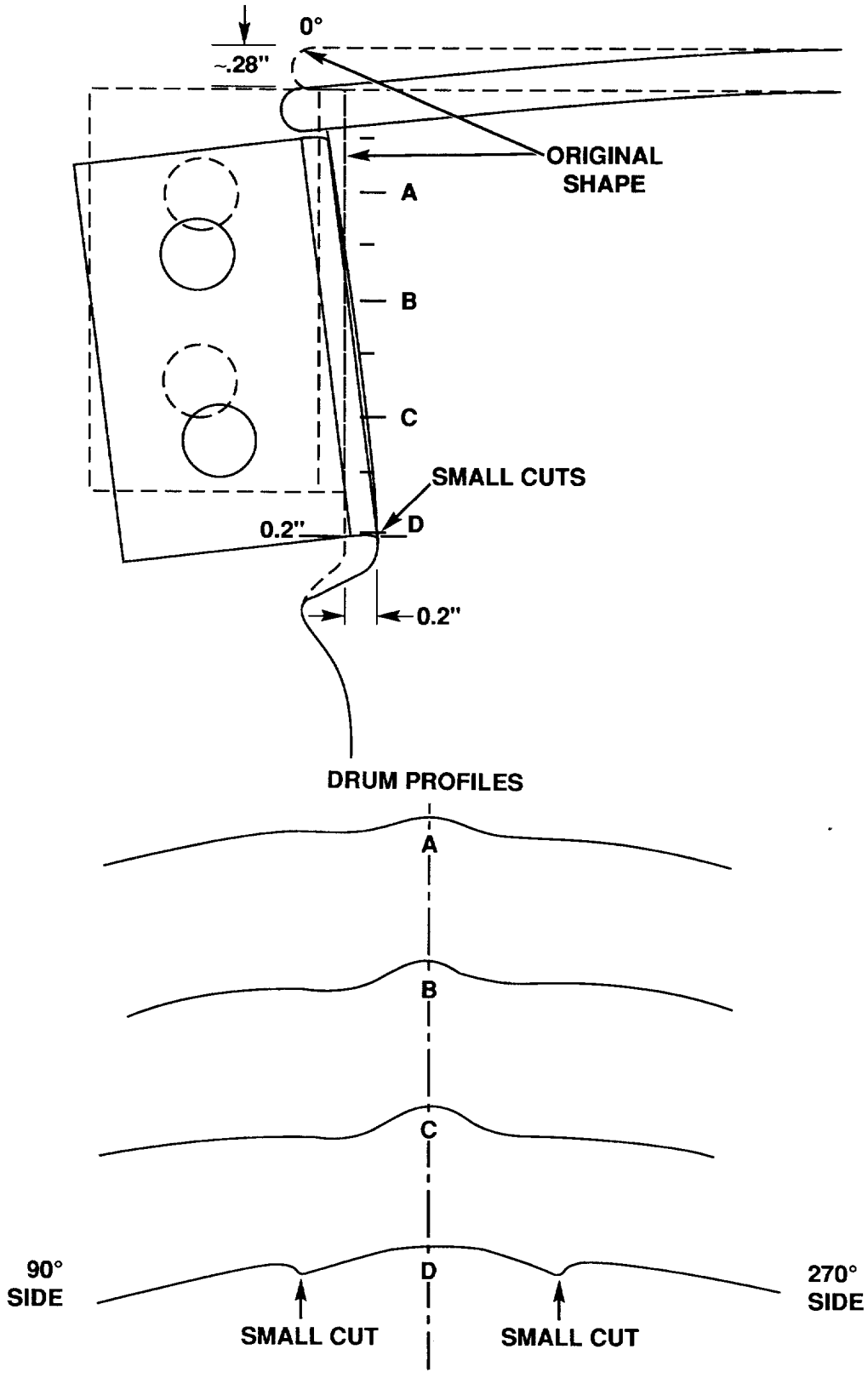

Figure 7-6. Deformation Sketch

These cuts were of concern because they formed vents that might be detrimental in a fire. It was assumed that the cuts would be significantly larger as a result of a 30-foot drop test performed in the same orientation. LANL personnel then evaluated and redesigned the locking ring before conducting subsequent tests. This evaluation also concluded that the change in locking ring configuration would have no negative effects on either the overpressure or water spray tests since these tests placed no structural demands on the ring. Thus no retesting of a unit for these two tests was necessary. (Performance of the new ring in a 4-foot normal condition drop test was later verified on a separate, certification test unit.[18])

The new design was a standard military-specification locking ring modified with machined bolt lugs (Figure 7-7). The designers also determined that the steel reinforcement ring on the bottom of the outer drum was unnecessary, and removed it. Weight decreased approximately 11 pounds as a result of these changes, making subsequent packages weigh an average of 70 pounds.

7.7 Disassembly

Before disassembly the test unit was weighed. A posttest weight of 82 pounds indicated no measurable change from pretest weight. A complete disassembly was performed after the normal conditions test series. Posttest torques on the locking ring bolts were measured to be 15 inch-pounds for the upper bolt and 20 inch-pounds for the lower bolt (assembly torques were 120 inch-pounds). The locking ring and drum lid were easily removed, and bolt lugs and welds on the locking ring were intact. The lid section of Celotex was tight in the drum because of inward deformations, but was removed intact. There was no indication of water inleakage; all Celotex was dry to the touch.

The inner container assembly was removed easily. The body section of Celotex was retained in the drum by the indentation at the 0° side.

After visual inspection and leak-testing of the inner container seal, the inner container was disassembled. Posttest torque on the V-clamp bolt was measured at 90 inch-pounds, a decrease of 10 inch-pounds from the assembly torque.

Upon removal of the inner container lid, the payload was noted to have rotated 22° clockwise in the container. Posttest torques on the RTG mounting bolts were as follows:

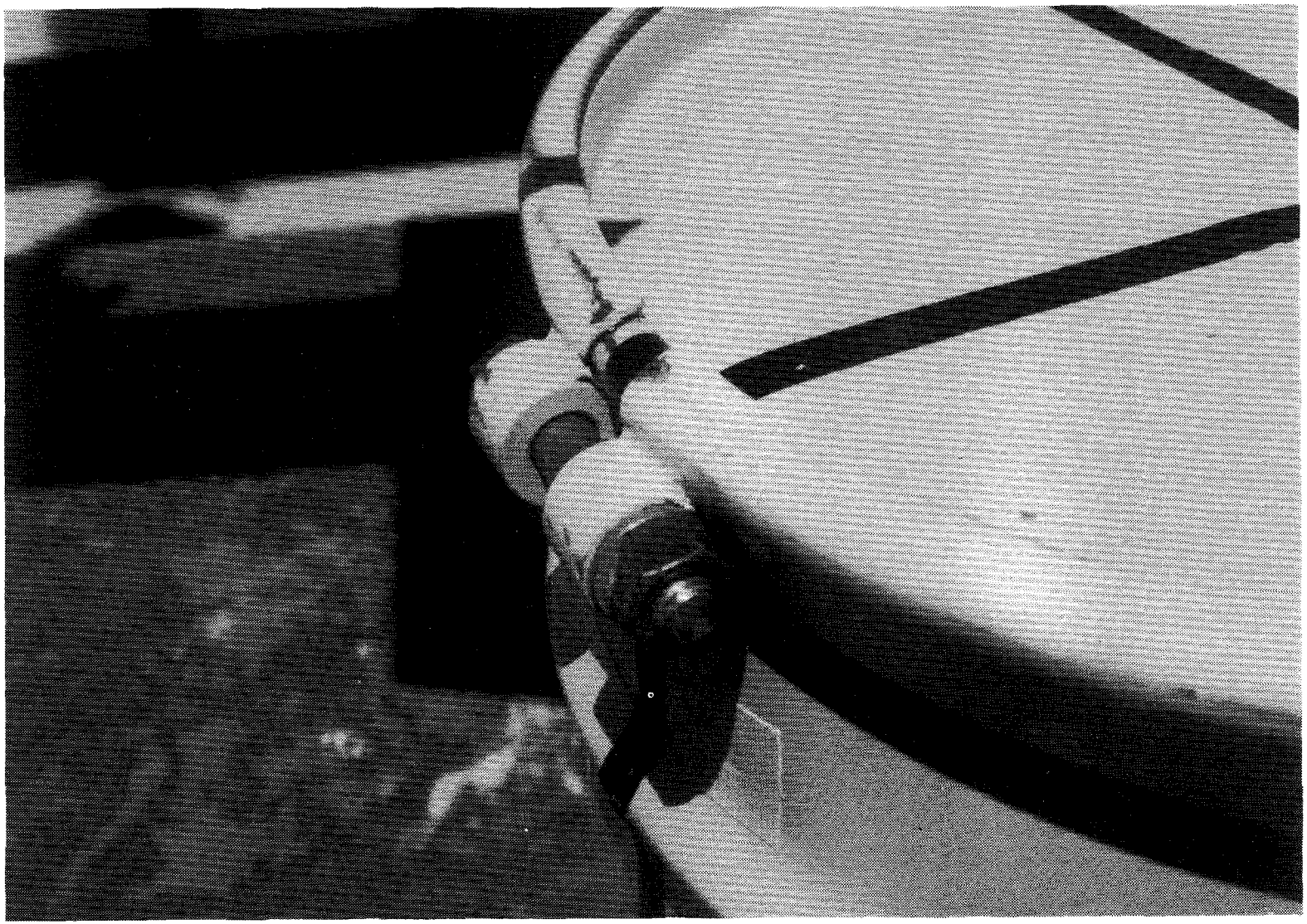

Figure 7-7. Redesigned Lid Locking Ring

Bolt	Location	Approximate Net Change in Torque (inch-pounds)
B1	0° upper RTG	0
B2	180° upper RTG	0
B5	0° lower RTG	-5
B6	180° lower RTG	0

7.8 Results--Nondestructive Examination

7.8.1 Leak Test

A posttest leak test of the inner container seal showed no detectable leak above the existing background of the leak test cavity (6.4×10^{-9} atm cm^3/sec). Appendix A contains a discussion on leak-test cavity background.

7.8.2 Inspection

A posttest dimensional inspection was performed on the inner container body and lid. No dimensional changes were detected within the accuracy of the inspection process for the inner container lid. The only apparent change to the inner container body was a slight difference in angular measurement of the flange. A decrease of 0.38° was noted near 180°. This change was in the opposite direction of the movement noted for the overpressure test. As with the overpressure test, movement may have been caused by loads induced during assembly of the V-clamp, rather than by the test itself. Appendix B contains complete inspection data and a discussion of accuracy.

8.0 CENTER OF GRAVITY OVER CORNER DROP TEST

8.1 Test Unit Preparation

Before assembly, the test unit inner container body, lid, and V-clamp were instrumented with the transducers defined in Section 5. Bolts (both instrumented and standard) for the RTGs were installed and torqued to specified values. Preload in the instrumented bolts was measured at this time. The bolt on the V-clamp was also torqued and the preload measured.

Helium leak-testing on the lid seal showed a leakage rate of $<2 \times 10^{-10}$ atm cm^3/sec (minimum detector sensitivity).

The inner container assembly was installed in an undamaged outer drum (S-1B) with new Celotex (S-1C). The inner assembly was oriented such that the V-clamp bolt was at 180°, the intended impact location of the drum. The welded seam of the drum was oriented at the 180° impact side. Internal instrumentation wiring was routed through the lid section of Celotex and out the center of the drum lid (Figure 8-1).

The redesigned drum lid locking ring was installed with the bolt lug oriented at 180°. The instrumented locking ring bolt was torqued to 180 inch-pounds, and the preload strain was measured and recorded.

8.2 Test Set-Up

This test was performed following the HS/RTG CG Over Corner Drop Test Procedure.[5] The test unit was installed in the cradle at an angle of 57° with the 180° side facing down, aligning the center of gravity of the unit over the lid locking ring nearest the bolt lug (Figure 8-2). Figure 8-3 shows the cradle and sliding beam assembly, raised to the final drop height of 32 feet, 4-3/4 inches. The midpoint of the instrumentation wiring was tied to a forklift mast approximately 15 feet above the ground to remove some of the cable weight from the test unit and to reduce the chance of the cables being impacted by the unit during the test.

8.3 Drop Test Event

Figure 8-4 shows the drop test. The test unit impacted at a velocity of 44.9 feet per second and an angle of 59°. Photographs A and B show the unit at decreasing heights above the target. Photograph D shows the unit just after impact. At approximately 10 to 15 ms, the unit began to rotate counterclockwise towards the lid (Photograph E and F).

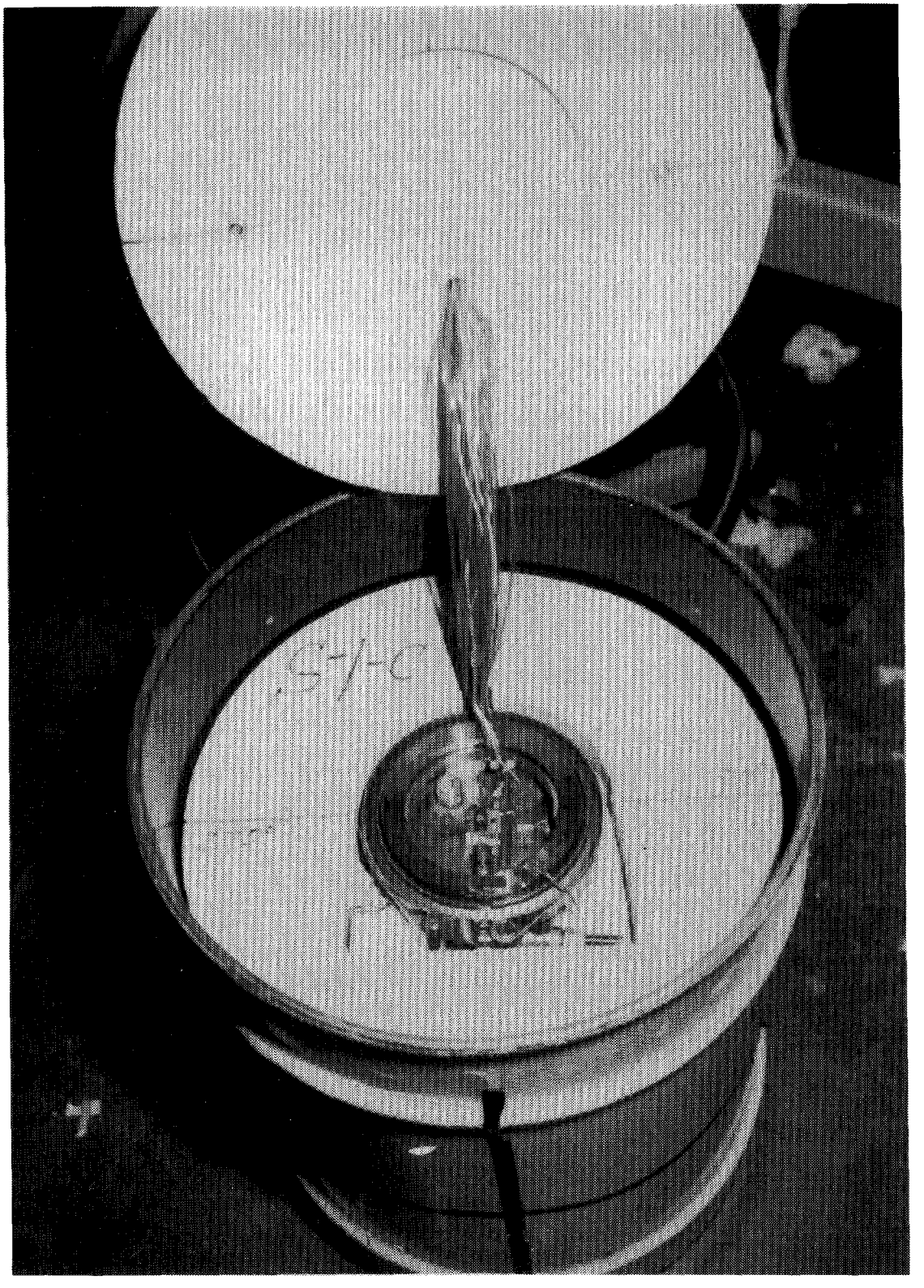

Figure 8-1. Test Unit Assembly

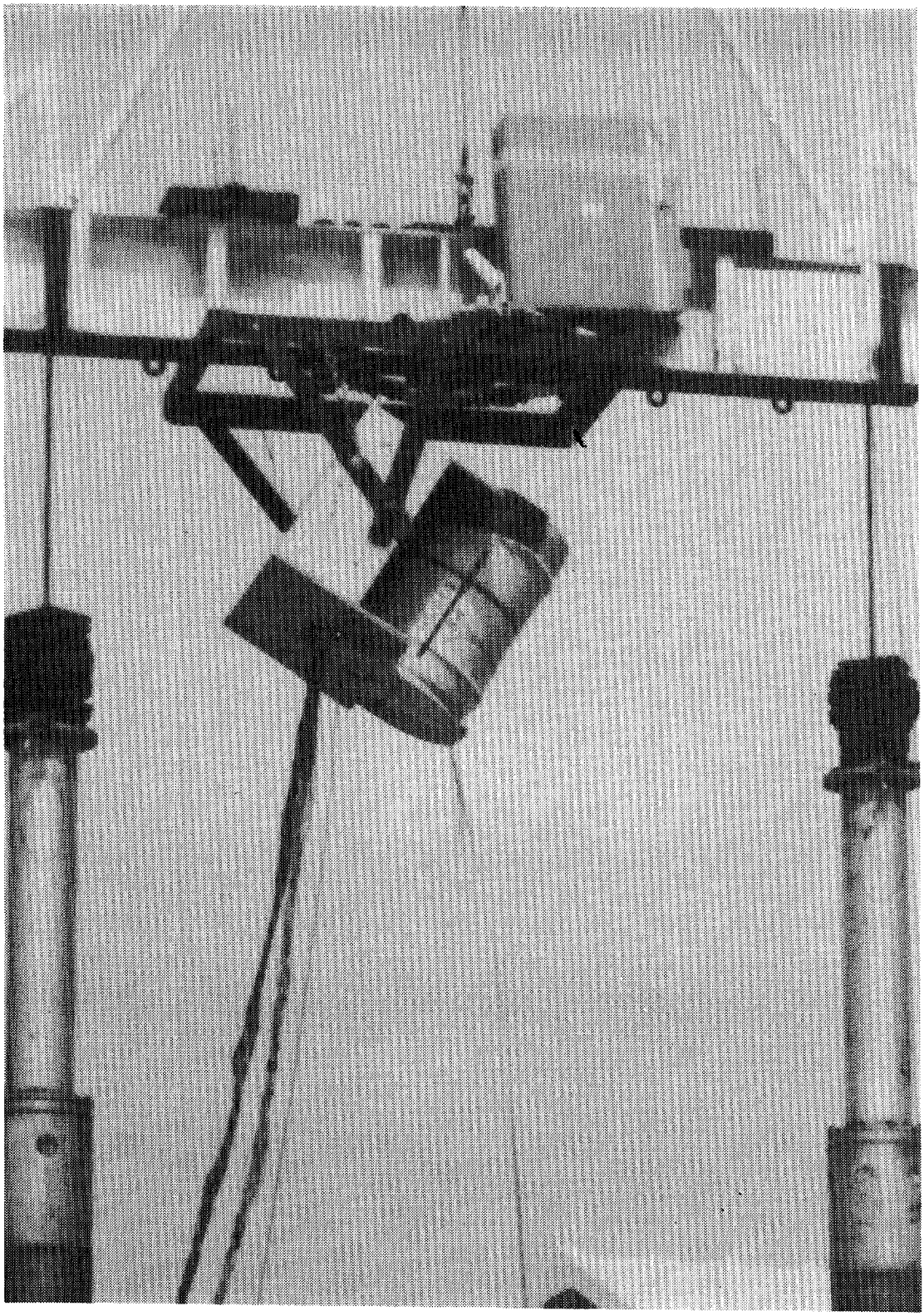

Figure 8-2. Test Unit in Cradle

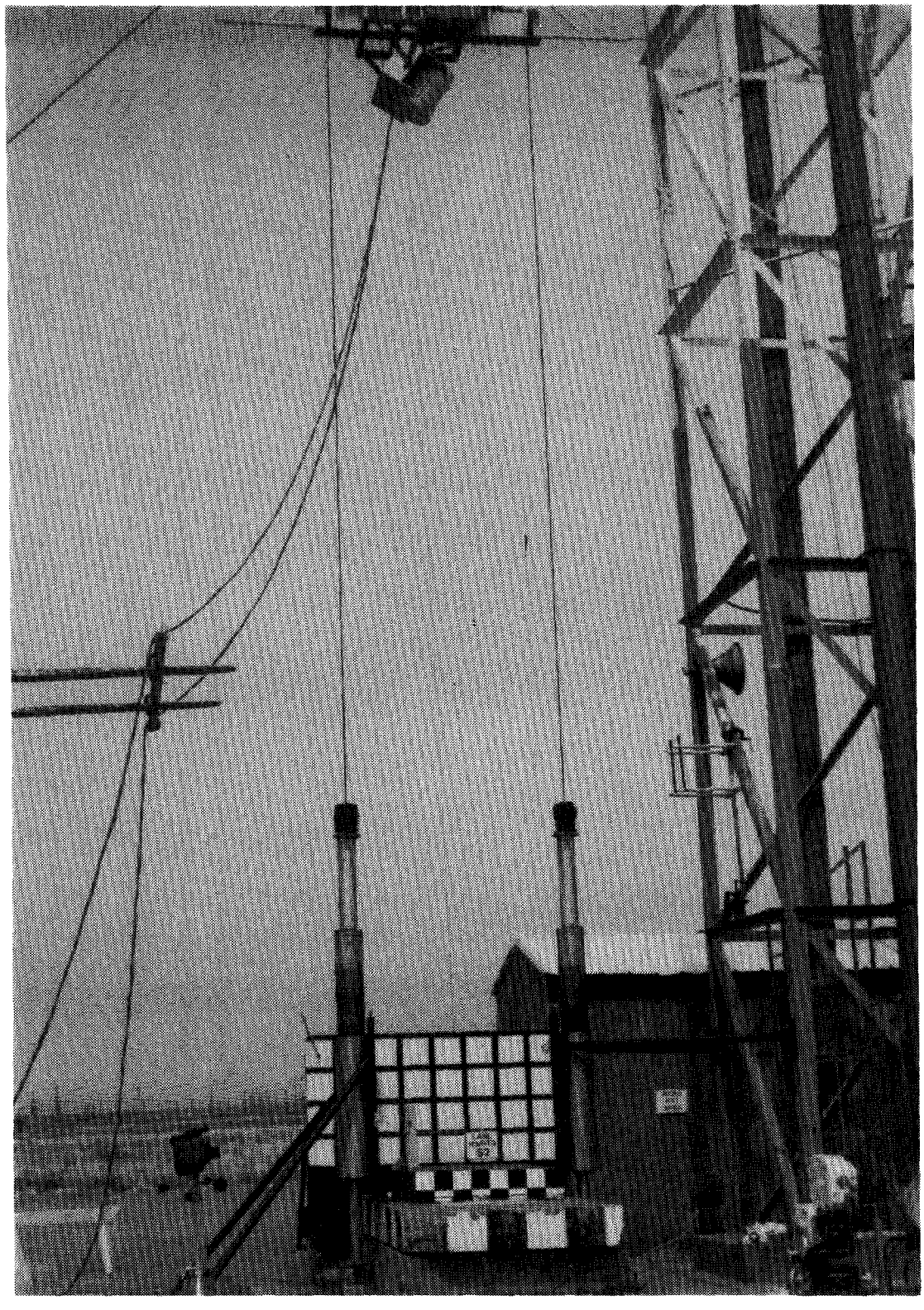

Figure 8-3. Test Set-Up

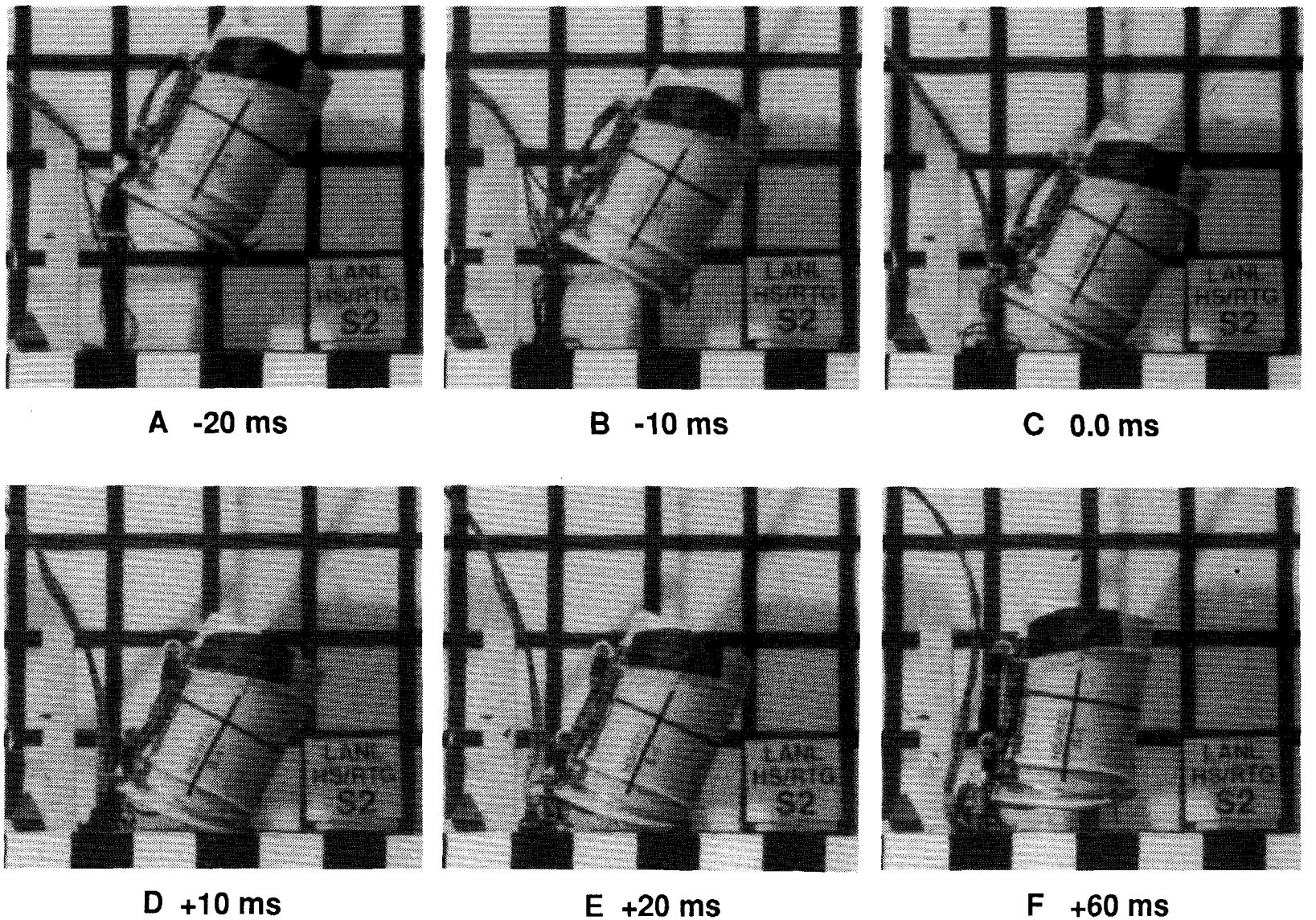

Figure 8-4. Test Sequence

Total impact duration was estimated to be 9 to 10 ms based on photometric and accelerometer data. The unit continued to rotate and fell off the raised target approximately 3.5 feet above the ground.

Package rotation after impact indicated that the center of gravity of the test unit was not accurately aligned over the impacting corner. Removing the reinforcement from the drum bottom shifted the center of gravity. This shift changed the angle required to properly align the CG over the impact corner, and was not reflected in the test set-up.

8.4 Exterior Deformations

Damage to the outer drum is shown in Figures 8-5 and 8-6. The deformed area is limited to the impact area extending to the upper (closest) rolled ring of the drum body, with a footprint approximately 11 inches wide. Maximum crush of the drum is estimated to be 2.5 inches at the clamp ring.

8.5 Disassembly

A complete disassembly was performed after the CG over corner test. Posttest torque on the locking ring bolts was measured at ~10 inch-pounds, a decrease from the 180 inch-pound assembly torque. Bolt preloads were not measured because of a wiring problem. The locking ring deformed with the drum but was easily removed. Bolt lugs and welds on the locking ring were intact. Deformations in the drum body consisted of dents in the side of the drum under the bolt lugs. No holes, cuts, or cracks were found under the ring or bolt lug; however, there was a small gap at exactly 180° between the ends of the locking ring where the lid had bent away from the lip of the drum. The interface between the lid and drum in the rest of the impact area was improved/enhanced; the edge of the lid was rolled around the drum lip. The lid was removed by lifting the 0° side and rotating off.

The lid section of Celotex was wedged tightly in place because of the inward deformations of the drum. This section was removed by cutting the section into two pieces and removing the piece in the undamaged area first (Figure 8-7). The inner container assembly was then removed easily. Drum deformations also held the body section of Celotex in place; no attempt was made to remove that section.

After visual inspection and leak-testing of the inner container seal, the inner container was disassembled. Posttest torque and preload of the V-clamp bolt were measured. Preload was 462 $\mu\varepsilon$, a decrease of 316 $\mu\varepsilon$ from the strain measured at assembly. The torque was 85 inch-pounds, a decrease of 15 inch-pounds from the 100 inch-pounds assembly torque. The V-clamp and lid were then removed.

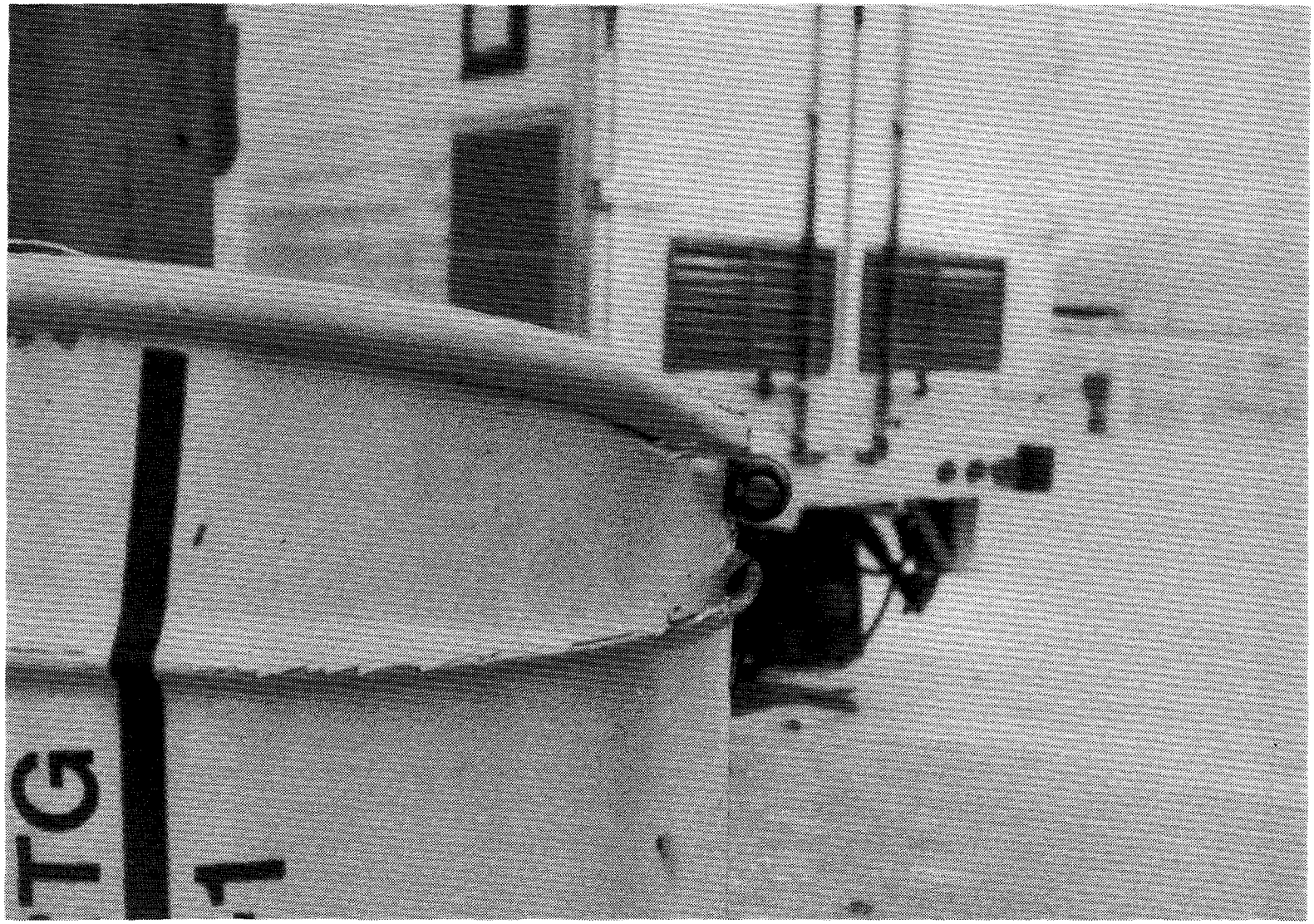

Figure 8-5. Outer Drum Deformations

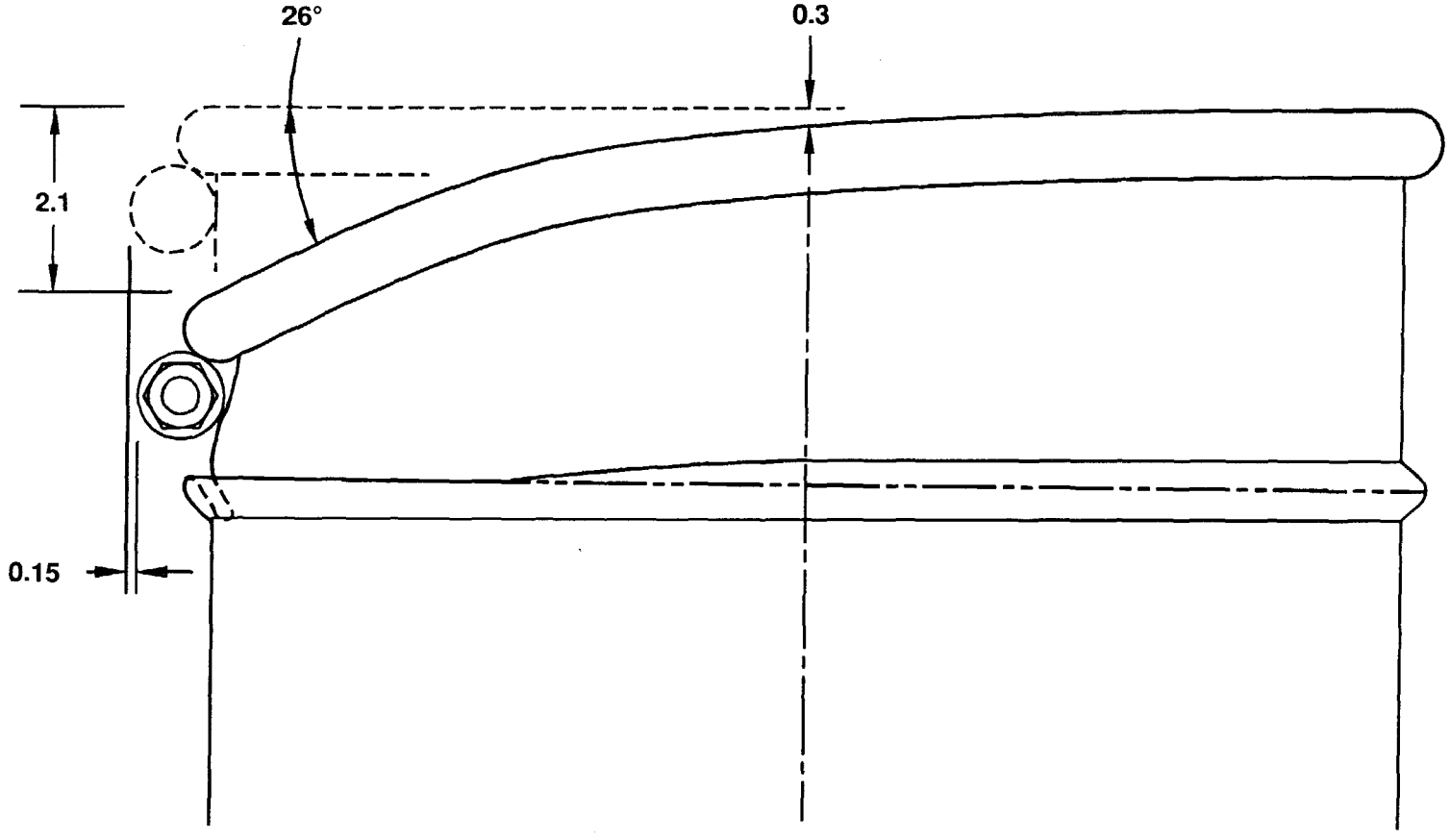

Figure 8-6. Drum Deformation Sketch

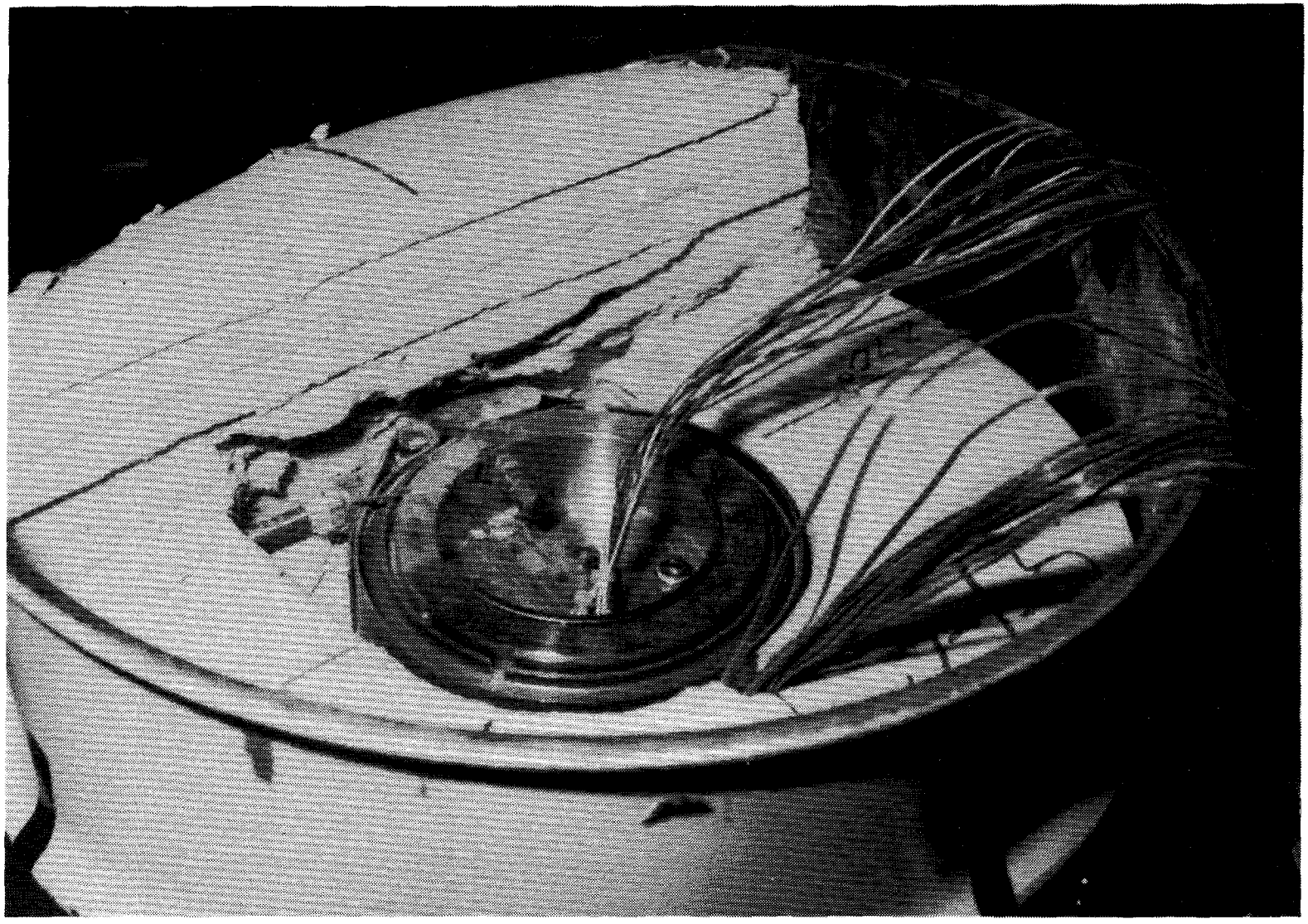

Figure 8-7. Removal of Lid Section Celotex

The payload assembly had rotated ~2° clockwise in the container. Tightness of the bolts securing the RTGs was checked as was the preload for the instrumented RTG bolts. Results are as follows:

Bolt	Location	Approximate Net Change in Torque (inch-pounds)	Approximate Net Change in Preload ($\mu\varepsilon$)
SB1	0° upper RTG	0	-106
SB2	180° upper RTG	-2	-12
B5	0° lower RTG	-5	NA
B6	180° lower RTG	-5	NA

8.6 Results--Nondestructive Examination

8.6.1 Leak Test

A posttest leak test of the inner container seal showed no detectable leak within the sensitivity of the leak detector ($<2 \times 10^{-10}$ atm cm^3/sec).

8.6.2 Inspection

No mechanical inspections of inner container components were performed at the conclusion of the CG over corner drop test. A visual inspection was made of the inner container components with no observable deformations noted.

The Celotex insulation was measured for deformations (Figure 8-8). As expected, the major deformation was a compression of the lid section in the immediate impact area. This movement translated into some compression of the body section of Celotex on the 180° side. Because the Celotex was quite rigid, the lid section rotated to fill the clearance between the top of the Celotex and the drum lid. This caused a gap of approximately 0.15 inch between the lid and body sections of Celotex at the 0° side.

The inner container assembly also slightly deformed the internal cavity of the Celotex. An indentation from the lid and V-clamp in the lid section indicated movement of 0.05 inch in the Z direction. Movement in the Y direction was negligible. Figure 8-8 shows the decreases in Celotex thickness.

8.7 Results--Transducer Data

8.7.1 Accelerometer Data

Instrumentation for the CG over corner test included eight accelerometers as defined in Section 5.2, mounted in biaxial configurations at four locations: A2Y and A2Z on the

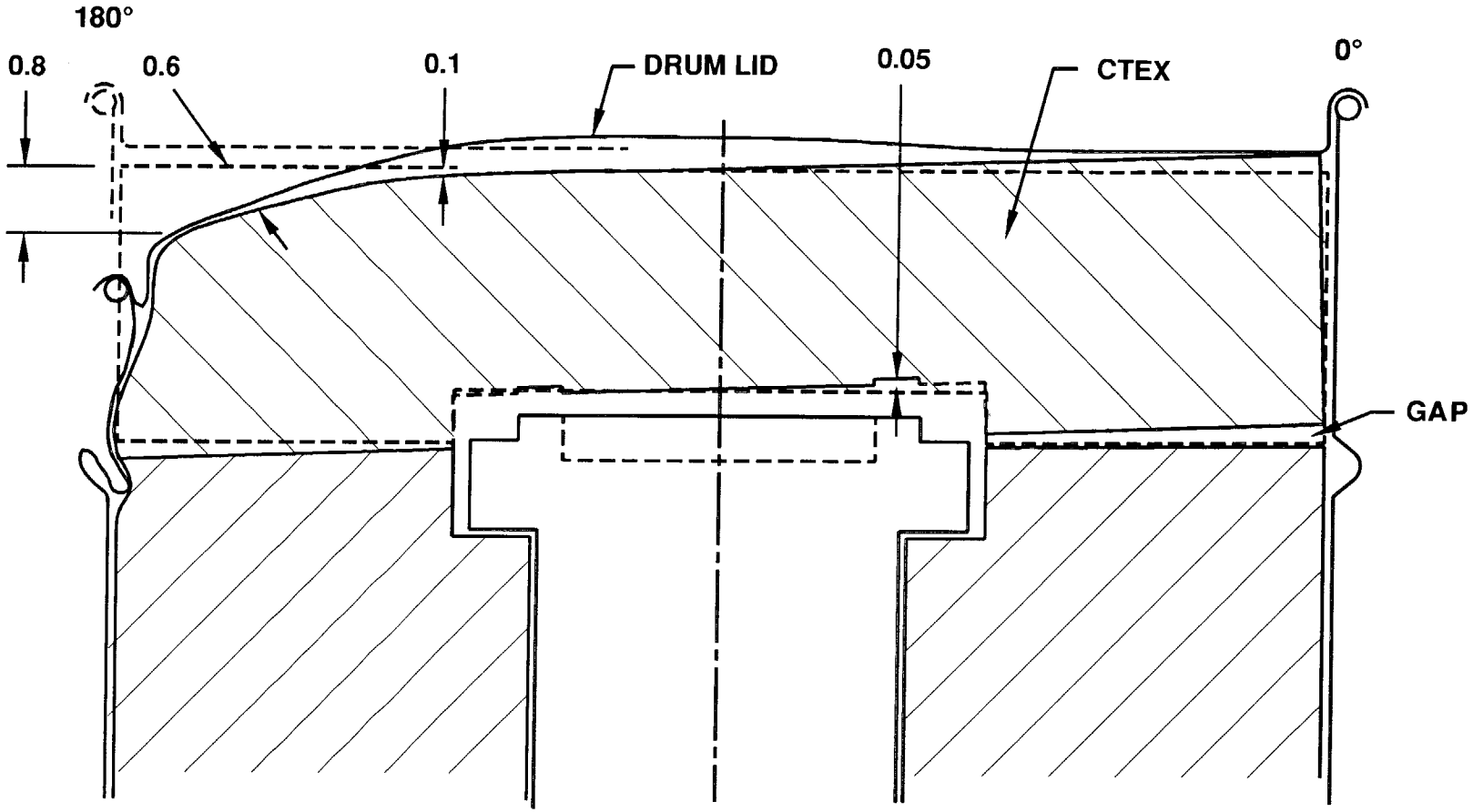

Figure 8-8. Celotex Deformations

exterior of the outer drum, A5Y and A5Z on the inner container body, A8Y and A8Z on the inner container lid, and A9Y and A9Z on the payload assembly. The values presented are based on data that has been filtered at 1,000 Hz. Figure 8-9 shows a layout of the accelerometers with the peak deceleration values labeled. Table 8-1 lists the designation, calibration value, measured peak value, and confidence level of each accelerometer. (The inverted signal of all Z accelerometers was a result of mounting orientation relative to drop orientation.)

Decelerations of the outer drum were measured by A2Y and A2Z mounted on the center of the 0° side of the drum. Plots of these data are shown in Figures 8-10 and 8-11. The Y rather than the Z accelerometer indicated the higher deceleration. This may be explained by the fact that the drum's major direction of crush was in the Z direction, cushioning the impact. This is verified by measured crush in each direction (Section 8.5.2) and by longer event times for the Z-direction accelerometers (as indicated by an integration of the pulses). Also, the unit began to rotate almost immediately after impact, adding to the deceleration of AY2.

Inner container decelerations were measured by A5Y and A5Z mounted on the 180° side of the body and by A8Y and A8Z mounted on the lid. The response of the inner container is shown in Figures 8-12 and 8-13. All pulses showed a time delay of approximately 1 ms from outer drum impact. Both Y and Z direction accelerometers had decreased peaks and averages compared to the transducers on the outer drum because of the cushioning effect of the Celotex mineral board. As with the outer drum accelerometers, the decelerations tended to be higher in the Y direction.

Response of the payload assembly was measured by accelerometers A9Y and A9Z. Data from these transducers are shown in Figures 8-14 and 8-15. These pulses showed a time delay of approximately 1.5 ms from outer drum impact. The pair followed the trend of the other accelerometers.

8.7.2 Strain Gage Data

Instrumentation for the CG over corner drop test included 28 strain gages as defined in Section 5.1. These gages measured surface strain on the exterior of the inner container body and lid on the 180°(impact), 90°, and 0° sides. Gages were also mounted on the V-clamp ring and bolt. Table 8-2 lists the gage designation, measured peak strain, strain offset, and confidence level of each measurement. All data presented has been filtered at 1,000 Hz.

In general, measured strains were low (below 100 $\mu\varepsilon$), with a few notable exceptions. Gages S1, S2, and S3 on the lid indicated strains of 165 to 290 $\mu\varepsilon$ (Figure 8-16). Peak strains on these channels occurred much later after initial

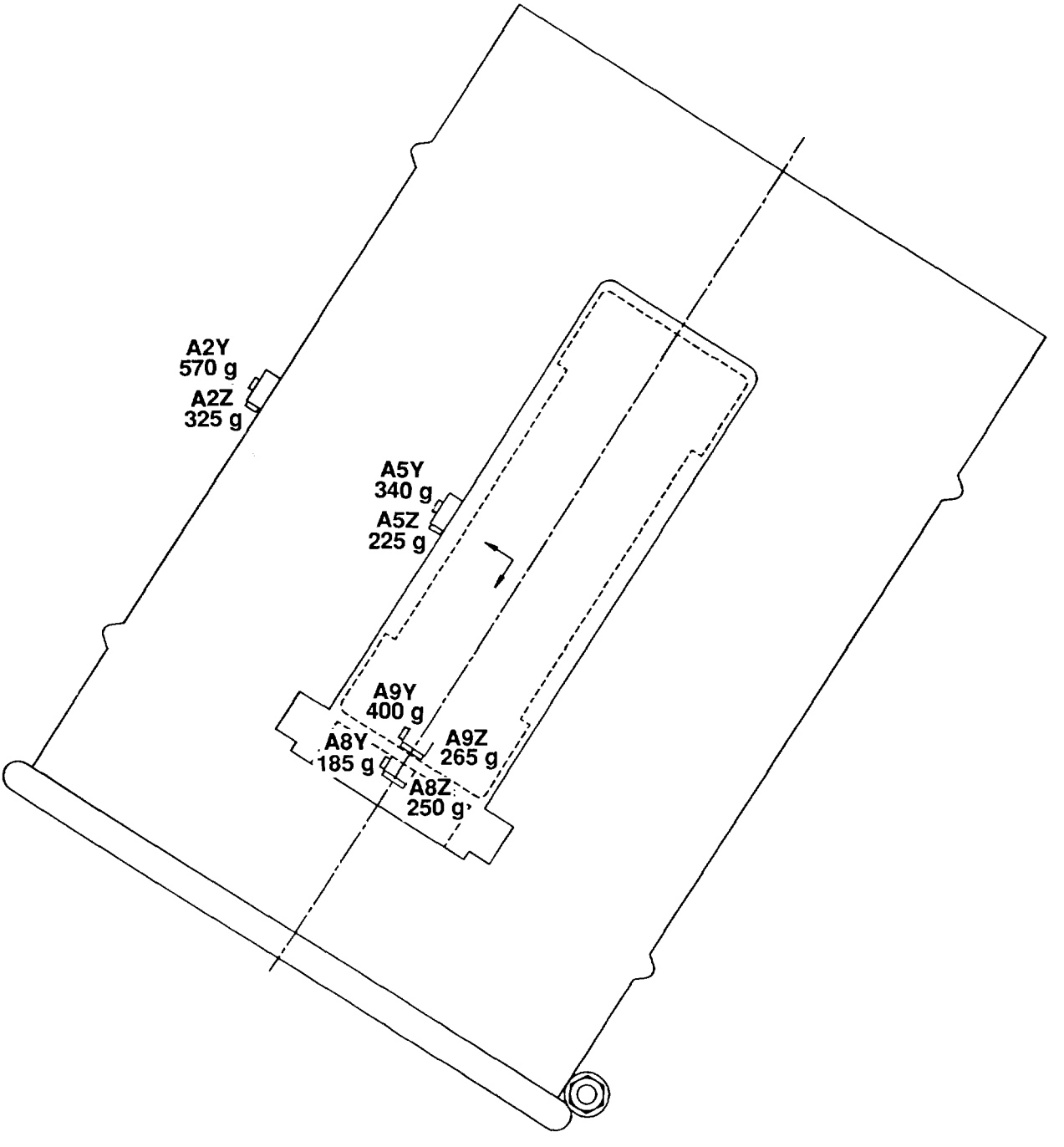

Figure 8-9. Peak Accelerations--CG Over Corner Drop Test

TABLE 8-1

Accelerometer Data--CG Over Corner Drop Test

Component	Accelero-meter Designation	Cali-bration Value (g)	Peak Accele-ration (g)	Confidence Level
Outer Drum	A2Y	8,000	570	High
	A2Z	8,000	-325	High
Inner Container	A5Y	8,000	340	High
	A5Z	8,000	-255	High
Inner Lid	A8Y	8,000	185	High
	A8Y	8,000	-250	High
Payload	A9Y	8,000	400	Good
	A9Y	8,000	-265	High

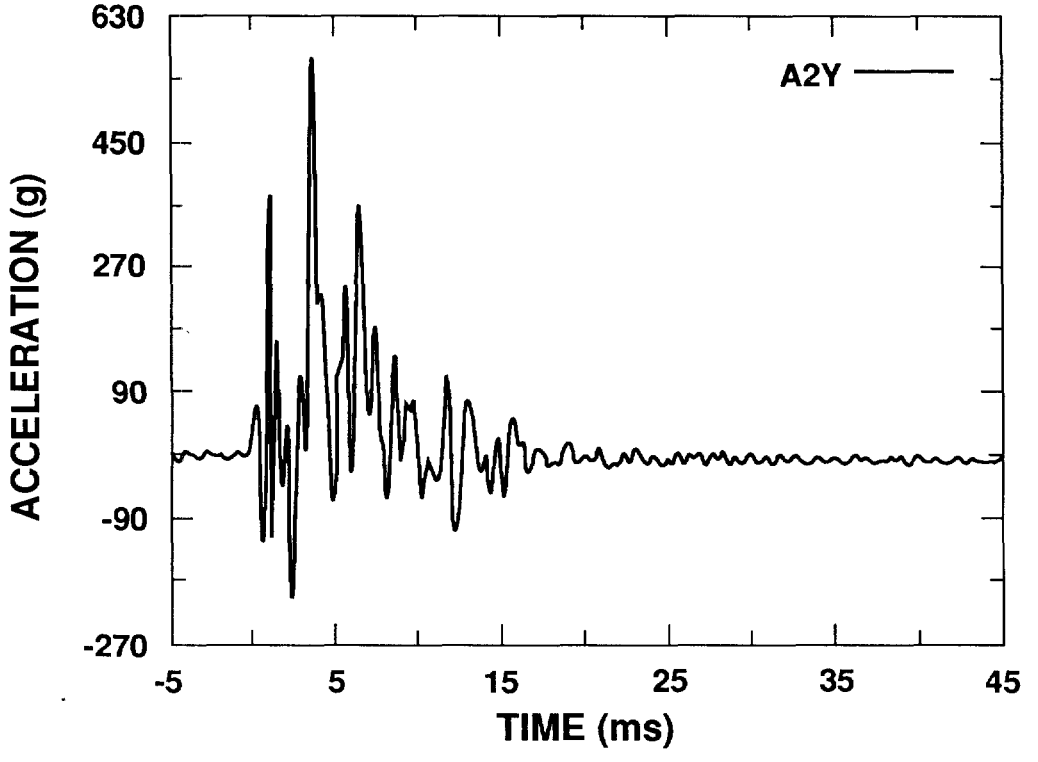

Figure 8-10. Plot of Data from Accelerometer A2Y

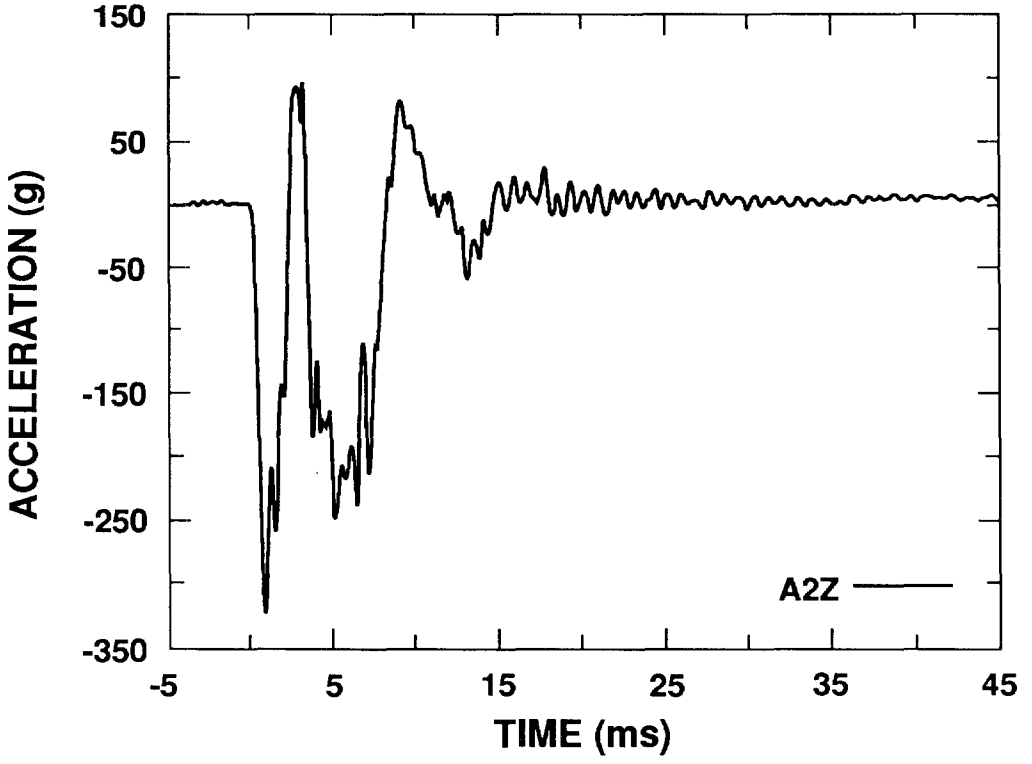

Figure 8-11. Plot of Data from Accelerometer A2Z

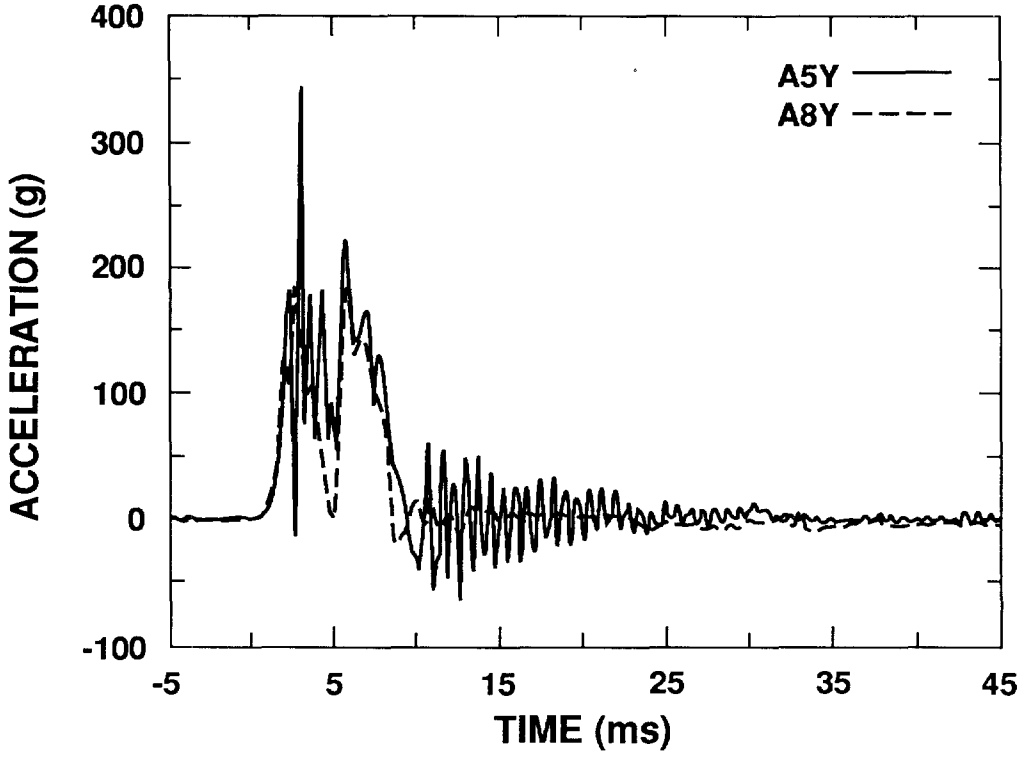

Figure 8-12. Plots of Data from Accelerometers A5Y and A8Y

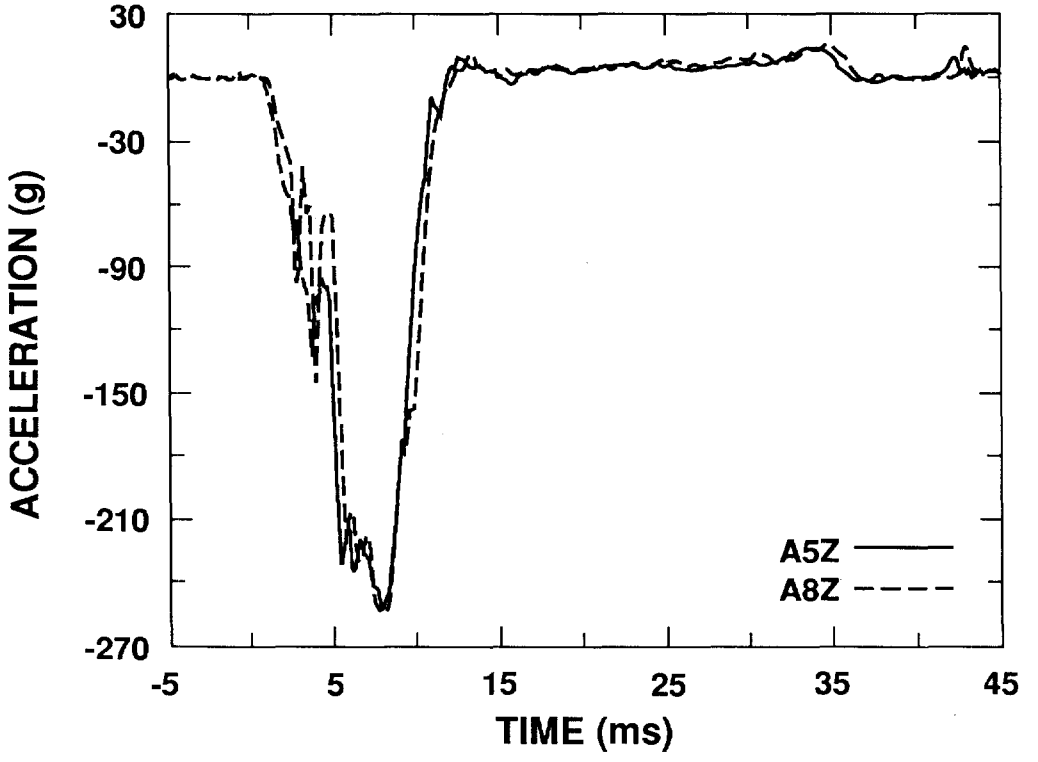

Figure 8-13. Plots of Data from Accelerometers A5Z and A8Z

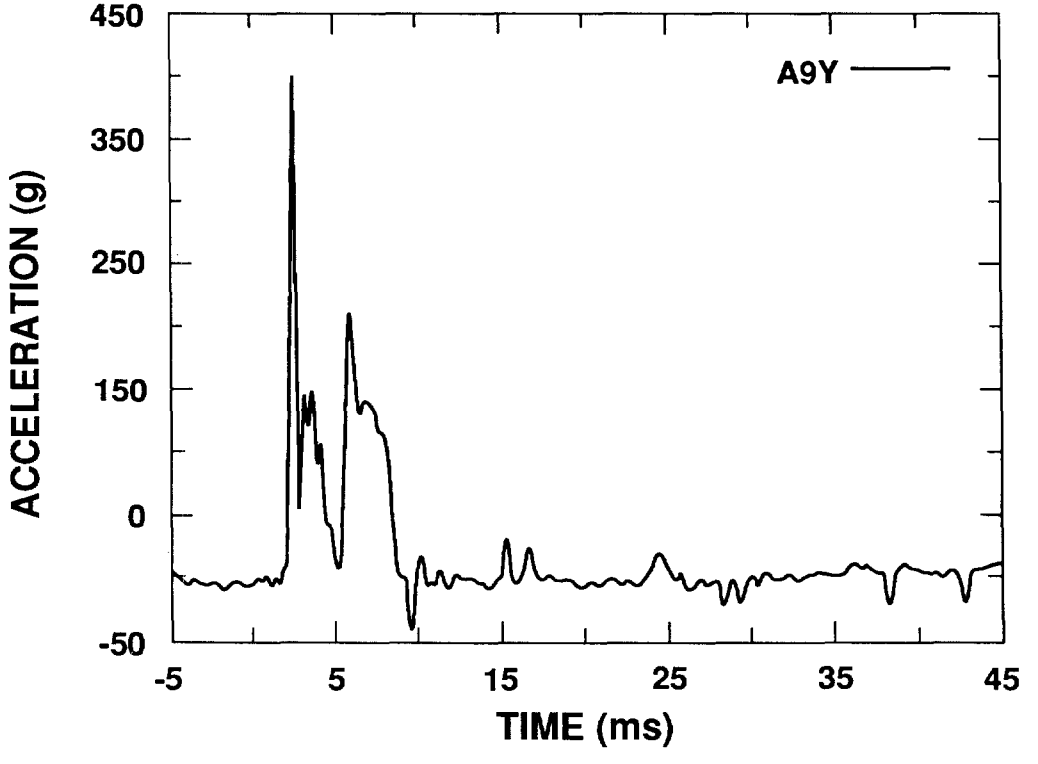

Figure 8-14. Plot of Data from Accelerometer A9Y

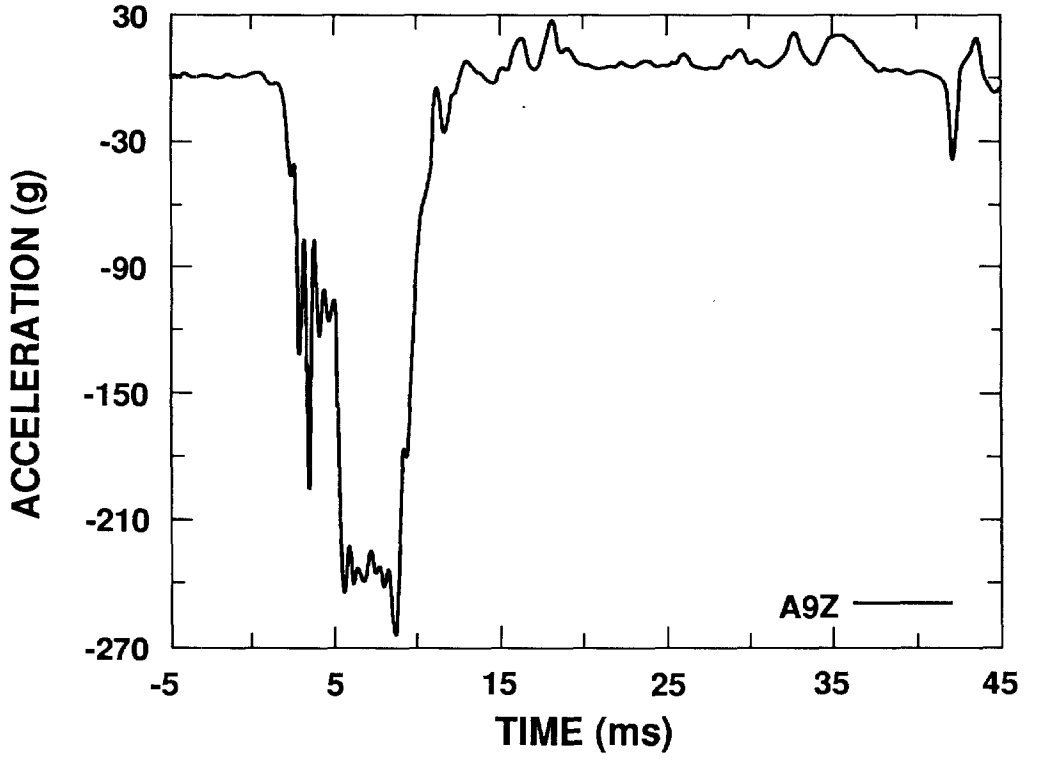

Figure 8-15. Plot of Data from Accelerometer A9Z

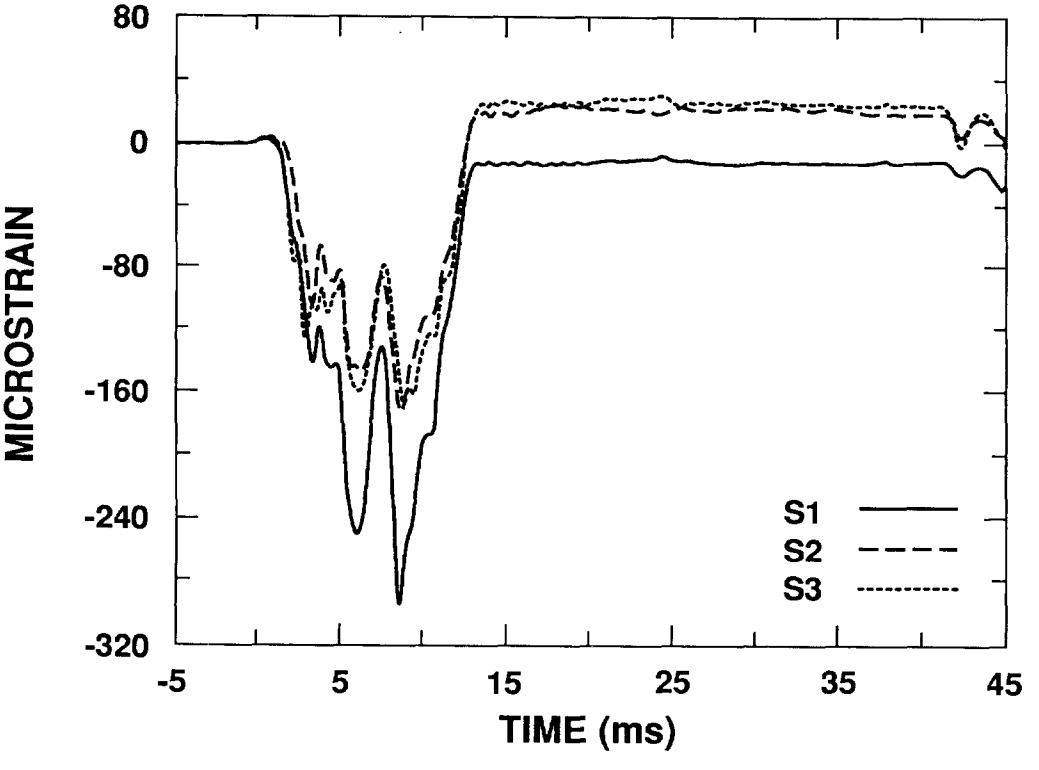

Figure 8-16. Plots of Data from Gages S1, S2, and S3

TABLE 8-2

Strain Gage Data--CG Over Corner Drop Test

Component/ Location	Gage Desig-nation	Peak Strain ($\mu\varepsilon$)	Strain Offset ($\mu\varepsilon$)	Confidence Level
Lid	S1	-290	-10	High
	S2	-175	25	High
	S3	-165	25	High
Lid Flange	S5	-20	22	High
	S6	75	5	High
Top of Body	S7	95	20	High
	S8	48	-15	High
	S9	70	-10	High
	S10	68	-5	High
	S11	370	60	High
	S12	265	65	High
Body Flange	S15	1175	450	Good
	S16	95	90	High
Center of Body	S17	92	10	High
	S18	-120	0	High
	S19	175	-15	High
	S20	200	10	High
	S21	-200	-10	Good
	S22	-125	-10	Reject
Bottom of Body	S25	40	0	High
	S26	26	0	High
	S27	132	0	High
	S28	37	3	High
	S29	-34	-2	High
	S30	-43	3	High
V-Clamp	S33	85	65	High
	S34	310	320	Good
	S35	73	58	High

impact (8.5 ms versus 3 to 4 ms for most body channels) and are believed to be caused by the payload striking the lid.

The highest strain was recorded for gage S15, which is a radial direction gage on the flange of the body. This strain of 1,175 $\mu\varepsilon$ (Figure 8-17) may underestimate the actual strain as the unfiltered data show a slight clipping of the signal. Additionally, this gage showed the highest strain offset of 450 $\mu\varepsilon$, which indicates yielding of the flange in the impact area. (No mechanical inspection was made immediately after this test but inspections made after the series of three drop tests indicated movement of the flange on the impact side.) Gages S11 and S12 on the body near the flange on 180° showed higher than average peak strains of 370 $\mu\varepsilon$ and 265 $\mu\varepsilon$ (Figure 8-18).

An area of higher than average strains was observed around the center plane of the body, measured by gages S17 through S22. These gages recorded peak strains ranging from 100 to 200 $\mu\varepsilon$ (Figures 8-19 through 8-21).

Strains in the inner container V-clamp were measured by gages S33 and S35 on the band of the clamp and gage S34 on the clamp bolt. An offset in these data indicates a change in the strain put in the clamp at assembly. Figure 8-22 shows plots of data from the gages on the band. These plots show a tension loading and high offset. This is believed to be caused by tension in the band, concentrated on the bolting side at assembly, and then transferred around the band during the event. Data from gage S34 are somewhat confusing. While the pulse shape and peak times correlate with gages S33 and S35, the data show tension (positive signal) loading with a 320 $\mu\varepsilon$ offset (Figure 8-23). This result conflicts with the bolt preload measurement at disassembly, which showed a net loss of 316 $\mu\varepsilon$ preload and should have resulted in a negative offset in the data. There are two possible explanations: the signal was inverted by the data acquisition system, or the bolt underwent a combination of loosening and bending.

8.7.3 Instrumented Bolt Data

Instrumentation included strain-gaged bolts in the upper (lid end) RTG mounted in the payload assembly, designated as SB1 and SB2, and in the locking ring of the outer drum, SB3. Table 8-3 contains the instrumented bolt data obtained. Bolt SB1 (Figure 8-24) loaded in tension and then released slightly. This correlates marginally with the strains measured at disassembly, which indicated a loss of approximately 100 $\mu\varepsilon$ during the test. No data was obtained from bolt SB2.

Figure 8-25 shows the plot from bolt SB3 in the drum locking ring. This bolt initially loaded in tension and then released 155 $\mu\varepsilon$ (negative offset in plot) of the 236 $\mu\varepsilon$ preload strain present at assembly.

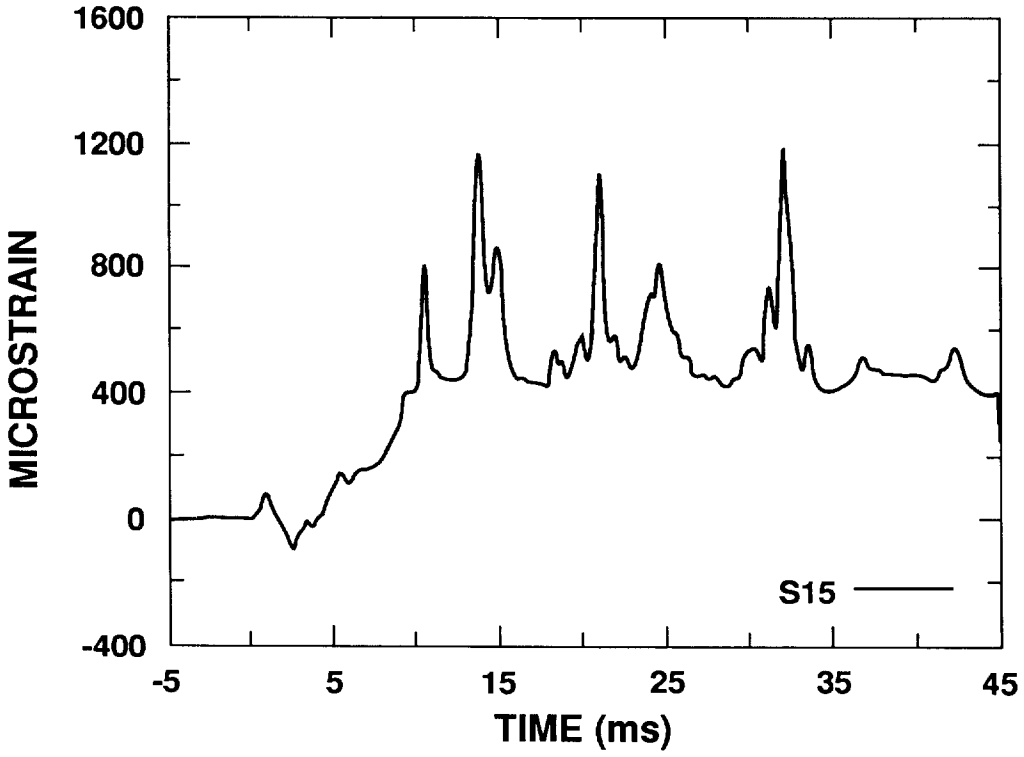

Figure 8-17. Plot of Data from Gage S15

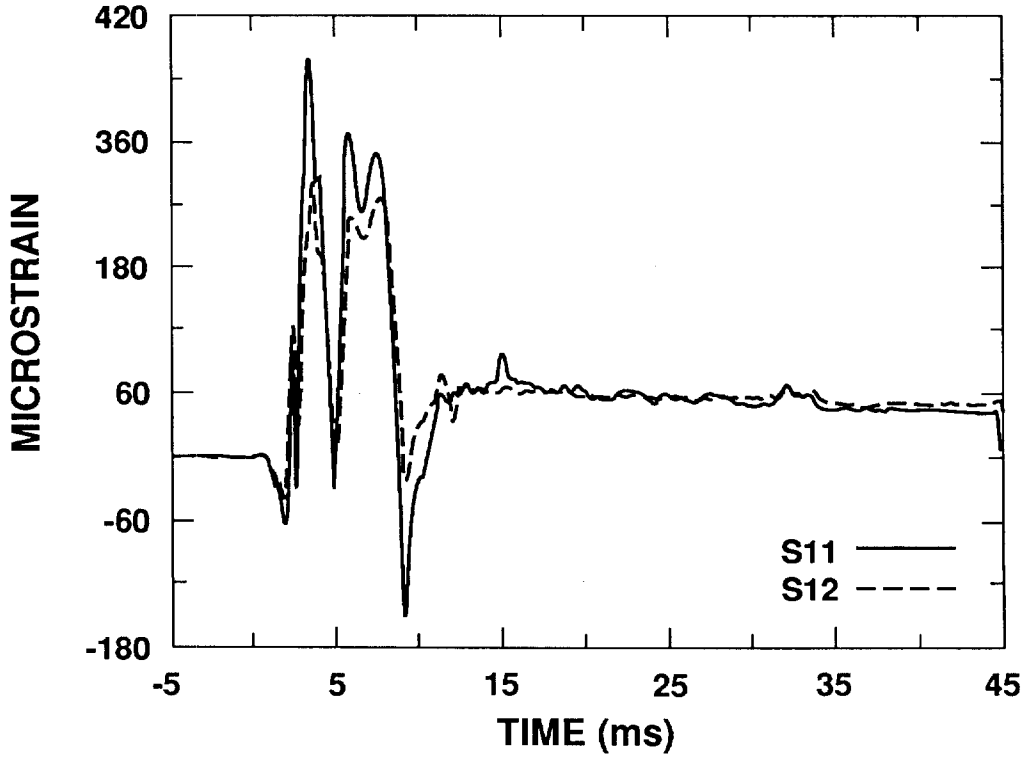

Figure 8-18. Plots of Data from Gages S11 and S12

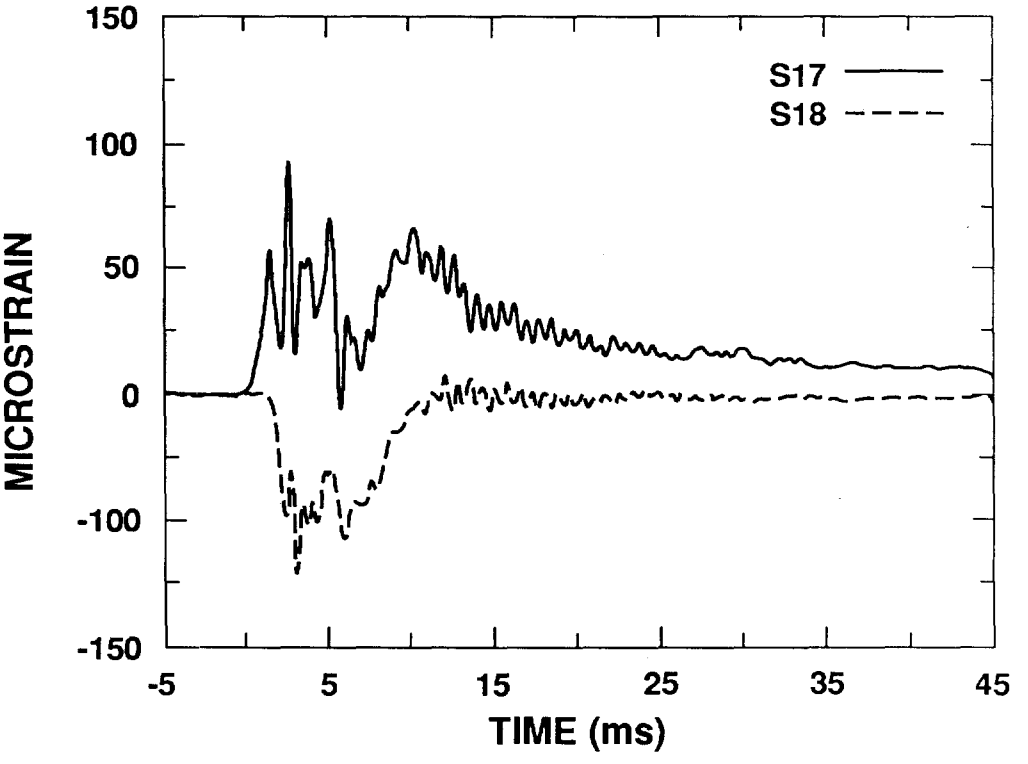

Figure 8-19. Plots of Data from Gages S17 and S18

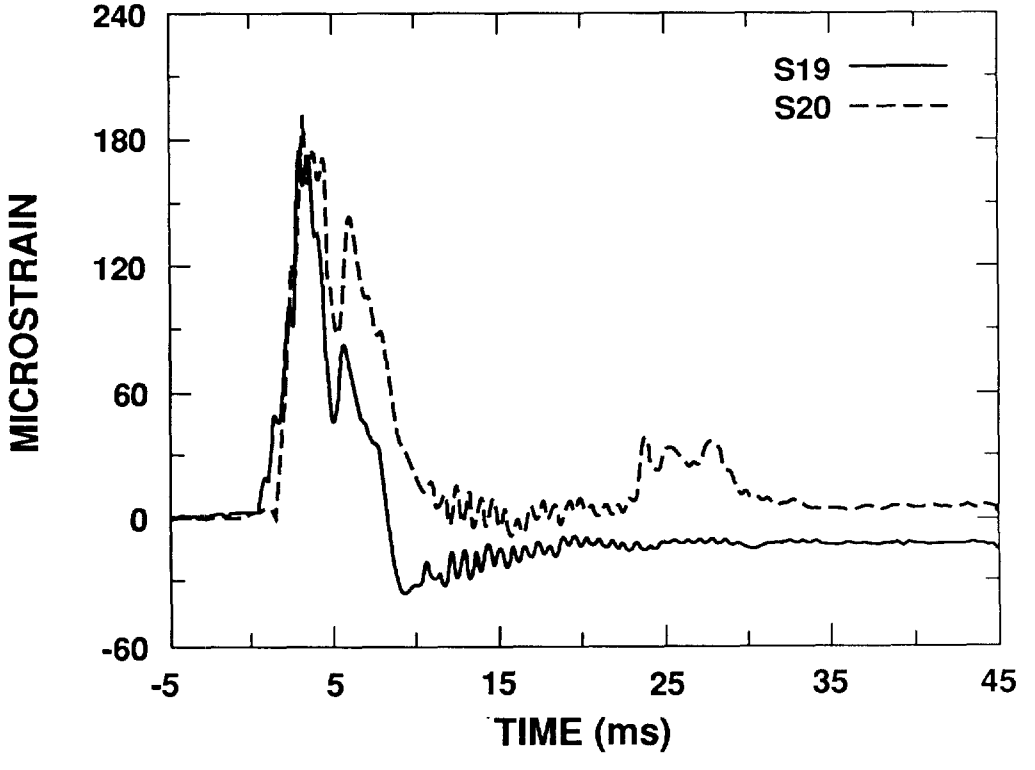

Figure 8-20. Plots of Data from Gages S19 and S20

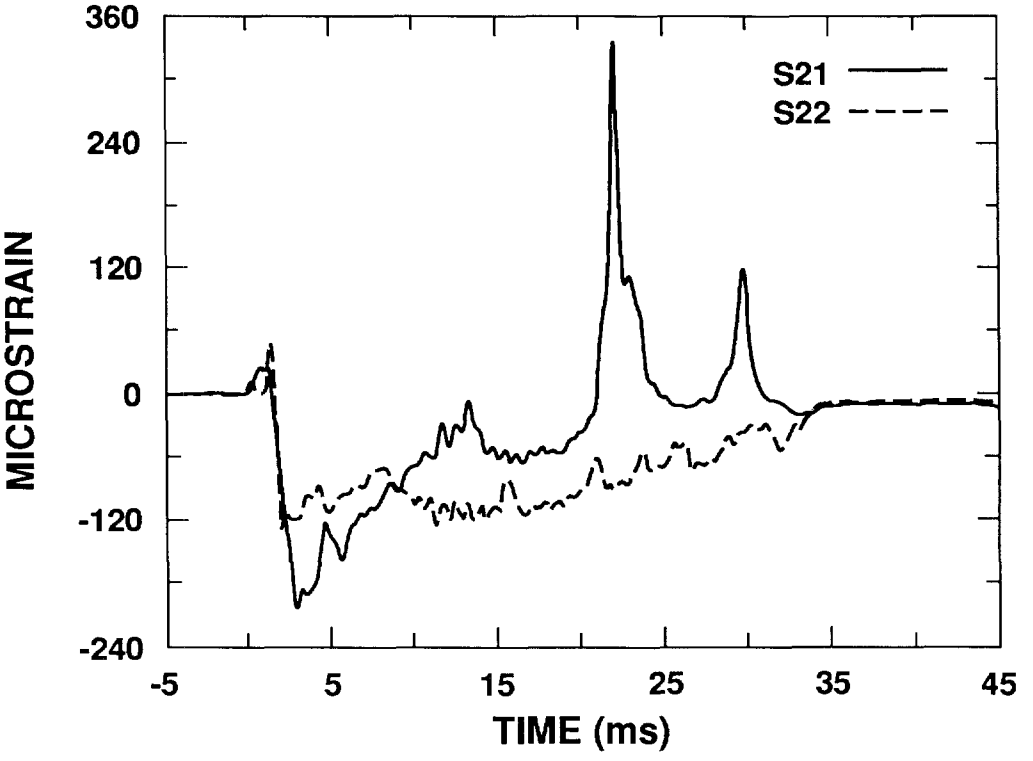

Figure 8-21. Plots of Data from Gages S21 and S22

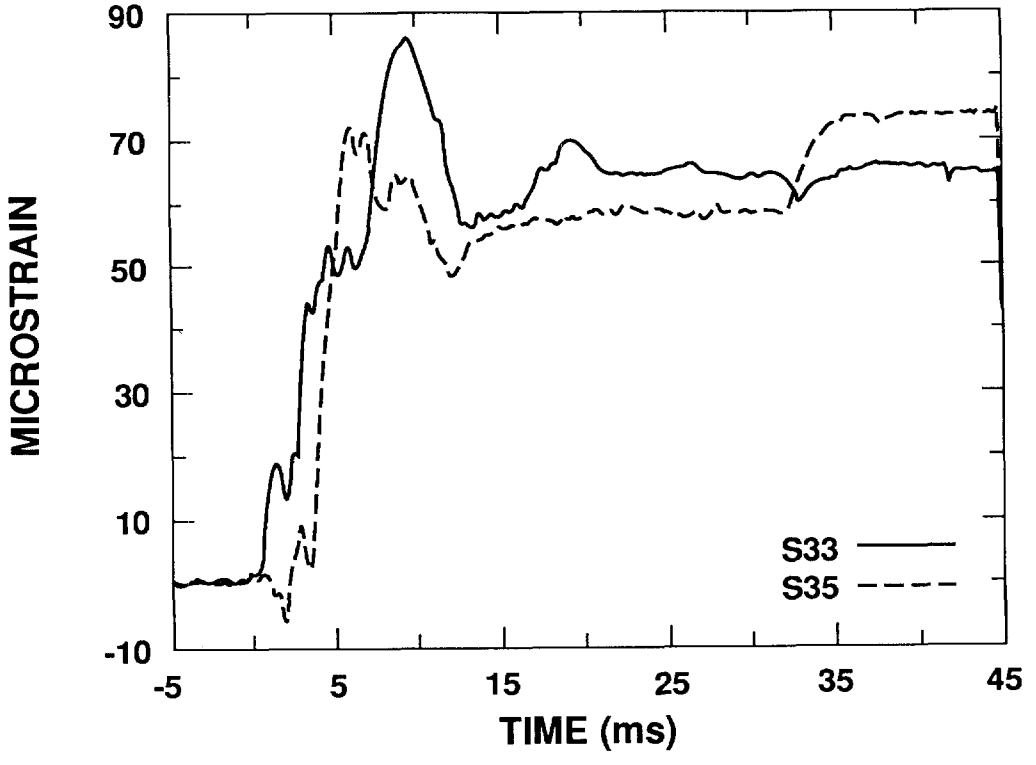

Figure 8-22. Plots of Data from Gages S33 and S35

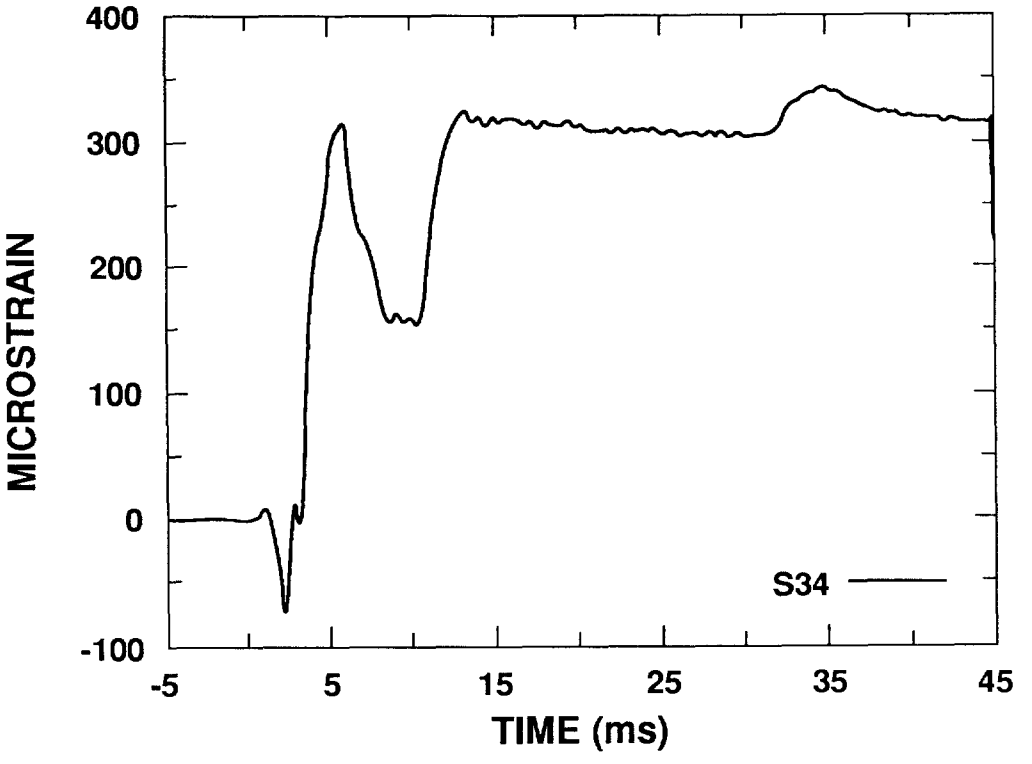

Figure 8-23. Plot of Data from Gage S34

TABLE 8-3

Instrumented Bolt Data--CG Over Corner Drop Test

Component/ Location	Bolt Desig- nation	Peak Strain ($\mu\varepsilon$)	Strain Offset ($\mu\varepsilon$)	Confidence Level
RTG 0°	SB1	110	-20	High
RTG 180°	SB2	no data	no data	Reject
Locking ring	SB3	70	-155	High

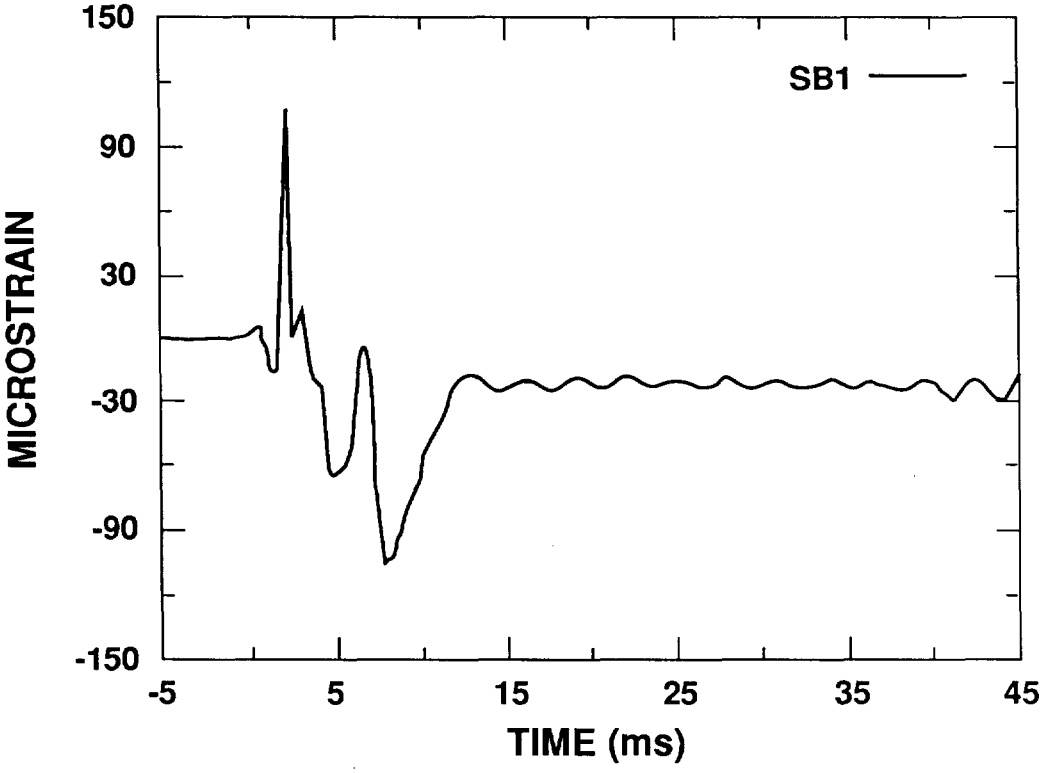

Figure 8-24. Plot of Data from Bolt SB1

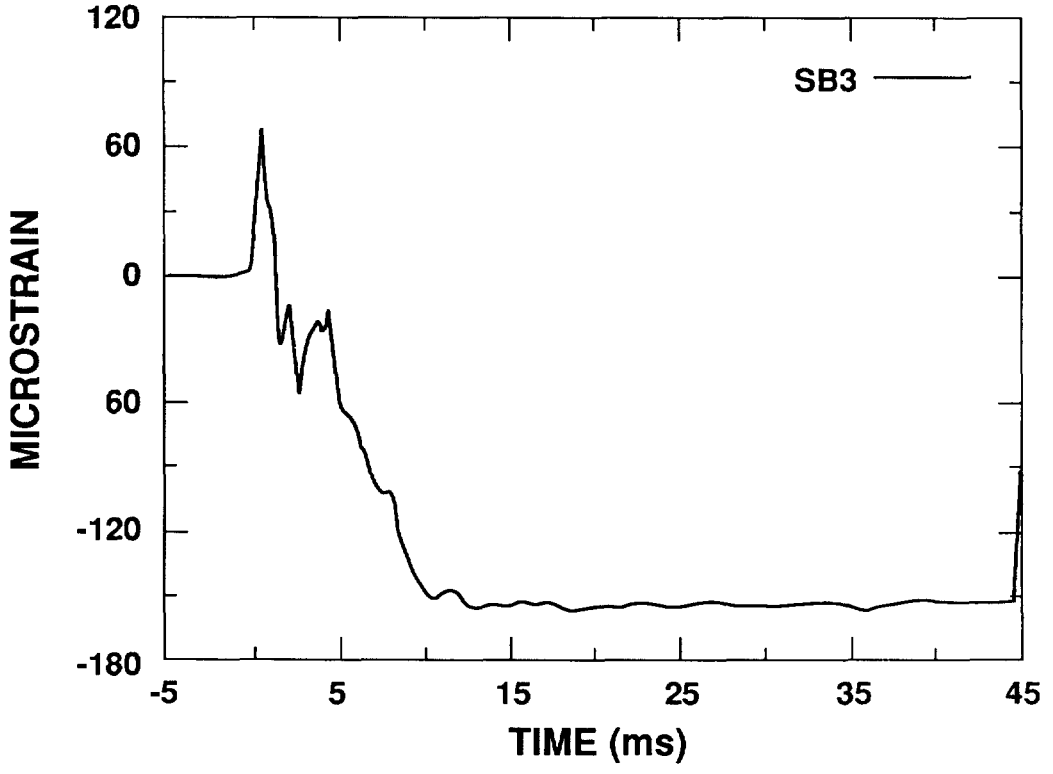

Figure 8-25. Plot of Data from Bolt SB3

9.0 SIDE DROP TEST

9.1 Test Unit Preparation

Before assembly, the test unit inner container body, lid, and V-clamp were instrumented with the transducers defined in Section 5. Bolts (both instrumented and standard) for the RTGs were installed and torqued to specified values. Preload in the instrumented bolts was measured at this time. The bolt on the V-clamp was also torqued, and the preload measured and recorded.

Helium leak-testing of the inner container seal revealed a leakage rate of 2.0×10^{-10} atm cm^3/sec (equal to minimum sensitivity of the detector).

The inner container assembly was installed in an undamaged outer drum (S-1C) with new Celotex (S-1D). The inner assembly was oriented such that the V-clamp bolt was at 180°, the intended impact side of the drum. The welded seam of the drum was also oriented at 180°. Instrumentation wiring was routed through the lid section of Celotex and out the center of the drum lid as was done for the CG over corner drop test. An undamaged drum lid locking ring was installed with the bolt lug oriented at 180°. The instrumented locking ring bolt was torqued to 180 inch-pounds, and preload strain was measured and recorded.

9.2 Test Set-Up

This test was performed following the HS/RTG Side Drop Test Procedure.[6] Figure 9-1 shows the test unit mounted in the cradle with the drum axis at an angle of 0° (horizontal) with the 180° side faced down to impact the target. Because the locking ring bolt lug was located at the 180° side, that end of the drum impacted the target first, with the bottom end impacting next. The cradle and sliding beam assembly were raised so that the lowest point of the unit was 32 feet, 4-1/2 inches above the target (Figure 9-2). The midpoint of the instrumentation wiring was tied to a forklift mast approximately 15 feet above the ground to remove some of the cable weight from the test unit. This also reduced the chance of impacting the test unit on the instrumentation cables.

9.3 Drop Test

The drop test is shown in Figure 9-3. The test unit impacted at a velocity of 45.8 feet per second and an angle of 1° (lid end lower). Photographs A and B show the unit at decreasing heights above the target. Photograph D shows the unit just after impact and Photographs E and F show the unit

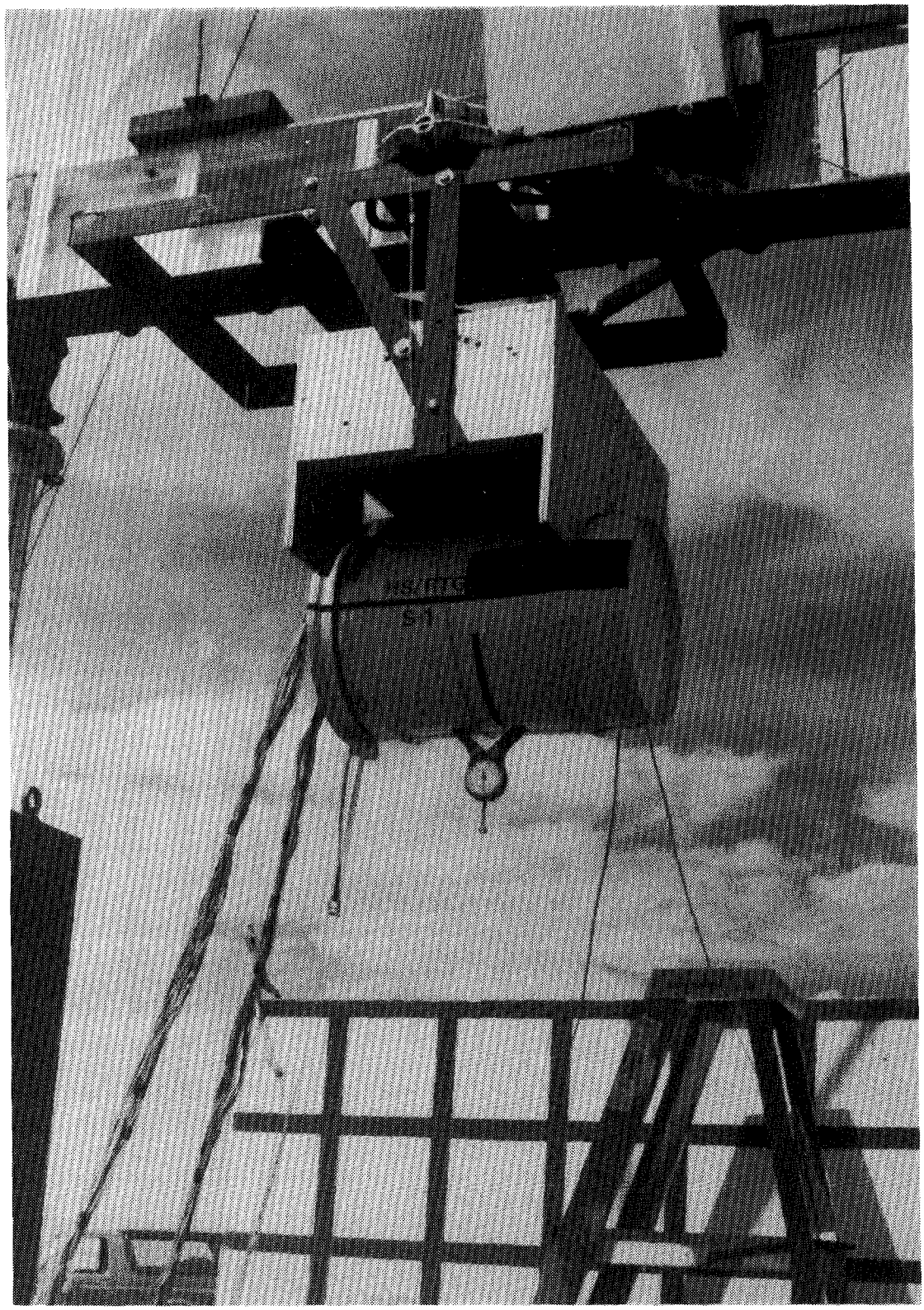

Figure 9-1. Test Unit in Cradle

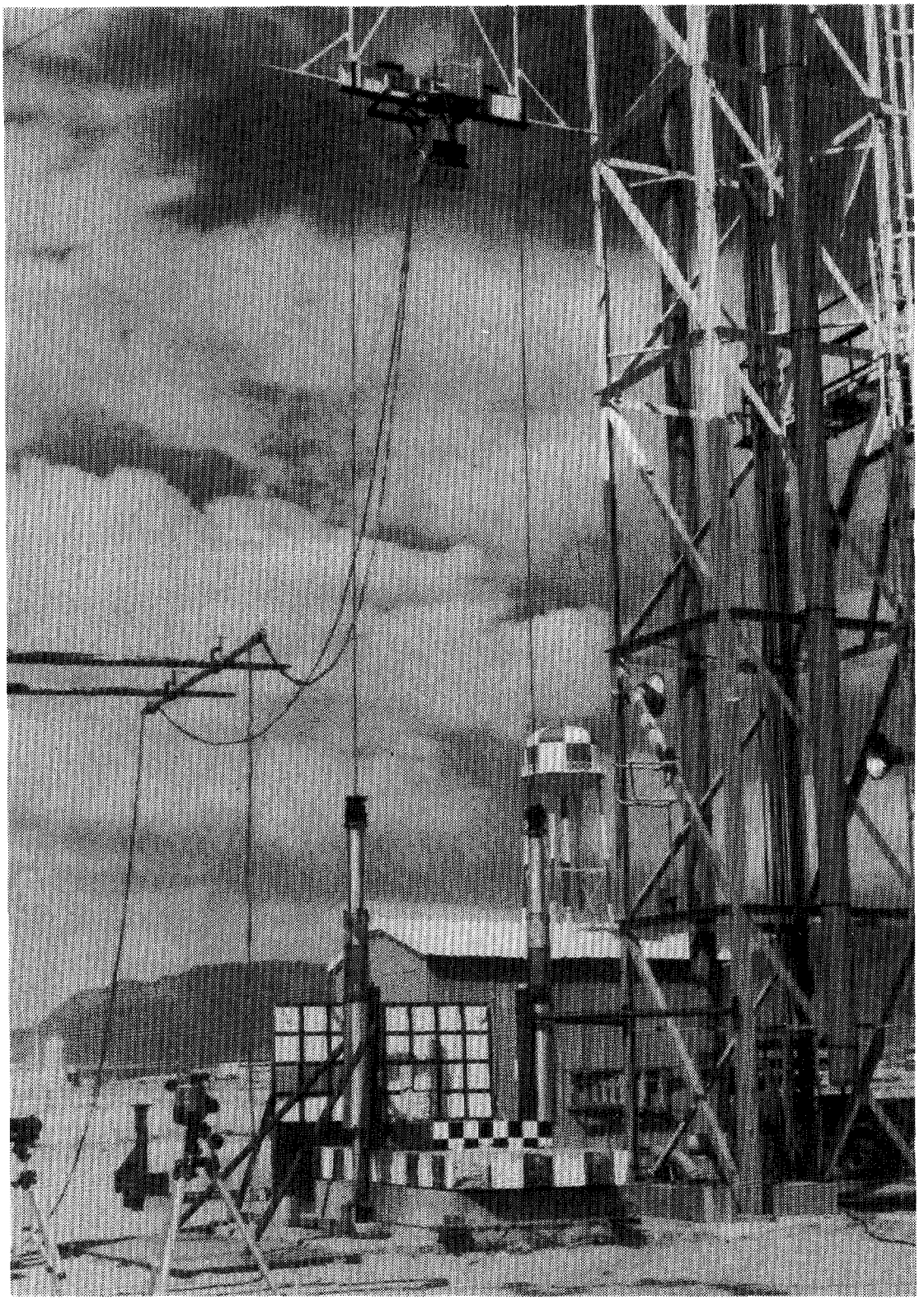

Figure 9-2. Test Set-Up

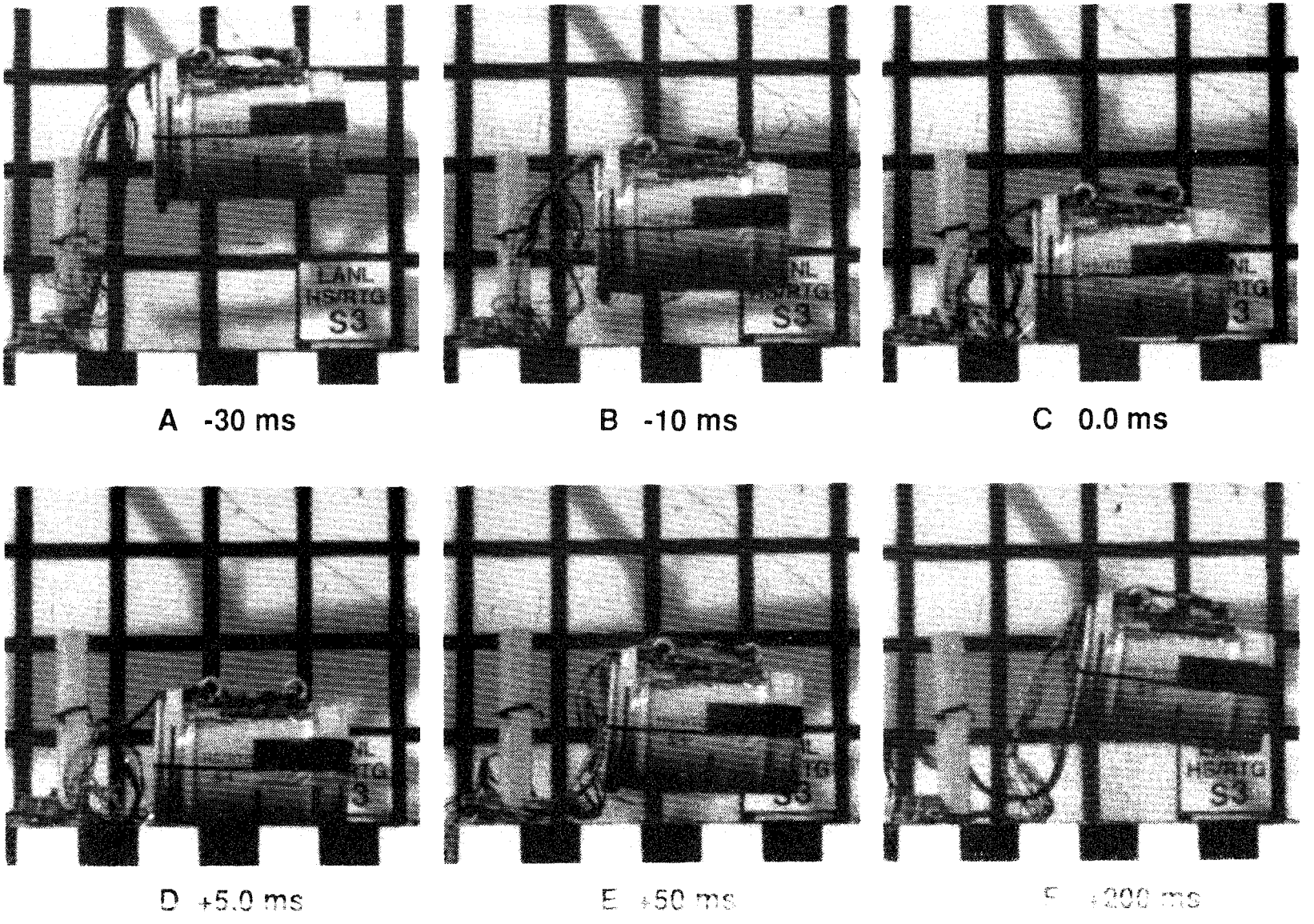

Figure 9-3. Test Sequence

rebounding off the target and at maximum rebound height. Total impact duration was estimated to be 4 ms. The unit came to rest on the 180° (impact) side on the target.

9.4 Exterior Deformations

Damage to the outer drum is shown in Figures 9-4 and 9-5. The drum deformed along the length of the impact side, with the largest deformation where the locking ring bolt lug was driven into the drum. No tears or cracked welds were evident. Figure 9-5 illustrates deformation depths at each end of the unit.

9.5 Disassembly

After the side drop test, the test unit was completely disassembled. Posttest torque on the locking ring bolt could not be measured because the lug and bolt had been driven into the drum and neither the bolt head nor the nut was accessible. Posttest preload (strain) was measured to be 20 $\mu\varepsilon$, a decrease of 214 $\mu\varepsilon$ from the assembly preload. The deformed locking ring remained in close contact with the drum lip and lid (Figure 9-4). The bolt lugs and welds on the locking ring were intact. Deformations in the drum body consisted of dents in the side of the drum under the bolt lugs. No holes, cuts, or cracks were found under the ring or bolt lug. However, there was a small gap at exactly 180°, between the ends of the locking ring (Figure 9-6), where the lid had bent away from the lip of the drum. The lid was easily removed.

Inward deformations of the drum on the 180° side wedged the lid section of Celotex tightly in place. This section was removed by cutting the section into two pieces and removing the piece in the undamaged area first. The inner container assembly was then removed easily. No attempt was made to remove the body section of Celotex, which was held in place by drum deformations.

After visual inspection and leak-testing of the inner container seal, the inner container was disassembled. Both posttest torque and preload of the V-clamp bolt were measured. Preload was 510 $\mu\varepsilon$, a decrease of 220 $\mu\varepsilon$ from the 730 $\mu\varepsilon$ strain measured at assembly. Torque was approximately 95 inch-pounds, a decrease of 5 inch-pounds from the 100 inch-pound assembly torque. The V-clamp and lid were then removed.

The payload assembly had rotated ~2° clockwise in the container. Tightness of the bolts securing the RTGs was checked as was the preload for the instrumented RTG bolts. Results are as follows:

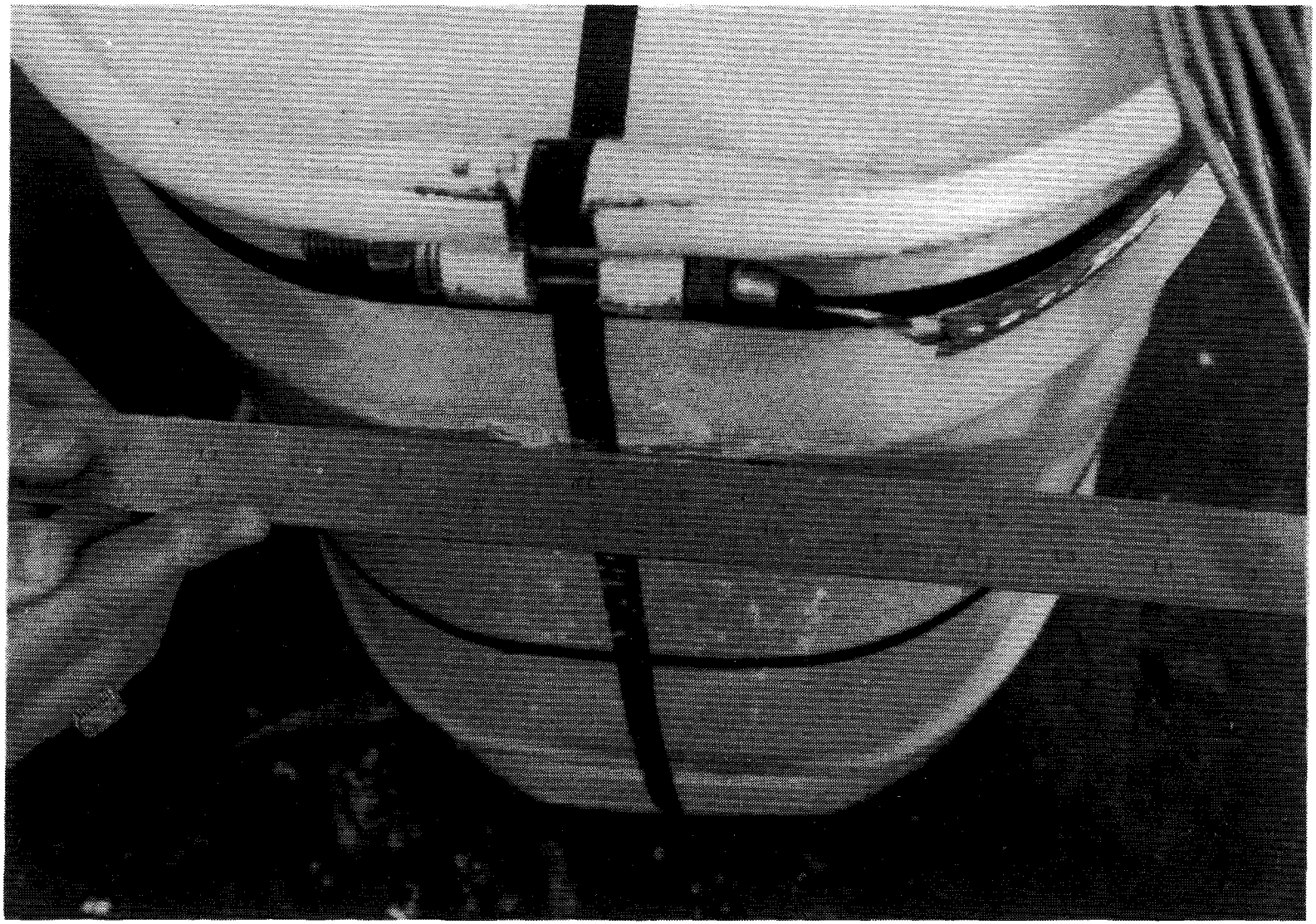

Figure 9-4. Outer Drum Deformations

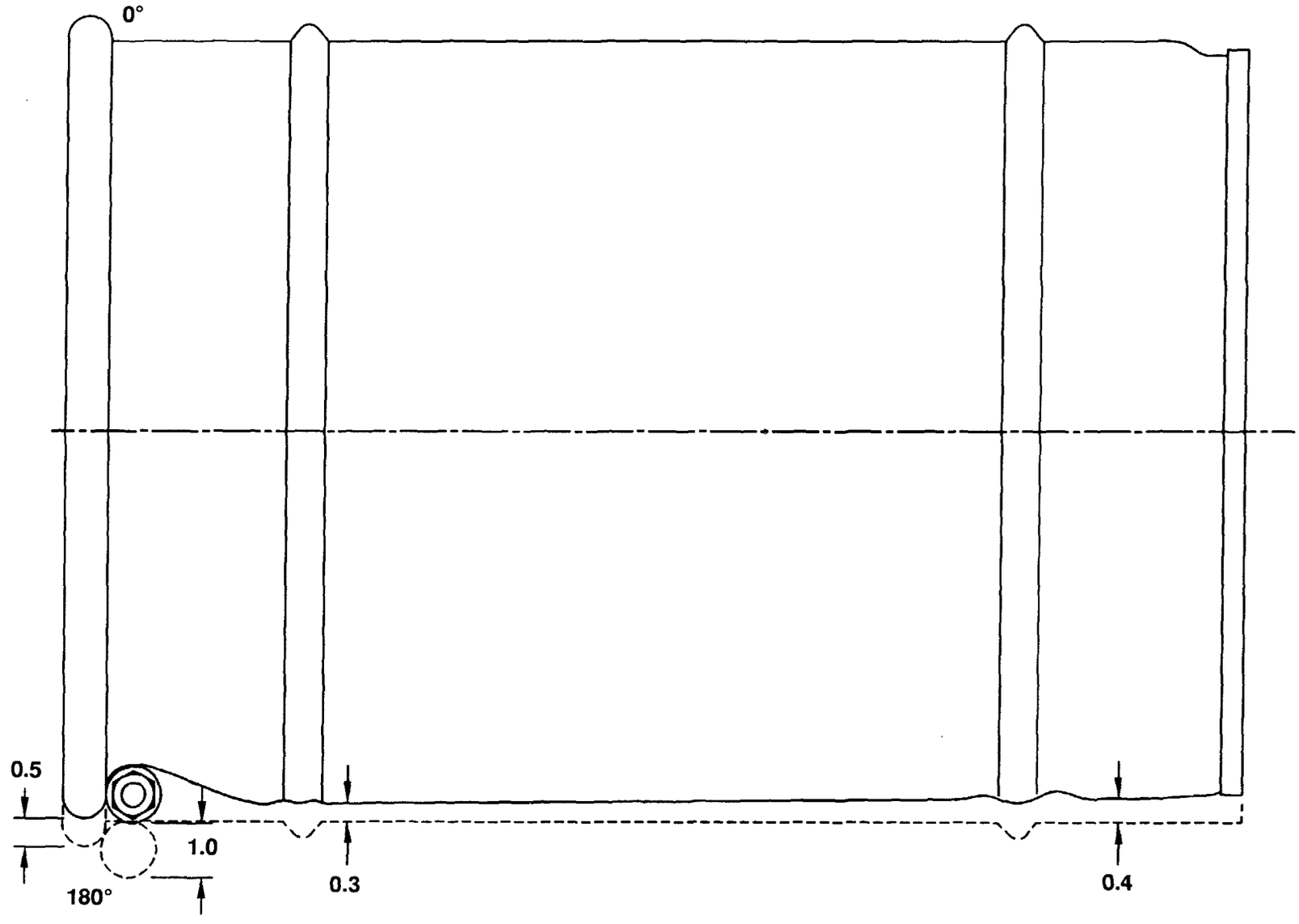

Figure 9-5. Drum Deformation Sketch

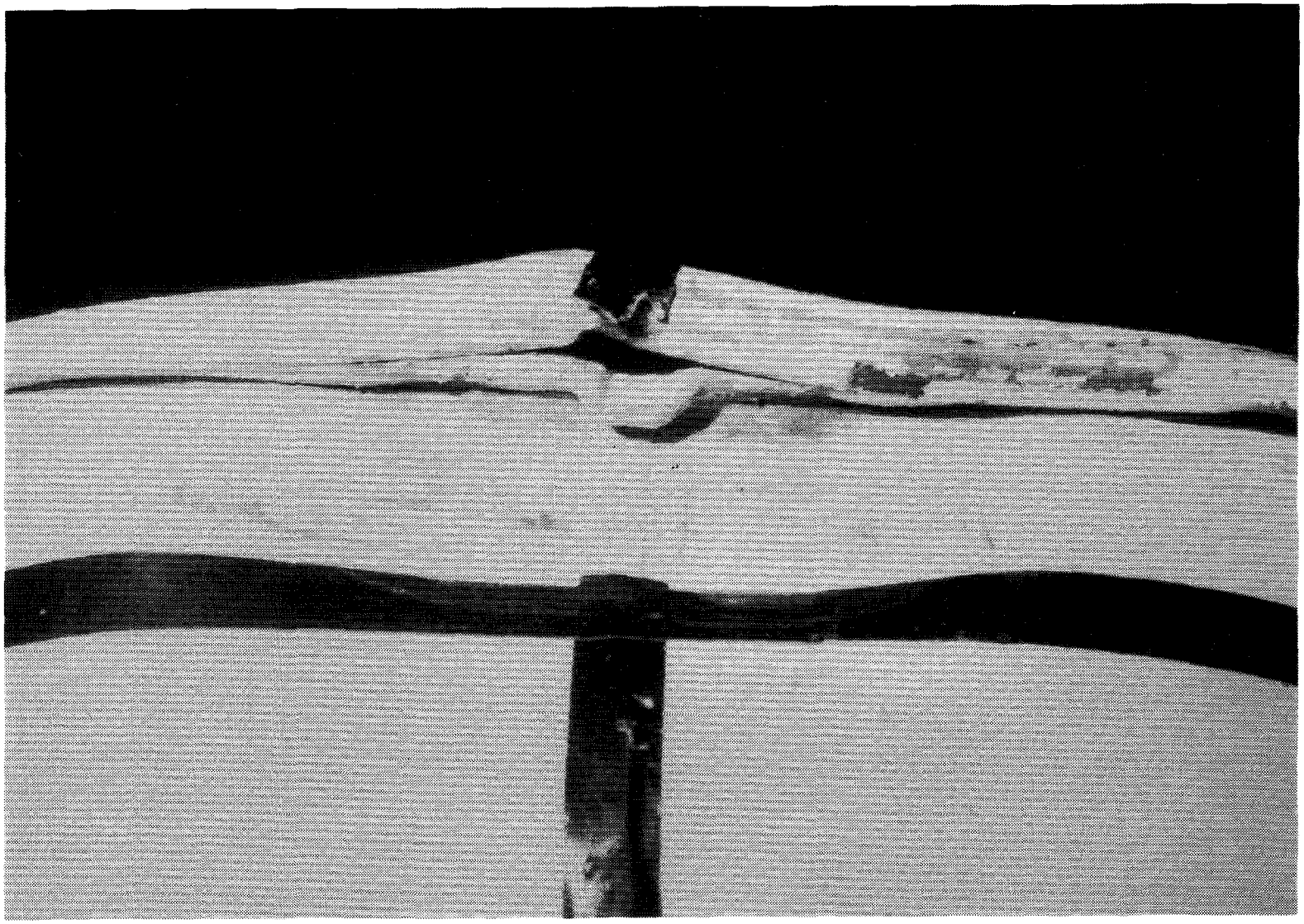

Figure 9-6. Drum Lip Deformations

Bolt	Location	Approximate Net Change in Torque (inch-pounds)	Approximate Net Change in Preload ($\mu\varepsilon$)
SB1	0° upper RTG	-15	-434
SB2	180° upper RTG	0	-186
B5	0° lower RTG	-25	NA
B6	180° lower RTG	-10	NA

Of note is the significant loss of torque and preload on bolts SB1 and B5. Both of these bolts are in the upper (0° side) locations of the RTGs (Figure 5-9). These bolts were subjected to high loads during impact as a result of the mass of the RTGs and the geometry of their locations.

9.6 Results--Nondestructive Examination

9.6.1 Leak Test

A posttest leak test of the inner container seal showed a leakage rate of 4×10^{-10} atm cm^3/sec (background).

9.6.2 Inspection

No mechanical inspections of the inner container components were performed at the conclusion of the side drop test. A visual inspection was made of the inner container components with no observable deformations noted. Section 10.6.2 gives inspection results after the subsequent drop test.

Major damage to the Celotex consisted of indentations from the locking ring lugs. Celotex deformations along the remainder of the 180° side are not as severe as the drum exterior might indicate. Most drum deformation simply removed the gap which existed between the outside diameter of the Celotex and the interior drum walls, resulting in actual crush of only 0.05 to 0.10 inch along the side.

A crack was observed in the Celotex surface at the 180° side of the inner container assembly (Figure 9-7). This may have been caused by 1) downward forces exerted by the heavy lid end of the inner container, or 2) inward impact forces attempting to collapse the inner cavity. The crack did not appear to constitute a heat path in a thermal test scenario.

9.7 Results--Transducer Data

9.7.1 Accelerometer Data

Instrumentation for the side drop test included six accelerometers as defined in Section 5.2. All were oriented

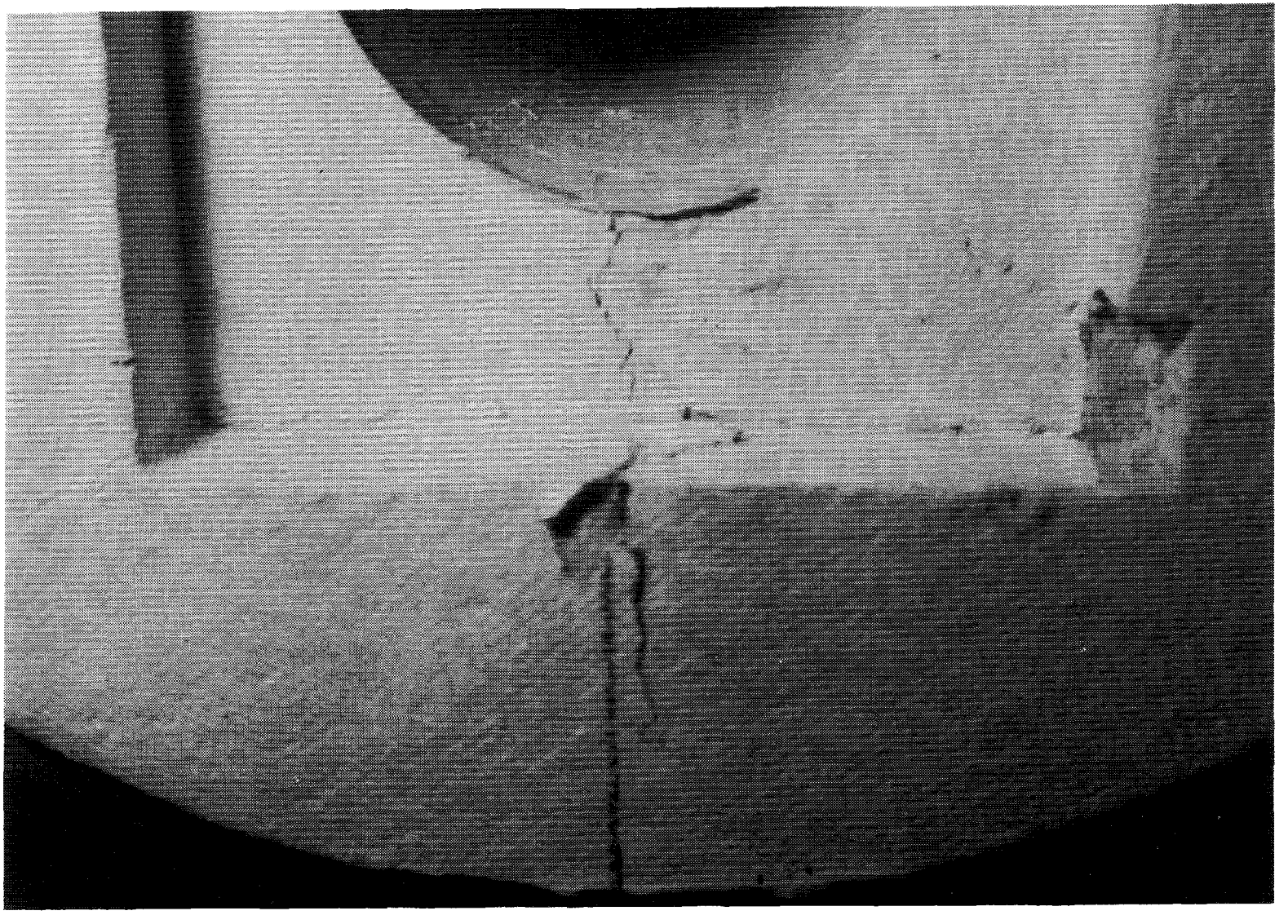

Figure 9-7. Crack in Surface of Celotex

in the Y direction, i.e., the direction of impact. Mounting locations consisted of A1Y and A4Y on the outer drum, A5Y and A7Y on the inner container body, A8Y on the inner container lid, and A9Y on the payload assembly. Values presented are based on data that have been filtered at 1,000 Hz. Figure 9-8 shows a layout of the accelerometers with the peak deceleration values labeled. Table 9-1 lists the designation, location, calibration value, measured peak acceleration, and confidence level of each transducer.

Decelerations of the outer drum were measured by A1Y near the lid end and A4Y near the bottom end. Plots of these data are shown in Figure 9-9. The peak acceleration measured by A1Y is approximately half that of A4Y even though A1Y measured the initial impact. Because of the small crush area (under the bolt lug), the lid end of the unit crushed approximately twice the amount of the bottom end (1.0 inch under the bolt versus 0.4 inch at the bottom end). Also, the bolt lug acted as a rotation point which may have accelerated the bottom end into the target creating a slapdown effect.

Inner container decelerations were measured by A5Y at the center of the body, A7Y at the bottom of the body, and A8Y on the lid. Response of the inner container assembly at these three locations is shown in Figure 9-10. All pulses showed a time delay of approximately 1 ms from outer drum impact. Inner container pulse peaks were about one-half of the outer drum peaks at respective ends as a result of the cushioning effect of the Celotex insulation. Accelerometer A5Y was also the approximate average of A7Y and A8Y.

Response of the payload assembly was measured by accelerometer A9Y. Data from this transducer appear in Figure 9-11. This pulse showed a time delay of 1.5 ms from initial outer drum impact and consisted of a single, high spike.

9.7.2 Strain Gage Data

Instrumentation for the side drop test included 28 strain gages as defined in Section 5.1. These gages measured surface strain on the exterior of the inner container body and lid on the 180° (impact), 90°, and 0° sides. Gages also were mounted on the V-clamp ring and bolt. Table 9-2 lists the gage designation, measured peak strain, strain offset, and confidence level of each measurement. All data presented have been filtered at 1,000 Hz.

As in the CG over corner test, measured strains at many locations were low (below 100 $\mu\varepsilon$). Notable exceptions are discussed below.

Gages S7 through S12 on the top (lid) end of the inner container body recorded generally higher strains than in the

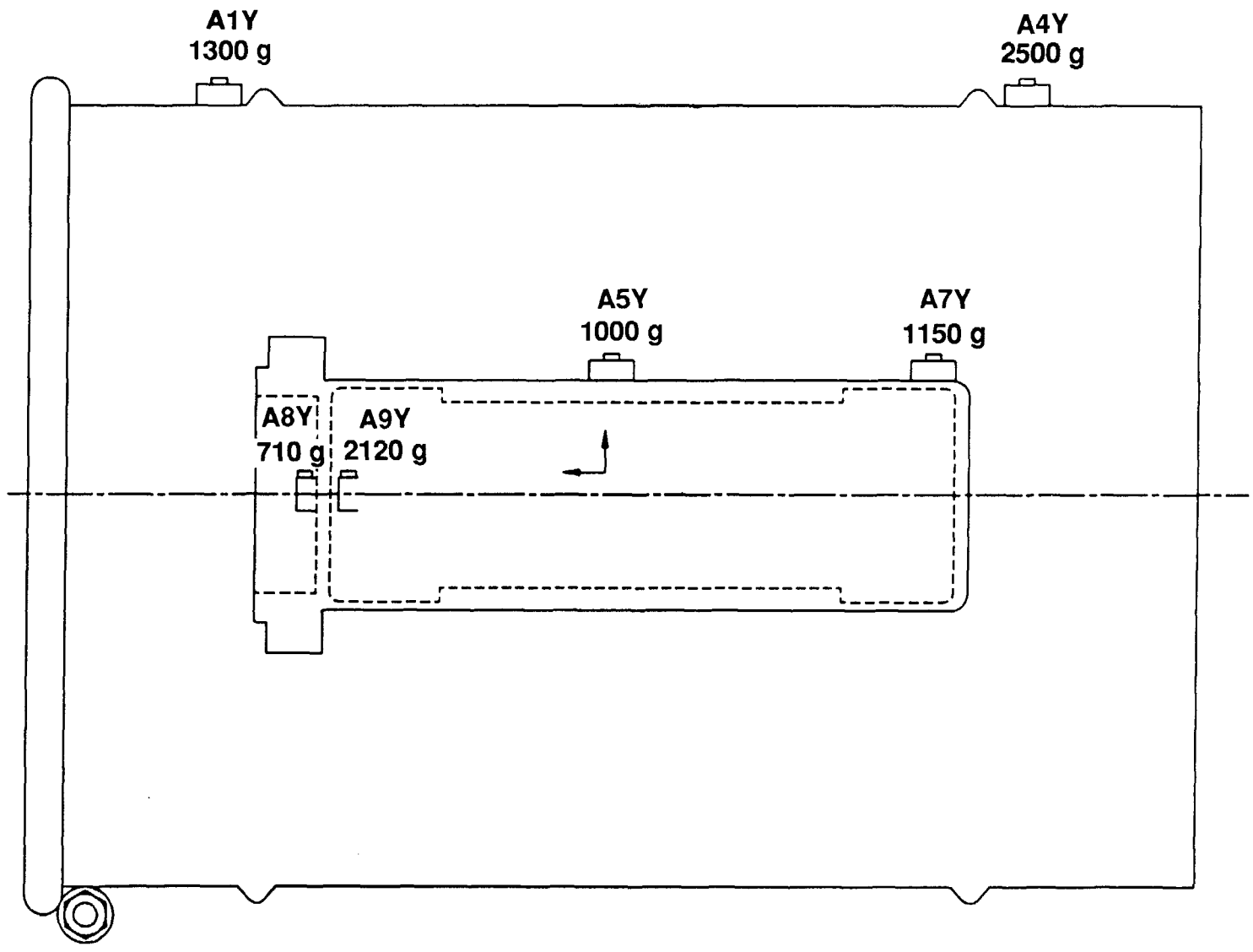

Figure 9-8. Peak Accelerations--Side Drop Test

TABLE 9-1

Accelerometer Data--Side Drop Test

Component	Accelero-meter Designation	Cali-bration Value (g)	Peak Accele-ration (g)	Confidence Level
Outer Drum	A1Y	4,000	1,300	High
	A4Y	4,000	2,500	High
Inner Container	A5Y	4,000	1,000	High
	A7Y	4,000	1,150	High
Inner Lid	A8Y	4,000	710	High
Payload	A9Y	4,000	2,120	High

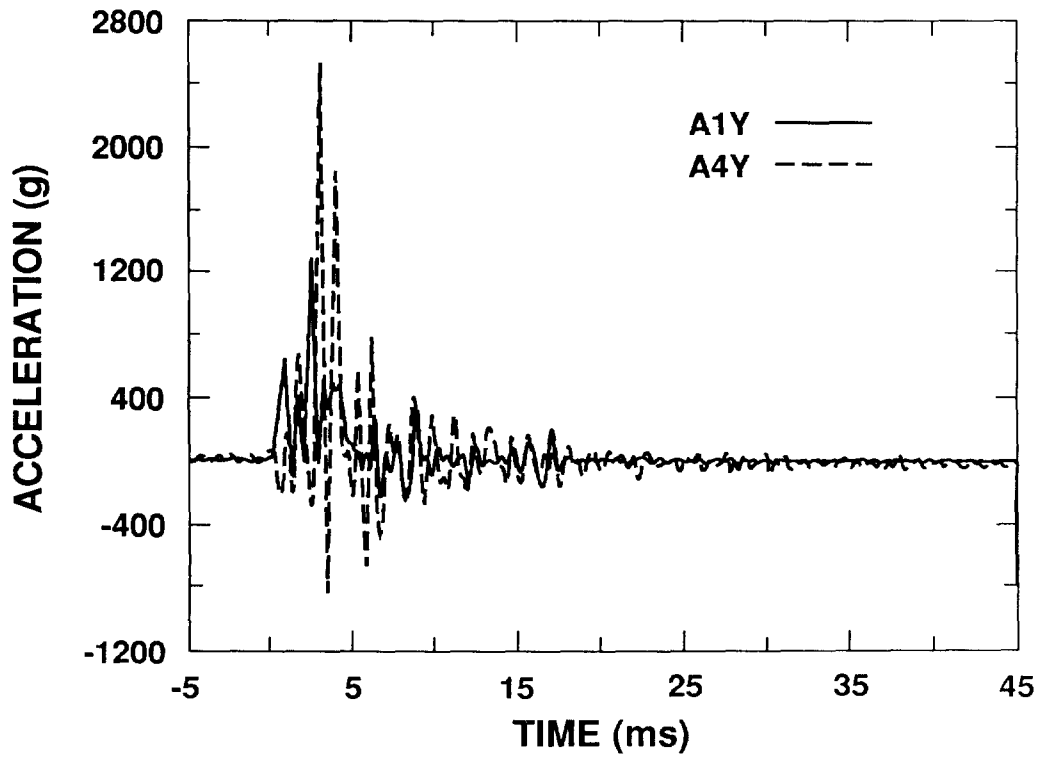

Figure 9-9. Plots of Data from Accelerometers A1Y and A4Y

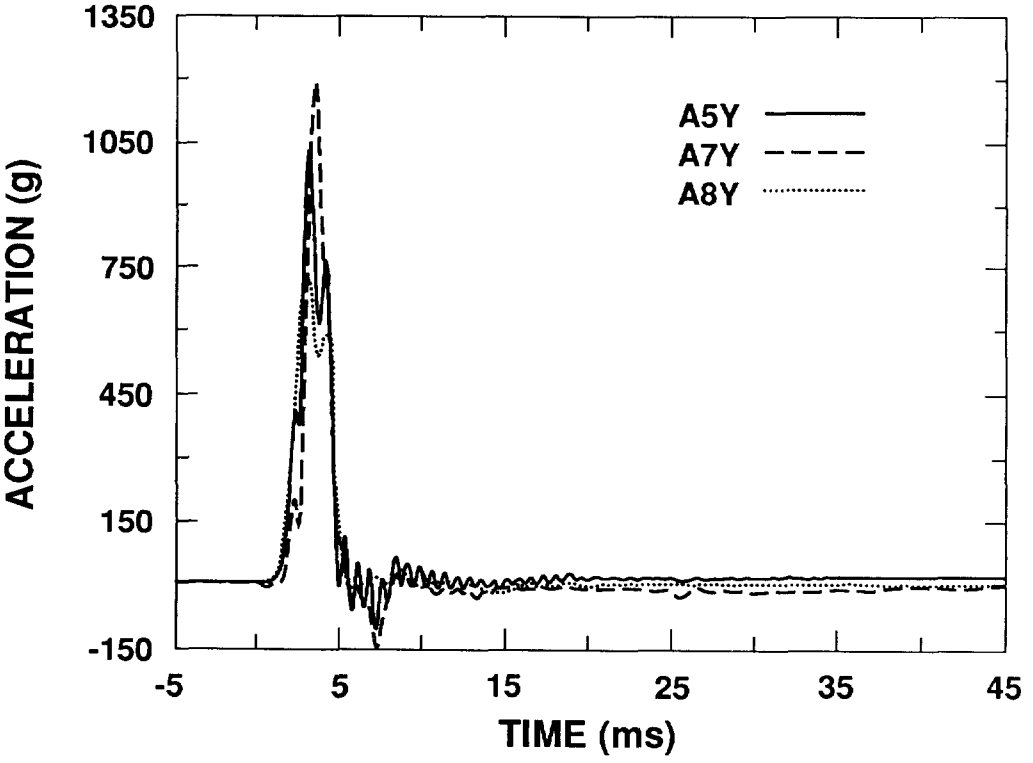

Figure 9-10. Plots of Data from Accelerometers A5Y, A7Y, and A8Y

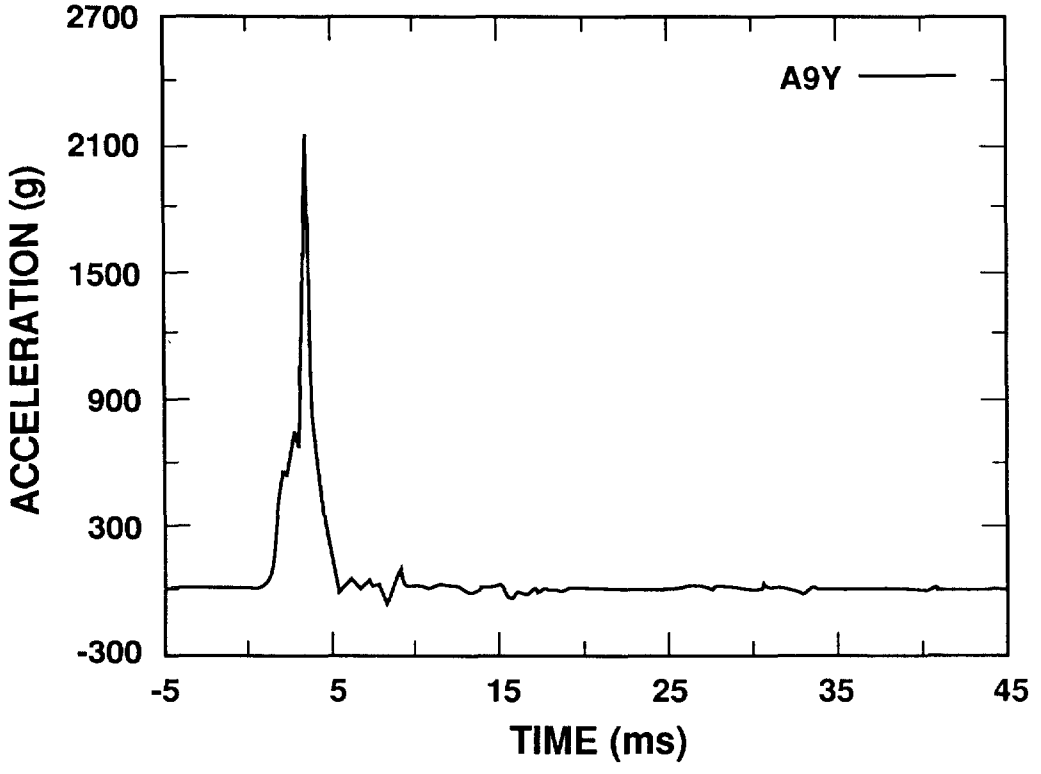

Figure 9-11. Plot of Data from Accelerometer A9Y

TABLE 9-2

Strain Gage Data--Side Drop Test

Component/ Location	Gage Designation	Peak Strain ($\mu\varepsilon$)	Strain Offset ($\mu\varepsilon$)	Confidence Level
Lid	S1	-90	25	High
	S2	-80	0	High
	S3	-85	30	High
Lid Flange	S5	-42	3	High
	S6	72	-3	High
Top of Body	S7	240	-80	High
	S8	155	-70	High
	S9	-185	60	High
	S10	-25	40	High
	S11	920	120	High
	S12	680	70	High
Body Flange	S15	360	210	High
	S16	155	60	High
Center of Body	S17	-240	70	High
	S18	-400	-10	High
	S19	560	0	High
	S20	540	25	High
	S21	-680	20	High
	S22	-550	-15	High
Bottom of Body	S25	155	5	High
	S26	-45	-3	High
	S27	-130	0	High
	S28	55	5	High
	S29	85	5	High
	S30	-60	0	High
V-Clamp	S33	75	0	High
	S34	-290	30	High
	S35	44	-5	High

CG over corner test and ranged from -185 to 920 $\mu\varepsilon$. The highest strains of 920 and 680 $\mu\varepsilon$ were measured by gages S11 and S12, which are located at the 180° (impact) side. Plots of these channels are illustrated in Figures 9-12 through 9-14.

Gages located on the flange of the body at 180° (S15 and S16) measured strains of 360 and 155 $\mu\varepsilon$ (Figure 9-15). Offset of 210 $\mu\varepsilon$ measured by gage S15 was the highest indicated for the side drop test. (No mechanical inspection was made immediately after this test but inspections made after the series of three drop tests indicated movement of the flange at the 180° side. Gages S11 and S12 mentioned above are located quite close to this area.)

Another area of higher than average strains was around the center plane of the body, measured by gages S17 through S22. These gages saw peak strains ranging from -400 to 680 $\mu\varepsilon$ (Figures 9-16 through 9-18).

Strains in the inner container V-clamp were measured by gages S33 and S35 on the band of the clamp and gage S34 on the clamp bolt. Little change occured in the offsets (preload strains) for this test. Figure 9-19 shows plots of data from the gages on the band and Figure 9-20 shows the bolt data.

9.7.3 Instrumented Bolt Data

Instrumentation included strain gaged bolts in the upper (lid end) RTG mounted in the payload assembly, SB1 and SB2, and in the locking ring of the outer drum, SB3. Designation, location, calibration level, peak value, and confidence level for each instrumented bolt are listed in Table 9-3.

Both of the instrumented RTG bolts were severely loaded in tension, overranging the recording system and truncating the output signals. Data from these channels, although rejected during posttest evaluation due to overranging, do show tension in each of the bolts was a minimum of 1350 $\mu\varepsilon$. Strain offset of each bolt correlates with the decrease in preload measured at disassembly (see Section 9.5 and Table 9-3).

Figure 9-21 shows the plot from bolt SB3 in the drum locking ring. This bolt initially loaded in tension and then released 115 $\mu\varepsilon$ (negative offset in plot) of the 234 $\mu\varepsilon$ preload strain present at assembly. (Static strain measured at disassembly indicated a loss of 214 $\mu\varepsilon$, Section 9.5.)

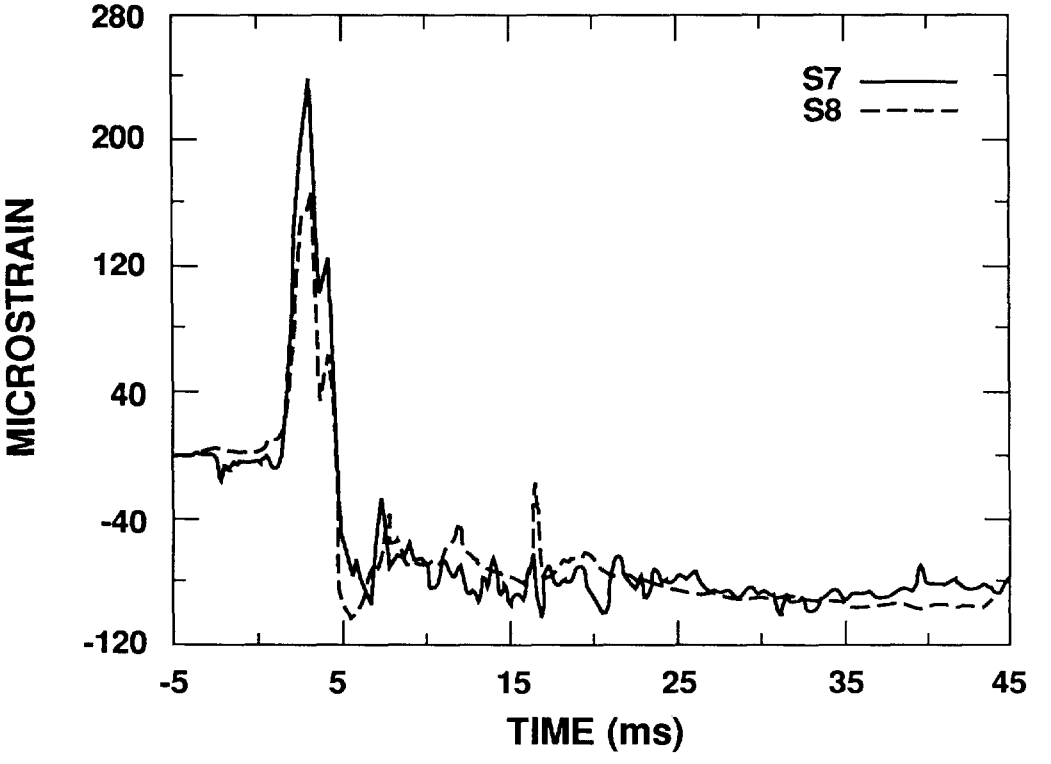

Figure 9-12. Plots of Data from Gages S7 and S8

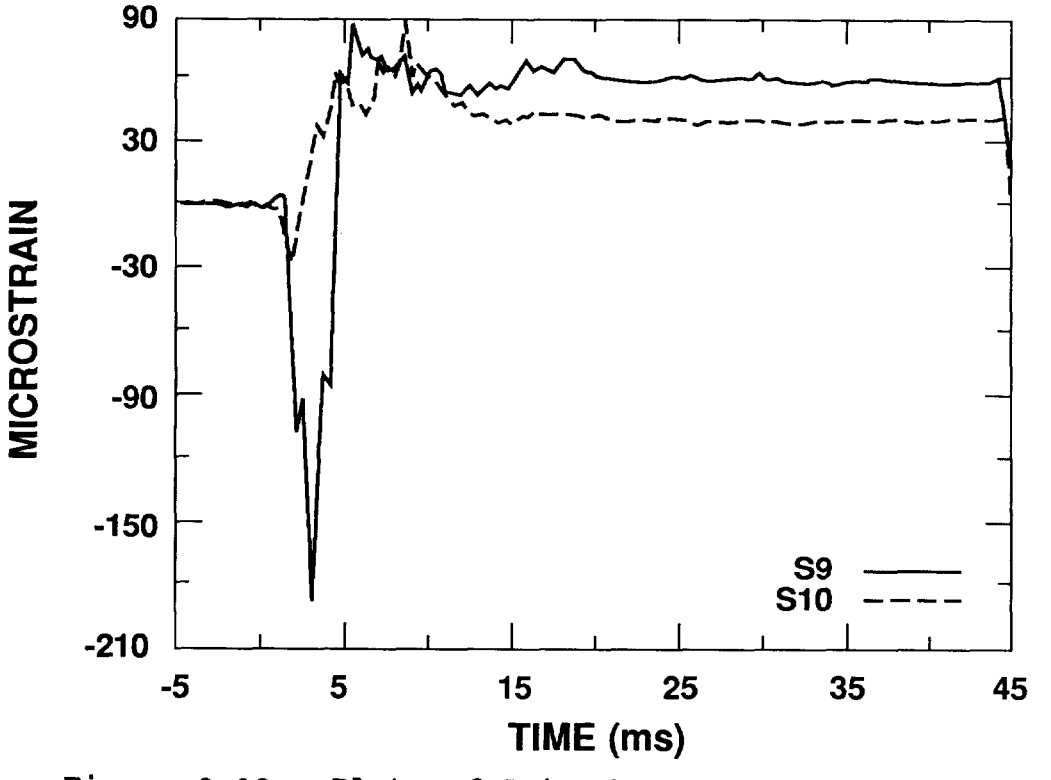

Figure 9-13. Plots of Data from Gages S9 and S10

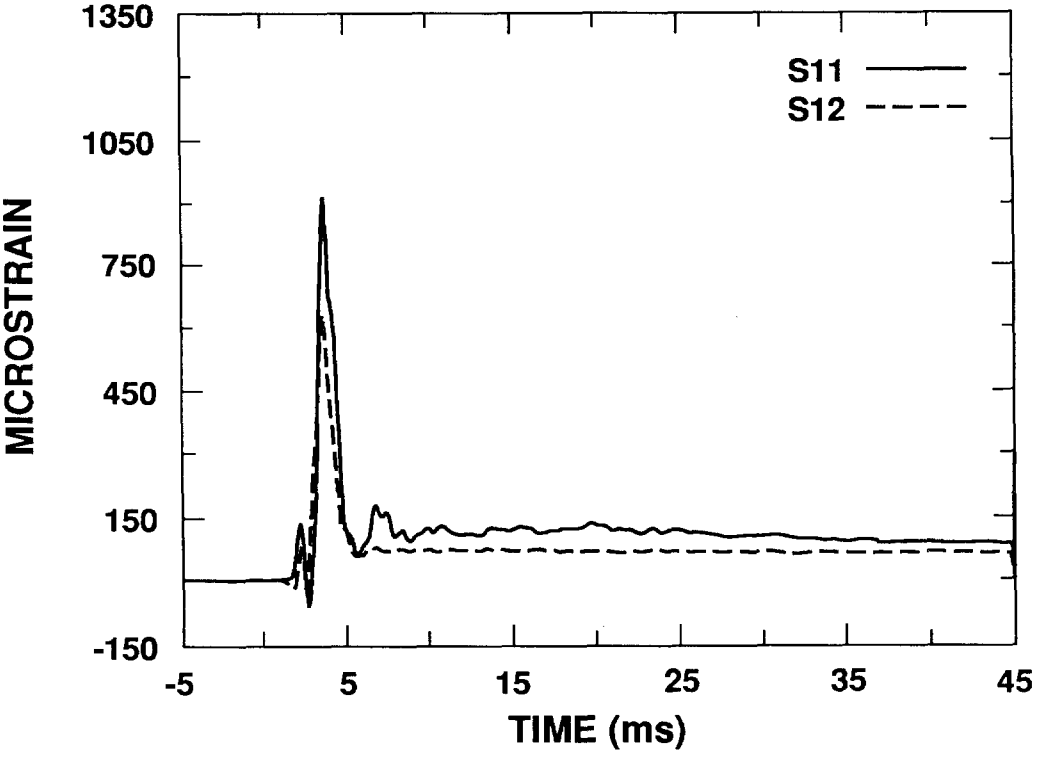

Figure 9-14. Plots of Data from Gages S11 and S12

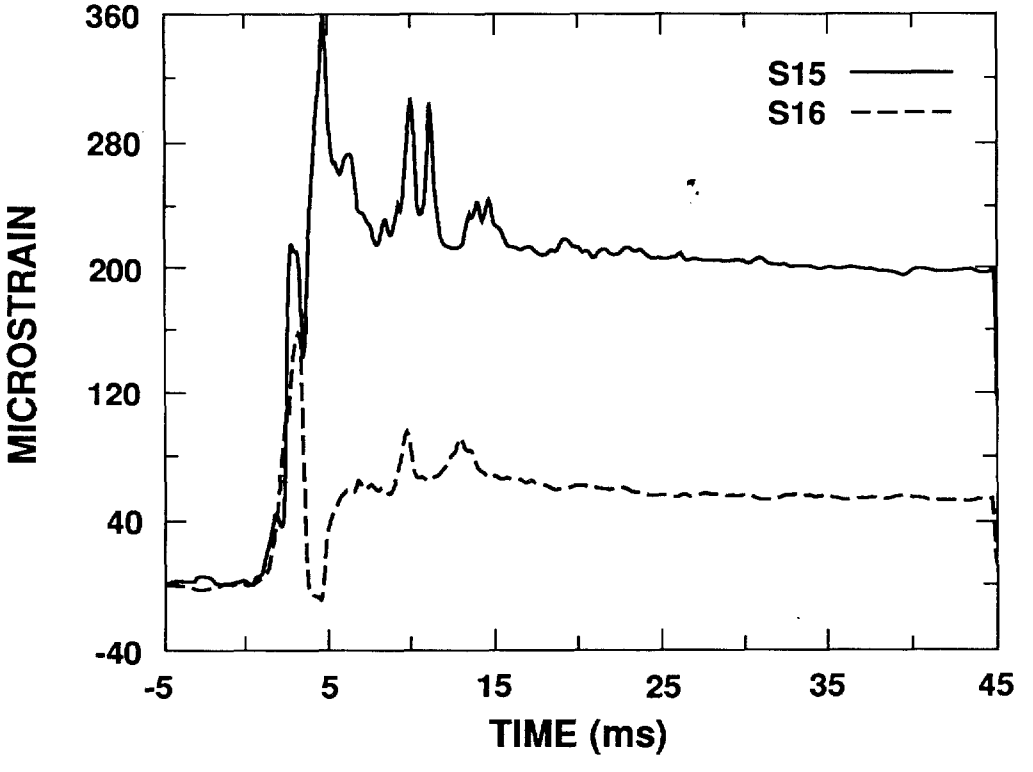

Figure 9-15. Plots of Data from Gages S15 and S16

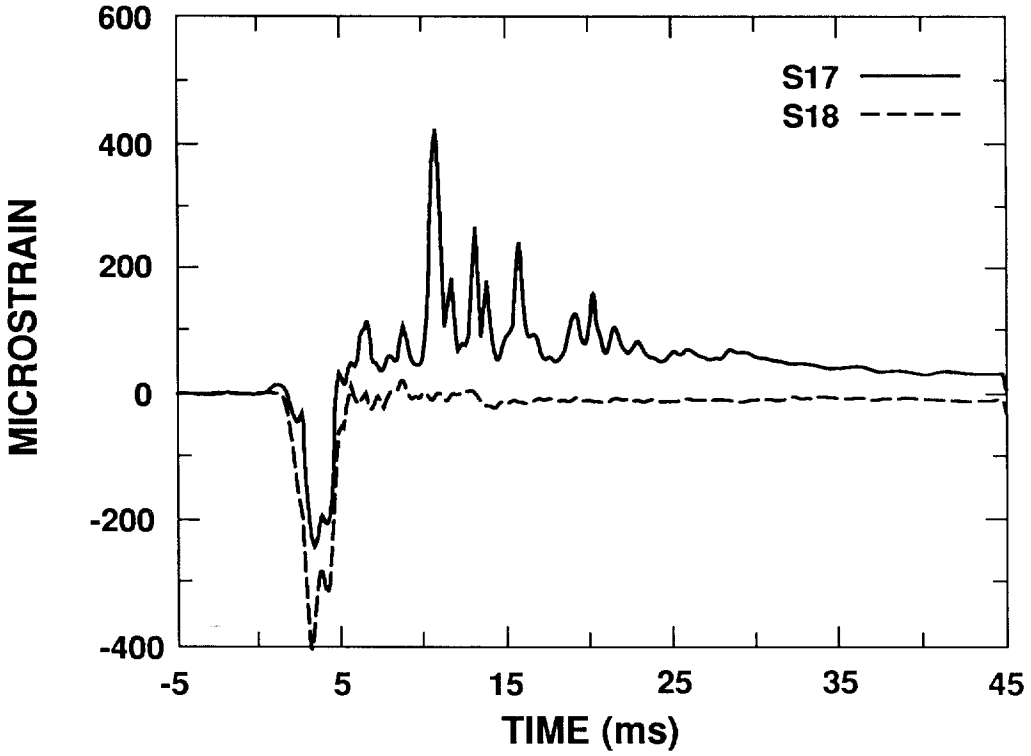

Figure 9-16. Plots of Data from Gages S17 and S18

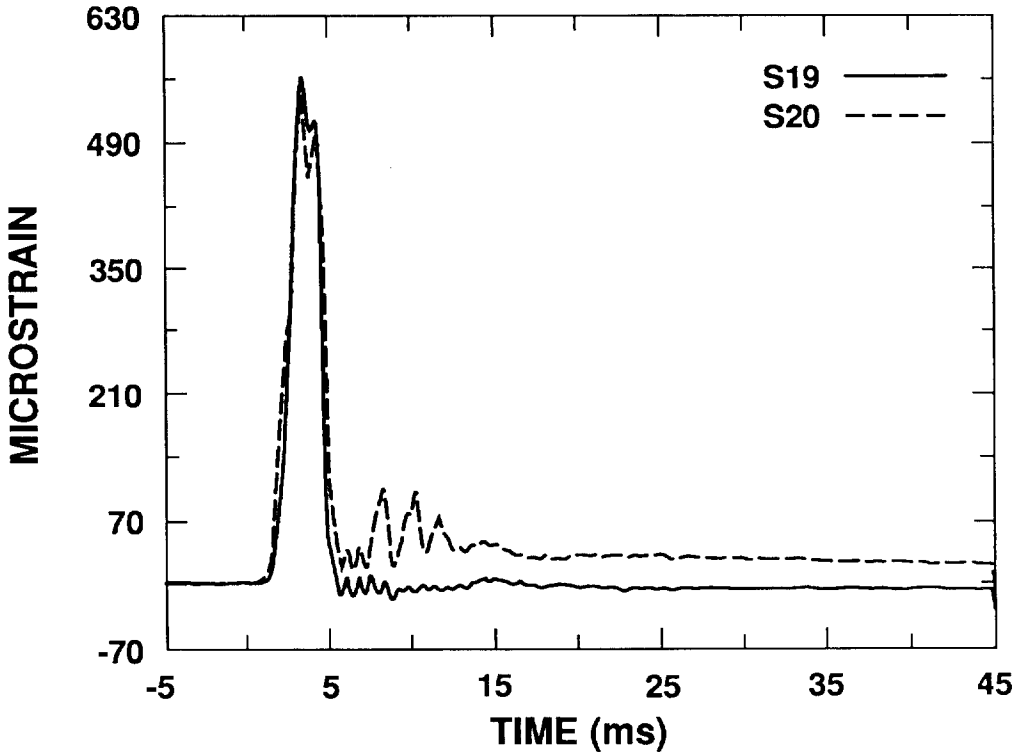

Figure 9-17. Plots of Data from Gages S19 and S20

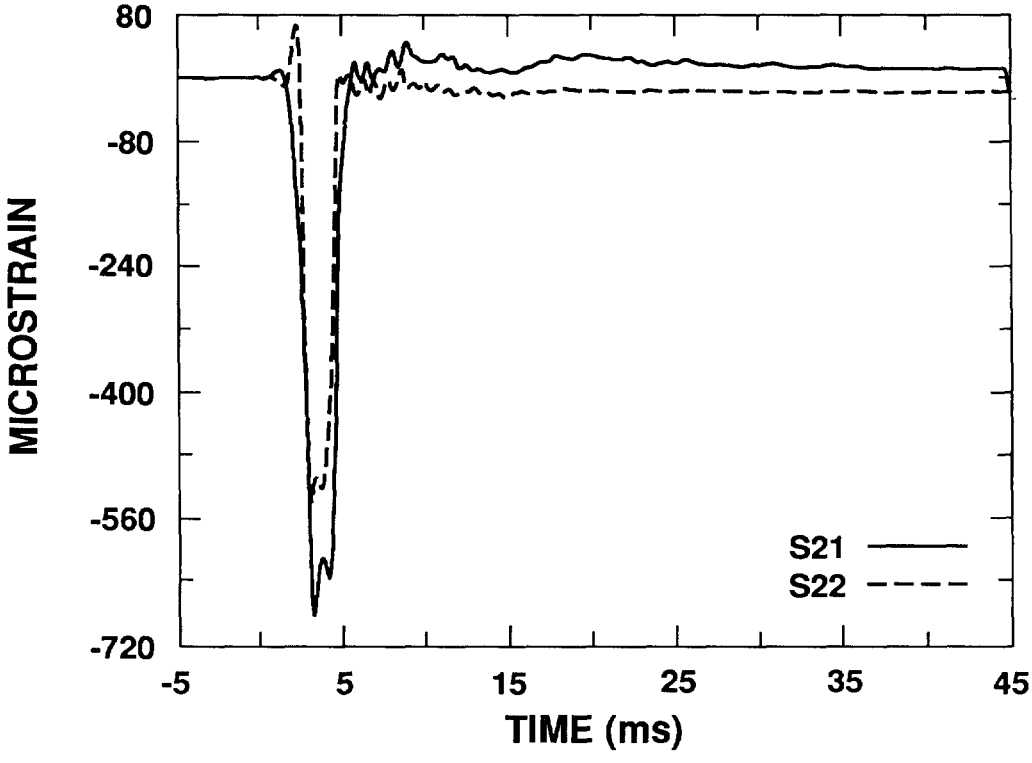

Figure 9-18. Plots of Data from Gages S21 and S22

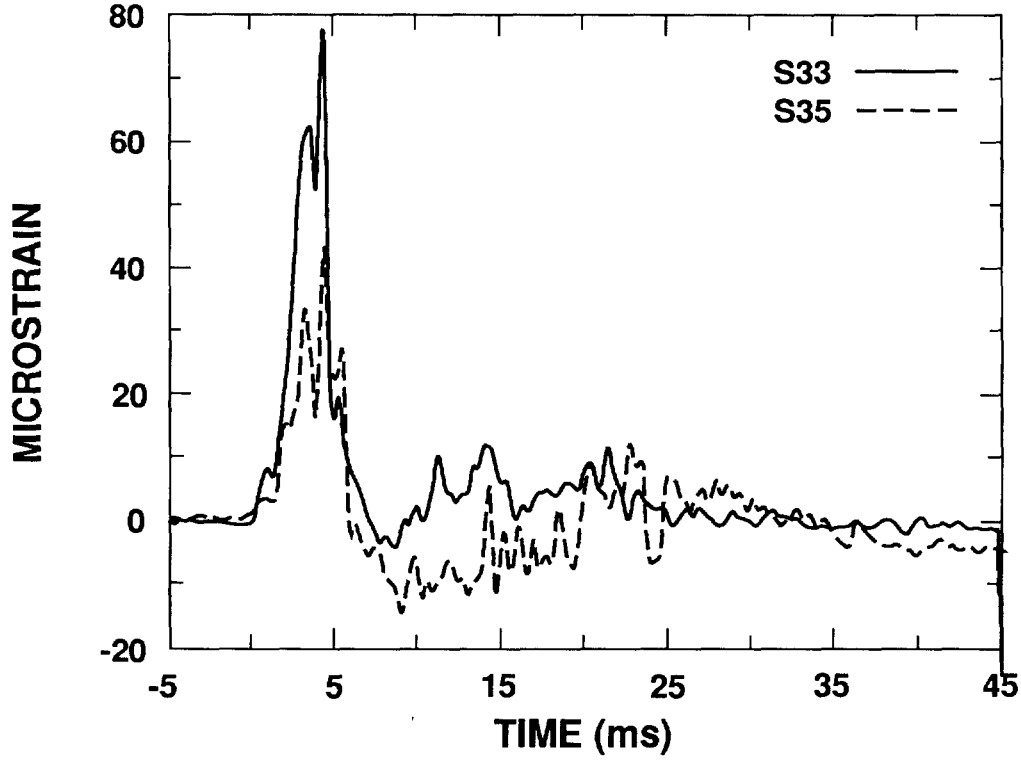

Figure 9-19. Plots of Data from Gages S33 and S35

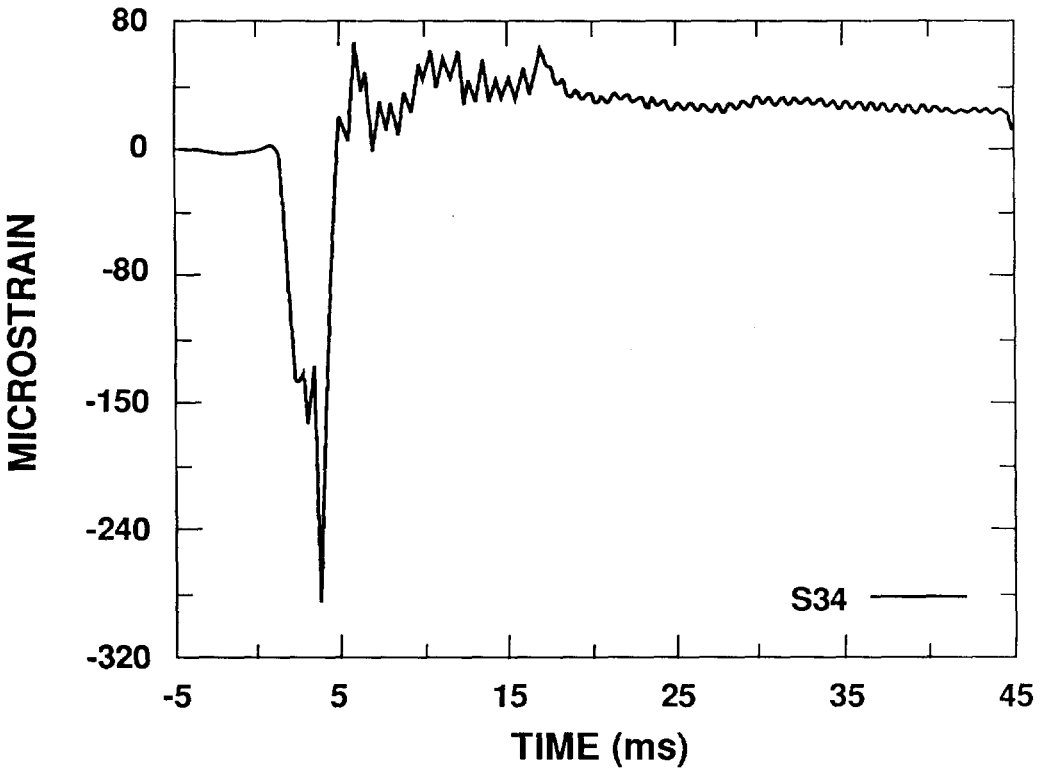

Figure 9-20. Plot of Data from Gage S34

TABLE 9-3

Instrumented Bolt Data--Side Drop Test

Component/ Location	Bolt Desig- nation	Peak Strain ($\mu\varepsilon$)	Strain Offset ($\mu\varepsilon$)	Confidence Level
RTG 0°	SB1	1350	-450	Reject
RTG 180°	SB2	1350	-100	Reject
Locking ring	SB3	150	-115	High

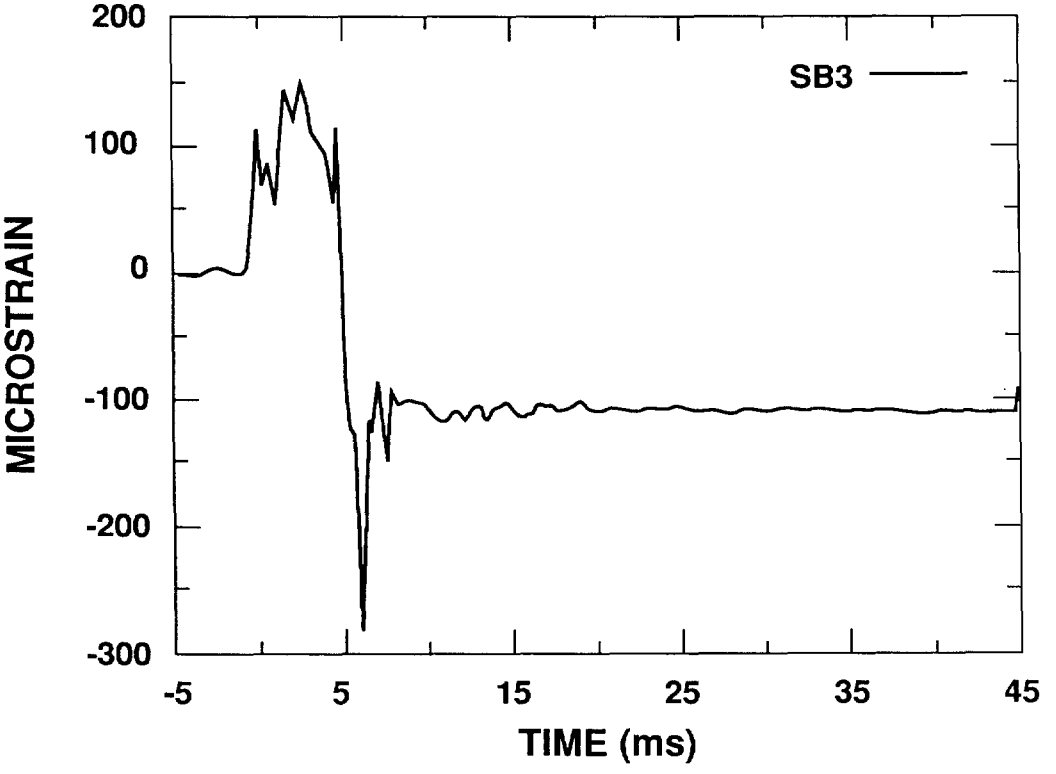

Figure 9-21. Plot of Data from Bolt SB3

10.0 END DROP TEST

10.1 Test Unit Preparation

Before assembly, the test unit inner container body, lid, and V-clamp were instrumented with the transducers defined in Section 5. Bolts (both instrumented and standard) for the RTGs were installed and torqued to specified values. Preload in the instrumented bolts was measured at this time. The bolt on the V-clamp was also torqued and the preload measured.

Helium leak-testing showed no detectable leakage of the inner container seal within the sensitivity of the leak detector (i.e., $<2 \times 10^{-10}$ atm cm^3/sec).

The inner container assembly was installed in the outer drum and Celotex used in the 4-foot normal condition drop test (Drum S-1A and Celotex S-1B). Minor drum damage resulting from the 4-foot test was repaired. A small deformation in the Celotex was not of concern because of its location with respect to the impact area for this test. All components were assembled in the same relative orientation as was used for the CG over corner drop tests (all suspected vulnerable areas located on the 180° side), even though there was no actual impact side. Internal instrumentation wiring was routed through the lid section of Celotex and out the center of the drum lid, leaving an extra service loop to allow for inner container movement. The redesigned drum lid locking ring was installed with the bolt lug oriented at 180°. The instrumented locking ring bolt was torqued to specification, and preload strain was measured and recorded.

10.2 Test Set-Up

This test was performed following the HS/RTG Bottom End Drop Test Procedure.[7] The cradle assembly was removed from the test facility's sliding beam assembly and a flat, horizontal mounting plate installed in its place. The test unit was installed with the lid mounted flush to the mounting plate. Three angled brackets held the drum by the lid locking ring (Figure 10-1). Explosive bolts fastened the brackets to the mounting plate and provided the release mechanism. The assembly (sliding beam, mounting plate, and test unit) was adjusted so that the bottom surface of the test unit was horizontal (axis at 90° to the target surface). Figure 10-2 shows the sliding beam assembly, raised to 32 feet, 4-1/2 inches (bottom surface of drum to target surface). The midpoint of the instrumentation wiring was tied to a forklift mast approximately 15 feet above the ground to remove some of the cable weight from the test unit and to reduce the possibility of impacting the test unit on the cables.

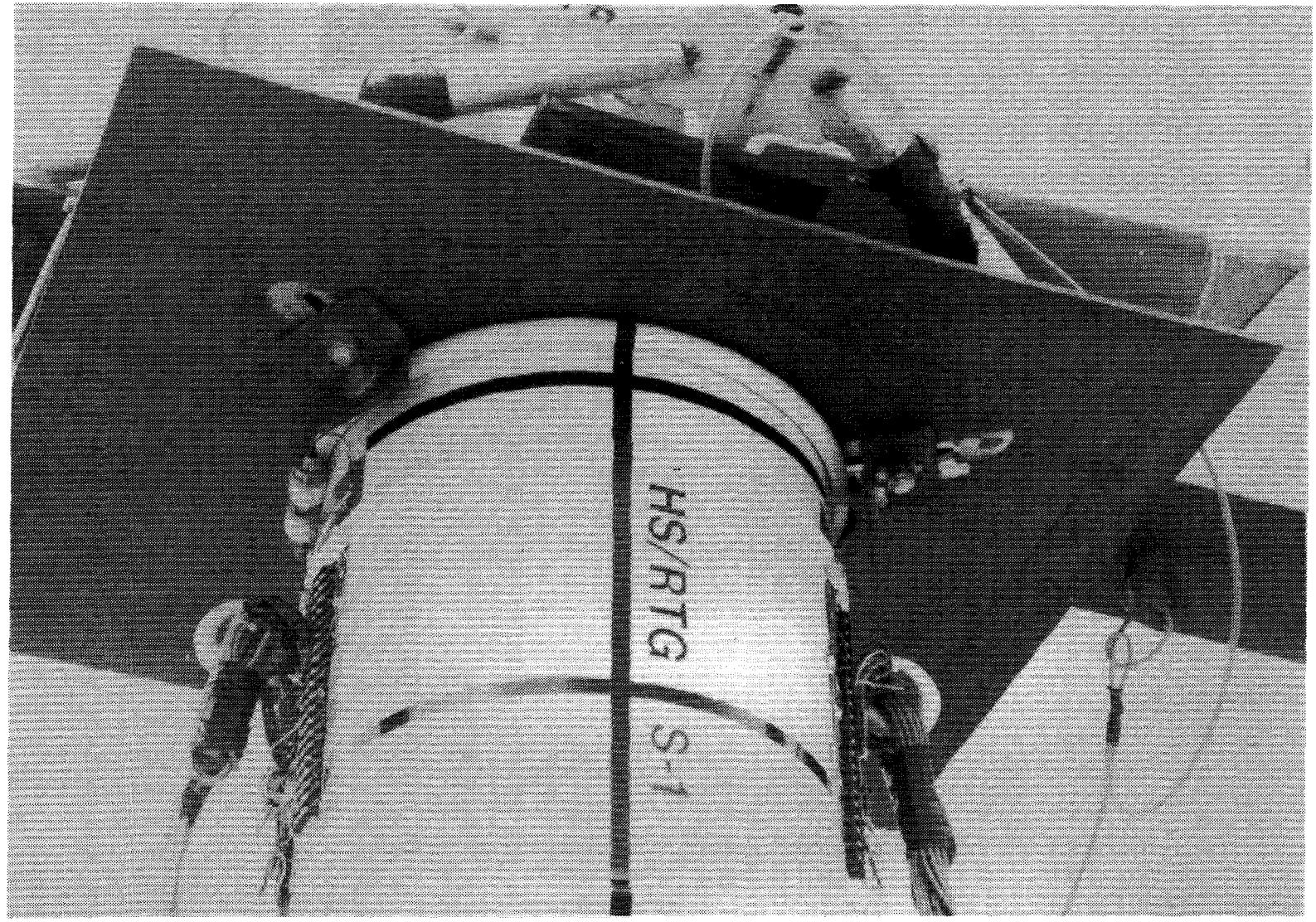

Figure 10-1. Test Unit Mounted to Plate

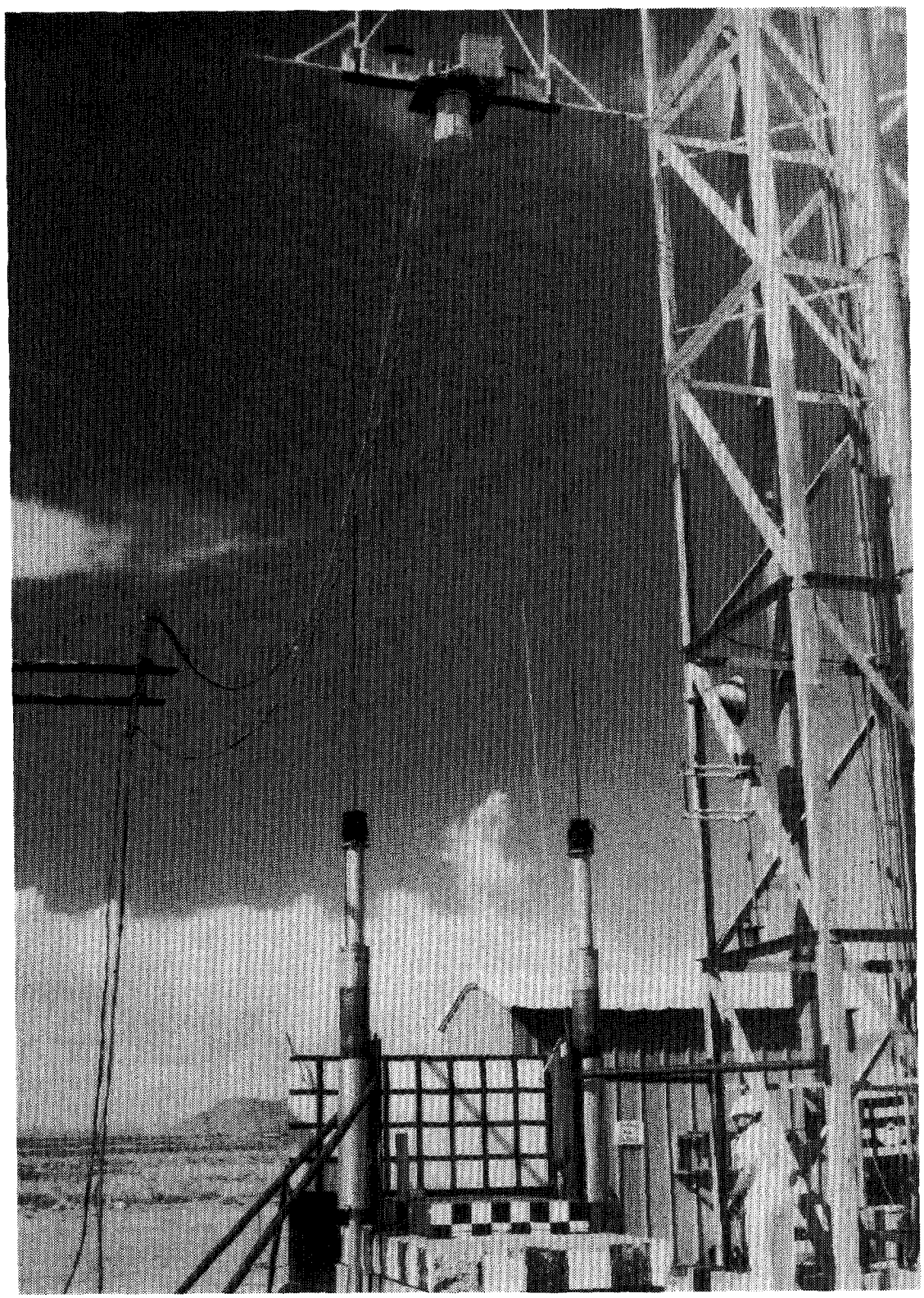

Figure 10-2. Test Set-Up

10.3 Drop Test

The drop test is shown in Figure 10-3. The test unit impacted at a velocity of 45.1 feet per second and an angle of 87°. Photographs A and B show the unit at decreasing heights above the target. Photograph D shows the unit just after impact and Photographs E and F show the unit rebounding off the target. Total impact duration was estimated to be 5 to 6 ms. The unit came to rest on the target.

Although the drop test was successful in that it provided the required impact velocity and angle, instrumentation problems were encountered. During the drop, shrapnel from the explosive bolts damaged instrumentation wiring (Figure 10-4). Many transducer leads were severed, causing a complete loss of data for those channels. Section 10.7 contains a list of affected channels. In addition, the digital recording system failed because of a power fluctuation. Data were recorded on the back-up magnetic tape system. Although this system did supply data, it is of lower quality, with a lower signal to noise ratio.

10.4 Exterior Deformations

Damage to the outer drum is shown in Figures 10-5, 10-6, and 10-7. Deformed area is limited to the bottom 2 inches of the drum. The bottom 1/2 inch of side wall, which is smaller in diameter than the drum itself, collapsed in an accordion fashion. Maximum crush measured 0.85 inch near the 180° side, correlating with photometric data showing this side of the drum impacted first. Average crush around the bottom was approximately 0.6 inch.

10.5 Disassembly

A complete disassembly was performed after the end drop test. Posttest torque on the locking ring bolts was measured at ~140 inch-pounds, a decrease of 40 inch-pounds from assembly. Bolt load was measured at 134 $\mu\varepsilon$, a decrease of 100 $\mu\varepsilon$ from assembly. These load losses are attributed to general shock and vibration during testing because the top of the drum saw no direct impacts. The locking ring and lid were easily removed, as was the lid section of Celotex.

Removing the inner container assembly revealed an indentation in the Celotex under the inner container V-clamp. The V-clamp was not in contact with the Celotex before the test, indicating that the bottom of the inner container assembly had deformed the bottom of the cavity 0.05 to 0.1 inch. The body section of Celotex, while snug around the bottom of the drum, was removable. Net change in drum height does not represent actual Celotex crush because most deformation was to the bottom lip and not to the actual bottom of the drum (Figure 10-7). Deformations to the Celotex at the

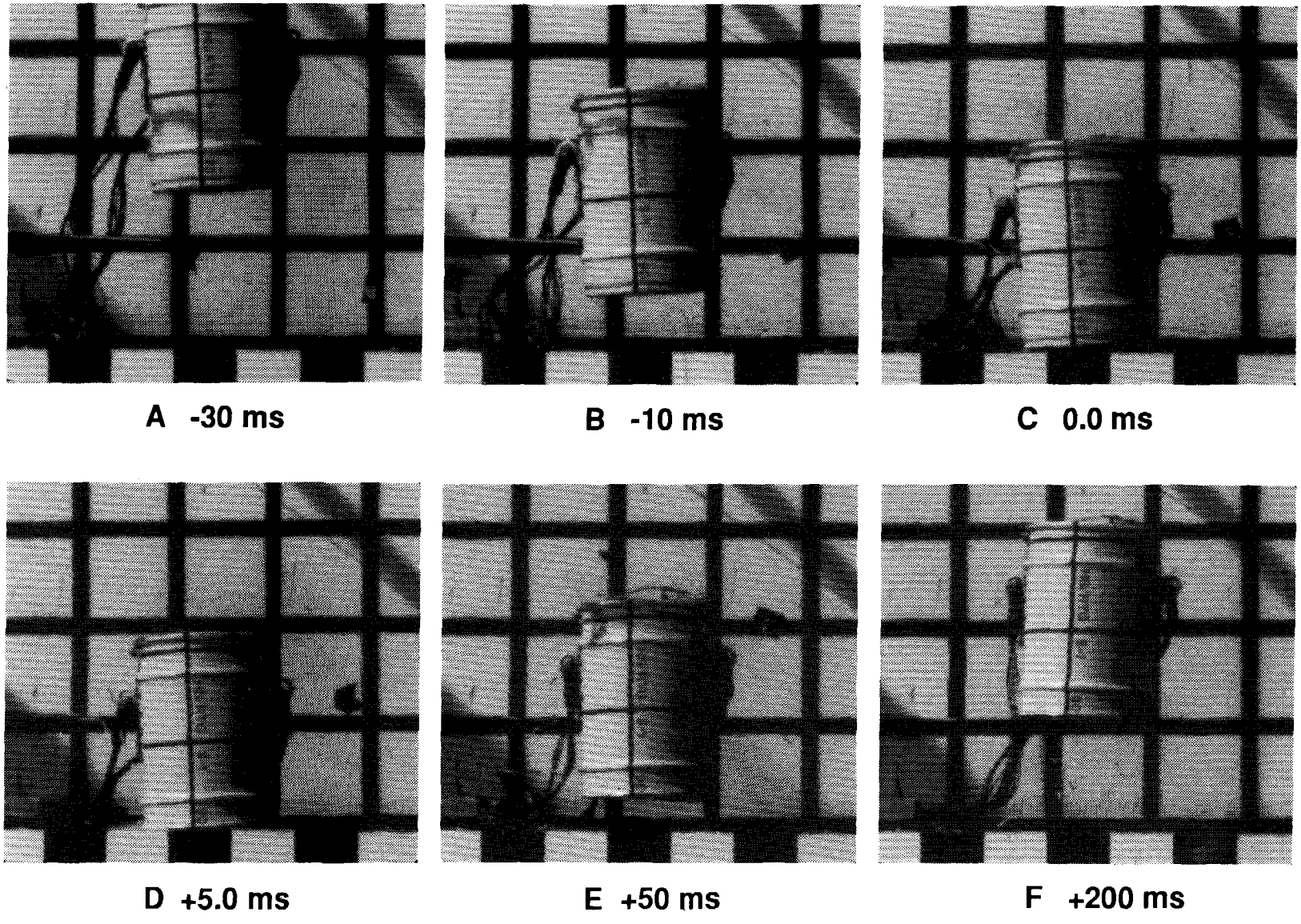

Figure 10-3. Test Sequence

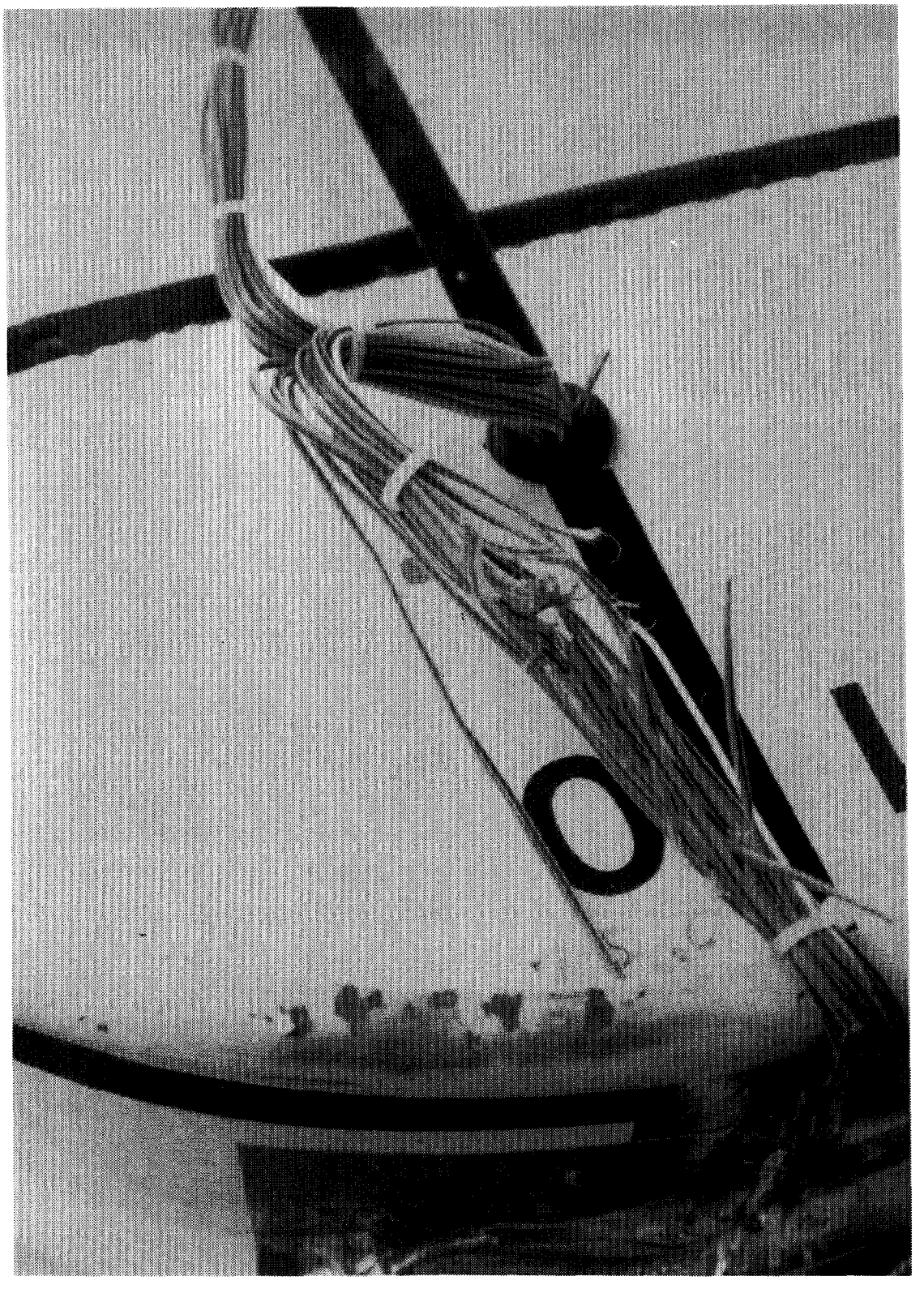

Figure 10-4. Wiring Damage

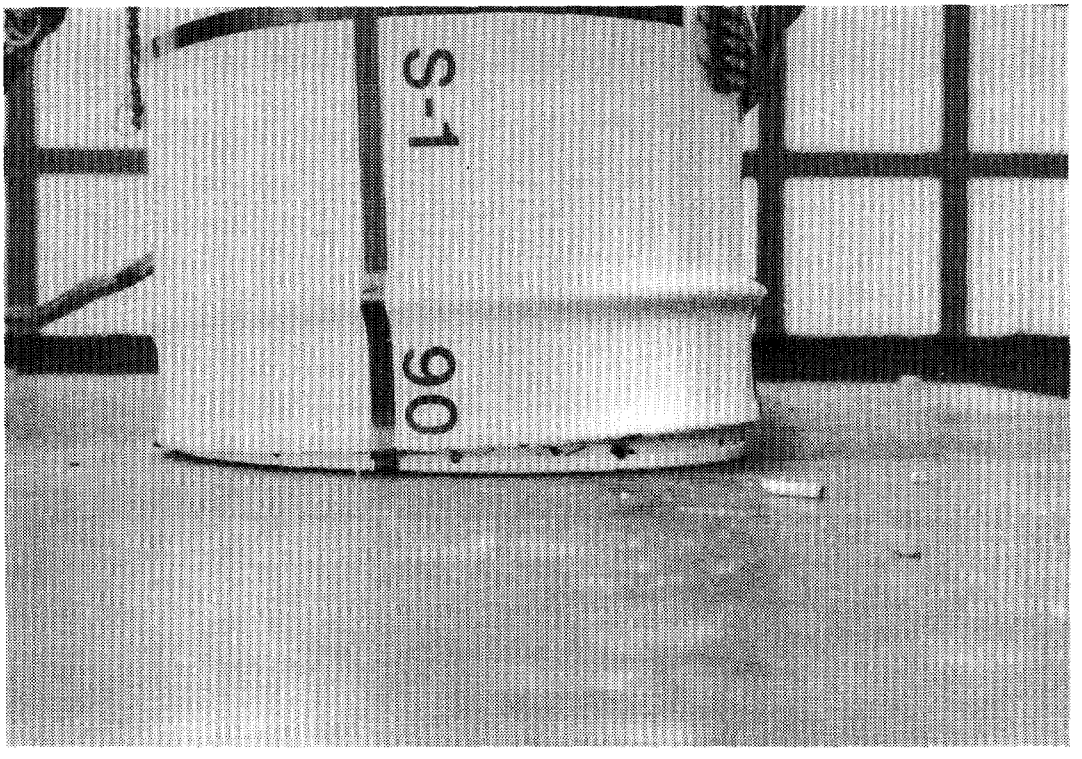

Figure 10-5. Posttest Deformations

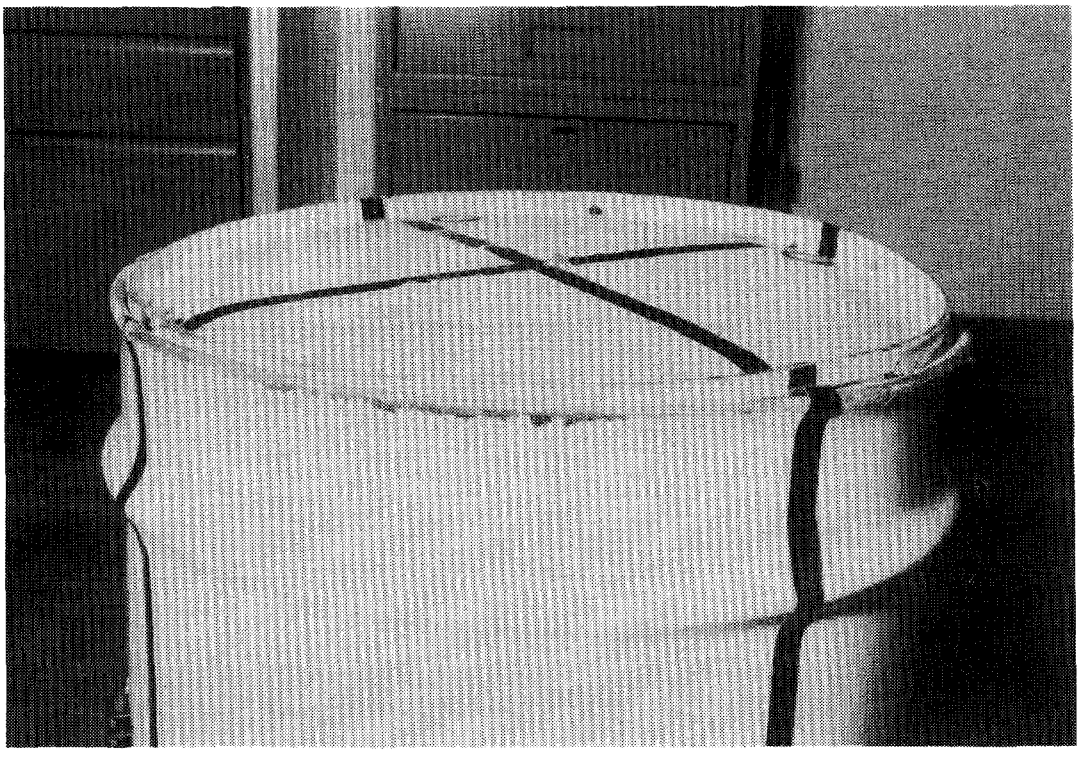

Figure 10-6. Outer Drum Deformations

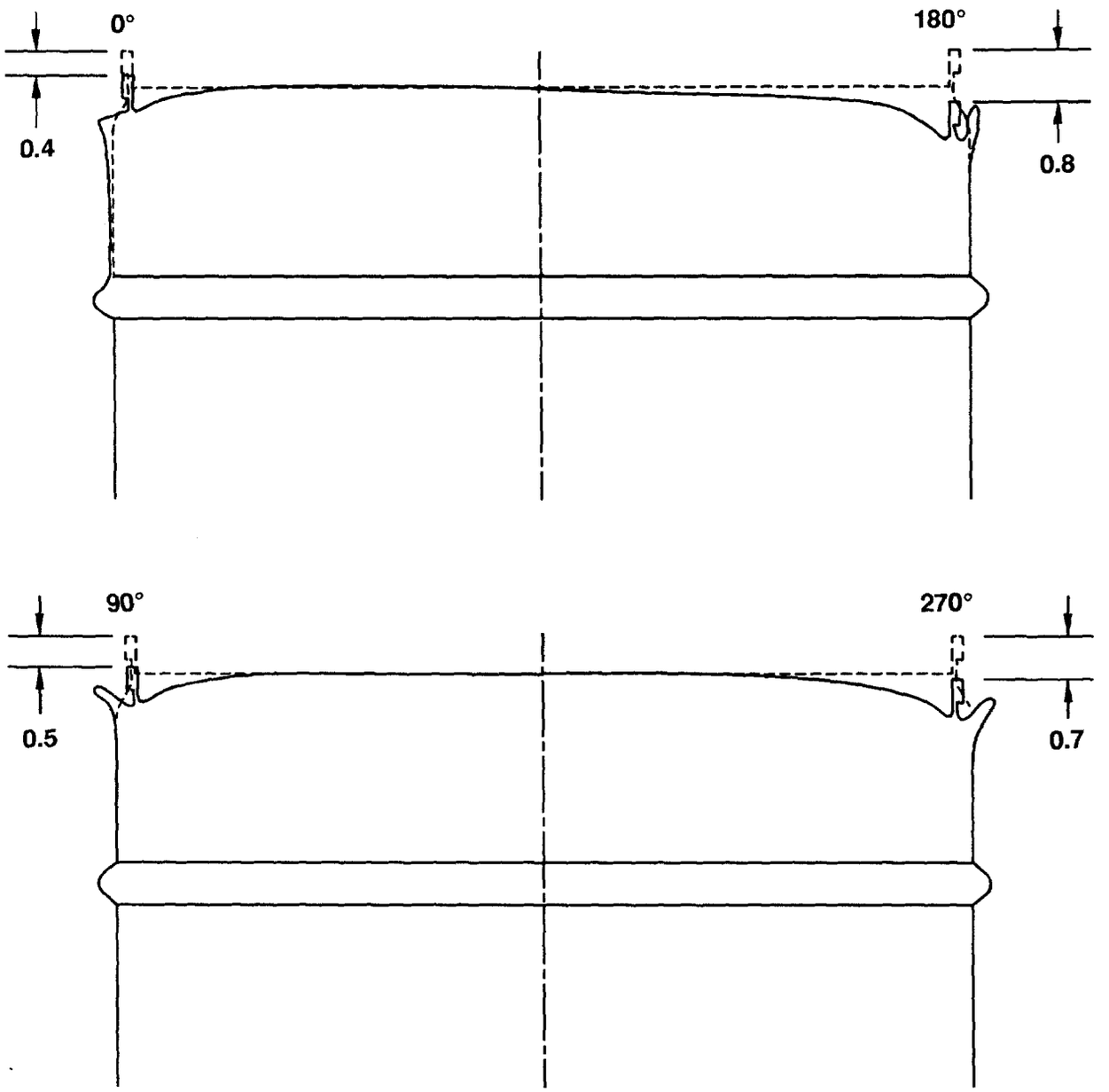

Figure 10-7. Sketch of Deformations

bottom (impact) region showed only slight crushing around the outer edge. Deformation averaged 0.20 inch around the outer edge and tapered to zero within 1 inch of the outer edge.

After visual inspection and leak-testing of the inner container seal, the inner container was disassembled. Post-test torque and preload strain of the V-clamp bolt were measured to be 618 $\mu\varepsilon$ and 85 inch-pounds, showing a decrease of 322 $\mu\varepsilon$ from the 940 $\mu\varepsilon$ assembly strain and a decrease of 15 inch-pounds from the assembly torque. The V-clamp and lid were then removed.

Orientation of the payload assembly remained at 0° with relation to the container body. Tightness of the bolts securing the RTGs was checked as well as the preload for the instrumented RTG bolts. RTG bolt data are listed below.

Bolt	Location	Approximate Net Change in Torque (inch-pounds)	Approximate Net Change in Preload ($\mu\varepsilon$)
SB1	0° upper RTG	-5	-288
SB2	180° upper RTG	0	-158
B5	0° lower RTG	-5	NA
B6	180° lower RTG	-5	NA

10.6 Results

A leak test of the inner container seal showed no detectable leak within the sensitivity of the leak detector (5×10^{-10} atm cm^3/sec).

A complete mechanical inspection of the inner container body and lid were performed at the conclusion of this test. No inspection was made after the CG over corner or side drop tests, and changes noted at this inspection could not be definitely attributed to a particular test.

There was no indication of deformation to either the lid or the cylindrical section of the container body. A very slight change of 0.2° was noted in the area of the flange near the 180° side. This was the same area of movement indicated by the inspections following the overpressure and normal conditions of transport tests. Relatively high strain and offsets were measured by gages S15 and S16 (on the flange at 180°), particularly in Test 3, the CG over corner drop test.

The Celotex insulation was measured for deformations as noted in Sections 10.4 and 10.5.

10.7 Results--Transducer Data

As mentioned in Section 10.3, many data channels were lost because of wiring damage. Affected transducers consisted of one accelerometer, one instrumented bolt, and 13 strain gages. An asterisk in the peak value column identifies these channels on the respective transducer data tables.

10.7.1 Accelerometer Data

Accelerometers for the end drop test consisted of six transducers as defined in Section 5.2. All were oriented in the Z direction, i.e., the direction of impact. Mounting locations consisted of A2Z and A3Z on opposite sides of the outer drum, A5Z and A6Z on opposite sides of the inner container body, A8Z on the inner container lid, and A9Z on the payload assembly. Values presented are based on data that has been filtered at 1,000 Hz. Figure 10-8 is a layout of the accelerometers with the peak deceleration values labeled. Table 10-1 lists the accelerometer designation, location, calibration value, peak acceleration measured, and confidence level of each transducer.

Decelerations of the outer drum were measured by A2Z and A3Z mounted on opposite sides at the center of the drum. Plots of these data with average peak values of 540 g were recorded (Figure 10-9).

Inner container body decelerations were measured by A5Z and A6Z (Figure 10-10). The pulses show a delay of 1 ms from initial drum impact. Both accelerometers recorded peak values of 750 g. These values appear to be inconsistent since they are higher than the decelerations recorded for the outer drum. The movement of the payload may have contributed to these higher peaks, which occur between 4 and 5 ms.

Accelerometer A9Z measured the response of the payload assembly (Figure 10-11). The plot shows a time delay of approximately 1.5 ms from outer drum impact. Although the measured peak is large, it does not contain the higher frequency content of the payload accelerometers noted on previous tests, possibly because of the felt cushion located at the bottom of the inner container.

10.7.2 Strain Gage Data

Instrumentation for the end drop test included 28 strain gages as defined in Section 5.1. These gages measured surface strain on the exterior of the inner container body and lid. Gages were also mounted on the V-clamp ring and bolt. Table 10-2 lists the gage designation, peak strain measured, strain offset, and confidence level of each measurement.

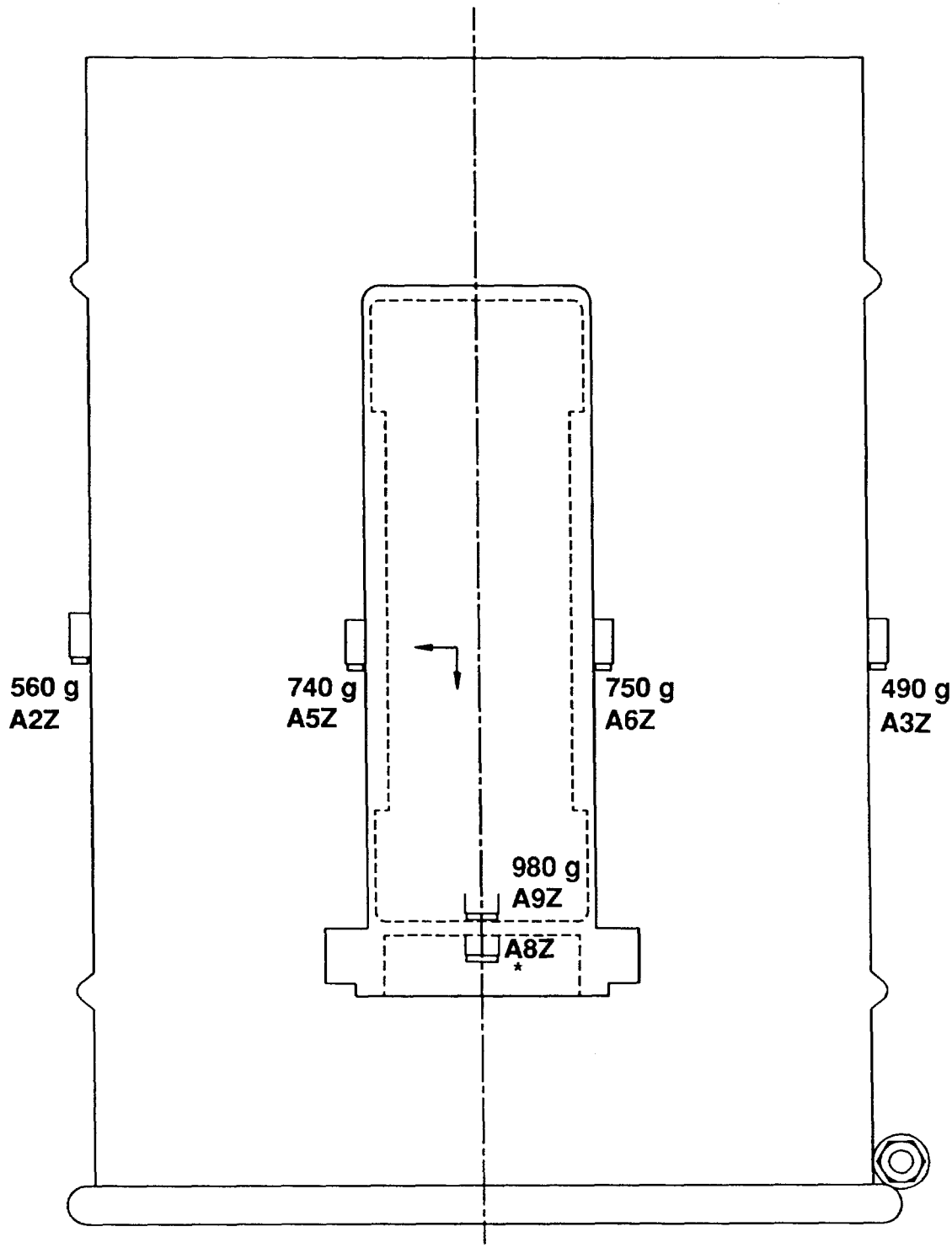

Figure 10-8. Peak Accelerations--End Drop Test

TABLE 10-1

Accelerometer Data--End Drop Test

Component	Accelerometer Designation	Calibration Value (g)	Peak Acceleration (g)	Confidence Level
Outer Drum	A2Z	4,000	560	High
	A3Z	4,000	490	High
Inner	A5Z	4,000	740	High
Container	A6Z	4,000	750	High
Inner Lid	A8Z	4,000	*	Reject
Payload	A9Z	4,000	980	High

*No data: wiring damage.

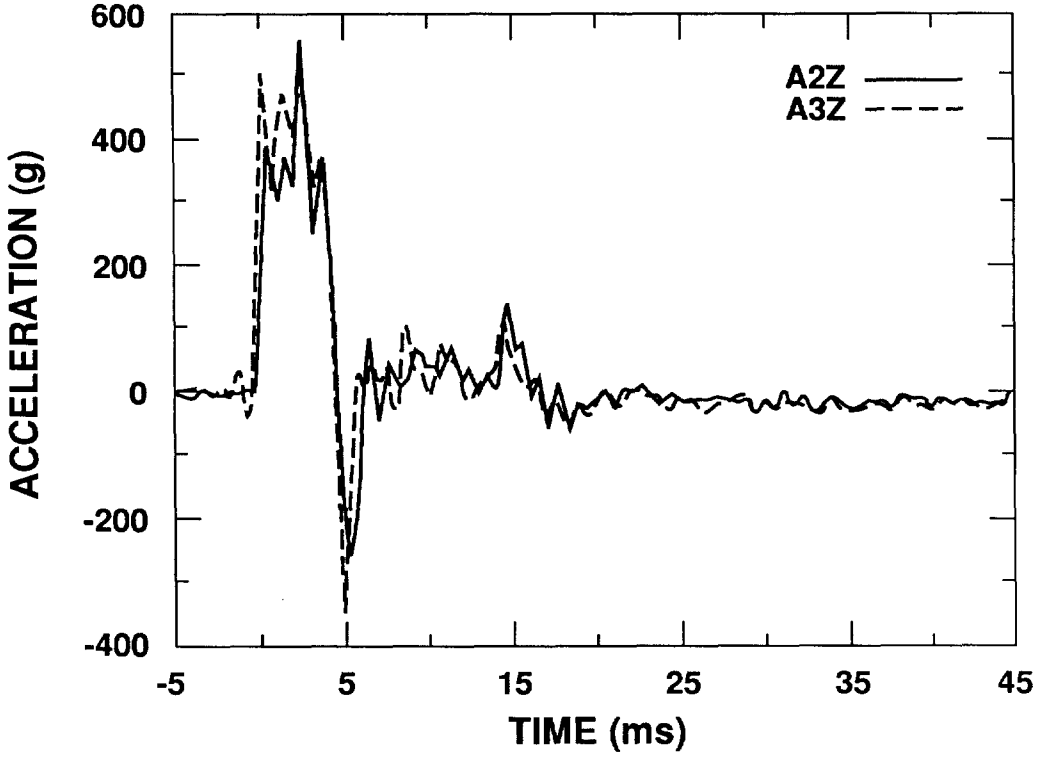

Figure 10-9. Plots of Data from Accelerometers A2Z and A3Z

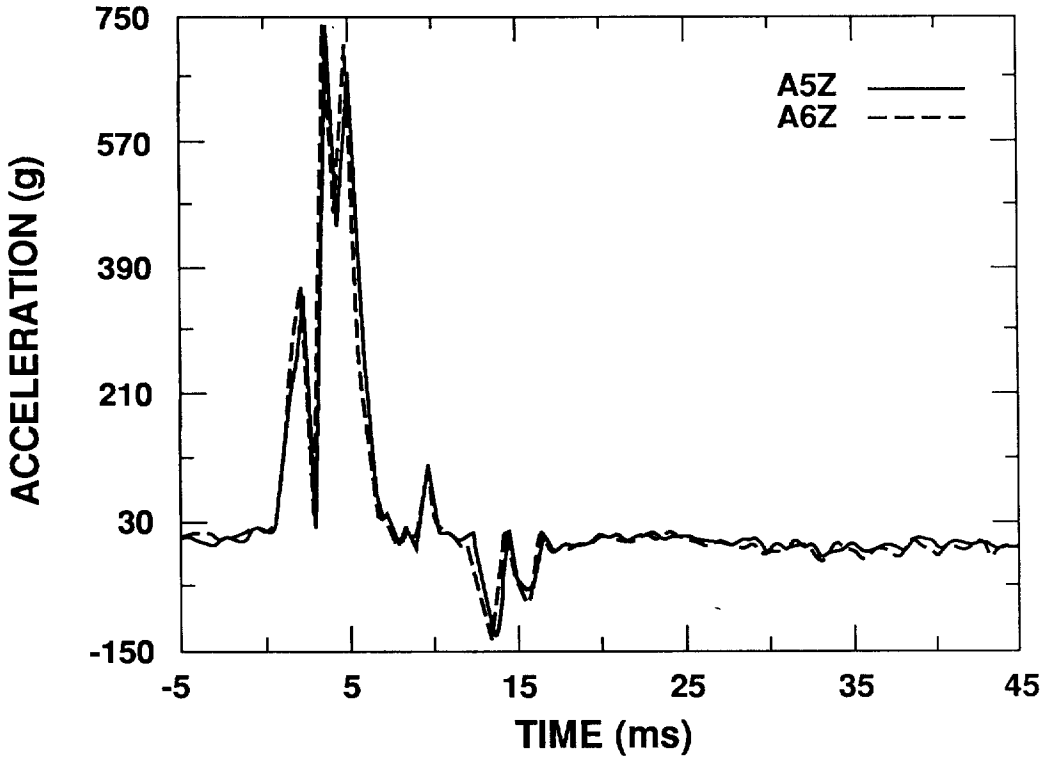

Figure 10-10. Plots of Data from Accelerometers A5Z and A6Z

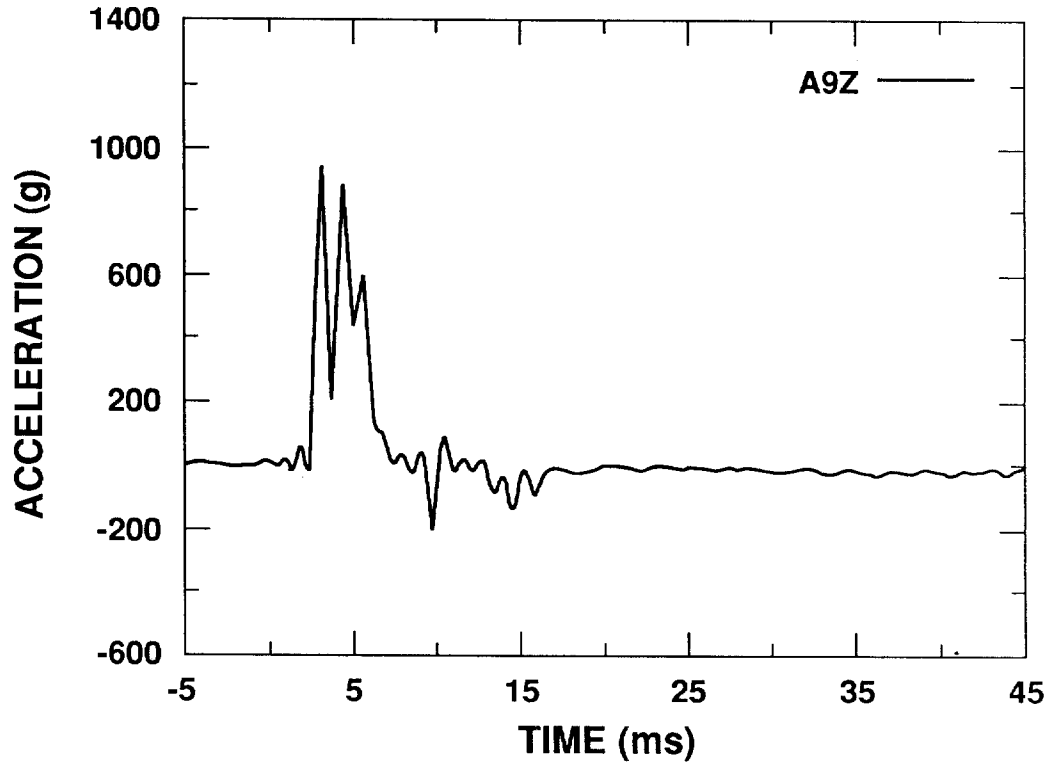

Figure 10-11. Plot of Data from Accelerometer A9Z

TABLE 10-2

Strain Gage Data--End Drop Test

Component/ Location	Gage Designation	Peak Strain ($\mu\varepsilon$)	Strain Offset ($\mu\varepsilon$)	Confidence Level
Lid	S1	*	*	Reject
	S2	95	10	High
	S3	1,100	0	Reject
Lid Flange	S5	95	-35	Good
	S6	115	65	Good
Top of Body	S7	*	*	Reject
	S8	12,000	0	Reject
	S9	180	0	Good
	S10	80	-5	Good/High
	S11	*	*	Reject
	S12	*	*	Reject
Body Flange	S15	*	*	Reject
	S16	105	65	High
Center of Body	S17	*	*	Reject
	S18	*	*	Reject
	S19	*	*	Reject
	S20	58	-5	High
	S21	*	*	Reject
	S22	*	*	Reject
Bottom of Body	S25	*	*	Reject
	S26	85	12	High
	S27	*	*	Reject
	S28	90	0	High
	S29	*	*	Reject
	S30	49	5	High
V-Clamp	S33	180	30	Good
	S34	-90	230	Good
	S35	710	80	Good

*No data: wiring damage.

A large number of the lost data channels were strain gage channels. Lacking other channels for comparison, this loss affected the confidence level of what may be accurate measurements.

As in the previous drop tests, most measured strains were low (below 100 $\mu\varepsilon$). Notable exceptions are explained below.

Gages S3 and S8 recorded unusually high peaks. Wide band data from these channels show the signal at the upper level of the recording system, indicating an open or shorted circuit. Data from these channels were rejected.

Gage S9 showed a peak strain of 180 $\mu\varepsilon$. Data from gages S9 and S10 are presented in Figure 10-12. The spike in S9 at 9 ms is also attributed to a wiring problem and that anomaly was not considered in the evaluation.

Strains in the inner container V-clamp were measured by gages S33 and S35 on the band of the clamp and gage S34 on the clamp bolt. An offset in these data indicates a change in the strain in the clamp at assembly. Figure 10-13 shows plots of data from the gages on the band. Although these do not correlate well, both of these plots show a tension loading and high offset. This may be caused by tension in the band, concentrated at the bolting side at assembly, which was transferred around the band during the impact. Data from gage S34 is confusing. The pulse does not correlate well with the band gages, and a high positive (tension) offset occurs quite late in the event (Figure 10-14). This tension offset conflicts with the bolt preload measured at disassembly, which showed a net loss of 230 $\mu\varepsilon$ preload, and should have resulted in a negative offset in the data. There are two possible explanations: the signal was inverted by the data acquisition system or the bolt underwent a combination of loosening and bending.

10.7.3 Instrumented Bolt Data

Instrumentation included strain-gaged bolts in the upper (lid end) RTG mounted in the payload assembly, SB1 and SB2, and in the locking ring of the outer drum, SB3. Table 10-3 contains the instrumented bolt data. Bolt SB1 (Figure 10-15) loaded in tension to 1,500 $\mu\varepsilon$ and then released slightly. This correlates with the strains measured at disassembly, which indicated a loss of approximately 200 $\mu\varepsilon$ during the test. Although no data were obtained from bolt SB2, preload recorded at disassembly showed a loss of 158 $\mu\varepsilon$ from the assembly preload measurement.

The plot from bolt SB3 on the drum locking ring is shown in Figure 10-16. This bolt initially loaded in tension and then released 70 $\mu\varepsilon$ (negative offset in plot). This correlates to the static strain measurement at disassembly, which indicated a loss of 100 $\mu\varepsilon$ from the assembly strain.

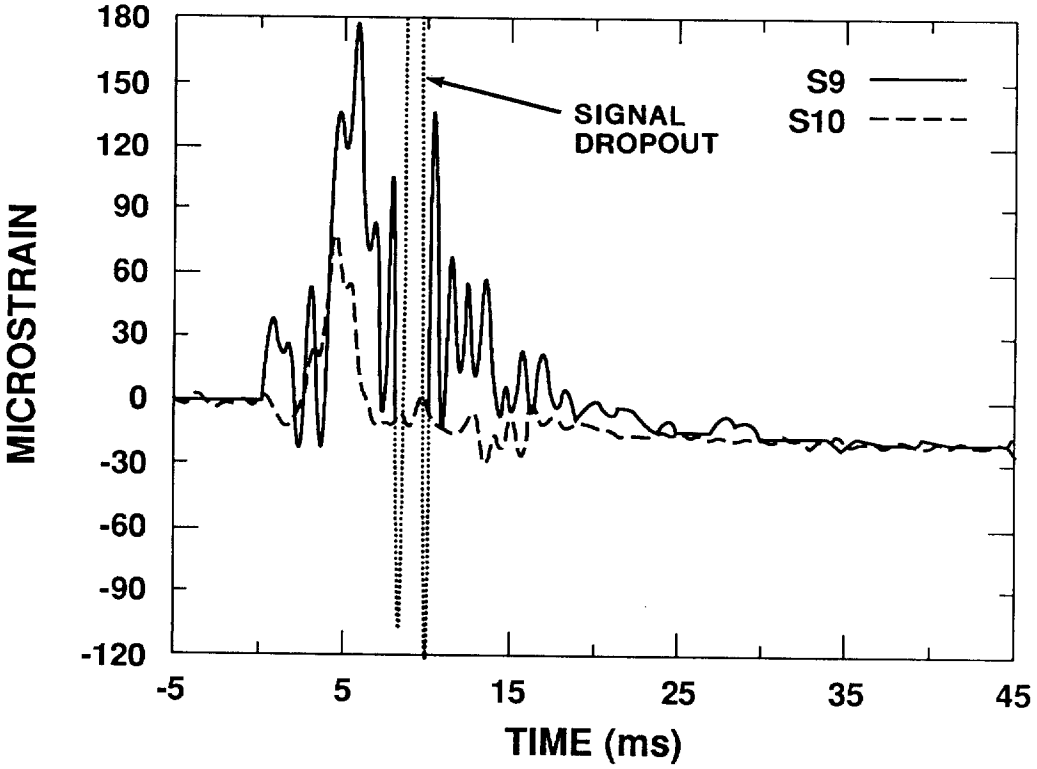

Figure 10-12. Plots of Data from Gages S9 and S10

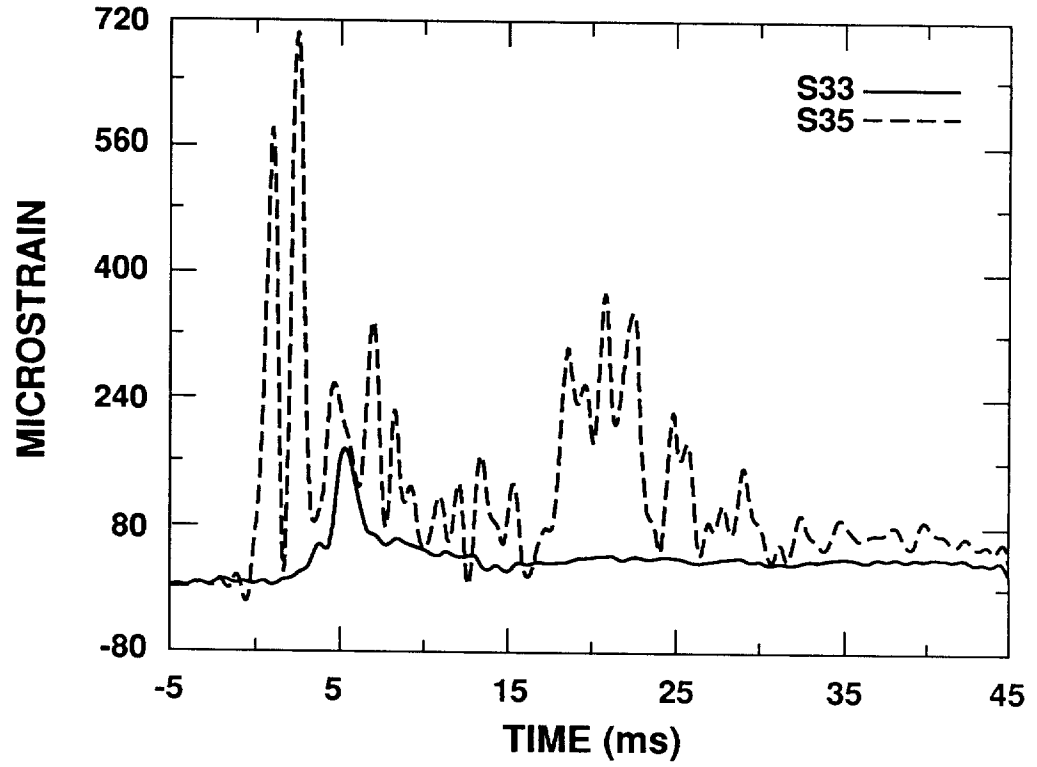

Figure 10-13. Plots of Data from Gages S33 and S35

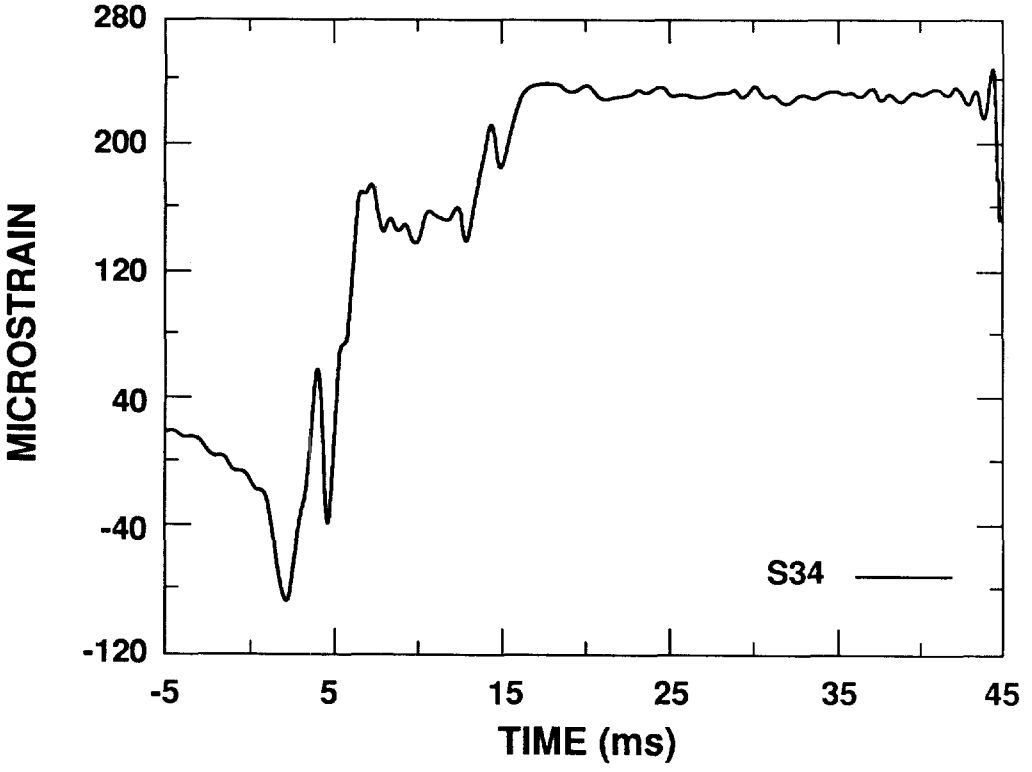

Figure 10-14. Plot of Data from Gage S34

TABLE 10-3

Instrumented Bolt Data--End Drop Test

Component	Bolt Designation	Peak Strain ($\mu\varepsilon$)	Strain Offset ($\mu\varepsilon$)	Confidence Level
RTG 0°	SB1	1,500	-200	High
RTG 180°	SB2	*	*	Reject
Locking ring	SB3	205	-70	High

*No data: wiring damage.

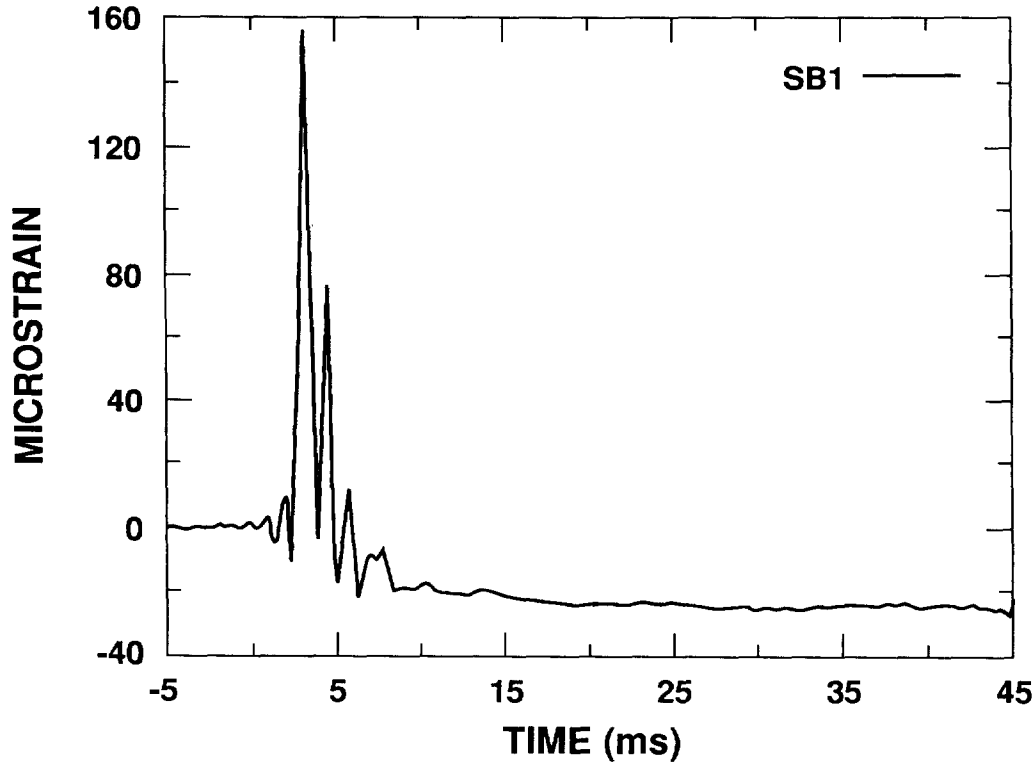

Figure 10-15. Plot of Data from Bolt SB1

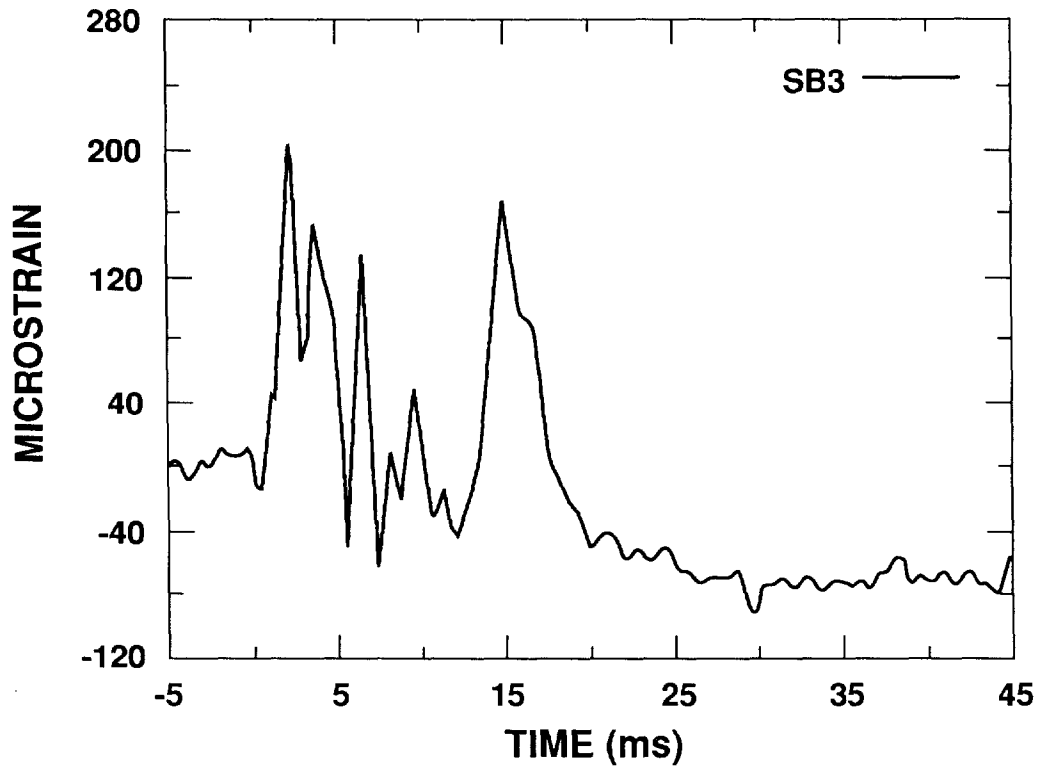

Figure 10-16. Plot of Data from Bolt SB3

11.0 PUNCTURE TESTS

Five puncture tests were performed. One test was performed on each of the three previously drop-tested units, with the punch attacking the damaged area. Two additional punch tests were performed, directing the punch at the lid locking ring. All tests were a minimum 40-inch free fall drop onto 6-inch diameter, mild steel spikes that conformed to the requirements of 10 CFR 71.73.[1] Each spike and integral base was welded to the drop target. Two different length spikes were used: an 8-inch-long spike for the three tests which attacked previously damaged areas and a 24-inch-long version to attack the lid locking ring. The five punch test configurations are shown in Figure 11-1. All punch tests followed the HS/RTG 40-inch Puncture Test Procedure.[8]

All punch tests were conducted at ambient temperature. No instrumentation was used for the puncture tests. Nondestructive evaluations included a leak test after each test (or pair of tests) on each test unit and a mechanical inspection of the inner container after the last test. Details of the test sequence and related operations are contained in Section 3.

11.1 Tests A and B--Center of Gravity Over Corner Test Unit

11.1.1 Test Unit Preparation

The RTG payload and inner container assembly were assembled in standard fashion. Torque on the RTG bolts and the V-clamp bolt was measured during assembly. This would be the only assembly of the inner container for the entire series of punch tests.

Helium leak-testing of the inner container seal demonstrated a leakage rate of 4×10^{-10} atm cm^3/sec. This small rate was a result of outgassing of the O-ring material. Appendix A contains a detailed description of the leak tests performed.

The inner container assembly was installed in the drum/Celotex combination, which was tested in the center of gravity over corner drop test (drum S-1B, Celotex S-1C). The lid section of Celotex, which was cut for removal after the corner drop test, was refit into the drum without difficulty. This cut was believed to have negligible effect on either Celotex or general package performance. The damaged lid and locking ring were also easily re-installed. A standard (noninstrumented) locking ring bolt was installed and tightened to 10 inch-pounds, the approximate torque on the bolt after the corner drop test.

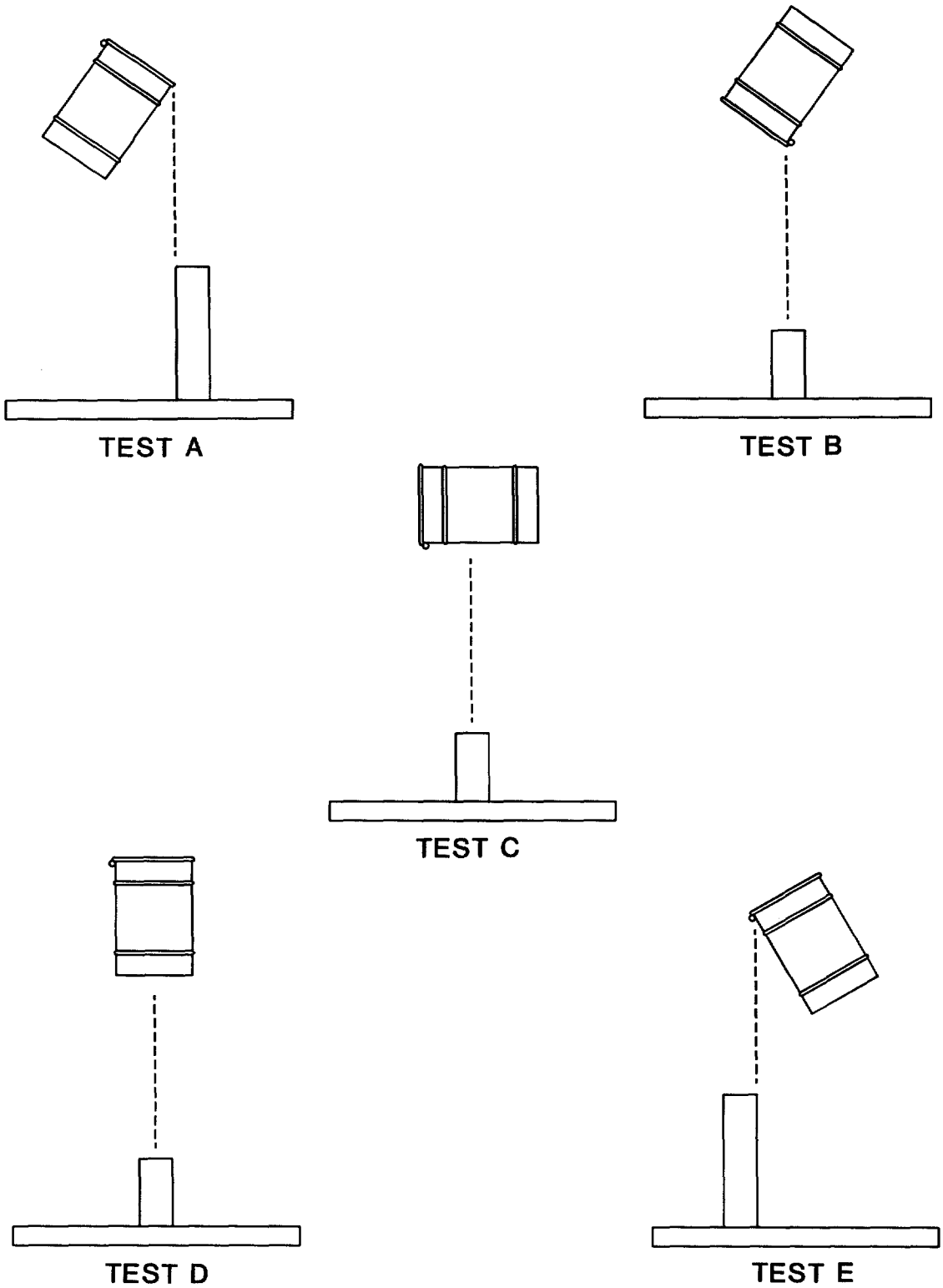

Figure 11-1. Punch Test Configurations

11.1.2 Test Set-Up--Test A

Test A, the first test, was configured to attack the lid locking ring at the 0° side in an attempt to remove the locking ring (much like removing a bottle cap).

A 24-inch-long spike was welded to the facility target, allowing the test unit to free fall along the spike until impact at the desired location near the top of the package. The test container was attached to the adjustable cradle and set at 54° from horizontal (Figure 11-2). Drop height was set at 40-3/4 inches from the top of the spike to the impact location of the locking ring.

11.1.3 Test Event--Test A

The test sequence is shown in Figure 11-3. The test unit impacted the spike as intended and immediately rotated counterclockwise. The bottom of the drum impacted the spike base. The test unit remained on the raised target.

11.1.4 Posttest Observations

Deformation caused by the spike is shown in Figure 11-4. Damage was limited to a small indentation in the side of the drum; no damage or movement of the locking ring was noted. (A deformation of the lip of the drum was noted at disassembly after Test B and is shown in Figure 11-4.) In addition, the drum bottom lip received a dent from impacting the corner of the puncture spike base.

11.1.5 Results

No disassembly of the test unit was performed after Test A, nor was a leak test performed at this time. The test sequence proceeded with Test B on the same test unit.

11.1.6 Test Set-Up--Test B

An 8-inch-long spike was welded to the target in place of the 24-inch-long spike. Again the unit was attached to the adjustable cradle and set at 54° from horizontal (Figure 11-5). Drop height was set at 40-3/4 inches from the top of the spike to the lowest surface of the package.

11.1.7 Test Event--Test B

The test sequence is shown in Figure 11-6. The damaged corner of the test unit impacted the spike as intended. The unit rebounded approximately 3 inches, and the lid of the unit struck the spike again. The unit then rotated and fell off the spike, coming to rest on the target.

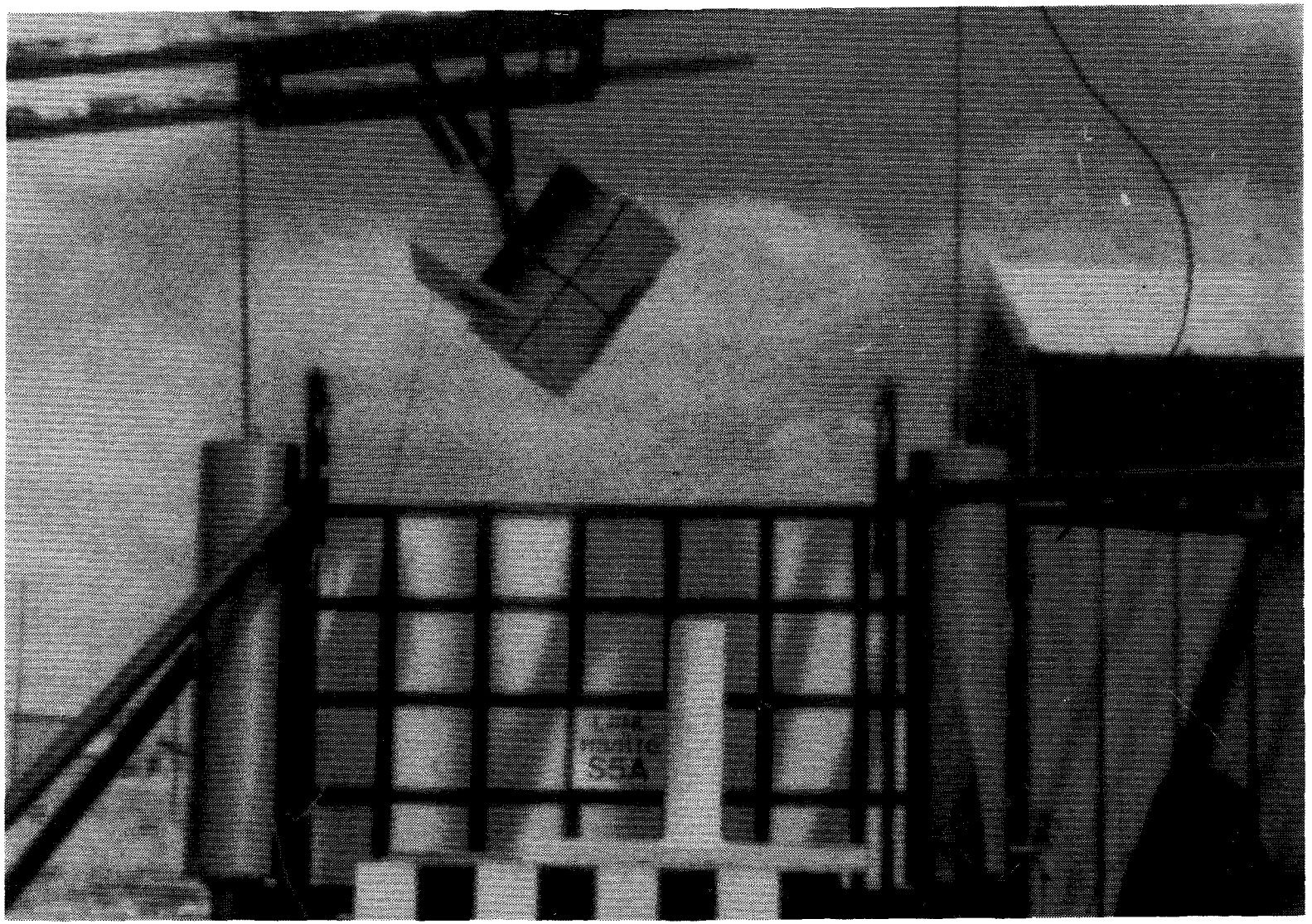

Figure 11-2. Test Set-Up--Test A

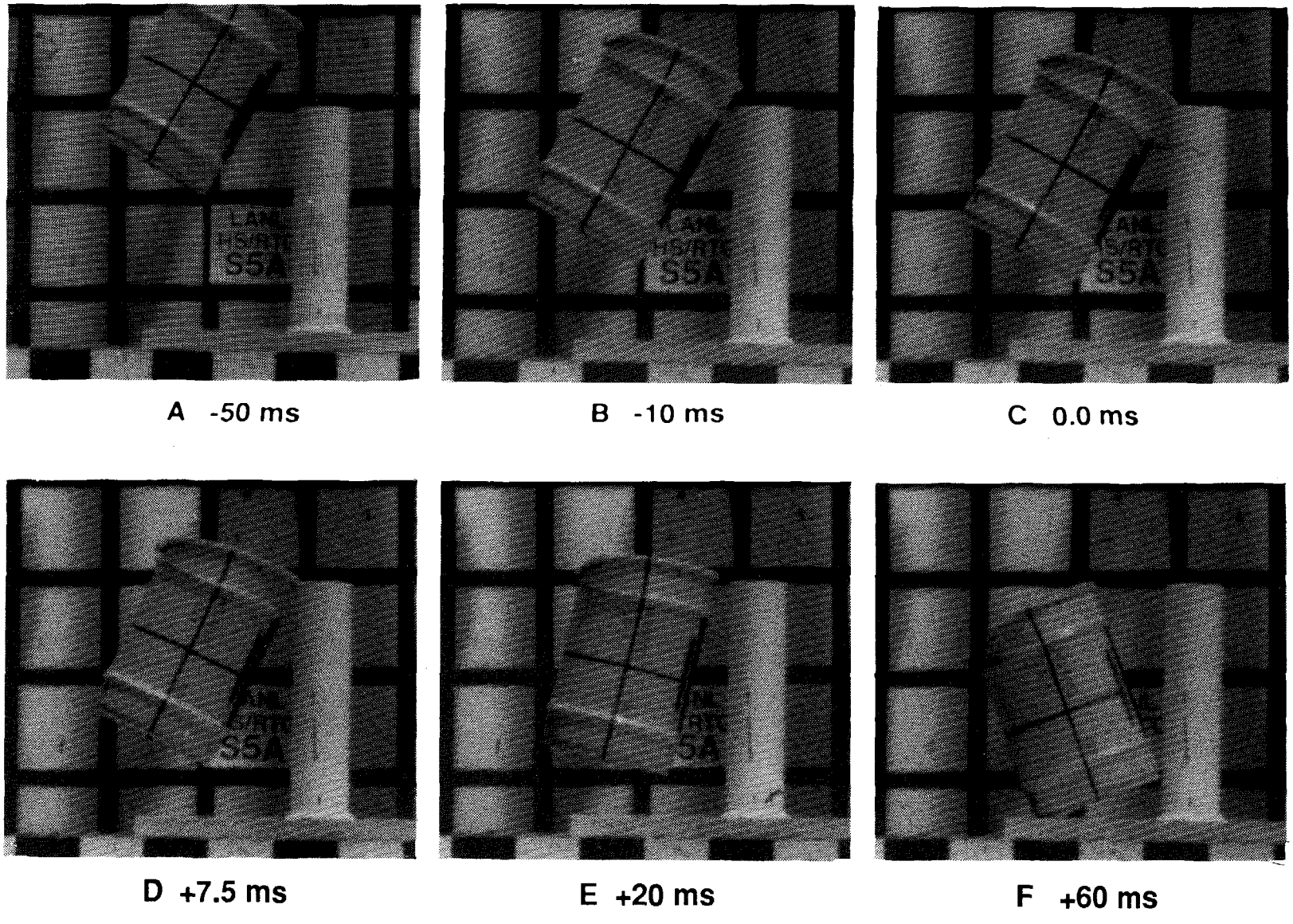

Figure 11-3. Test Sequence--Test A

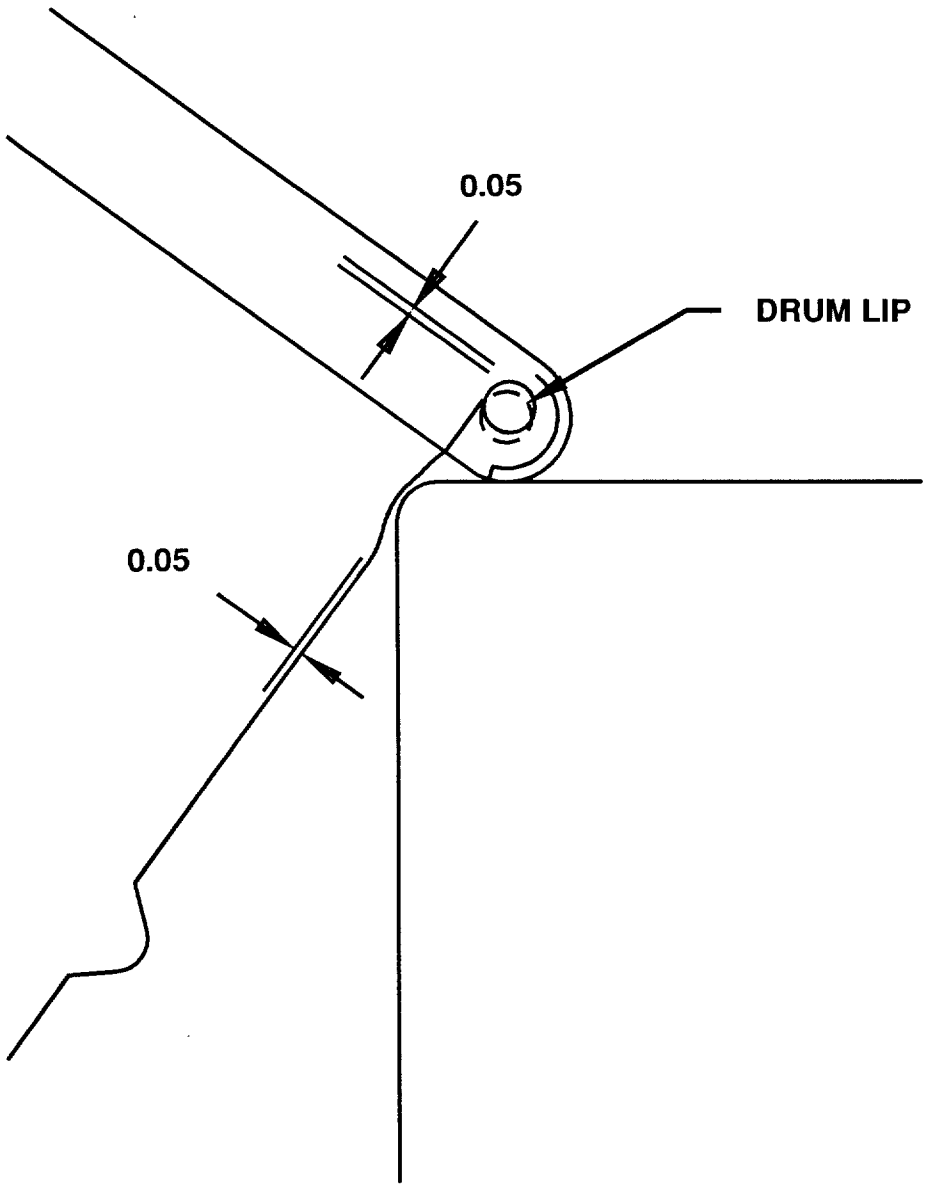

Figure 11-4. Impact Area Deformations--Test A

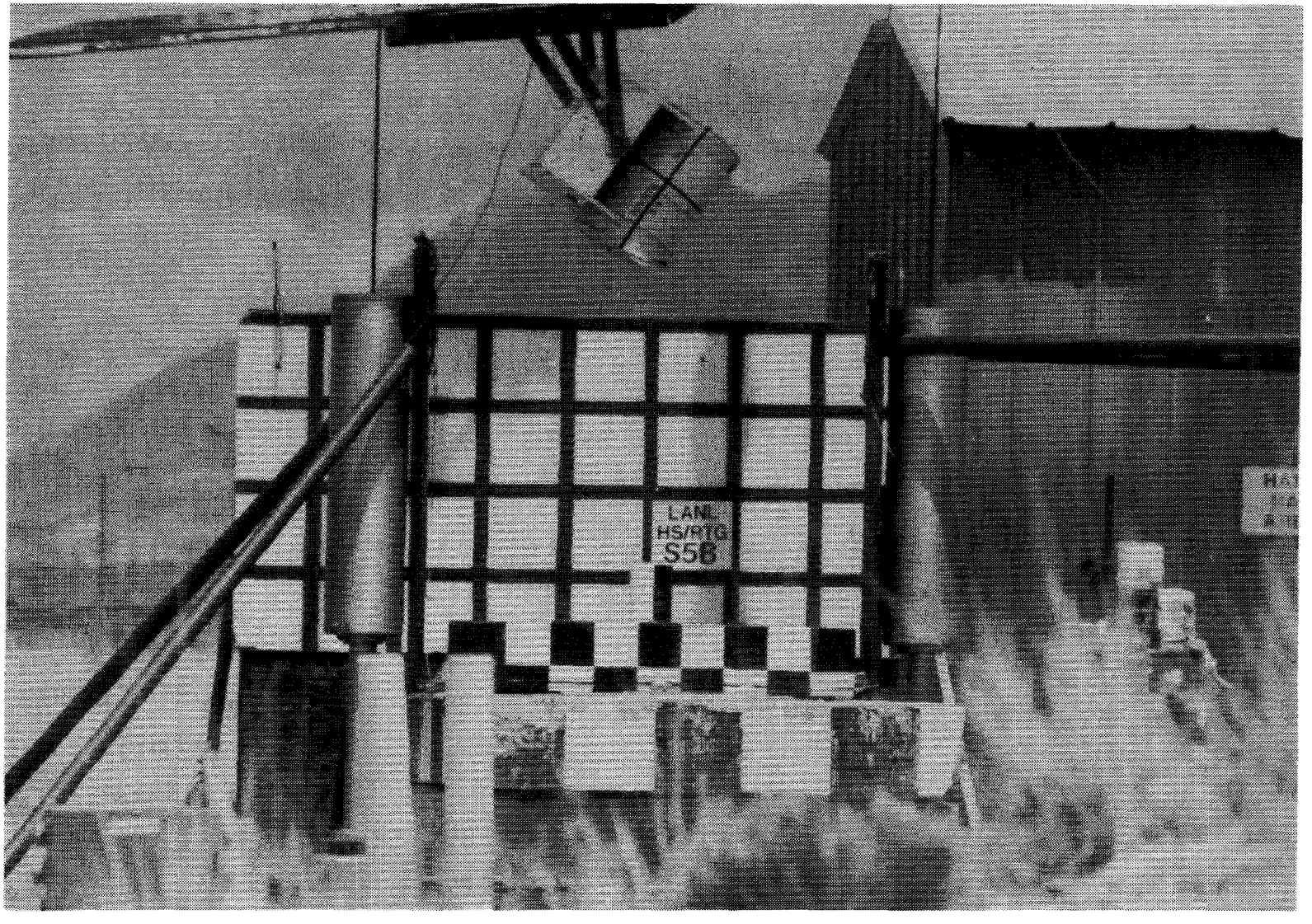

Figure 11-5. Test Set-Up--Test B

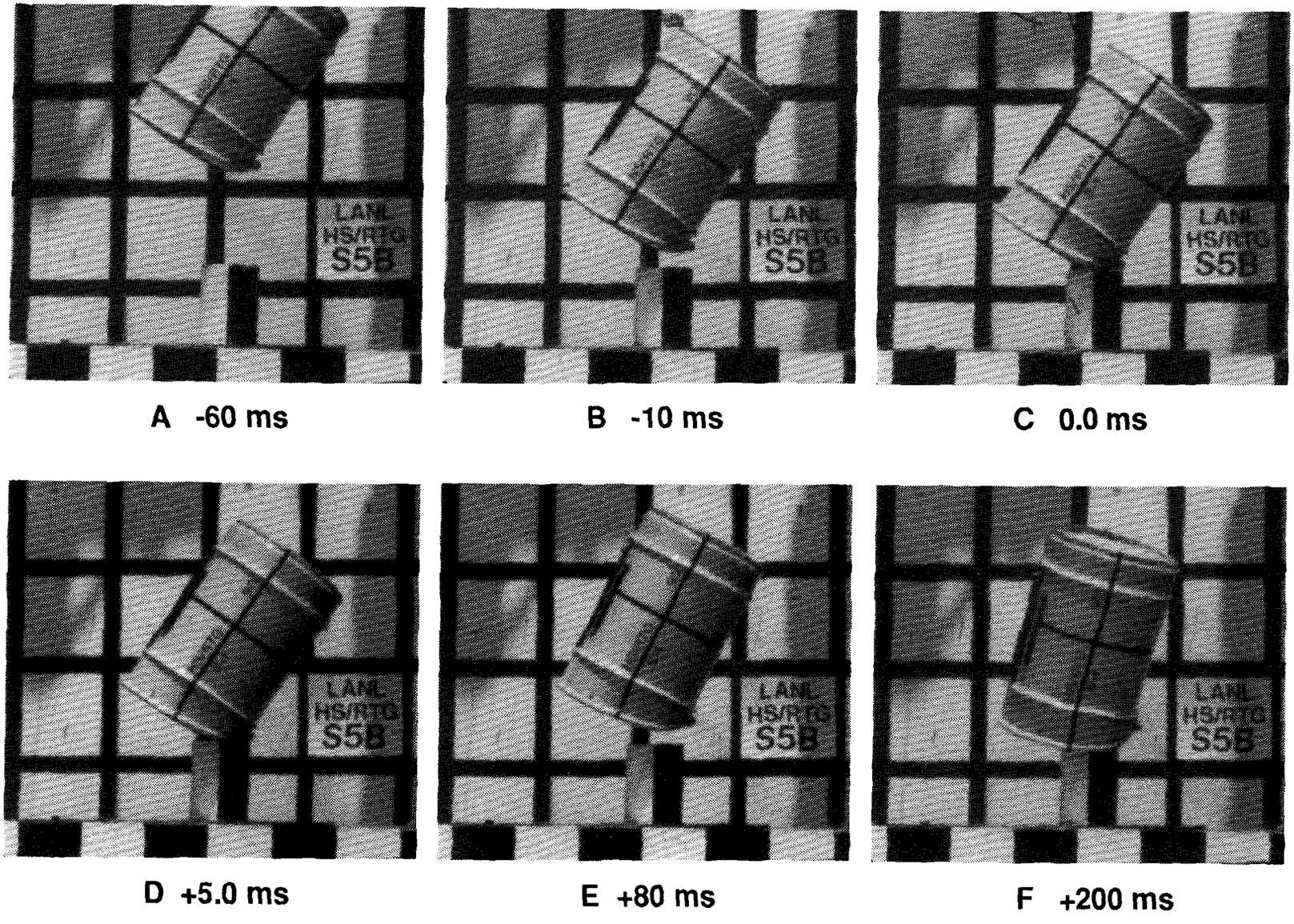

Figure 11-6. Test Sequence--Test B

11.1.8 Posttest Observations

Damage caused by this test is illustrated in Figure 11-7. There were no obvious changes to the initial impact area of the unit. A small crescent-shaped dent in the lid was caused by the secondary impact. Measurements showed an additional crush of approximately 0.05 to 0.10 inch in the immediate impact area.

11.1.9 Results

To allow removal of the inner container, the test unit was partially disassembled. Tightness of the lid locking ring bolt was unchanged from assembly (~10 inch-pounds). The drum lid was removed without difficulty. The lid section of Celotex was removed in the existing two parts; no additional cutting was necessary.

The inner container was removed for leak-testing, which showed a leakage rate of 3×10^{-10} atm cm^3/sec.

No mechanical inspections of the inner container were performed after this test.

11.2 Test C--Side Drop Test Unit

11.2.1 Test Unit Preparation

No assembly of the inner container was required because a posttest disassembly was not performed. Neither was the assembly leak-tested; leak testing performed after the previous test served as the assembly leak test for the side drop test unit.

The inner container assembly was installed in the drum/Celotex combination, which was tested in the 30-foot side drop test (drum S-1C and Celotex S-1D). The lid section Celotex, which had been cut for removal after the side drop test, was refit into the drum without difficulty. The cut was believed to have negligible effect on either the Celotex or general package performance. The damaged lid and locking ring were also re-installed without difficulty. A standard (noninstrumented) locking ring bolt was installed and tightened by hand (the approximate torque on the bolt after the side drop test).

11.2.2 Test Set-Up--Test C

This test was designed to attack the previously damaged side (180°) of the test unit. The 8-inch-long spike used for the previous test was left in place on the target. The test container was rigged to the adjustable cradle and set at 0° (horizontal). The unit was aligned over the punch such that

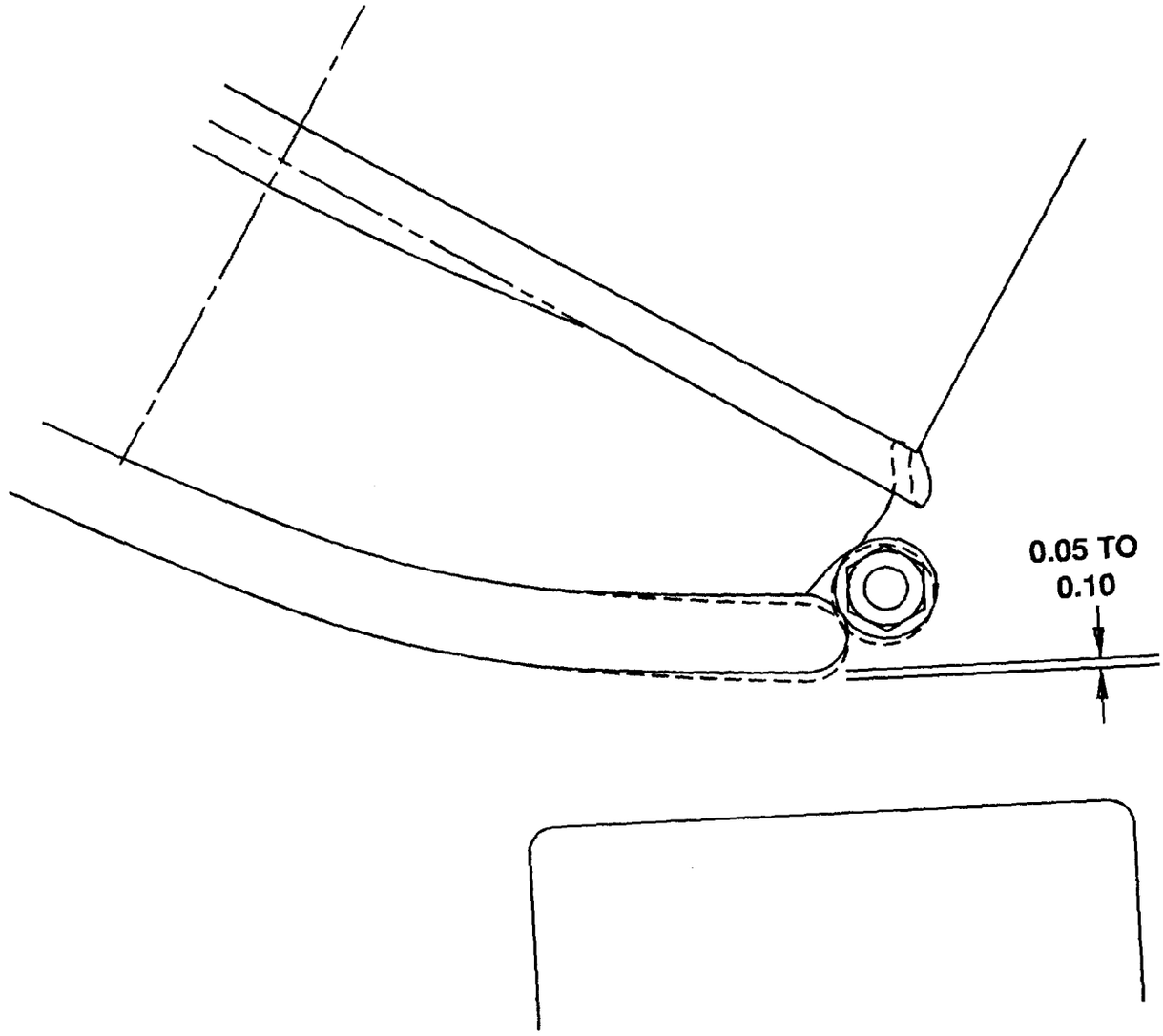

Figure 11-7. Deformations--Test B

the center of the punch would impact the side of the drum approximately 7 inches from the lid end. This was considered to be the worst case orientation because it directed the punch at an area of minimum insulation thickness. Figure 11-8 shows the test set-up.

Drop height was set at 40-5/8 inches from the top of the spike to the side of the drum.

11.2.3 Test Event--Test C

The test sequence is shown in Figure 11-9. The test unit impacted the spike as intended and then rotated clockwise off the spike, continued rolling off the edge of the raised target, and landed on the ground.

11.2.4 Posttest Observations

The deformation caused by the spike is illustrated in Figure 11-10. Damage consisted of a small indentation in the side of the drum. Maximum deformation of approximately 0.2 inch was located 10 inches from the lid end, a point relating to the edge of the spike nearest the center of gravity of the unit.

11.2.5 Results

The package was partially disassembled after the test to allow removal of the inner container. The lid and locking ring were removed without difficulty. Lid section Celotex was removed in the existing two parts; no additional cutting was necessary. The inner container was easily removed for leak-testing.

A helium leak test of the inner container seal demonstrated no detectable leakage above the existing background of the test cavity (2.4×10^{-9} atm cm^3/sec). This background was higher than for other leak tests and was attributed to residual helium from the previous leak test. Appendix A contains a discussion of leak-testing and permeation.

Mechanical inspections of the inner container components were not performed.

11.3 Tests D and E--End Drop Test Unit

11.3.1 Test Unit Preparation

No assembly of the inner container was required because a posttest disassembly was not performed. Neither was the assembly leak-tested; leak testing performed after the previous test served as the assembly leak test for the side drop test unit.

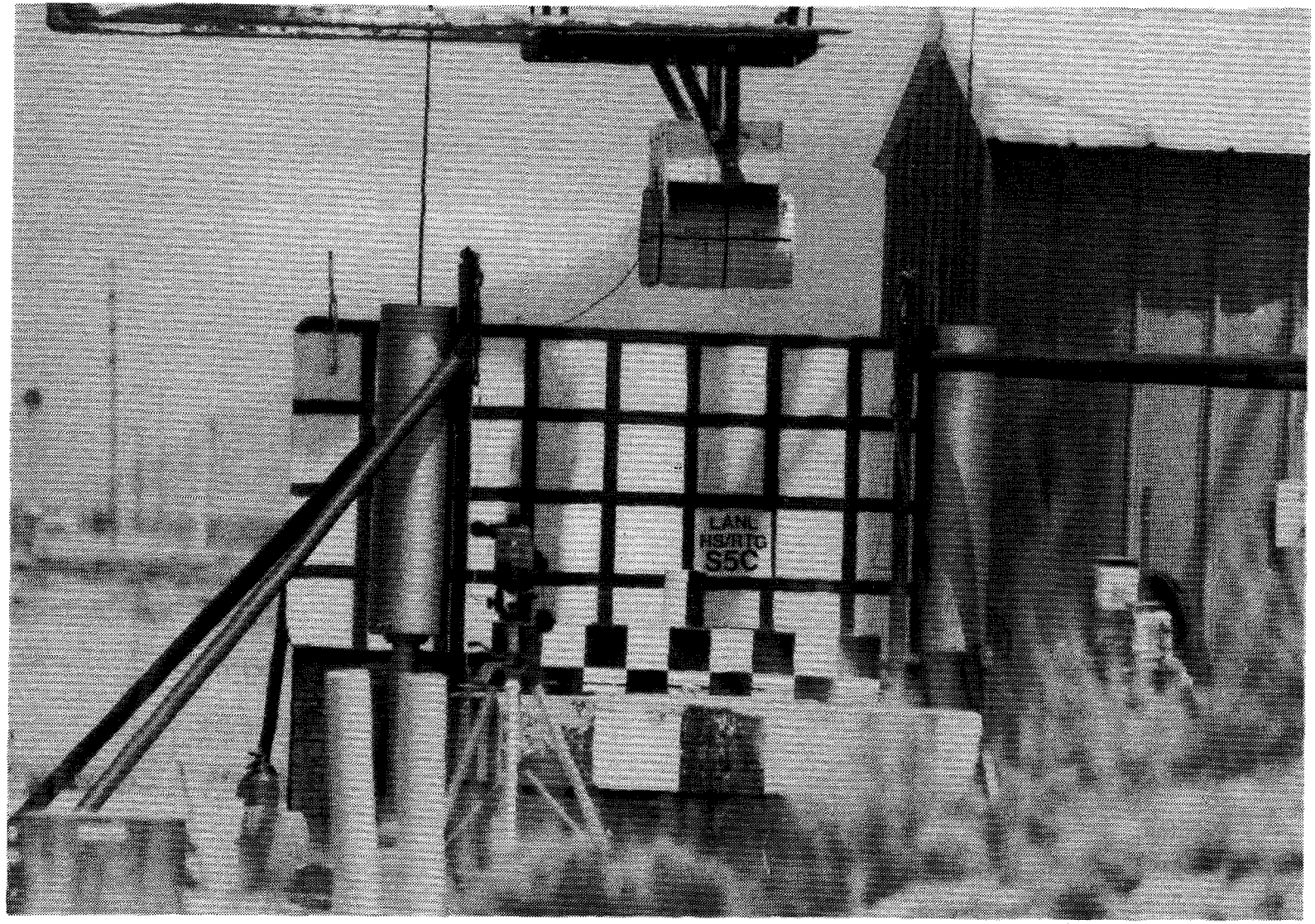

Figure 11-8. Test Set-Up--Test C

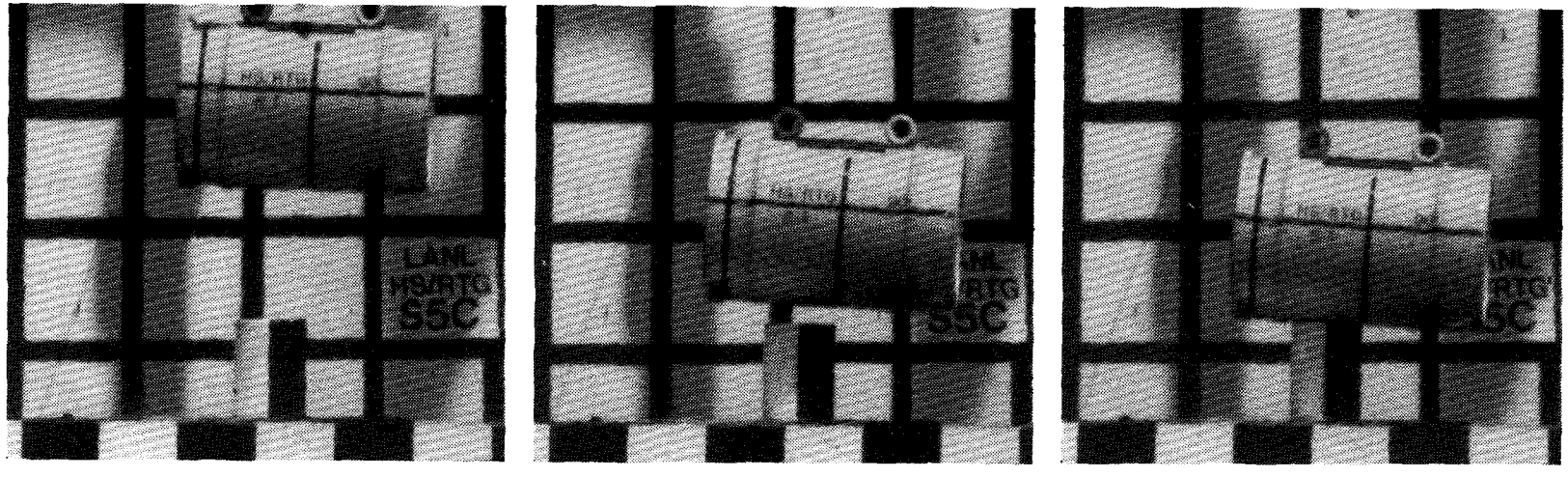

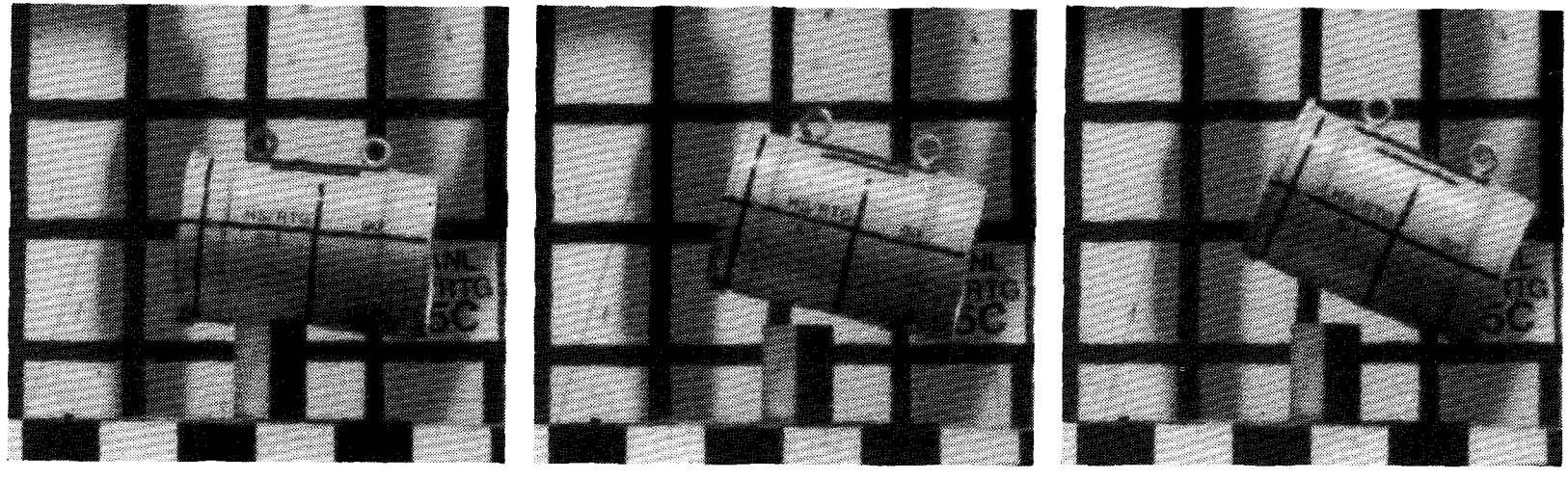

Figure 11-9. Test Sequence--Test C

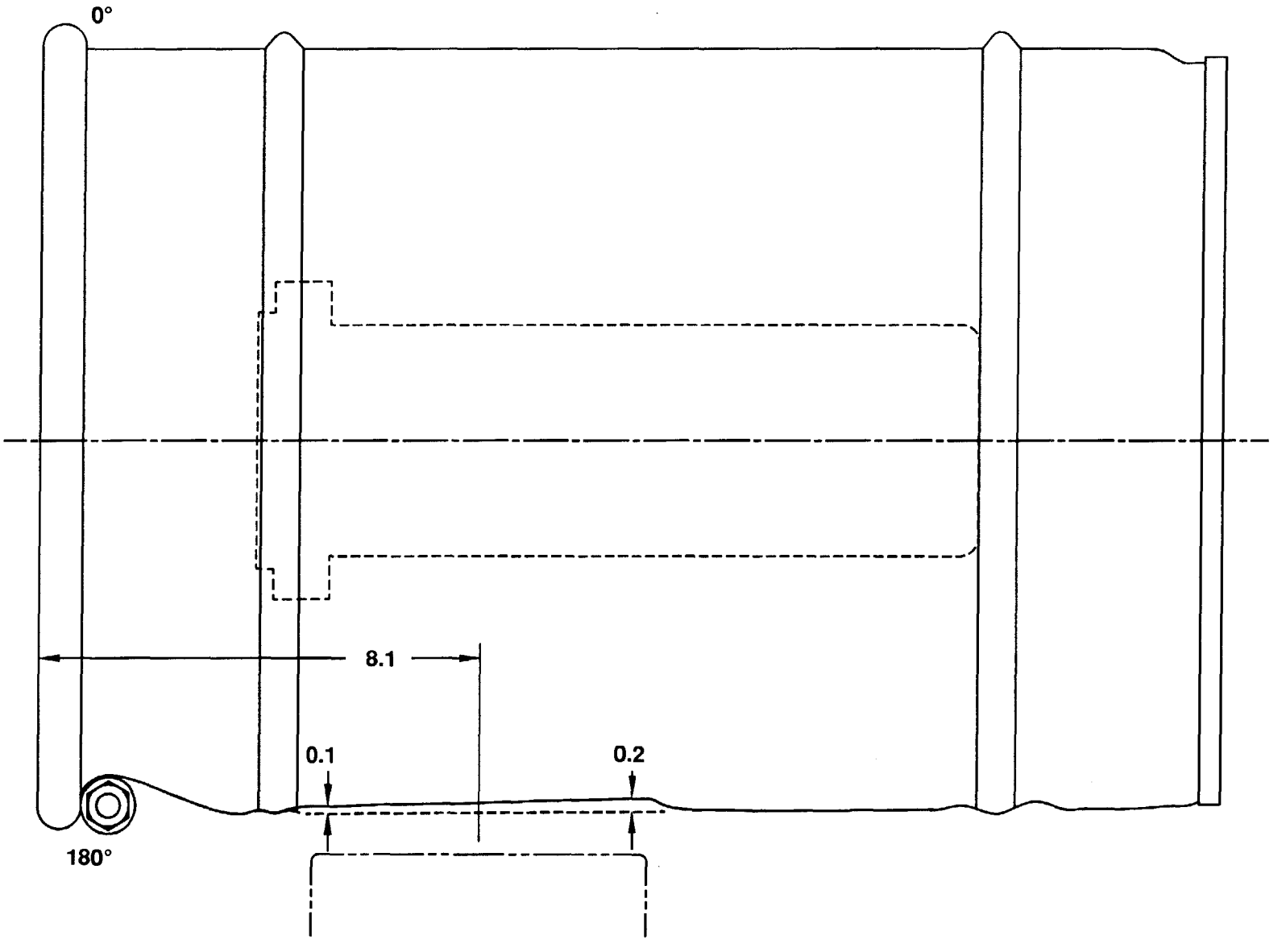

Figure 11-10. Deformations--Test C

The inner container assembly was installed in the drum/ Celotex combination which had been used in the 30-foot bottom end drop test (drum S-1A and Celotex S-1B). The lid section of Celotex, lid, and locking ring, were easily re-installed because this area was not deformed during the end drop test. A standard (noninstrumented) locking ring bolt was installed and tightened to 180 inch-pounds.

11.3.2 Test Set-Up--Test D

This test was configured to punch the center of the bottom of the drum. This was the end deformed by the 30-foot test. The 8-inch-long spike used for the previous test was left in place on the target. Wire rope was used to suspend the test unit in a vertical orientation (Figure 11-11).

Drop height was set at 40-3/4 inches from the top of the spike to the impact surface of the drum.

11.3.3 Test Event--Test D

The test sequence is shown in Figure 11-12. The test unit impacted the spike approximately 1 inch off center, rebounded 5 to 6 inches, and struck the spike a second time before falling to the target. The unit rolled off the raised target and came to rest on the ground.

11.3.4 Posttest Observations

Figure 11-13 illustrates the deformation caused by the spike. The punch area was deformed an average of 0.15 inch in relation to the surrounding area.

11.3.5 Posttest Activities

No disassembly of the test unit was performed after Test D nor was a leak test performed. The test sequence proceeded with Test E using the same test unit.

11.3.6 Test Set-Up--Test E

Test E was a second attempt to remove a lid locking ring. This test attacked the bolt lug of the lock ring. The lug was believed to be a vulnerable area because the larger protrusion could be struck squarely by the spike.

A 24-inch-long spike was welded to the target in place of the 8-inch-long spike. As in Test A, this configuration allowed the test unit to free fall along the spike until impact of the desired location near the top of the package. The test container was mounted to the adjustable cradle and

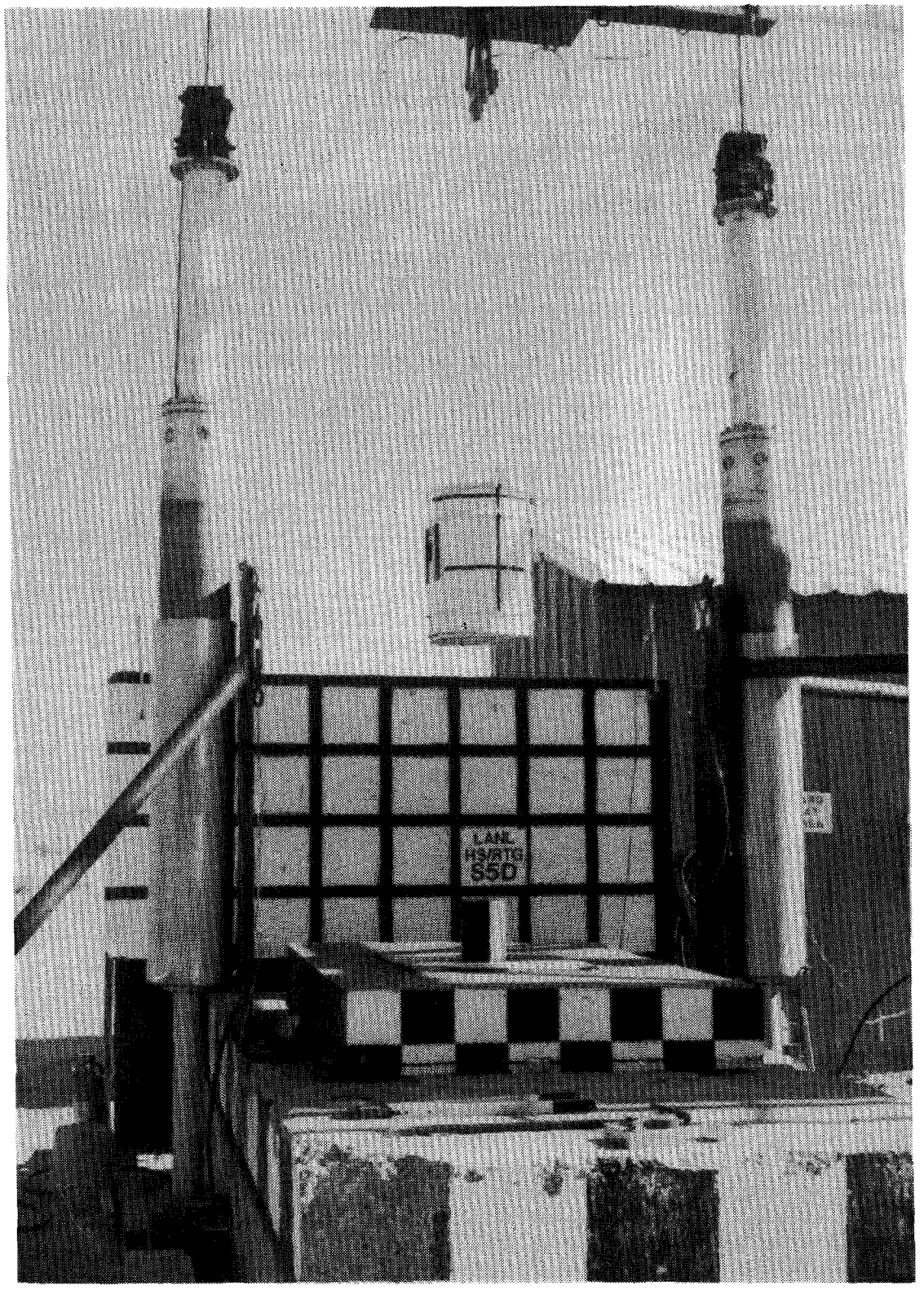

Figure 11-11. Test Set-Up--Test D

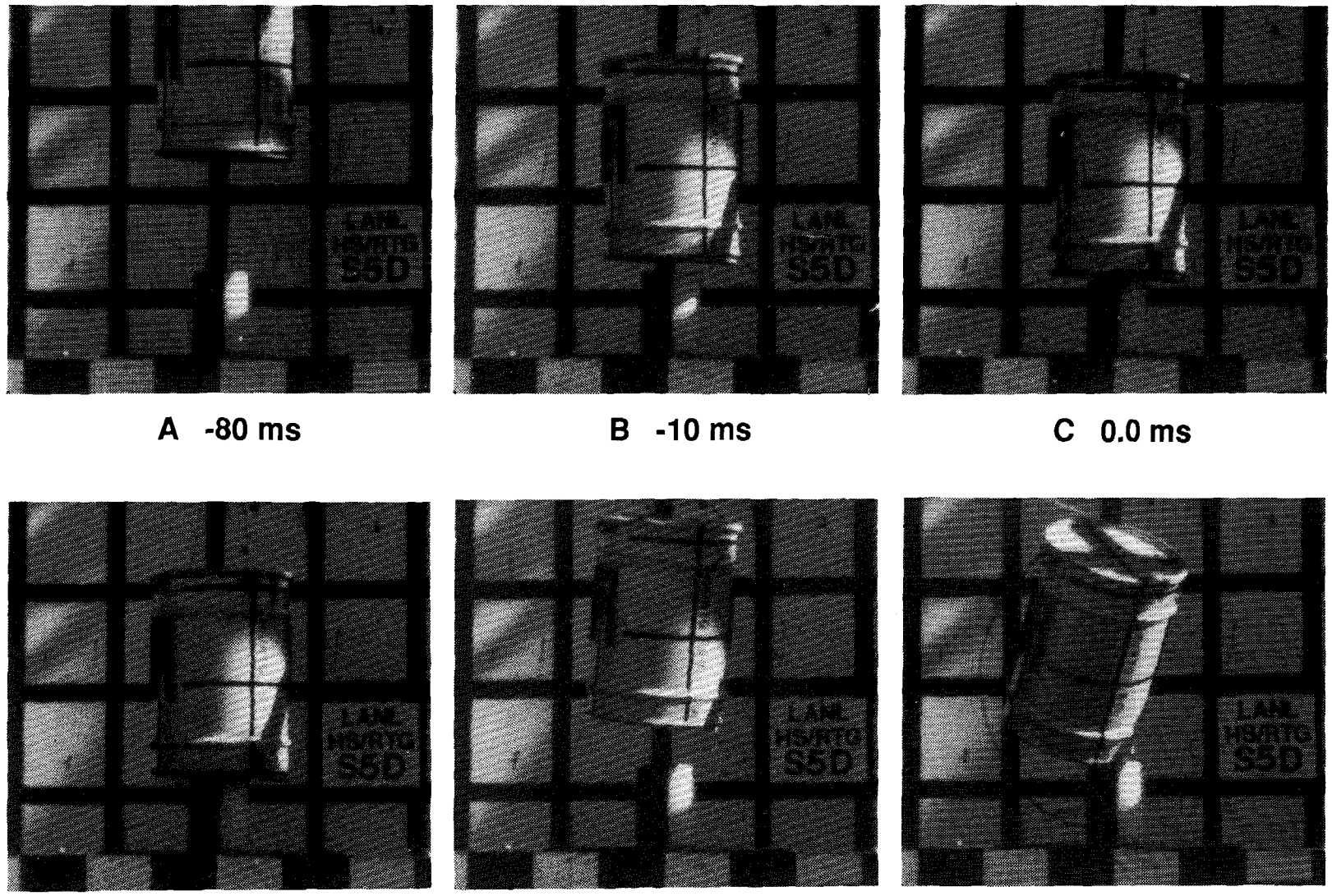

Figure 11-12. Test Sequence--Test D

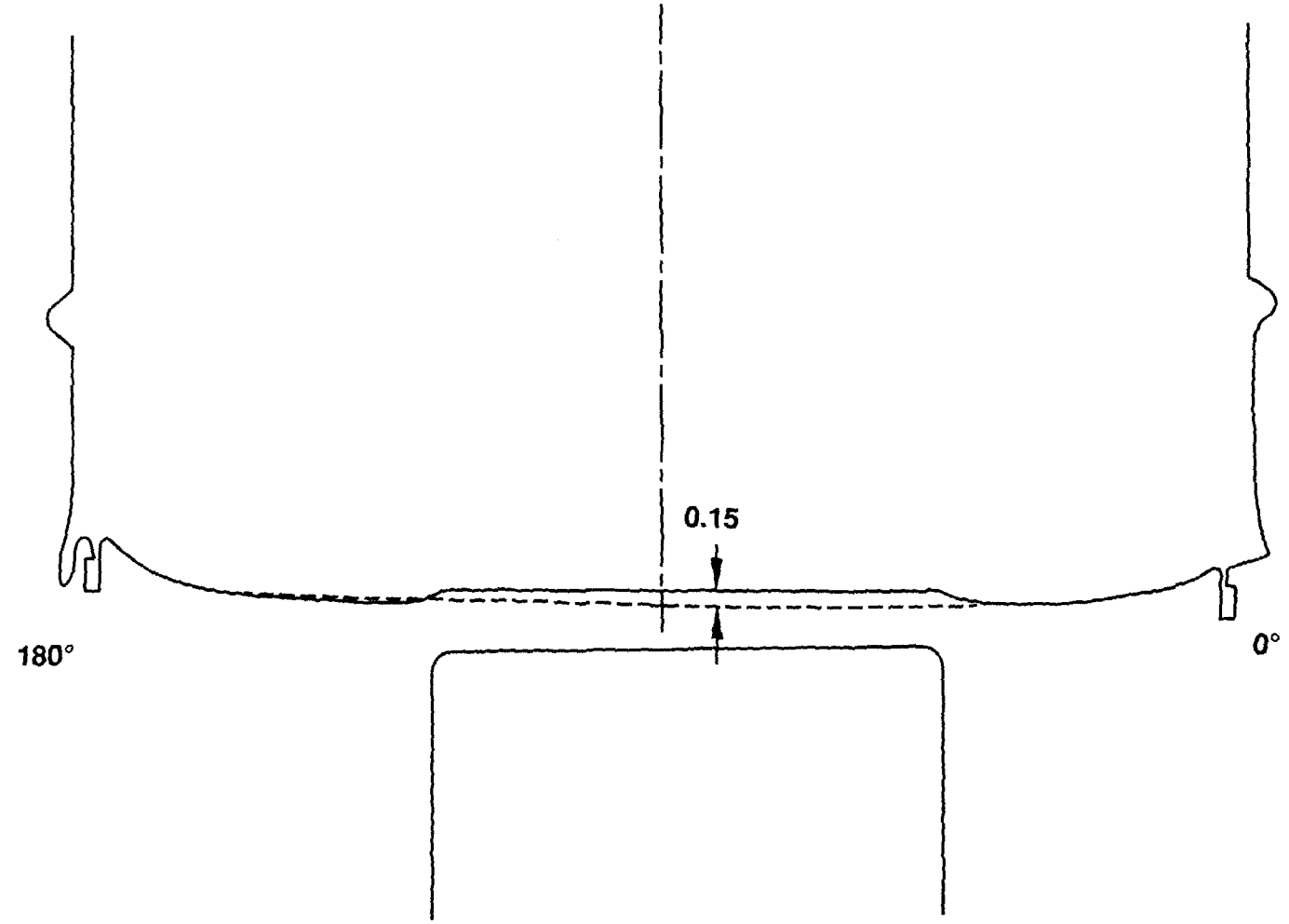

Figures 11-13. Deformations--Test D

set at 60° from horizontal (Figure 11-14). Drop height was set at 40-1/2 inches from the top surface of the spike to the underside of the locking ring lug.

11.3.7 Test Event--Test E

The test sequence is shown in Figure 11-15. The locking ring lug struck the spike as intended. The unit rotated clockwise after impact, allowing the bottom of the unit to strike the corner of the spike base, and came to rest on the target.

11.3.8 Posttest Observations

Punch area deformations are shown in Figure 11-16. The locking ring lug was driven into the side of the drum slightly. The locking ring and drum lip moved upward approximately 0.1 inch. The bottom edge of the drum deformed slightly as a result of impacting the corner of the spike base.

11.3.9 Disassembly

The test unit was completely disassembled after Test E. Locking ring bolt torque was measured at 50 inch-pounds, a decrease of 130 inch-pounds from the assembly torque. Despite minor damage, the locking ring and lid were easily removed. The lid section of Celotex was snug in the drum but removable. Two slight indentations were noted in the area of the locking ring lugs.

11.3.10 Results

A helium leak test of the inner container seal showed no detectable leakage above cavity background, 1.2×10^{-9} atm cm^3/sec.

Posttest dimensional inspections were performed on the inner container body and lid. No dimensional changes were detected within the accuracy of the inspection process for the inner container lid.

The only detectable change to the inner container body was a minor change in the angular measurement of the flange. Decreases of 0.20° and 0.17° were noted near 135° and 180°, respectively, in the same direction of movement noted after the three drop tests. As with all other tests, movement may have been caused by loads induced during assembly of the V-clamp, rather than by the test itself. Complete inspection data and a discussion of accuracy are contained in Appendix B.

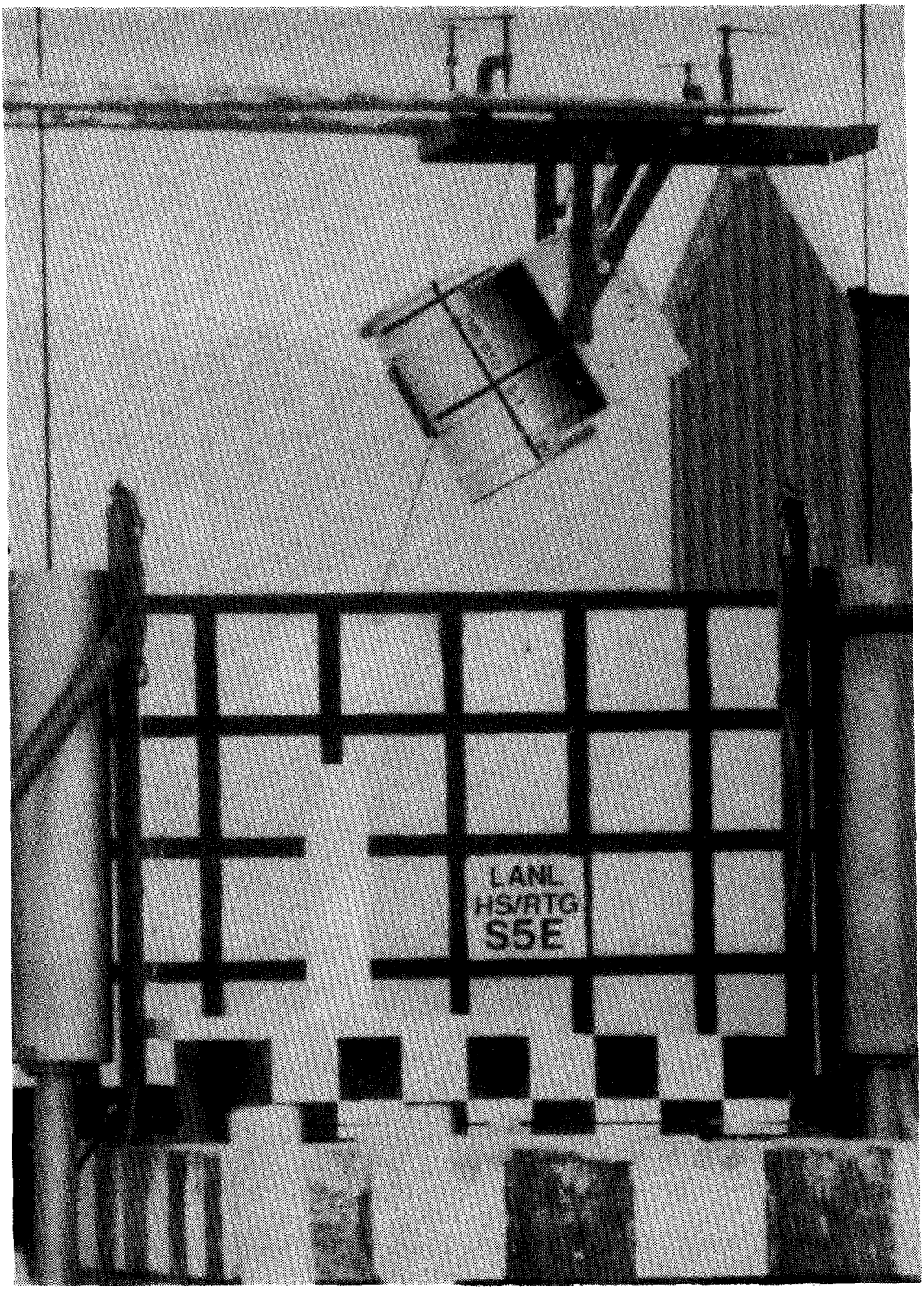

Figure 11-14. Test Set-Up--Test E

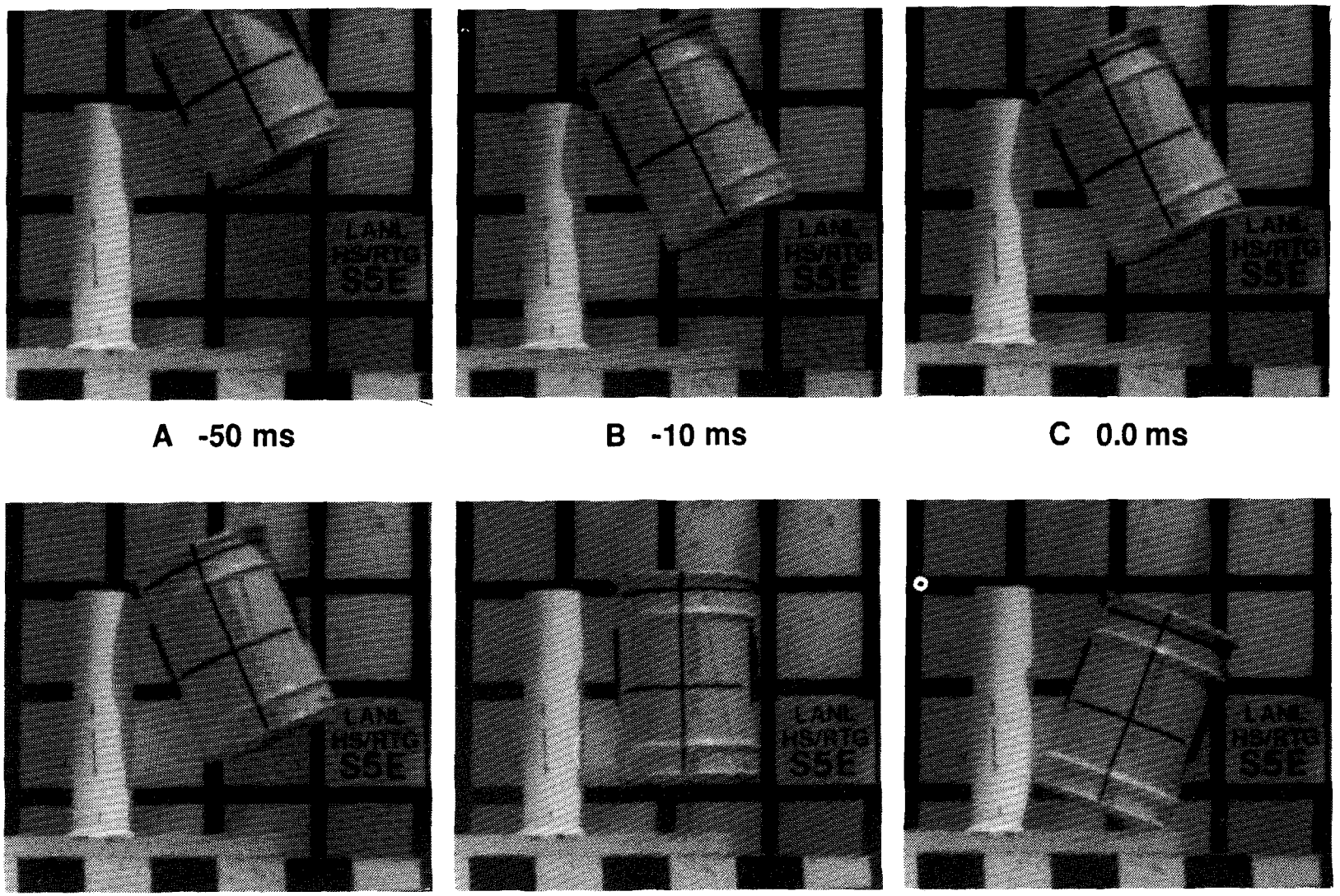

Figure 11-15. Test Sequence--Test E

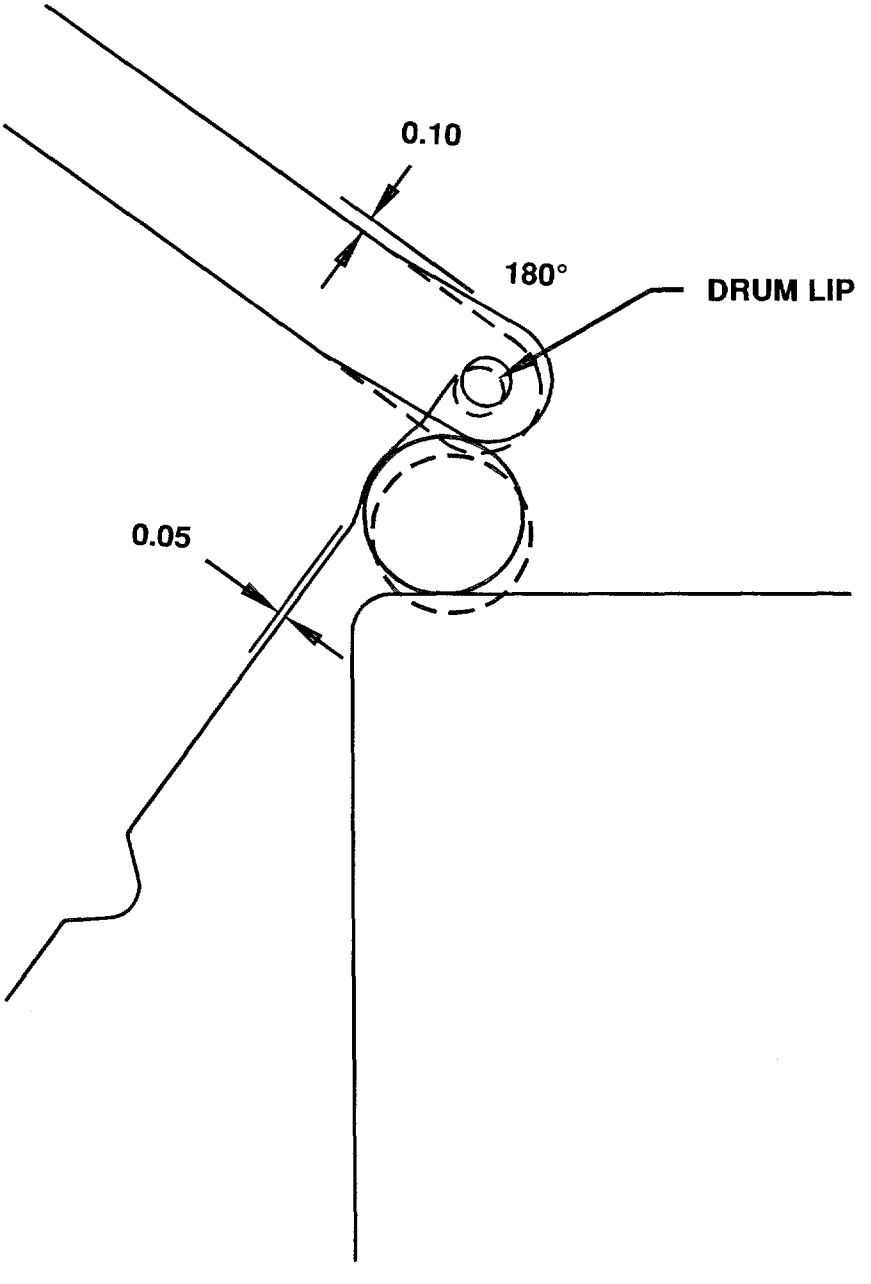

Figure 11-16. Deformations--Test E

12.0 SUMMARY

The inner container assembly met the primary criteria of no leakage rate greater than 1.0×10^{-7} atm cm^3/sec. Leakage rate measurements were performed a total of seven times during the test series.

The design of the locking ring proved questionable when the drum was cut during the 4-foot normal conditions drop test. The redesigned ring used on all subsequent tests performed satisfactorily in that it retained the drum lid without creating any potential vents in the drum wall. The performance of the redesigned ring during a 4-foot drop was verified on a separate certification test unit.[18]

The inner container body and lid were not damaged as a result of the tests. A minor dimensional change was noted on the body flange, at the 180° side. Rather than caused by the tests, this angular change appeared to be a flexing of the flange, resulting from forces exerted by the V-clamp during assembly. The change was also random from test to test because it was a positive change in two posttest inspections and a negative change in two others, resulting in the slight change of 0.2° for the entire test series.

The outer drum assembly satisfactorily performed its function of containing and protecting the Celotex insulation. The drum deformed in each drop test at the immediate impact location, cushioning the inner container assembly; however, these deformations were not excessive because they did not significantly decrease the thickness of insulation at any location around the inner container. The maximum change in insulation thickness occurred during the 30-foot CG over corner drop test, which decreased insulation thickness 0.5 inch from the original 3.5 inches in an angular direction of impact. Side and end drop tests produced changes in insulation thicknesses of less than 0.1 inch.

During the test series, the integrity of the outer drum was not diminished by cracked welds or tears (other than during the initial 4-foot drop test) which would expose the Celotex insulation during a later fire scenario. The side impact test did produce a small gap at the lid/drum lip interface. Located between the ends of the locking ring, this gap constituted a potential vent of approximately 0.1 $in.^2$. (The drum is fabricated with four 0.25-inch-diameter [0.05-$in.^2$] holes as vents.)

Strain measurements of the inner container body and lid were generally low with one-half of all measurements below 100 $\mu\varepsilon$ and three-quarters of all measurements below 200 $\mu\varepsilon$. Two notable exceptions are the body flange during the CG over corner drop test, which indicated a strain of 1,175 $\mu\varepsilon$,

and the center area of the body in the side drop tests, which showed strains ranging from 240 to 920 $\mu\varepsilon$.

Strains in the drum lid locking ring bolt were low in all three drop tests, with measurements ranging from 70 to 205 $\mu\varepsilon$.

Strains measured by the instrumented bolts securing the RTGs varied with the drop orientation of the test unit. Only a small amouunt of tension load was produced in the bolts during the CG over corner test. Loads in excess of 1,350 $\mu\varepsilon$ were recorded in both the end drop and side drop tests. The end drop loaded the bolts in direct tension. The bolts indicated a large tension component in the side drop test as a result of moment of the RTG.

Accelerations on the inner container assembly also varied with test unit drop orientation. Accelerations in the CG over corner test were approximately 300 g for the inner container assembly and 400 g for the payload. These accelerations were the lowest of the three drop orientations as a result of the amount of drum crush cushioning the contents. The side and end drop tests crushed much less and consequently had higher accelerations. For the end drop test the inner container was subjected to accelerations of approximately 750 g on the inner container body and 1,000 g on the payload assembly. Inner container body and payload accelerations averaged 1,000 and 2,100 g, respectively, during the side drop test.

REFERENCES

1 "Packaging and Transportation of Radioactive Material," U.S. Nuclear Regulatory Commission, Code of Federal Regulations, Title 10, Part 71, Washington, DC, 1989.

2 "Test Specification: HG/RTG Shipping Container," Hazpact-HS/RTG-03, Los Alamos National Laboratory, November 1989.

3 "Overpressure Test Procedure: HS/RTG Shipping Container," LANL-O, Sandia National Laboratories, 1990.

4 "Normal Conditions Test Procedure: HS/RTG Shipping Container," LANL-1, Sandia National Laboratories, 1990.

5 "CG Over Corner Drop Test Test Procedure HS/RTG Shipping Container," LANL-S2, Sandia National Laboratories, 1990.

6 "Side Drop Test Procedure: HS/RTG Shipping Container," LANL-S3, Sandia National Laboratories, 1990.

7 "Bottom End Drop Test Procedure: HS/RTG Shipping Container," LANL-S4, Sandia National Laboratories, 1990.

8 "40 Inch Puncture Test Procedure: HS/RTG Shipping Container," LANL-S5, Sandia National Laboratories, 1990.

9 "Transportation Systems Development Quality Assurance Program Plan," Department 6320, Sandia National Laboratories, June 1988.

10 "Test Program Plan: HS/RTG Shipping Container," LANL-TPP, Sandia National Laboratories, 1990.

11 "Quality Assurance Program Plan: HS/RTG Shipping Container," LANL-QAPP, Sandia National Laboratories, 1990.

12 "Advisory Material for the IAEA Regulations for the Safe Transport of Radioactive Material," International Atomic Energy Agency (IAEA), Safety Series No. 37, 1985.

13 "Instrumentation Uses to Determine Structural Responses Under Various Test Conditions," A. Gonzales, SAND 87-2645, Sandia National Laboratories Report.

14 "Inspection Procedure: HS/RTG Shipping Container," LANL-10, Sandia National Laboratories, 1990.

15 "Instrumentation and Assembly Procedure: HS/RTG Shipping Container," LANL-8, Sandia National Laboratories, 1990.

16 "Leak Test Procedure: HS/RTG Shipping Container," LANL-9, Sandia National Laboratories, 1990.

17 "American National Standards for Radioactive Materials Leakage Tests on Packages for Shipment," American National Standards Institute (ANSI), Standard N14.5, January 16, 1987.

18 "Certification Testing of the Los Alamos National Laboratory Heat Source/Radioisotopic Thermoelectric Generator Shipping Container," D. Bronowski, M. Madsen, SAND 91-1064, Sandia National Laboratories Report.

APPENDIX A

LEAK TESTING

Leak testing is a form of nondestructive evaluation used for detecting and measuring leaks in a pressurized or evacuated system. The method of leak testing used for the evaluation of the HS/RTG inner container seal was a mass spectrometer envelope technique using helium as a tracer gas. The leak tests were performed following ANSI N14.5[17] guidelines and a project-specific procedure.[16]

Inner container and leak test configurations are shown in Figures A-1 and A-2. The mass spectrometer leak detector was connected to a test cavity formed by two concentric O-rings. The payload cavity was evacuated and backfilled with helium tracer gas. The leak detector measured the amount of tracer gas leaking across the inner O-ring. (The function of the outer O-ring is to form the test cavity, and it is not itself tested in this configuration.)

Maximum allowable leakage rate for the container was 1.0×10^{-7} atm cm^3/sec. In accordance with ANSI N14.5, required minimum sensitivity of the detector was 5.0×10^{-8}. Leak test sensitivity refers to how small a physical leak can be detected. The mass spectrometer leak detector used is capable of detecting a leak of 2.0×10^{-10} atm cm^3/sec. Actual test sensitivity was dependent on cavity background, which varied somewhat from test to test. High backgrounds, resulting from both outgassing and permeation, decreased sensitivity to the 10^{-9} range for several tests.

The majority of higher backgrounds were due to permeation and subsequent release of helium from the O-rings. Helium, because of its small molecular size, readily permeates viton seal material. Helium also requires a significant period of time to diffuse from the seal, leading to a high background for any tests performed in rapid succession, i.e., on a daily basis. A graph illustrating helium permeation is shown in Figure A-3.

The leak detector was calibrated using a 10^{-8} cm^3/sec range leak standard before and after each test, ensuring the required detector sensitivity and establishing the scale for quantitative measurements.

The payload cavity was evacuated to 0.01 atm and backfilled to 1 atm with high-purity helium, assuring a high (near 100 percent) concentration of tracer gas. Each leak test was monitored for a minimum of 3 minutes, sufficient time to ensure detector response. Helium was then removed to avoid severe permeation of the O-rings.

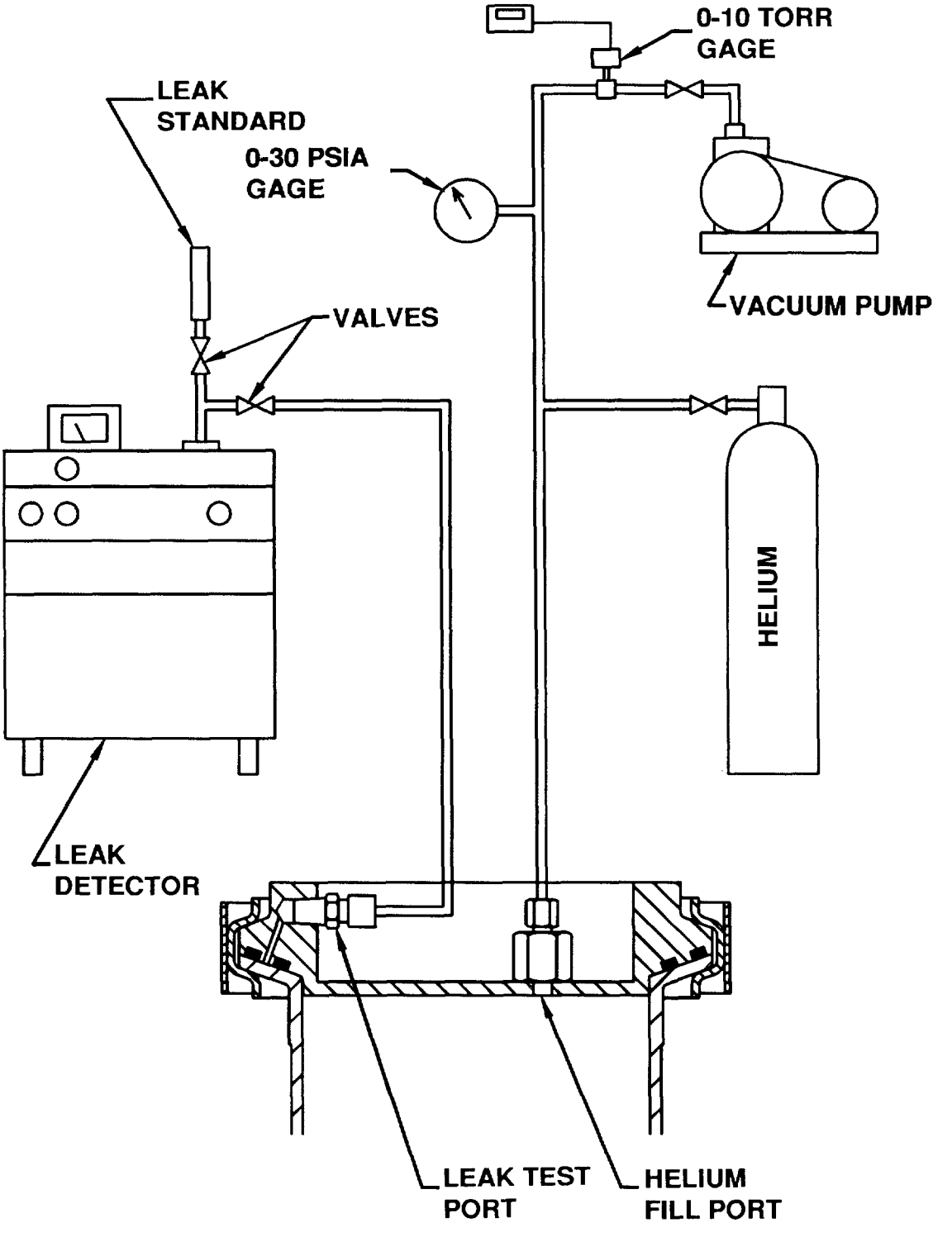

Figure A-1. Leak Test Configuration

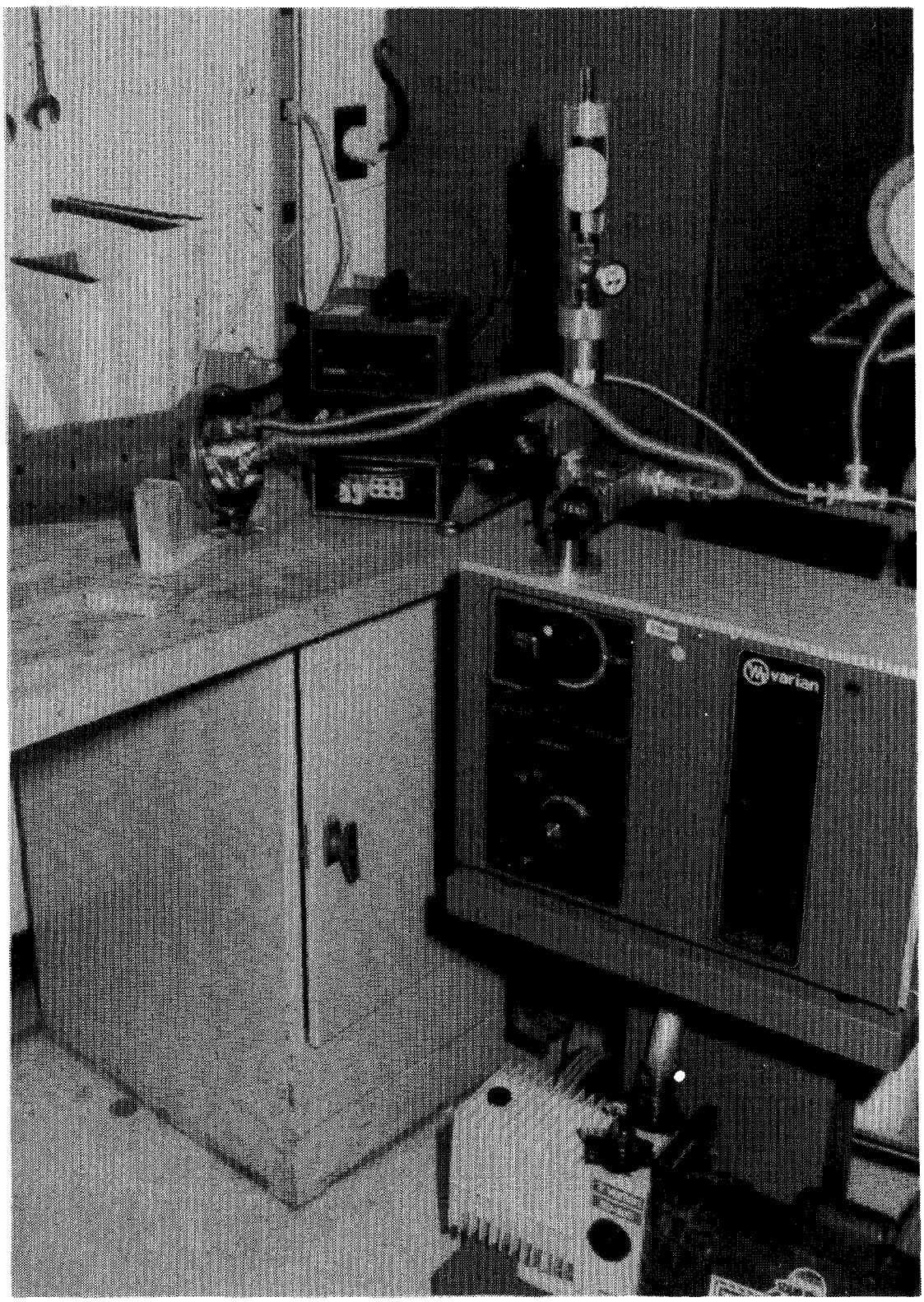

Figure A-2. Leak Test Set-Up

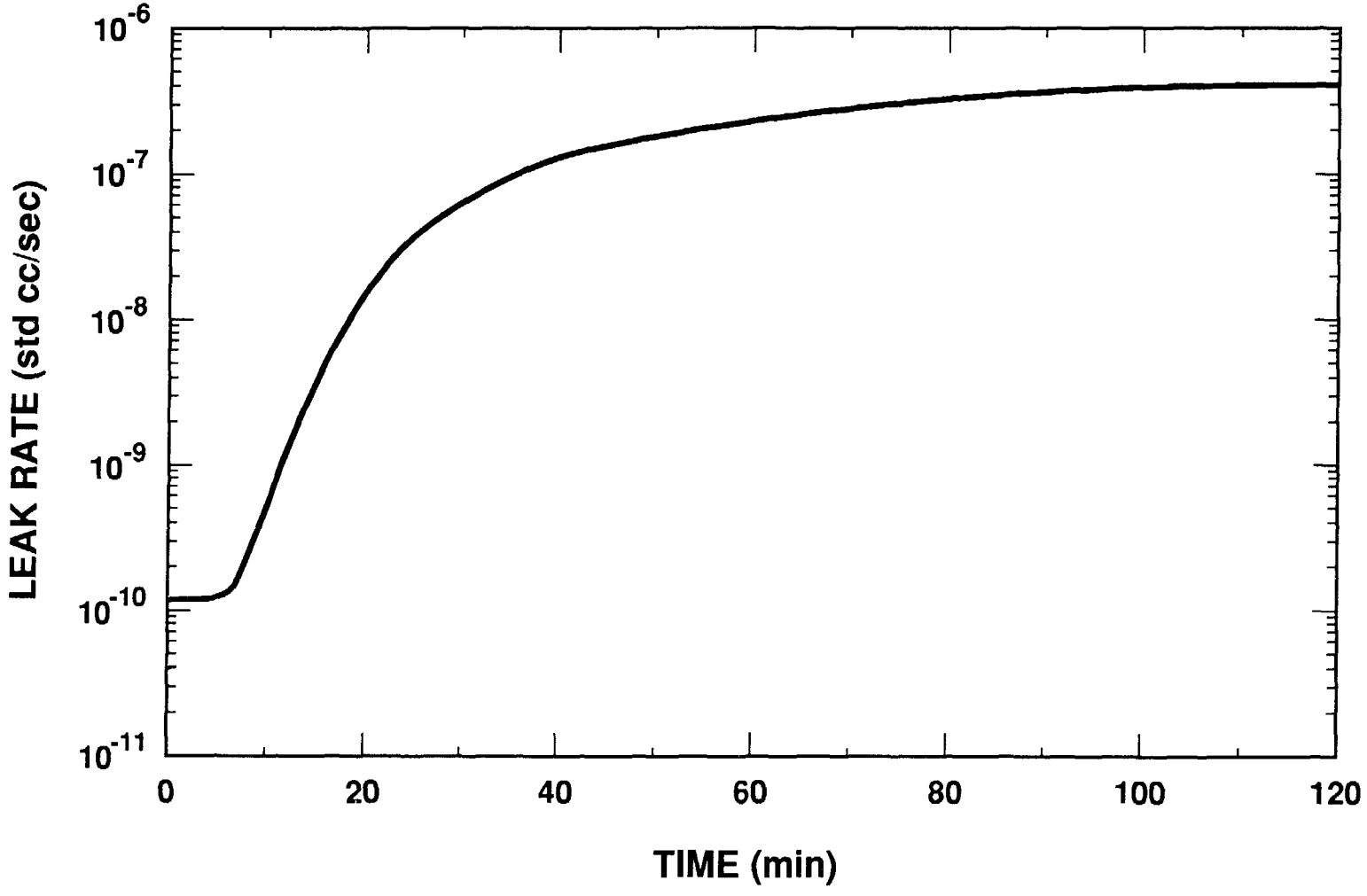

Figure A-3. Helium Permeation of Container O-Rings

Each leak test was repeated once as an assurance measure immediately following a posttest calibration check of the initial leak test. Helium permeation was evident during each of the repeated tests.

When possible, the test cavity was evacuated overnight to remove helium from the seals, ensuring a low background for the next post test leak test. Higher backgrounds of up to 2.4 x 10^{-9} atm cm^3/sec were evident in instances where the constrained test schedule did not permit prolonged evacuation times.

APPENDIX B

DIMENSIONAL INSPECTION

Dimensional inspections were performed on the inner container lid and body components before, during, and after the test sequence. These inspections were made to detect any dimensional changes as a result of the tests.

Inspection points used for all inspections are shown in Figure B-1 for the inner container body and Figure B-2 for the lid. All inspections were performed by Sandia National Laboratories (SNL) Mechanical Measurements Department 7485 using calibrated equipment. All inspection data and calculated changes are presented on a test-by-test basis in Tables B-1 through B-10.

The measuring equipment employed could accurately reproduce measurements within 0.0005 inch. Overall inspection accuracy is dependent on this equipment as well as the repeatability of the inspection set-up. The lid set-up was easily repeated with a high degree of accuracy. Overall inspection accuracies for lid dimensions are $\pm$0.001 inch for linear dimensions and 0.015° for angular dimensions.

Accuracies relating to inner container body measurements varied with the location of the measurement. The set-up from which radial measurements were made is shown in Figure B-3. The open end of the body was used as the datum as well as a mounting surface. Measurements in this immediate area (R5 and R6 inspection points) were quite accurate, typically $\pm$0.001 inch. However, this surface was not perfectly square with the centerline, requiring the use of thin shims at various locations. A small change in shim thickness made a larger change in a radial measurement at the far, closed end. For example, a change of 0.001 inch under the flange affects radial measurements at the far end by over 0.002 inch as a result of geometry. Difficulty in reproducing this set-up was magnified by slight angular movements of the flange near the 180° side requiring different shims at each set-up. Centerline offsets at the far end were generally 0.002 to 0.003 inch, with one set-up (post normal conditions test inspection) misaligned by 0.005 inch. Because these offsets were in random directions, the errors were additive in many cases, making the total inaccuracy 0.006 to 0.008 inch at the far end of the body. Inspection accuracies for other inner container body locations are as follows: length measurements = $\pm$0.001 inch and angular measurements = $\pm$0.015°.

Conclusions

All indicated changes in body radial and length measurements are believed to be due to inaccuracies in set-up. Real changes are indicated in angular measurements of the body flange (Figure B-1) at and near the 180° side. No real changes to the inner container lid were indicated in the data.

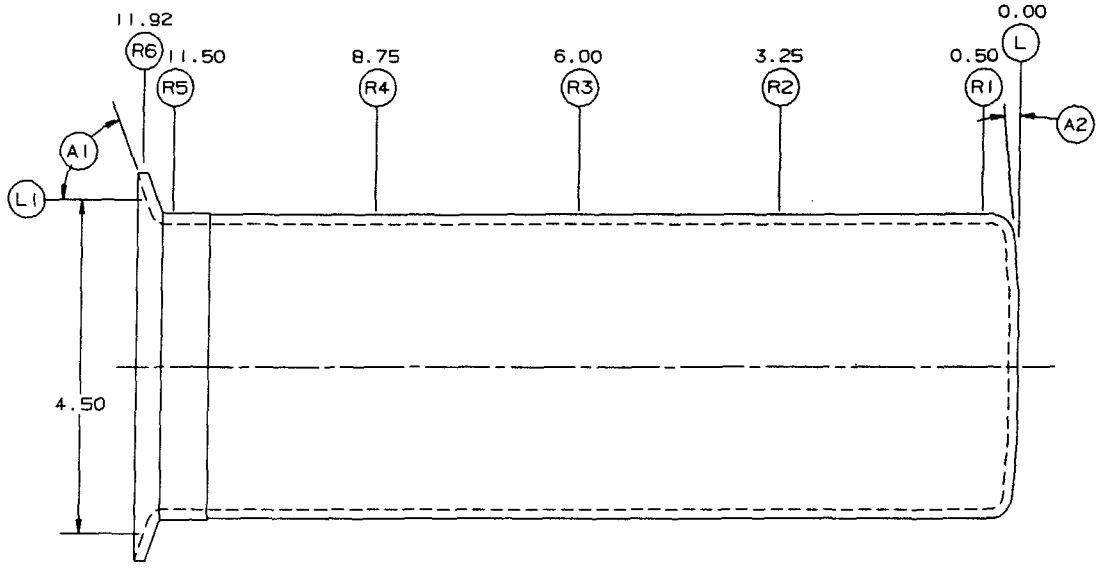

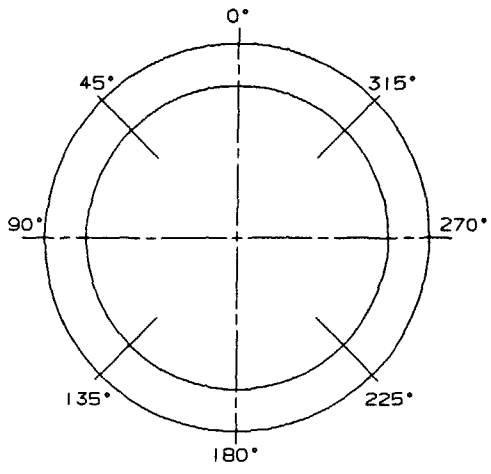

INSPECT POINT	MEASURE TYPE	LOCATION OF MEASUREMENT		
		LENGTH	REF RAD	REF ANGLE
1	RADIUS	R1	2.04	0°
2	RADIUS	R1	2.04	45°
3	RADIUS	R1	2.04	90°
4	RADIUS	R1	2.04	135°
5	RADIUS	R1	2.04	180°
6	RADIUS	R1	2.04	225°
7	RADIUS	R1	2.04	270°
8	RADIUS	R1	2.04	315°
9	RADIUS	R2	2.04	0°
10	RADIUS	R2	2.04	45°
11	RADIUS	R2	2.04	90°
12	RADIUS	R2	2.04	135°
13	RADIUS	R2	2.04	180°
14	RADIUS	R2	2.04	225°
15	RADIUS	R2	2.04	270°
16	RADIUS	R2	2.04	315°
17	RADIUS	R3	2.04	0°
18	RADIUS	R3	2.04	45°
19	RADIUS	R3	2.04	90°
20	RADIUS	R3	2.04	135°
21	RADIUS	R3	2.04	180°
22	RADIUS	R3	2.04	225°
23	RADIUS	R3	2.04	270°
24	RADIUS	R3	2.04	315°

INSPECT POINT	MEASURE TYPE	LOCATION OF MEASUREMENT		
		LENGTH	REF RAD	REF ANGLE
25	RADIUS	R4	2.04	0°
26	RADIUS	R4	2.04	45°
27	RADIUS	R4	2.04	90°
28	RADIUS	R4	2.04	135°
29	RADIUS	R4	2.04	180°
30	RADIUS	R4	2.04	225°
31	RADIUS	R4	2.04	270°
32	RADIUS	R4	2.04	315°
33	RADIUS	R5	2.07	0°
34	RADIUS	R5	2.07	45°
35	RADIUS	R5	2.07	90°
36	RADIUS	R5	2.07	135°
37	RADIUS	R5	2.07	180°
38	RADIUS	R5	2.07	225°
39	RADIUS	R5	2.07	270°
40	RADIUS	R5	2.07	315°
41	RADIUS	R6	2.61	0°
42	RADIUS	R6	2.61	45°
43	RADIUS	R6	2.61	90°
44	RADIUS	R6	2.61	135°
45	RADIUS	R6	2.61	180°
46	RADIUS	R6	2.61	225°
47	RADIUS	R6	2.61	270°
48	RADIUS	R6	2.61	315°

INSPECT POINT	MEASURE TYPE	LOCATION OF MEASUREMENT		
		LOCATION	REF DIM	REF ANGLE
49	LENGTH	L1	11.87	0°
50	LENGTH	L1	11.87	45°
51	LENGTH	L1	11.87	90°
52	LENGTH	L1	11.87	135°
53	LENGTH	L1	11.87	180°
54	LENGTH	L1	11.87	225°
55	LENGTH	L1	11.87	270°
56	LENGTH	L1	11.87	315°
57	ANGULAR	A1	70°	0°
58	ANGULAR	A1	70°	45°
59	ANGULAR	A1	70°	90°
60	ANGULAR	A1	70°	135°
61	ANGULAR	A1	70°	180°
62	ANGULAR	A1	70°	225°
63	ANGULAR	A1	70°	270°
64	ANGULAR	A1	70°	315°
65	ANGULAR	A2	5°	0°
66	ANGULAR	A2	5°	45°
67	ANGULAR	A2	5°	90°
68	ANGULAR	A2	5°	135°
69	ANGULAR	A2	5°	180°
70	ANGULAR	A2	5°	225°
71	ANGULAR	A2	5°	270°
72	ANGULAR	A2	5°	315°

Figure B-1. Inspection Points--Body

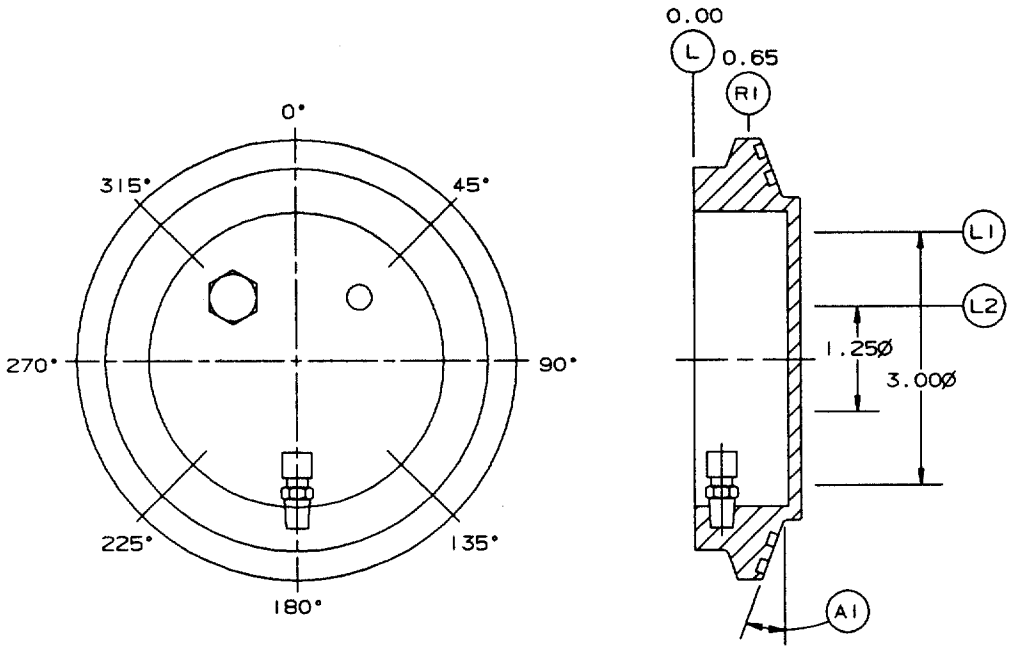

INSPECT POINT	MEASURE TYPE	LOCATION OF MEASUREMENT		
		LENGTH	REF DIM	REF ANGLE
1	RADIUS	R1	2.61	0°
2	RADIUS	R1	2.61	45°
3	RADIUS	R1	2.61	90°
4	RADIUS	R1	2.61	135°
5	RADIUS	R1	2.61	180°
6	RADIUS	R1	2.61	225°
7	RADIUS	R1	2.61	270°
8	RADIUS	R1	2.61	315°
9	ANGLE	A1	20°	0°
10	ANGLE	A1	20°	45°
11	ANGLE	A1	20°	90°
12	ANGLE	A1	20°	135°
13	ANGLE	A1	20°	180°
14	ANGLE	A1	20°	225°
15	ANGLE	A1	20°	270°
16	ANGLE	A1	20°	315°
17	LENGTH	L1	1.25	0°
18	LENGTH	L1	1.25	45°
19	LENGTH	L1	1.25	90°
20	LENGTH	L1	1.25	135°
21	LENGTH	L1	1.25	180°
22	LENGTH	L1	1.25	225°
23	LENGTH	L1	1.25	270°
24	LENGTH	L1	1.25	315°
25	LENGTH	L2	1.25	0°
26	LENGTH	L2	1.25	90°
27	LENGTH	L2	1.25	180°
28	LENGTH	L2	1.25	270°

Figure B-2. Inspection Points--Lid

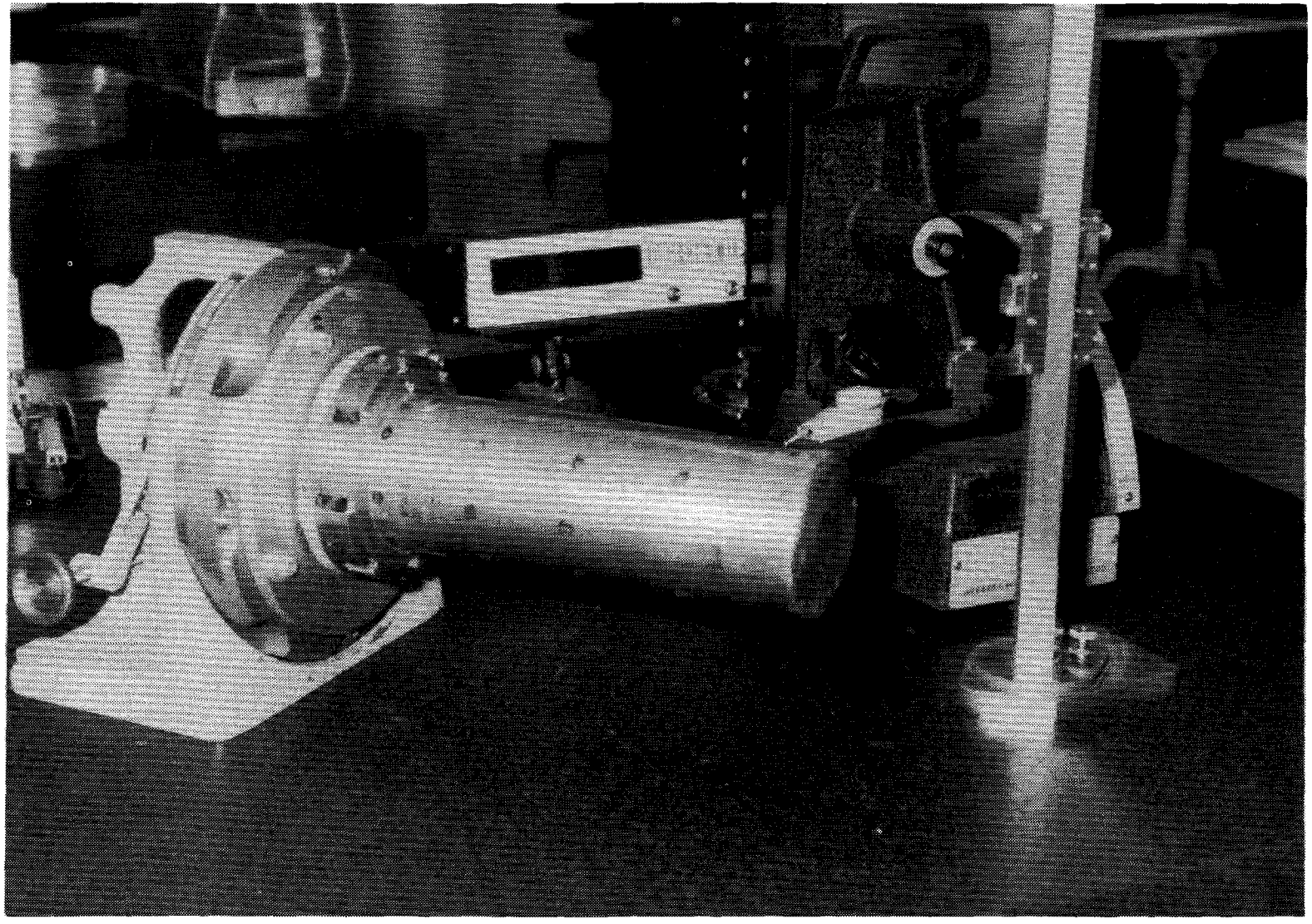

Figure B-3. Inspection Setup--Inner Container Body

TABLE B-1

Overpressure Test--Body

Radial Measurements

Location	Pretest	Posttest	Change	Location	Pretest	Posttest	Change
R1-000	2.039	2.042	0.003	R2-000	2.043	2.042	-0.001
R1-045	2.038	2.044	0.006	R2-045	2.041	2.044	0.003
R1-090	2.041	2.043	0.002	R2-090	2.043	2.044	0.001
R1-135	2.043	2.042	-0.001	R2-135	2.045	2.044	-0.001
R1-180	2.047	2.040	-0.007	R2-180	2.047	2.043	-0.004
R1-225	2.045	2.039	-0.006	R2-225	2.046	2.043	-0.003
R1-270	2.045	2.038	-0.007	R2-270	2.045	2.041	-0.004
R1-315	2.042	2.038	-0.004	R2-315	2.044	2.041	-0.003

Location	Pretest	Posttest	Change	Location	Pretest	Posttest	Change
R3-000	2.045	2.042	-0.003	R4-000	2.048	2.046	-0.002
R3-045	2.044	2.044	0.000	R4-045	2.046	2.047	0.001
R3-090	2.044	2.044	0.000	R4-090	2.043	2.048	0.005
R3-135	2.044	2.045	0.001	R4-135	2.043	2.048	0.005
R3-180	2.044	2.044	0.000	R4-180	2.042	2.045	0.003
R3-225	2.045	2.044	-0.001	R4-225	2.046	2.045	-0.001
R3-270	2.045	2.043	-0.002	R4-270	2.047	2.043	-0.004
R3-315	2.045	2.042	-0.003	R4-315	2.048	2.041	-0.007

Location	Pretest	Posttest	Change	Location	Pretest	Posttest	Change
R5-000	2.078	2.077	-0.001	R6-000	2.614	2.610	-0.004
R5-045	2.076	2.076	0.000	R6-045	2.611	2.610	-0.001
R5-090	2.070	2.076	0.006	R6-090	2.607	2.610	0.003
R5-135	2.070	2.078	0.008	R6-135	2.602	2.610	0.008
R5-180	2.070	2.076	0.006	R6-180	2.601	2.608	0.007
R5-225	2.074	2.074	0.000	R6-225	2.605	2.608	0.003
R5-270	2.076	2.070	-0.006	R6-270	2.608	2.608	0.000
R5-315	2.078	2.072	-0.006	R6-315	2.613	2.608	-0.005

Angular Measurements

Location	Pretest	Posttest	Change	Location	Pretest	Posttest	Change
A1-000	69.927	69.888	-0.039	A2-000	3.993	3.938	-0.055
A1-045	69.846	69.807	-0.039	A2-045	3.963	3.924	-0.039
A1-090	70.036	70.040	0.004	A2-090	3.897	3.797	-0.100
A1-135	70.004	70.224	0.220	A2-135	3.737	3.676	-0.061
A1-180	69.814	70.130	0.316	A2-180	3.653	3.622	-0.031
A1-225	70.011	70.028	0.017	A2-225	3.667	3.604	-0.063
A1-270	69.814	69.826	0.012	A2-270	3.774	3.749	-0.025
A1-315	69.929	69.869	-0.060	A2-315	3.932	3.885	-0.047

TABLE B-1 (Continued)

Overpressure Test--Body

Length Measurements

Location	Pretest	Posttest	Change
L1-000	11.879	11.880	0.001
L1-045	11.880	11.881	0.001
L1-090	11.879	11.879	0.000
L1-135	11.881	11.880	-0.001
L1-180	11.881	11.880	-0.001
L1-225	11.881	11.880	-0.001
L1-270	11.881	11.881	0.000
L1-315	11.880	11.880	0.000

TABLE B-2

Overpressure Test--Lid

Radial Measurements

Location	Pretest	Posttest	Change
R1-000	2.610	2.611	0.001
R1-045	2.610	2.610	0.000
R1-090	2.610	2.610	0.000
R1-135	2.610	2.610	0.000
R1-180	2.610	2.609	-0.001
R1-225	2.609	2.610	0.001
R1-270	2.609	2.610	0.001
R1-315	2.609	2.610	0.001

Angular Measurements

Location	Pretest	Posttest	Change
A1-000	19.898	19.902	0.004
A1-045	19.922	19.927	0.005
A1-090	19.900	19.898	-0.002
A1-135	19.990	19.993	0.003
A1-180	19.916	19.922	0.006
A1-225	19.895	19.900	0.005
A1-270	19.915	19.915	0.000
A1-315	19.814	19.817	0.003

Length Measurements

Location	Pretest	Posttest	Change
L1-000	1.249	1.247	-0.002
L1-045	1.250	1.248	-0.002
L1-090	1.250	1.248	-0.002
L1-135	1.250	1.248	-0.002
L1-180	1.249	1.248	-0.001
L1-225	1.248	1.248	0.000
L1-270	1.248	1.248	0.000
L1-315	1.246	1.246	0.000

Location	Pretest	Posttest	Change
L2-000	1.247	1.246	-0.001
L2-045	1.248	1.247	-0.001
L2-090	1.248	1.247	-0.001
L2-135	1.248	1.248	0.000
L2-180	1.248	1.247	-0.001
L2-225	1.248	1.247	-0.001
L2-270	1.247	1.246	-0.001
L2-315	1.246	1.246	0.000

TABLE B-3

Normal Conditions Tests--Body

Radial Measurements

Location	Pretest	Posttest	Change	Location	Pretest	Posttest	Change
R1-000	2.042	2.039	-0.003	R2-000	2.042	2.040	-0.002
R1-045	2.040	2.035	-0.005	R2-045	2.041	2.039	-0.002
R1-090	2.039	2.034	-0.005	R2-090	2.041	2.039	-0.002
R1-135	2.040	2.039	-0.001	R2-135	2.043	2.043	0.000
R1-180	2.043	2.044	0.001	R2-180	2.045	2.045	0.000
R1-225	2.046	2.046	0.000	R2-225	2.047	2.046	-0.001
R1-270	2.049	2.045	-0.004	R2-270	2.047	2.045	-0.002
R1-315	2.046	2.041	-0.005	R2-315	2.045	2.041	-0.004

Location	Pretest	Posttest	Change	Location	Pretest	Posttest	Change
R3-000	2.044	2.042	-0.002	R4-000	2.044	2.045	0.001
R3-045	2.043	2.042	-0.001	R4-045	2.044	2.044	0.000
R3-090	2.043	2.042	-0.001	R4-090	2.044	2.044	0.000
R3-135	2.044	2.044	0.000	R4-135	2.046	2.045	-0.001
R3-180	2.045	2.045	0.000	R4-180	2.047	2.044	-0.003
R3-225	2.047	2.045	-0.002	R4-225	2.049	2.046	-0.003
R3-270	2.046	2.044	-0.002	R4-270	2.048	2.046	-0.002
R3-315	2.045	2.041	-0.004	R4-315	2.047	2.046	-0.001

Location	Pretest	Posttest	Change	Location	Pretest	Posttest	Change
R5-000	2.073	2.073	0.000	R6-000	2.609	2.610	0.001
R5-045	2.071	2.074	0.003	R6-045	2.608	2.611	0.003
R5-090	2.072	2.071	-0.001	R6-090	2.608	2.610	0.002
R5-135	2.074	2.074	0.000	R6-135	2.608	2.608	0.000
R5-180	2.076	2.074	-0.002	R6-180	2.608	2.606	-0.002
R5-225	2.078	2.074	-0.004	R6-225	2.608	2.605	-0.003
R5-270	2.076	2.074	-0.002	R6-270	2.609	2.607	-0.002
R5-315	2.075	2.074	-0.001	R6-315	2.609	2.609	0.000

Angular Measurements

Location	Pretest	Posttest	Change	Location	Pretest	Posttest	Change
A1-000	69.909	69.894	-0.015	A2-000	3.924	3.920	-0.004
A1-045	69.844	69.802	-0.042	A2-045	3.916	3.909	-0.007
A1-090	70.034	70.005	-0.029	A2-090	3.838	3.801	-0.037
A1-135	70.232	70.019	-0.213	A2-135	3.687	3.668	-0.019
A1-180	70.159	69.955	-0.204	A2-180	3.625	3.635	0.010
A1-225	70.002	70.002	0.000	A2-225	3.654	3.602	-0.052
A1-270	69.829	69.834	0.005	A2-270	3.643	3.729	0.086
A1-315	69.889	69.862	-0.027	A2-315	3.888	3.875	-0.013

Table B-3 (Continued)

Normal Conditions Tests--Body

Length Measurements

Location	Pretest	Posttest	Change
L1-000	11.879	11.879	0.000
L1-045	11.880	11.880	0.000
L1-090	11.879	11.879	0.000
L1-135	11.880	11.880	0.000
L1-180	11.880	11.881	0.001
L1-225	11.880	11.880	0.000
L1-270	11.881	11.881	0.000
L1-315	11.879	11.879	0.000

TABLE B-4

Normal Conditions Tests--Lid

Radial Measurements

Location	Pretest	Posttest	Change
R1-000	2.609	2.609	0.000
R1-045	2.609	2.609	0.000
R1-090	2.609	2.610	0.001
R1-135	2.609	2.610	0.001
R1-180	2.609	2.610	0.001
R1-225	2.609	2.610	0.001
R1-270	2.609	2.610	0.001
R1-315	2.609	2.610	0.001

Angular Measurements

Location	Pretest	Posttest	Change
A1-000	19.901	19.897	-0.004
A1-045	19.926	19.918	-0.008
A1-090	19.894	19.899	0.005
A1-135	19.958	19.995	0.037
A1-180	19.919	19.921	0.002
A1-225	19.905	19.906	0.001
A1-270	19.922	19.924	0.002
A1-315	19.822	19.820	-0.002

Length Measurements

Location	Pretest	Posttest	Change
L1-000	1.248	1.249	0.001
L1-045	1.249	1.249	0.000
L1-090	1.249	1.249	0.000
L1-135	1.249	1.249	0.000
L1-180	1.249	1.250	0.001
L1-225	1.249	1.250	0.001
L1-270	1.249	1.249	0.000
L1-315	1.247	1.248	0.001

Location	Pretest	Posttest	Change
L2-000	1.247	1.247	0.000
L2-045	1.247	1.248	0.001
L2-090	1.248	1.248	0.000
L2-135	1.248	1.249	0.001
L2-180	1.248	1.248	0.000
L2-225	1.248	1.248	0.000
L2-270	1.247	1.248	0.001
L2-315	1.245	1.246	0.001

TABLE B-5

Drop Tests--Body

Radial Measurements

Location	Pretest	Posttest	Change	Location	Pretest	Posttest	Change
R1-000	2.039	2.042	0.003	R2-000	2.040	2.042	0.002
R1-045	2.035	2.044	0.009	R2-045	2.039	2.044	0.005
R1-090	2.034	2.043	0.009	R2-090	2.039	2.044	0.005
R1-135	2.039	2.042	0.003	R2-135	2.043	2.044	0.001
R1-180	2.044	2.040	-0.004	R2-180	2.045	2.043	-0.002
R1-225	2.046	2.039	-0.007	R2-225	2.046	2.043	-0.003
R1-270	2.045	2.038	-0.007	R2-270	2.045	2.041	-0.004
R1-315	2.041	2.038	-0.003	R2-315	2.041	2.041	0.000

Location	Pretest	Posttest	Change	Location	Pretest	Posttest	Change
R3-000	2.042	2.042	0.000	R4-000	2.045	2.046	0.001
R3-045	2.042	2.044	0.002	R4-045	2.044	2.047	0.003
R3-090	2.042	2.044	0.002	R4-090	2.044	2.048	0.004
R3-135	2.044	2.045	0.001	R4-135	2.045	2.048	0.003
R3-180	2.045	2.044	-0.001	R4-180	2.044	2.045	0.001
R3-225	2.045	2.044	-0.001	R4-225	2.046	2.045	-0.001
R3-270	2.044	2.043	-0.001	R4-270	2.046	2.043	-0.003
R3-315	2.041	2.042	0.001	R4-315	2.046	2.041	-0.005

Location	Pretest	Posttest	Change	Location	Pretest	Posttest	Change
R5-000	2.073	2.077	0.004	R6-000	2.610	2.610	0.000
R5-045	2.074	2.076	0.002	R6-045	2.611	2.610	-0.001
R5-090	2.071	2.076	0.005	R6-090	2.610	2.610	0.000
R5-135	2.074	2.078	0.004	R6-135	2.608	2.610	0.002
R5-180	2.074	2.076	0.002	R6-180	2.606	2.608	0.002
R5-225	2.074	2.074	0.000	R6-225	2.605	2.608	0.003
R5-270	2.074	2.070	-0.004	R6-270	2.607	2.608	0.001
R5-315	2.074	2.072	-0.002	R6-315	2.609	2.608	-0.001

Angular Measurements

Location	Pretest	Posttest	Change	Location	Pretest	Posttest	Change
A1-000	69.894	69.888	-0.006	A2-000	3.920	3.938	0.018
A1-045	69.802	69.807	0.005	A2-045	3.909	3.924	0.015
A1-090	70.005	70.040	0.035	A2-090	3.801	3.797	-0.004
A1-135	70.019	70.224	0.205	A2-135	3.668	3.676	0.008
A1-180	69.955	70.130	0.175	A2-180	3.635	3.622	-0.013
A1-225	70.002	70.028	0.026	A2-225	3.602	3.604	0.002
A1-270	69.834	69.826	-0.008	A2-270	3.729	3.749	0.020
A1-315	69.862	69.869	0.007	A2-315	3.875	3.885	0.010

TABLE B-5 (Continued)

Drop Tests--Body

Length Measurements

Location	Pretest	Posttest	Change
L1-000	11.879	11.880	0.001
L1-045	11.880	11.881	0.001
L1-090	11.879	11.879	0.000
L1-135	11.880	11.880	0.000
L1-180	11.881	11.880	-0.001
L1-225	11.880	11.880	0.000
L1-270	11.881	11.881	0.000
L1-315	11.879	11.880	0.001

TABLE B-6

Drop Tests--Lid

Radial Measurements

Location	Pretest	Posttest	Change
R1-000	2.609	2.611	0.002
R1-045	2.609	2.610	0.001
R1-090	2.610	2.610	0.000
R1-135	2.610	2.610	0.000
R1-180	2.610	2.609	-0.001
R1-225	2.610	2.610	0.000
R1-270	2.610	2.610	0.000
R1-315	2.610	2.610	0.000

Angular Measurements

Location	Pretest	Posttest	Change
A1-000	19.897	19.902	0.005
A1-045	19.918	19.927	0.009
A1-090	19.899	19.898	-0.001
A1-135	19.995	19.993	-0.002
A1-180	19.921	19.922	0.001
A1-225	19.906	19.900	-0.006
A1-270	19.924	19.915	-0.009
A1-315	19.820	19.817	-0.003

Length Measurements

Location	Pretest	Posttest	Change
L1-000	1.249	1.247	-0.002
L1-045	1.249	1.248	-0.001
L1-090	1.249	1.248	-0.001
L1-135	1.249	1.248	-0.001
L1-180	1.250	1.248	-0.002
L1-225	1.250	1.248	-0.002
L1-270	1.249	1.248	-0.001
L1-315	1.248	1.246	-0.002

Location	Pretest	Posttest	Change
L2-000	1.247	1.246	-0.001
L2-045	1.248	1.247	-0.001
L2-090	1.248	1.247	-0.001
L2-135	1.249	1.248	-0.001
L2-180	1.248	1.247	-0.001
L2-225	1.248	1.247	-0.001
L2-270	1.248	1.246	-0.002
L2-315	1.246	1.246	0.000

TABLE B-7

Puncture Tests--Body

Radial Measurements

Location	Pretest	Posttest	Change	Location	Pretest	Posttest	Change
R1-000	2.039	2.042	0.003	R2-000	2.043	2.042	-0.001
R1-045	2.038	2.044	0.006	R2-045	2.041	2.044	0.003
R1-090	2.041	2.043	0.002	R2-090	2.043	2.044	0.001
R1-135	2.043	2.042	-0.001	R2-135	2.045	2.044	-0.001
R1-180	2.047	2.040	-0.007	R2-180	2.047	2.043	-0.004
R1-225	2.045	2.039	-0.006	R2-225	2.046	2.043	-0.003
R1-270	2.045	2.038	-0.007	R2-270	2.045	2.041	-0.004
R1-315	2.042	2.038	-0.004	R2-315	2.044	2.041	-0.003

Location	Pretest	Posttest	Change	Location	Pretest	Posttest	Change
R3-000	2.045	2.042	-0.003	R4-000	2.048	2.046	-0.002
R3-045	2.044	2.044	0.000	R4-045	2.046	2.047	0.001
R3-090	2.044	2.044	0.000	R4-090	2.043	2.048	0.005
R3-135	2.044	2.045	0.001	R4-135	2.043	2.048	0.005
R3-180	2.044	2.044	0.000	R4-180	2.042	2.045	0.003
R3-225	2.045	2.044	-0.001	R4-225	2.046	2.045	-0.001
R3-270	2.045	2.043	-0.002	R4-270	2.047	2.043	-0.004
R3-315	2.045	2.042	-0.003	R4-315	2.048	2.041	-0.007

Location	Pretest	Posttest	Change	Location	Pretest	Posttest	Change
R5-000	2.078	2.077	-0.001	R6-000	2.614	2.610	-0.004
R5-045	2.076	2.076	0.000	R6-045	2.611	2.610	-0.001
R5-090	2.070	2.076	0.006	R6-090	2.607	2.610	0.003
R5-135	2.070	2.078	0.008	R6-135	2.602	2.610	0.008
R5-180	2.070	2.076	0.006	R6-180	2.601	2.608	0.007
R5-225	2.074	2.074	0.000	R6-225	2.605	2.608	0.003
R5-270	2.076	2.070	-0.006	R6-270	2.608	2.608	0.000
R5-315	2.078	2.072	-0.006	R6-315	2.613	2.608	-0.005

Angular Measurements

Location	Pretest	Posttest	Change	Location	Pretest	Posttest	Change
A1-000	69.927	69.888	-0.039	A2-000	3.993	3.938	-0.055
A1-045	69.846	69.807	-0.039	A2-045	3.963	3.924	-0.039
A1-090	70.036	70.040	0.004	A2-090	3.897	3.797	-0.100
A1-135	70.004	70.224	0.220	A2-135	3.737	3.676	-0.061
A1-180	69.814	70.130	0.316	A2-180	3.653	3.622	-0.031
A1-225	70.011	70.028	0.017	A2-225	3.667	3.604	-0.063
A1-270	69.814	69.826	0.012	A2-270	3.774	3.749	-0.025
A1-315	69.929	69.869	-0.060	A2-315	3.932	3.885	-0.047

TABLE B-7 (Continued)

Puncture Tests--Body

Length Measurements

Location	Pretest	Posttest	Change
L1-000	11.879	11.880	0.001
L1-045	11.880	11.881	0.001
L1-090	11.879	11.879	0.000
L1-135	11.881	11.880	-0.001
L1-180	11.881	11.880	-0.001
L1-225	11.881	11.880	-0.001
L1-270	11.881	11.881	0.000
L1-315	11.880	11.880	0.000

TABLE B-8

Puncture Tests--Lid

Radial Measurements

Location	Pretest	Posttest	Change
R1-000	2.610	2.611	0.001
R1-045	2.610	2.610	0.000
R1-090	2.610	2.610	0.000
R1-135	2.610	2.610	0.000
R1-180	2.610	2.609	-0.001
R1-225	2.609	2.610	0.001
R1-270	2.609	2.610	0.001
R1-315	2.609	2.610	0.001

Angular Measurements

Location	Pretest	Posttest	Change
A1-000	19.898	19.902	0.004
A1-045	19.922	19.927	0.005
A1-090	19.900	19.898	-0.002
A1-135	19.990	19.993	0.003
A1-180	19.916	19.922	0.006
A1-225	19.895	19.900	0.005
A1-270	19.915	19.915	0.000
A1-315	19.814	19.817	0.003

Length Measurements

Location	Pretest	Posttest	Change
L1-000	1.249	1.247	-0.002
L1-045	1.250	1.248	-0.002
L1-090	1.250	1.248	-0.002
L1-135	1.250	1.248	-0.002
L1-180	1.249	1.248	-0.001
L1-225	1.248	1.248	0.000
L1-270	1.248	1.248	0.000
L1-315	1.246	1.246	0.000

Location	Pretest	Posttest	Change
L2-000	1.247	1.246	-0.001
L2-045	1.248	1.247	-0.001
L2-090	1.248	1.247	-0.001
L2-135	1.248	1.248	0.000
L2-180	1.248	1.247	-0.001
L2-225	1.248	1.247	-0.001
L2-270	1.247	1.246	-0.001
L2-315	1.246	1.246	0.000

TABLE B-9

All Tests--Body

Radial Measurements

Location	Pretest	Posttest	Change	Location	Pretest	Posttest	Change
R1-000	2.034	2.035	0.001	R2-000	2.041	2.042	0.001
R1-045	2.036	2.039	0.003	R2-045	2.041	2.043	0.002
R1-090	2.041	2.045	0.004	R2-090	2.043	2.046	0.003
R1-135	2.048	2.051	0.003	R2-135	2.044	2.048	0.004
R1-180	2.048	2.053	0.005	R2-180	2.044	2.049	0.005
R1-225	2.045	2.050	0.005	R2-225	2.042	2.046	0.004
R1-270	2.040	2.043	0.003	R2-270	2.041	2.043	0.002
R1-315	2.036	2.038	0.002	R2-315	2.040	2.042	0.002

Location	Pretest	Posttest	Change	Location	Pretest	Posttest	Change
R3-000	2.044	2.045	0.001	R4-000	2.049	2.049	0.000
R3-045	2.043	2.045	0.002	R4-045	2.047	2.048	0.001
R3-090	2.044	2.046	0.002	R4-090	2.044	2.046	0.002
R3-135	2.043	2.047	0.004	R4-135	2.043	2.045	0.002
R3-180	2.042	2.047	0.005	R4-180	2.042	2.046	0.004
R3-225	2.042	2.046	0.004	R4-225	2.043	2.046	0.003
R3-270	2.043	2.045	0.002	R4-270	2.045	2.047	0.002
R3-315	2.043	2.044	0.001	R4-315	2.049	2.048	-0.001

Location	Pretest	Posttest	Change	Location	Pretest	Posttest	Change
R5-000	2.075	2.078	0.003	R6-000	2.609	2.609	0.000
R5-045	2.075	2.077	0.002	R6-045	2.609	2.609	0.000
R5-090	2.071	2.073	0.002	R6-090	2.608	2.609	0.001
R5-135	2.067	2.071	0.004	R6-135	2.607	2.609	0.002
R5-180	2.067	2.070	0.003	R6-180	2.606	2.609	0.003
R5-225	2.071	2.033	-0.038	R6-225	2.606	2.608	0.002
R5-270	2.073	2.076	0.003	R6-270	2.606	2.608	0.002
R5-315	2.075	2.077	0.002	R6-315	2.608	2.608	0.000

Angular Measurements

Location	Pretest	Posttest	Change	Location	Pretest	Posttest	Change
A1-000	69.954	69.816	-0.138	A2-000	3.625	3.593	-0.032
A1-045	70.005	69.979	-0.026	A2-045	3.576	3.574	-0.002
A1-090	69.905	69.896	-0.009	A2-090	3.729	3.584	-0.145
A1-135	69.999	70.018	0.019	A2-135	3.855	3.759	-0.096
A1-180	70.016	70.014	-0.002	A2-180	3.945	3.890	-0.055
A1-225	69.912	69.892	-0.020	A2-225	3.979	3.901	-0.078
A1-270	69.997	69.994	-0.003	A2-270	3.894	3.859	-0.035
A1-315	69.871	69.817	-0.054	A2-315	3.663	3.666	0.003

TABLE B-9 (Continued)

All Tests--Body

Length Measurements

Location	Pretest	Posttest	Change
L1-000	11.880	11.881	0.001
L1-045	11.877	11.878	0.001
L1-090	11.875	11.875	0.000
L1-135	11.872	11.871	-0.001
L1-180	11.872	11.870	-0.002
L1-225	11.875	11.874	-0.001
L1-270	11.877	11.877	0.000
L1-315	11.880	11.881	0.001

TABLE B-10

All Tests--Lid

Radial Measurements

Location	Pretest	Posttest	Change
R1-000	2.609	2.610	0.001
R1-045	2.609	2.610	0.001
R1-090	2.609	2.610	0.001
R1-135	2.609	2.611	0.002
R1-180	2.609	2.611	0.002
R1-225	2.609	2.611	0.002
R1-270	2.609	2.611	0.002
R1-315	2.609	2.611	0.002

Angular Measurements

Location	Pretest	Posttest	Change
A1-000	19.902	19.914	0.012
A1-045	19.895	19.892	-0.003
A1-090	19.962	19.954	-0.008
A1-135	19.963	19.956	-0.007
A1-180	19.936	19.942	0.006
A1-225	19.950	19.952	0.002
A1-270	19.869	19.877	0.008
A1-315	19.869	19.881	0.012

Length Measurements

Location	Pretest	Posttest	Change
L1-000	1.245	1.247	0.002
L1-045	1.248	1.248	0.000
L1-090	1.248	1.248	0.000
L1-135	1.248	1.248	0.000
L1-180	1.248	1.248	0.000
L1-225	1.248	1.248	0.000
L1-270	1.247	1.247	0.000
L1-315	1.244	1.245	0.001

Location	Pretest	Posttest	Change
L2-000	1.244	1.244	0.000
L2-045	1.246	1.246	0.000
L2-090	1.246	1.246	0.000
L2-135	1.246	1.246	0.000
L2-180	1.246	1.246	0.000
L2-225	1.246	1.245	-0.001
L2-270	1.244	1.244	0.000
L2-315	1.242	1.242	0.000

DISTRIBUTION LIST

No. of
Copies

205 U.S. Department of Energy
Office of Scientific and
Technical Information
Attn: DOE/OSTI-4500-R74 UC-722
Oak Ridge, TN 37830

26 Los Alamos National Laboratory
Attn: A. Guthrie
R. Sharp (20)
N. King
Group HSE3 M.S. G726
G. Rinehart
Group NMT9 M.S. E502
M. Lewis
D. Trujillo
Group MEE4 M.S. G787
D. Summers
Group QOO M.S. G736
Los Alamos, NM 87845

5	3141	S. A. Landenberger
8	3145	Document Processing for DOE/OSTI
3	3151	G. L. Esch, Actg.
5	5222	M. M. Madsen
1	6000	D. L. Hartley
1	6300	R. W. Lynch
1	6320	R. E. Luna, Actg. Attn: TTC Master File
25	6320	TTC Library
1	6321	M. G. Vannoni, Actg.
1	6322	G. F. Hohnstreiter
1	6323	T. L. Sanders
10	6323	D. R. Bronowski
1	6323	W. L. Uncapher
1	8524	Livermore Library

*U.S. GOVERNMENT PRINTING OFFICE 1991-0-573-038/44043